Genetically Tailored Yeast Strains for Cell-based Biosensors in White Biotechnology

DISSERTATION

zur Erlangung des akademischen Grades
Doctor rerum naturalium
(Dr. rer. nat.)

vorgelegt der
Fakultät Mathematik und Naturwissenschaften
der Technischen Universität Dresden

von

Annett Groß

geboren am 19.09.1982 in Freital

Gutachter: Prof. Dr. Gerhard Rödel
Prof. Dr. Günter Vollmer

Eingereicht am 30.09.2011
Verteidigt am 23.01.2012

... and a thousand years ago there was a strain, one who wished to apart from the infamous BY4741. Yes, this strain was jealous as it was never used to bring smiles and bake bread. But one day it was presented with the *ring of fluorescence* and there it was, illuminated by a tailor-made accessory ...

inspired by J. L. Gaugler during thesis revision

Authorship Declaration

I, Annett Groß, confirm that this dissertation and the experiments presented in it are my own achievement. The dissertation has not yet been presented in this or similar form to any other authority.

Where I have consulted the published work of others, this is always clearly attributed. Where I have quoted from the work of others, the source is always given. With the exception of such quotations, this dissertation is entirely my own work. I have acknowledged all main sources of help. If my research follows on from previous work or is part of a larger collaborative research project, I have made clear exactly what was done by others and what I have contributed myself.

Ich, Annett Groß, versichere, dass ich diese Dissertation und die darin vorgestellten Arbeiten selbstständig verfasst und durchgeführt habe. Die Dissertation wurde bisher weder im Inland noch im Ausland in gleicher oder ähnlicher Form einer anderen Prüfungsbehörde vorgelegt.

Die aus fremden Quellen direkt oder indirekt übernommenen Gedanken sind als solche kenntlich gemacht. Mit Ausnahme dieser angegebenen Zitate ist die Dissertation ohne unzulässige Hilfe Dritter und ohne Benutzung anderer Hilfsmittel angefertigt worden. Sofern Arbeiten von Vorgängern fortgeführt wurden oder diese Teil eines größeren Verbundprojektes waren, wurde eindeutig gekennzeichnet, welche Arbeiten von Dritten und welche Arbeiten selbst durchgeführt wurden.

Dresden, September 2011

Annett Groß

List of Publications

The following publications have evolved from or are related to this work. Where they form a part of it, this is referred to in the text and listed in the bibliography.

Peer-reviewed scientific article

Groß, A., Rödel, G., Ostermann, K., May 2011. Application of the yeast pheromone system for controlled cell-cell communication and signal amplification. Lett Appl Microbiol 52(5), 521–526.

Patent applications

Ostermann, K., Groß, A., Zierau, O., Diel, P., Vollmer, G., Lehmann, S., Rataj, F., Rödel, G., Jul 2010. Method for verification and/or identifying hormonally effective substances. WO Patent 2010072767.

Ostermann, K., Pompe, W., Rödel, G., Groß, A., Dec 2008. Device and a method for the detection and amplification of a signal. WO Patent 2009000918.

Ostermann, K., Pompe, W., Böttcher, H., Rödel, G., Groß, A., Nov 2008. Whole-cell sensor. WO Patent 2008132178.

Conference contributions

Groß, A., Ostermann, K., Rödel, G., Nov 2010. The *Saccharomyces cerevisiae* pheromone system: a versatile tool in whole-cell sensor applications. Max-Bergmann-Symposium in Dresden, Germany, 16 Nov 2010. *Poster presentation*

Groß, A., Ostermann, K., Rödel, G., Nov 2008. Design of fluorescent yeast whole cell sensors. Max-Bergmann-Symposium in Dresden, Germany, 4–6 Nov 2008. *Oral presentation*

Acknowledgement

Writing this dissertation has been the most significant academic challenge I have ever had to face. Without the guidance, support and encouragement of the following people, this work would not have been completed (yet) and it is to them that I owe my deepest gratitude.

I would like to thank Professor Gerhard Rödel for giving me the opportunity to do a doctorate in his research group and to act as a supervisor despite his numerous other academic and professional commitments. His knowledge, thoughtful criticism and commitment to high standards inspired and motivated me. I also want to thank Professor Günter Vollmer for reviewing this thesis.

I am truly thankful to Dr. Kai Ostermann for his imperturbable optimism, encouraging words, and all the time and attention despite busy terms.

I owe sincere and earnest thankfulness to my colleague Jennifer L. Gaugler who kindly proofread and commented the substantial manuscript, respectively, and enriched revision with an enjoyable sense of humour, too. All my former and present colleagues I would like to thank for the friendly atmosphere in the lab and our office, for vivid discussions, motivation and aid one another during the challenges we were all facing together. In addition, our sportful 'TRödel-AG' runs have been great fun.

I am obliged to all colleagues from the Institute of Materials Science, GMBU and UMEX who participated in the MBC projects with interest and enthusiasm. I especially thank Rocco Liebschner for great support during nano-plotting experiments and Georg Rode for literal supply of solutions.

Finally, I am truly indebted and thankful to my dear boyfriend Hagen Mölle for his love, support and non-limited patience with my personal as well as LaTeX's technical kinks and, of course, to my lovely family and friends who have always encouraged but also taught me to realise that working is not everything.

Table of Contents

List of Tables

List of Figures

List of Abbreviations

Standard abbreviations follow the guidelines of the Biochemical Journal (`http://www.biochemj.org/bj/bji2a.htm#table1`) and the recommendations of the IUPAC–IUBMB Joint Commission on Biochemical Nomenclature (`http://www.chem.qmul.ac.uk/iubmb/`). [URLs were last accessed on 28 September 2011.]

αF	α-factor
A. U.	Arbitrary unit
AvGFP	*Aequorea victoria* GFP
CFP	Cyan fluorescent protein
ddH_2O	Double-distilled water
E. coli	*Escherichia coli*
Em	Emission wavelength
Ex	Excitation wavelength
FP	Fluorescent protein
FSC	Forward scatter channel
GFP	Green fluorescent protein
GRAS	Generally recognised as safe
IfG	Institute of Genetics
kb	Kilo base pairs
MAPK	Mitogen-activated protein kinase
MBC	Molecular designed Biological Coating
MCS	Multiple cloning site
MM	Mineral medium
N-lim	Nitrogen limitation medium
OD_{600}	Optical density at 600 nm
ORF	Open reading frame
P-lim	Phosphorus limitation medium
pers. comm.	Personal communication
PMT	Photomultiplier tube
RFP	Red fluorescent protein
RFU	Relative fluorescence units
RNU	Relative nephelometer units

RT ..... Room temperature
S-lim ..... Sulphur limitation medium
S. cerevisiae ..... *Saccharomyces cerevisiae*
sd ..... Standard deviation
SSC ..... Side scatter channel
w/o ..... Without
YFP ..... Yellow fluorescent protein

Introduction

White biotechnology or industrial biotechnology is the application of living cells or their enzymes to generate useful products in industrial scale. Today, a palette of products ranging from dietary supplements to pharmaceuticals and biofuels is generated by fermentation. However, economic efficiency relies on precise and continuous process control which is only partially met by physical or physicochemical sensors. Genetically 'tailored' microorganisms equipped with fluorescent reporters in conjunction with optical analysis techniques might solve this problem in the near future.

Whole cell-based biosensors have the unique potential to near-line monitor both product yield and biological availability of nutrients during the entire fermentation process. The applicability of sensor cells in numerous examples of use has been demonstrated as a proof of concept. But there is still a wide gap between academic and commercial achievements (Kissinger, 2005). Developed cell-based biosensors meet economical, political and ethical concerns. Major issues impeding implementation of this technology include costs and time of development, selectivity, sensitivity, robustness and reproducibility.

Molecular designed Biological Coating

The presented work was done in the framework of the BMBF[1]-funded initiative 'Molecular designed Biological Coating' (MBC), a 'Regional Growth Core' that aims at the establishment and extension of innovative competences of local industry and research institutes. The city and the periphery of Dresden feature a number of small-scale enterprises with unique know-how in the fields of material coating, microelectronics, plant and biomedical engineering, sensorics and diagnostics. Moreover, close collaboration with the local research infrastructure was developed during the last decade. The unique feature of this strong network lies in the immobilisation of genetically engineered biomolecules and living cells on non-biological materials. Visions of the MBC platform include the establishment of a flexible technology to generate tailored and biologically active surfaces, its medium-term implementation in (supra-regional) industry and its extension to specific demands of costumers from industry and medicine. The potential of the MBC platform and participating collaboration partners was developed and extended in a cluster of six

[1] Federal Ministry of Education and Research

projects between 2007 and 2010. Among these, two projects with the codes 'FOBIO' and 'MaBioS' were of direct relevance for this work.

FOBIO[2] aims at the realisation of a new concept of photobioreactors for the synthesis of dietary supplements and biopharmaceuticals using immobilised microalgae. Microalgae are valuable resources of products, e.g. fatty acids, hydrocarbons, antioxidants and colouring substances, that are of interest for pharmaceutical, cosmetic, feed and food industry. Their yield and purity strongly depends on good vitality and biological activity of the producing microalgae. Photobioreactors enable controlled fermentation of microalgae and efficient supply of light and air, but productivity depends on a number of further determinants. Parameters such as temperature, pH and carbon dioxide concentration can be measured in-line using physical sensors. Sufficient supply with nutrients is essential too, but conventional methods are performed off-line and provide no information about the biological relevance of the analysed nutrients.

Therefore, a photobioreactor prototype for microalgae cultivation based on electrode-free light sources and fermentation process control based on recombinant *S. cerevisiae* cells have been proposed for development in the project FOBIO. The industrial partner UMEX GmbH Dresden, specialist in the development of photochemistry and photobiology equipment, was responsible for the construction of fermentation vessels with integrated light sources that allow optimal growth of phototropic microalgae. The GMBU e. V., Department Dresden is a non-profit organisation for industrial research. This partner optimised sol-gel immobilisation and fermentation of microalgae in photobioreactors as well as the synthesis efficiency of target products. The innovative use of baker's yeast *Saccharomyces* (*S.*) *cerevisiae* as a robust whole cell-based sensor for process monitoring should be examined as a proof of concept at the Institute of Genetics/TU Dresden. Respective nutrient sensor cells should monitor the biological availability of important macronutrients (nitrogen, phosphorus and sulphur) by means of converting the input information (i.e. the availability of a nutrient) into a fluorescence output signal that can be measured by a light-sensitive detector. The basic concept is depicted in Figure 1. By now, this invention is also protected by Patent WO 2008132178 entitled 'Whole-cell sensor' (Ostermann et al., 2008a).

In detail, promoters[3] that feature specifically higher or lower expression levels of the target gene under one particular nutrient limitation (Section 1.2.1) are fused to genes encoding GFP-like fluorescent proteins (Section 1.1.4). Prototype *S. cerevisiae* sensor cells harbour one detection construct to monitor the biological availability of one distinct nutrient. Dual-colour sensor cells feature two detection constructs and expression of a fluorescence reporter gene pair with well-distinguishable excitation and emission spectra

[2] The original project title is 'Photobioreaktoren und Kultivierungsverfahren auf der Basis elektrodenloser UV/VIS-Strahlungsquellen'.

[3] In the context of this work, the term 'promoter' describes an approximately 1-kb DNA fragment that comprises the (regulatory) region immediately adjacent to the 5'-end of the referring gene.

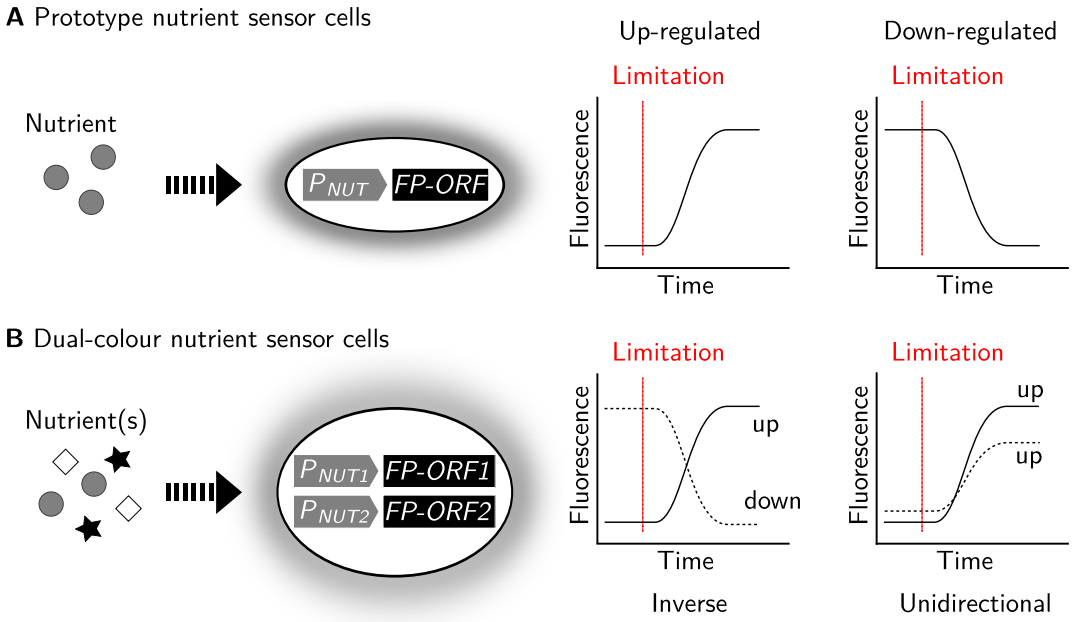

Figure 1: Concept of prototype and dual-colour yeast nutrient sensor cells. **A** Single-colour sensor cells carry one detection construct comprising a nutrient-responsive promoter (P_{NUT}) fused to a fluorescence reporter gene (*FP-ORF*). Upon limitation, the promoter is specifically up-regulated or down-regulated yielding in fluorescence increase or decline, respectively. **B** Dual-colour sensor cells exploit two different nutrient-responsive promoters for the expression of fluorescence reporter genes whose excitation and emission spectra can be separated. Expression profiles of the two detection constructs can be inverse or unidirectional.

such as green/red or cyan/yellow. These advanced sensor cells can be used to monitor either the same or different nutrients and the mode of expression can be unidirectional, inverse, etc. This dual-colour strategy can be applied to increase accuracy, double-check specificity or monitor multiple limitations and cross-reactivity.

MaBioS[4] is a pilot project to extend the capability of the MBC technology and address new markets. It aims at the junction of innovative generation of recombinant hybrid-biomolecules (tailored S-layers, hydrophobins) or microorganisms (tailored bacteria, yeast cells) and novel immobilisation techniques (microfluidics, nano-printing) to deposit biological structures in precise layers. To this end, industrial know-how from the GeSiM GmbH Rossendorf and research expertise of the TU Dresden Institutes of Genetics and Materials Science were combined. The GeSiM GmbH develops technical equipment for precise and automated nano-printing of particles on materials while the Institute of Genetics generates, evaluates and provides genetically engineered proteins and cells. Non-destructive and reliable deposition of bioparticles on non-biological, basic materials is finally optimised at the Institute of Materials Science.

Extension of the MBC technology should be realised using several economically rewarding examples. One key aspect is the generation and immobilisation of genetically

[4] The original project title is 'Maßgeschneiderte biofunktionalisierte Schichtsysteme und Mikroorganismen'.

engineered yeast cells that function as biosensors. To implement for instance *S. cerevisiae* nutrient sensor cells in photobioreactors or other fermentation processes, immobilisation of the sensor cells might be beneficial. Firstly, immobilisation is an essential step in the development of microbial biosensors in its understanding as a technical device (Sections 1.1.1 and 1.1.5). Secondly, sensor cells that are coimmobilised with the cultivated species might be able to monitor nutrient shifts in their direct microenvironment. Thus, the access of sensor cells to nutrients and detection of output signals after immobilisation has to be probed. Most microbial biosensors are based on a single cell type. They link an analyte-responsive promoter with the expression of a reporter gene resulting in a response that is directly proportional to the input signal. Such microbial biosensors might suffer from low sensitivity. As a countermeasure, a cellular communication and signal amplification system based on the natural mating pheromone system of *S. cerevisiae* (Section 1.3) was established. Detection of the input signal (analyte) by sensor cells and production of the output signal (fluorescence) by reporter cells is spatially separated and reconnected by pheromone signalling between both cell types (Fig. 2).

Basically, *S. cerevisiae* sensor cells exploit an analyte-responsive promoter for expression of the *MFα1* gene. In the presence of the analyte, sensor cells produce and secrete α-factor that is perceived by nearby reporter cells displaying the α-factor receptor. Binding of the pheromone triggers both natural mating response and artificial reporter response, i.e. expression of a gene encoding a GFP-like fluorescent protein from the pheromone-responsive *FIG1* promoter. Thereby one single sensor cell can activate a number of reporter cells. Another signal amplification circuit is offered by implementation of cells with expression of *MFα1* from the *FIG1* promoter. These amplifier cells are stimulated by α-factor to produce and release more α-factor molecules.

Spatial separation of analyte sensing and fluorescence generation will most likely result in delayed response compared to single cell-based sensors because of additional time required for α-factor-expression, secretion and diffusion towards reporter cells. However, the benefit is adjustable amplification of weak signals by varying the ratio of pheromone-secreting and pheromone-responsive cells. Moreover, sensor/amplifier/reporter cells can be arranged in various patterns by immobilisation. The invention of a 'Device and a method for the detection and amplification of a signal' is currently protected by a further in-house patent (WO 2009000918; Ostermann et al., 2008b).

Objectives

This work was performed in the framework of two MBC projects termed FOBIO and MaBioS. It focuses on the design of fluorescent *S. cerevisiae*-based sensor and reporter cells for white biotechnology and extension of the conventional single-cell/single construct principle of typical yeast biosensor systems and approaches. In detail, this work pursued

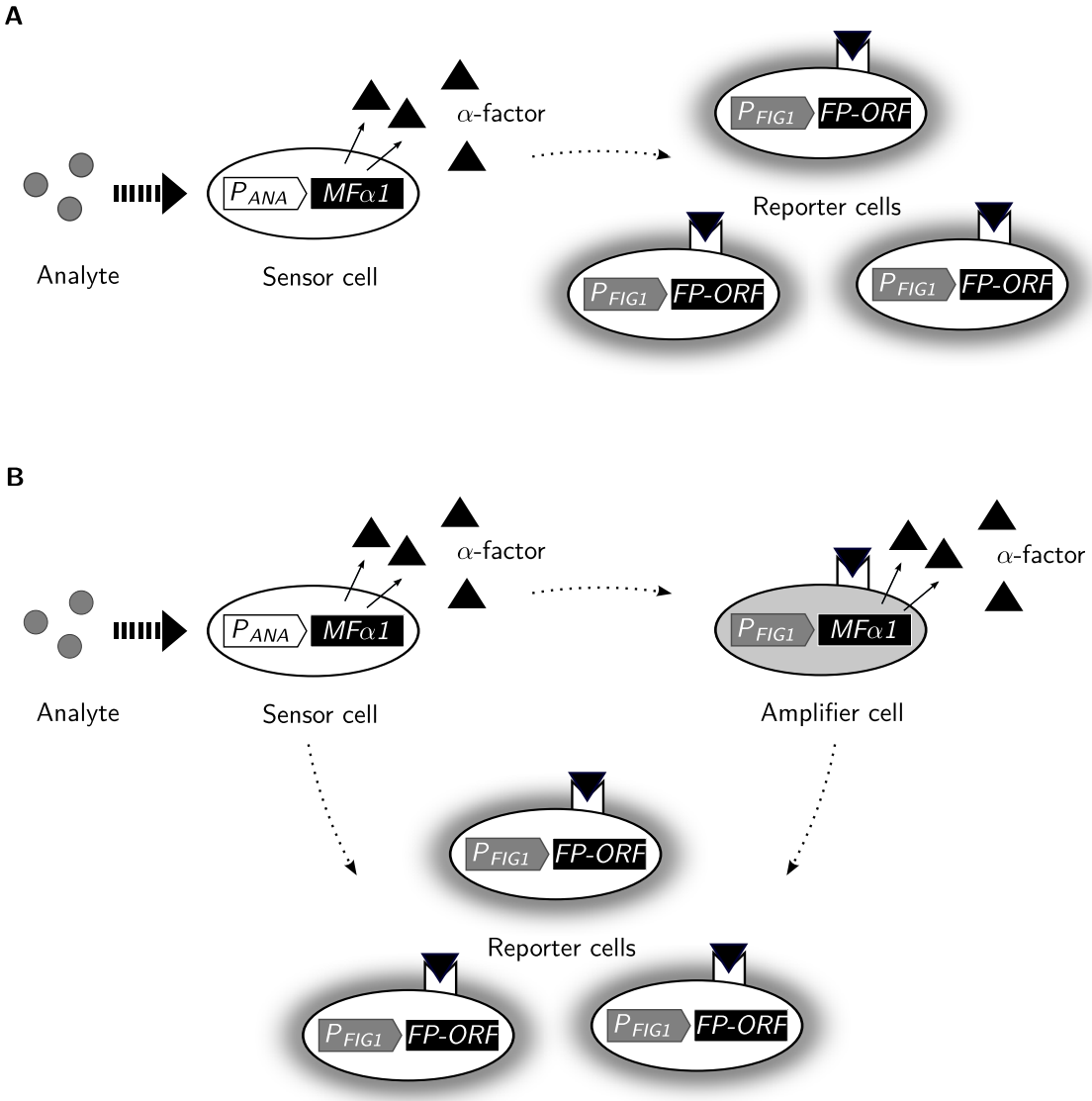

Figure 2: Concept of a *S. cerevisiae* pheromone-based cellular communication and signal amplification system. **A** Upon analyte-activation, a single sensor cell can trigger fluorescence in a number of reporter cells. Sensor cells carry a detection construct comprising an analyte-specific promoter (P_{ANA}) fused to the *MFα1* gene. They express and secrete α-factor in response to the analyte. This triggers both natural and artificial mating response in nearby reporter cells displaying α-factor-receptors and harbouring a detection construct for expression of a fluorescence reporter gene (*FP-ORF*) from the pheromone-responsive *FIG1* promoter (P_{FIG1}). **B** Another amplification circuit is generated by implementation of cells that link the *FIG1* promoter to the *MFα1* gene. These amplifier cells increase the level of α-factor molecules in response to α-factor.

the following objectives.

In the first part, a set of *S. cerevisiae* strains that can monitor the biological availability of three macronutrients (nitrogen, phosphorus and sulphur) should be generated and extensively evaluated. Such prototype sensor cells should be equipped with a detection plasmid that links a 'signature' promoter to a reporter gene encoding a GFP-like fluorescent protein. This includes the selection of convenient, i.e. specific and sensitive nutrient-responsive promoters that feature either higher or lower expression under one particular nutrient limitation. Globally changed gene expression in *S. cerevisiae* in response to nutrient limitation has been analysed before (Boer et al., 2003; Tai et al., 2005). Sensor cell performance and time trends of fluorescence should be evaluated on the level of single cells and total population using different conventional fluorescence detection methods. Specificity, sensitivity, selectivity and fluorescence regeneration of selected sensor cells should be primarily characterised in selective yeast media with defined nutrient concentrations. With regard to potential application in white biotechnology, sensor cell performance in microalgae media obtained before or after fermentation should be probed.

As mentioned, this work further aimed at expanding the principle of classical sensor cells that are based on a single cell type and produce a single output signal. Multi-parameter sensor cells represent an attractive option. Therefore, the potential of dual-colour sensor cells should be probed. A common drawback of whole cell-based sensor systems is low sensitivity. As a countermeasure, an amplification circuit based on the pheromone system of *S. cerevisiae* should be established. A set of required plasmid constructs was generated previously (Groba, 2007). Prerequisites for sufficient fluorescence generation should be examined, for instance by mixing α-factor-secreting cells and α-factor-perceiving/fluorescence-emitting reporter cells.

To implement sensor cells in existing transducer systems, their immobilisation is beneficial. Gentle cell entrapment methods based on calcium-alginate or agarose in a limited extent should be applied. One important question addressed the functionality of immobilised sensor cells. Hence, fluorescence signal production/acquisition in the hydrogel matrix should be studied as well.

Chapter 1

Theory

1.1 Implementation of *S. cerevisiae* in cell-based biosensor applications

1.1.1 An overview of microbial biosensors

Chemical and physical methods have been used over the past decades to measure particular properties of target samples. This traditional approach allows for highly precise and sensitive determination of analyte concentrations or even the exact composition of mixtures. However, such exhaustive examinations require costly instrumentation, specialised laboratory equipment and fail to monitor an impact on living systems or biological availability of target analytes. Numerous bioassays and bioreporter systems have been described as a complementary approach to partially meet these requirements. There has been growing interest to implement biosensors in environmental, medical, toxicological, defence or food and fermentation applications (Barthelmebs et al., 2010; Pancrazio et al., 1999).

In general understanding, biosensors are a class of analytical devices that couple a biological recognition element with a physical transducer to convert signals conducive for processing (Belkin, 2003; Lei et al., 2006; Su et al., 2011). Despite this, microbiologists frequently use the term 'biosensor' or 'microbial biosensor' in the context of whole cell-based biosensors to describe only the responsive microbial strain.

A wide variety of biomolecules, organelles or even whole cells have been implemented as biological sensing elements. Among the latter, microorganisms are advantageous due to cost efficiency in fabrication, ease of maintenance and inherent specificity and selectivity. However, often mentioned drawbacks of microbial biosensors in comparison to enzyme-based sensors are occurrence of unwanted side reactions, long response time or poor sensitivity and detection limits (D'Souza, 2001).

Microbial biosensors are under development for over 30 years and many concepts have been proposed by now (Karube et al., 1977; Nakamura et al., 2008). Biosensors of the

first generation exploit intrinsic respiratory or metabolic functions of microorganisms, e.g. to estimate the biological oxygen demand, utilisation of metabolically related nutrients or the impact of contaminants (König et al., 1998; Li and Chu, 1991; Svitel et al., 1998). Developments in molecular genetics offered new methods to generate biosensor cells that feature heterologous expression of various reporter genes (Lei et al., 2006; Su et al., 2011). This promoted the trend to 'tailor' microbial biosensors on the DNA level. Besides adaptation of microbes to new target substrates and analytical techniques, genetic manipulation was used to improve selectivity and sensitivity.

Microbial sensor cells function as the interface between the target substrate that is usually a physical parameter or a chemical compound, and the transducer. Ideally, the analyte concentration can be correlated with the output signal. Among various sensing techniques, electrochemical and optical techniques are most widely used. Electrochemical detection techniques can be divided into the subcategories amperometry, potentiometry, conductometry, voltammetry and microbial fuel cell. Optical detection is usually based on colourimetry, luminescence or fluorescence. In this work, fluorescent reporters were used for signal transduction.

1.1.2 Optical microbial biosensors

Colourimetric microbial biosensors involve the generation of a dye that can be correlated with the analyte concentration. Applications using genetically engineered bacteria can be found occasionally in literature (Su et al., 2011). For detection, either a facile photospectrometer is required or colour change may be judged by naked eye.

Luminescent microbial biosensors use bacterial or eukaryotic luciferase as a reporter (Gu et al., 2004). Reporter gene expression in microbial sensor cells can be constitutive or inducible and both systems have different benefits and limitations in biosensing. Constitutive systems feature a high basal luciferase gene expression level that is reduced after addition of the target analyte. Such 'lights off' assays lack specificity and were rather developed for rapid determination of overall ecotoxicity of environmental pollutants. The most famous example is the *Vibrio fischeri* bioluminescence inhibition assay and several tests are available on market (Farré and Barceló, 2003; Parvez et al., 2006). Inducible 'lights on' systems pursue low basal expression that is increased in a concentration-dependent manner upon addition of chemicals or conditions such as stress. A multitude of assays using bacteria as the sensing element are reviewed in Gu et al. (2004) and Su et al. (2011).

Both, colourimetric and luminescent assays have the disadvantage that addition of an exogenous substrate and/or ATP is essential. Fluorescent proteins, in contrast, emit light without such additives after excitation with light of another (lower) wavelength. Fluorescence assays are attractive for detection *in vivo* since measurements cause no or little damage in the host (Pickup et al., 2005). Fluorescent microbial biosensors employ

an inducible or repressible promoter that drives expression of a fluorescence reporter gene. The output signal can be qualitative (on/off) or ideally proportional to the input signal. The majority of reported fluorescent cell-based biosensor concepts exploit optimised green fluorescent proteins (Gu et al., 2004; Su et al., 2011). However, there are some limitations in the use of fluorescent reporters in microbial biosensor applications (Gu et al., 2004; Yagi, 2007). Fluorophore maturation takes an additional amount of time after synthesis of the core protein which results in a delay of maximum fluorescence. Once generated, the proteins are very stable and robust to denaturation or degradation. This might be disadvantageous in 'lights off' assays such as toxicity tests. Additionally, the presence of naturally fluorescent molecules in cells might cause a high background signal.

1.1.3 Yeasts as sensing elements in biosensors

The majority of microbial biosensors that are reported to date are based on bacterial cells (Nakamura et al., 2008; Su et al., 2011). However, there are three significant drawbacks in their use. Prokaryote cells may be relative fragile in a sensor environment and performance might be limited due to restricted tolerance of bacteria to physical parameters such as pH, temperature and salts (Baronian, 2004). Moreover, response of prokaryotes to some substrates are different from those of eukaryotes.

Reviews by Baronian (2004), Parry (1999) and Walmsley and Keenan (2000) discussed the superiority of yeasts in cell-based biosensors. Yeasts share rapid growth on a broad range of carbon sources with bacteria but display better robustness and physicochemical tolerance. Additionally, probing toxicity or genotoxicity of analytes with yeasts has potentially more relevance for higher eukaryotes.

Among the manageable number of reported yeast biosensor approaches to date, studies strongly focus on baker's yeast. *S. cerevisiae* (from here on equivalent to yeast) is a commonly applied model organism with GRAS[1] status of use, a completely sequenced genome and systematic characterisation in respect of its genome, transcriptome, proteome and metabolome. Early studies suggested for instance to evaluate toxicity of several compounds and to assay antifungal agents with *S. cerevisiae* wild type cells by measuring perturbation of respiratory activity or metabolic retardation (Campanella et al., 1996; Karube and Suzuki, 1990). Mascini and Memoli (1986) described an electrochemical biosensor using yeast as the sensing element for detection of glucose and other carbohydrates. Recently, the proof of concept of a yeast-based biosensor to follow carbohydrate uptake and degradation to carbon dioxide was proposed (Martínez et al., 2007). In another study, gas production of *S. cerevisiae* was used to monitor food temperature in cold chain control (Kogure et al., 2005). Even quantitation of analyte

[1] Acronym for the phrase 'Generally recognised as safe'

concentrations with wild type yeast was shown. Baronian and Gurazada (2007) proposed a method to quantify estradiol by a voltammetric yeast sensor. Akyilmaz et al. (2007, 2006) and Garjonyte et al. (2006) developed amperometric biosensors using *S. cerevisiae* wild type cells in order to assay vital marker L-lysine, thiamine and lactic acid and thereby determining the nutritional value of food and dietary supplements.

To date, a multitude of plasmid vectors and methods for genetic manipulation of yeast are available. Biosensors using genetically engineered yeasts as the sensor element have been reported frequently. The majority features expression of a fluorescence or luminescence reporter gene from an inducible or repressible regulatory element (promoter) resulting in 'lights on' or 'lights off' signal output. Of particular interest is the detection of (geno)toxicity of environmental pollutants and hormone-active chemicals by *S. cerevisiae* as a model eukaryote. Other recombinant yeast sensor cells were designed to monitor one singular or groups of specific chemical compounds. Table 1.1 gives an overview on published *S. cerevisiae*-based sensor cells and implemented transducer technologies during the last ten years.

1.1.4 Fluorescent proteins

Humans have an 'inherent' enthusiasm about glowing things in nature. Scientific study and application of fluorescent proteins started with the pioneering work of Shimomura et al. (1962) who extracted a green fluorescent protein from jellyfish *Aequorea victoria* (AvGFP). But the true impact of this discovery became apparent about 30 years later when the AvGFP gene was cloned and successfully expressed in bacteria and nematode worms (Chalfie et al., 1994; Prasher et al., 1992). The crystal structure of AvGFP was identified in 1996 (Ormö et al., 1996). It forms a nearly perfect cylinder (β-barrel) that buries the chromophore in its centre, resulting from autocatalytic cyclisation and oxidation of the tripeptide Serine65–Tyrosine66–Glycine67.

These studies proved that GFP fluorescence requires no exogenous substrates or cofactors and may be a versatile tool in many fields of molecular biology. The potential to visualise promoter activity *in vivo* is of special interest in applied fields of biotechnology such as the development of microbial biosensors.

During the last decades, the natural diversity of fluorescent proteins and their photophysical properties were intensively studied (Chudakov et al., 2010; Day and Davidson, 2009). GFP-like and other fluorescent proteins have been identified in four metazoan phyla so far. This natural diversity was further extended by the generation of new variants with modified spectral and biochemical properties using random or site-directed mutagenesis.

Several so called 'enhanced' GFP variants were generated in early studies after the cloning of AvGFP cDNA (Chudakov et al., 2010). This yielded a set of GFP derivatives with fluorescence emission ranging from blue to yellow regions of the visible spectrum. A

Table 1.1: Biosensors using genetically modified *S. cerevisiae* as sensing element

Analyte	**Reporter gene**	**Shuttle**	**Transducer type**	**Reference**
Copper ions	*lacZ*	Plasmid	Amperometric	Lehmann et al. (2000)
Copper ions	*luc*	Plasmid	Luminescent	Leskinen et al. (2003)
Copper ions	*GFPuv*	Plasmid	Fluorescent	Shetty et al. (2004)
Copper ions	*PpyRE8*	Plasmid	Luminescent	Roda et al. (2011)
Toxicity of heavy metals	*GFP*	Plasmid	Fluorescent	Radhika et al. (2005)
Toxicity of heavy metals	*EGFP*	Genome	Fluorescent	Yang et al. (2005)
Arsenic	*EGFP*, *TurboRFP*	Plasmid	Fluorescent	IfG/TU Dresden (2010), unpublished
Herbicide toxicity	*luc*	Genome	Luminescent	Hollis et al. (2000)
Paraoxon toxicity	*yEGFP*, *yDsRed*	Plasmid	Fluorescent	Schofield et al. (2007)
Organophosphorus compounds	*EGFP*	Plasmid	Fluorescent	Fukuda et al. (2010)
Oxidative stress	*EGFP*	Plasmid	Fluorescent	Jayaraman et al. (2005)
Genotoxicity	*yEGFP*	Plasmid	Fluorescent	Afanassiev et al. (2000)
Genotoxicity	*lacZ*	Plasmid, genome	Colourimetric	Jia et al. (2002)
Genotoxicity	*yEGFP*	Plasmid	Fluorescent	Lichtenberg-Fraté et al. (2003)
Genotoxicity	*yEGFP*	Plasmid	Fluorescent	Cahill et al. (2004); Keenan et al. (2007)
Genotoxicity of pharmaceuticals	*yEGFP*	Plasmid	Fluorescent	Gompel et al. (2005)
Genotoxicity of dental biopolymers	*EGFP*	Genome	Fluorescent	Yang et al. (2005)
Genotoxicity	*lacZ*	Plasmid	Colourimetric	Ichikawa and Eki (2006)
Genotoxicity	*yEGFP*	Genome	Fluorescent	Benton et al. (2007)
Genotoxicity	*yEGFP*	Plasmid	Fluorescent	García-Alonso et al. (2010, 2009)
Odorants	mammalian olfactory signalling components, *luc*	Plasmid	Luminescent	Minic et al. (2005)
Helional	mammalian olfactory signalling components, *luc*	Plasmid	Conductometric	Marrakchi et al. (2007)

[Continued on Next Page]

Table 1.1: [Continued]

Analyte	Reporter gene	Shuttle	Transducer type	Reference
DNT, odorants	mammalian olfactory signalling components, *GFP*	Plasmid	Fluorescent	Dhanasekaran et al. (2009); Radhika et al. (2007)
Estradiol	*luc*	Plasmid	Luminescent	Leskinen et al. (2003)
Hormone active chemicals	*EYFP*, *lacZ*	Plasmid	Fluorescent, luminescent	Muddana and Peterson (2003)
Estradiol	*yEGFP*, *luc*, *lacZ*	Plasmid	Fluorescent, luminescent	Bovee et al. (2004a)
Estrogenic activity	*yEGFP*	Plasmid	Fluorescent	Bovee et al. (2004b)
Estrogenic/androgenic chemicals	*luc*	Plasmid	Luminescent	Leskinen et al. (2005)
Androgenic activity	*luc*	Plasmid	Luminescent	Michelini et al. (2005)
Estrogenic chemicals	*luxA luxB*, *lacZ*	Plasmid	Colourimetric, luminescent	Sanseverino et al. (2005)
Endocrine disrupting chemicals	*luc*	Plasmid	Luminescent	Fine et al. (2006)
Estradiol	*lacZ*	Plasmid	Fluorescent	Wozei et al. (2006)
Androgenic chemicals	*luxA luxB*	Plasmid	Luminescent	Eldridge et al. (2007)
(Anti)androgenic chemicals	*yEGFP*	Plasmid	Fluorescent	Bovee et al. (2007, 2008)
Hormone active chemicals	*lacZ*	Plasmid	Amperometric	Ino et al. (2009)
Estrogenic/androgenic activity, toxicity	*luxA luxB*	Plasmid	Luminescent	Sanseverino et al. (2009)
2-isopropylthioxanthone (ITX)	*yEGFP*	Plasmid	Fluorescent	Peijnenburg et al. (2010)
Mycotoxins	*luc*	Plasmid	Luminescent	Välimaa et al. (2010)
Foreign protein production	*EGFP*	Plasmid	Fluorescent	Shibasaki et al. (2003)

serine–to–threonine substitution in the chromophore of AvGFP resulted in a simplified excitation spectrum with a single peak near 490 nm (GFP^{S65T}; Heim et al., 1995). Further replacement of the adjacent amino acid yielded Enhanced GFP (EGFP) that exhibits even higher brightness and faster maturation than wild type GFP or the GFP^{S65T} variant (Cormack et al., 1996). At the same time, an AvGFP mutant for UV detection was developed using DNA shuffling (Crameri et al., 1996). GFPuv features three amino acid substitutions and three silent mutations, and excitation/emission maxima of 395/509 nm. Enhanced cyan fluorescent protein (ECFP) was generated by a tyrosine–to–tryptophan substitution in the chromophore of AvGFP and further mutations with positive effects in adjacent positions of the surrounding β-barrel (Heim et al., 1994; Heim and Tsien, 1996).

Mutagenesis strategies were also used to generate codon-optimised fluorescent protein variants for mammalian cells and yeast. Cormack et al. (1997) reported on the synthesis of an artificial, codon-optimised EGFP reporter gene (*yEGFP3*) for versatile application in yeasts *S. cerevisiae* and *Candida albicans*.

GFP is a natural monomer and passes this characteristic down to its derivatives. This can be advantageous, e.g. for fast maturation, rapid fluorescence development or lower toxicity (Chudakov et al., 2010). However, *in vivo* application of fluorescent proteins such as monitoring of promoter activity is not restricted to monomer-type reporters.

Green fluorescent TurboGFP and yellow fluorescent TurboYFP are improved variants of Copepoda and Hydrozoa GFP-like proteins that both form dimers (Shagin et al., 2004). TurboGFP is a fast maturing variant of the Copepoda green fluorescent protein ppluGFP2 with improved solubility and stability (Evdokimov et al., 2006). It was found to be slightly brighter than EGFP (Day and Davidson, 2009). TurboYFP was generated from Hydrozoa PhiYFP and forms weak dimers. PhiYFP is one of few authentic yellow fluorescent proteins in terms of emitted light (Chudakov et al., 2010; Shagin et al., 2004). It was discovered much later than artificial YFPs which have been genetically engineered from AvGFP, but ironically they share some similarities in key positions of the amino acid sequence (Wachter et al., 1998). Anyway, this discovery verifies that protein engineering can be worth the effort in order to adjust the spectral properties of fluorescent proteins.

As indicated above, mutations of green fluorescent proteins did not yield variants with fluorescence emission in the red region of the visible spectrum. This area was entered with the discovery of new fluorescent proteins in Anthozoa, Copepoda and Hydrozoa species (Chudakov et al., 2010). Interestingly, oligomerisation (dimers or tetramers) is common for these proteins. DsRed was one of the first studied Anthozoa fluorescent proteins (Matz et al., 1999). It is a tetrameric GFP-like protein that emits orange-red fluorescence. In order to accelerate maturation and to improve solubility of wild type DsRed, Bevis and Glick (2002) used site-directed and random mutagenesis and engineered optimised

DsRed variants. DsRedT4 was found to have superior maturation time and was suggested as a reporter in fast growing microorganisms like yeasts. TurboRFP is a dimeric GFP-like orange-red fluorescent protein (Merzlyak et al., 2007). It was derived from Anthozoa fluorescent protein eqFP578 by random mutagenesis and features fast maturation and high stability. Moreover it is one of the brightest red fluorescent proteins known so far (Day and Davidson, 2009).

The stability of most fluorescent proteins limits their application in dynamic expression studies or 'lights off' systems. To overcome this, destabilised fluorescent proteins for use in eukaryotes and prokaryotes were developed by fusion to peptide tags that mediate rapid protein turnover (Andersen et al., 1998; Li et al., 1998). Mateus and Avery (2000) generated a hybrid fluorescent protein that consists of a yeast codon-optimised EGFP and the 178 carboxyl-terminal amino acids of yeast G1 cyclin Cln2p. The latter segment includes the major putative PEST motif and was shown to promote rapid protein degradation (Salama et al., 1994). PEST regions – rich in proline, glutamic acid, serine and threonine – are commonly found in short-lived eukaryotic proteins and confer susceptibility to ubiquitin-proteasome dependent and independent degradation (Belizario et al., 2008; Rogers et al., 1986). Mateus and Avery observed efficient degradation of EGFPpest within two hours of the *S. cerevisiae* cell cycle and determined a reporter half-life of approximately 30 minutes.

Today, the palette of fluorescent protein reporters comprises over 100 different variants that span almost the entire visible spectrum from deep blue (emission peak at 434 nm) to far-red (emission peak at 650 nm). Nevertheless, the majority of reported fluorescent microbial biosensors are based on GFP derivatives with EGFP being a favourable reporter as can be seen in Table 1.1 and reviews by Baronian (2004), Lei et al. (2006) and Su et al. (2011).

In this work, green fluorescent proteins were used in the first instance for studying the versatile application of engineered *S. cerevisiae* cells to monitor the presence of target analytes as a proof of concept. Besides, the implementation of further reporters selected from the palette of fluorescent proteins ranging from blue to red was probed. In an advanced approach, the ability to monitor and distinguish two fluorescent proteins (TurboGFP/TurboRFP) in dual-colour sensor cells was examined.

1.1.5 Immobilisation of microbial sensor cells in hydrogel matrices

Immobilisation of microorganisms is an important but drastic step in biosensor fabrication (Baronian, 2004; D'Souza, 2001; Lei et al., 2006; Su et al., 2011). Efficient signal transfer from the signal-emitting sensor cell to the transducer benefits from close contact between these two components. Immobilisation can furthermore help to stabilise the microbes

with regard to operational stability, long-term or repetitive use, sensor durability and portability. Cells can be either attached to a membrane or entrapped between two membrane layers that can be mounted on the transducer surface, or rather be directly immobilised on the transducer surface in a polymer matrix.

Chemical immobilisation methods like covalent binding and cross-linking typically involve harmful chemicals and harsh reaction conditions. Both techniques are not convenient for the immobilisation of viable microbial cells (Lei et al., 2006).

Traditional physical methods including adsorption and entrapment bypass the use of cytotoxic chemicals and reactions. Immobilisation by adsorption relies on ionic, electrostatic or hydrophobic interactions. The principle is simple but adsorption alone is weak and leads to desorption of microbes over time (D'Souza, 2001; Lei et al., 2006). Many synthetic and natural polymers have been proposed for microbe entrapment in layers, beads, discs, etc. (Baronian, 2004; D'Souza, 2001). Ideally, the polymer allows sufficient diffusion of molecules, passes optical signals, is biologically inert and obtains mechanical stability. Natural polymers such as alginate, agarose, carrageen and chitosan are superior to synthetic polymers (e.g. polyacrylamide) with regard to biological compatibility.

Agarose is a linear polysaccharide and can be useful in the immobilisation of cells with certain tolerance to temperature. Concentrations of 0.5% (w/v) and a temperature below 37°C are necessary for sol-gel transition (Xiong et al., 2005). In 2007, Bettaieb et al. validated an electrochemical bacterial biosensor using agarose gel-entrapped *E. coli* cells. The immobilisation procedure includes a moderate heat step (40°C) to mix melted agarose with *E. coli* cells for entrapment.

In contrast, entrapment in alginate hydrogels can be performed at room temperature. Alginates constitute a family of linear, unbranched polysaccharides that are widely distributed in the cell walls of brown algae and bacteria. Commercial alginates are primarily extracted from brown algae species *Laminaria hyperborea*, *Ascophyllum nodosum* or *Macrocystis pyrifera* and converted to the soluble sodium salt of alginic acid (Tønnesen and Karlsen, 2002; Wee and Gombotz, 1998). The binary copolymer consists of 1,4'-linked β-D-mannuronic acid (M) and α-L-guluronic acid (G) residues with varying composition and sequence depending on the source of alginate. In detail, homopolymeric M or G blocks are separated by regions of random or alternating MG units. Viscosity, transmittance and functional properties of an alginate as immobilisation matrix correlates strongly with its molecular weight, composition and block structure (Inukai and Yonese, 1999; Smidsrød and Skjåk-Braek, 1990).

Gelation and cross-linking of alginate chains mainly results from stacking of G blocks by exchange of sodium ions with any divalent cations except magnesium ions. G blocks of one alginate chain can form junctions with many other chains resulting in a gel network. Calcium-alginate hydrogels are the most extensively studied and regarded as generally non-toxic and biocompatible (Gacesa, 1988; Smidsrød and Skjåk-Braek, 1990).

They are widely used for immobilisation of viable cells in large respective micro-sized beads, thin layers or even three-dimensional structures (Braschler et al., 2005; Fine et al., 2006; Sugiura et al., 2005; Xu et al., 2009). Concentrations of 1% (w/v) alginate and 3 mmol l^{-1} calcium chloride are sufficient to maintain spherical calcium-alginate beads with entrapped *S. cerevisiae* cells (Bleve et al., 2008).

The major limitation in using calcium-alginate as an immobilisation matrix is its instability in the presence of calcium chelators like EDTA/EGTA, phosphate, citrate or lactate, and anti-gelling agents like sodium or magnesium ions (Smidsrød and Skjåk-Braek, 1990; Wee and Gombotz, 1998). This might be particularly critical for environmental monitoring since processing solutions and wastewater often contain chelators (D'Souza, 2001). Numerous strategies have been proposed to stabilise calcium-alginate hydrogels. Smidsrød and Skjåk-Braek (1990) suggested to adjust the calcium ion concentration or to substitute calcium ions with stronger cross-linking yet bio-compatible divalent ions (barium, strontium), trivalent ions (titanium, aluminium, iron) or cationic polyelectrolytes (chitosan, poly-lysine).

Novel immobilisation concepts are based on hybrid entrapment–encapsulation methods that combine convenient immobilisation techniques and yield better cell activity and viability (Su et al., 2011). Attention has been drawn for instance on the optimisation of stability and membrane properties of calcium-alginate beads by covering respective beads with mineral layers (Coradin and Livage, 2007; Coradin et al., 2003). Success of these approaches was mainly based on realisation of biocompatible silica synthesis. The traditional sol-gel technology allows for the formation of alkoxide silica gels at room temperature and neutral pH but releases alcohols that can be toxic for entrapped cells. A promising alternative are aqueous silica gels based on sodium silicates and colloidal silica (Coiffier et al., 2001). An all-aqueous sol-gel encapsulation method that avoids the generation of alcohols was proposed by Yu et al. (2005).

The present work did not focus on advanced immobilisation techniques but rather probing performance of engineered *S. cerevisiae* sensor and reporter cells after immobilisation as a proof of concept. Thus, traditional and facile physical entrapment methods, in detail immobilisation in calcium-alginate hydrogels and – to a limited extent – in low gelling point agarose was performed.

All polymer networks can be seen as a diffusion barrier and embedded cells may suffer from reduced access to nutrients or analytes. For agarose and calcium-alginate hydrogels, pore sizes in the range of 200–400 nm and 5–200 nm were reported, respectively (Pernodet et al., 1997; Wee and Gombotz, 1998). Thus, both hydrogel networks contain pores that entrap yeast cells which are much larger (approximately 5–10 μm) but allow the diffusion of small molecules such as glucose or ethanol (Wee and Gombotz, 1998) and of small peptides such as α-factor which was of interest here (Jahn, 2011).

1.2 Nutrient metabolism of *S. cerevisiae*

Unicellular, non-motile microorganisms such as yeasts have limited capacities to store nutrients or evade limitations and are mainly dependent on accessible nutrients from their immediate environment. *S. cerevisiae* has evolved numerous strategies to cope with nutrient fluctuations. Rapid and adequate response is essential for survival. Thus, cells must sense quantity and quality of accessible nutrients and initiate their uptake, metabolisation or storage. The physiological response is a complex process that is regulated for instance on the level of DNA, RNA or proteins. This section introduces background information about the macronutrient metabolism of *S. cerevisiae* that are essential for the development of yeast nutrient sensor cells to monitor the (biological) availability of macronutrients nitrogen, phosphorus and sulphur.

1.2.1 Response of *S. cerevisiae* to macronutrient limitation

The response of model organism *S. cerevisiae* to changes of environmental parameters is well studied with regard to its transcriptome, proteome, metabolome and ionome. Developments in microarray technology enabled the systematic and global analysis of yeast's gene expression profile under certain growth conditions. The genome-wide transcriptional response of *S. cerevisiae* strain CEN.PK113–7D (*MAT***a**) to growth limitation by glucose, nitrogen, phosphorus, or sulphur in aerobic and anaerobic chemostat cultures was characterised in the studies by Boer et al. (2003) and Tai et al. (2005). Here, only limitation of the three latter macronutrients was of interest.

The authors proposed several 'signature' genes for unequivocal indication of nutrient deficiency. Transcript abundance of such signature genes was significantly different in one nutrient-limited growth condition when compared with its abundance in all other limitations, i.e. genes were specifically up-regulated or down-regulated under one of the nutrient limitations. However, genes were categorised as significantly changed if expression under the respective limitation was changed at least twofold[2] when compared with its expression in all other conditions. Therefore, available microarray data must be analysed in more detail for own studies in order to identify genes with the highest fold-change in expression and transcript abundance (see Section 3.2.2). In gene clusters that are specifically more highly expressed under one particular limitation, some relevant regulatory motifs are enriched. This might indicate affiliation to a regulon and activation upon a unique stimulus – a beneficial criterion for the selection of reliable sensor constructs.

In these studies, yeasts were fed with ammonium sulphate as the sole source of nitrogen

[2] The fold-change was determined using Significance Analysis of Microarrays (SAM) published by Tusher et al. (2001). This method assigns a score to each gene on the basis of change in gene expression relative to the standard deviation of repeated measurements. In plain language, expression changed two-fold at a 99% confidence level.

and sulphur as well as potassium phosphate as the sole source of phosphorus. Comparable studies probing the global impact of other nutrient sources on gene transcription in *S. cerevisiae* are only known for nitrogen. Usaite et al. (2006) revealed that growth on ammonium and several amino acids also results in significantly changed transcription of numerous genes that might be physiologically correlated.

A vast number of studies and reviews deals with aspects of the complex nutritional network and pathways of yeast – primarily the utilisation of glucose and nitrogen. Sensing and response to various sources of nitrogen, phosphorus and sulphur is briefly summarised.

1.2.2 Nitrogen regulation

S. cerevisiae can use a variety of amino acids and other organic amines or amids as sources of cellular nitrogen alone but most laboratory strains prefer glutamine, glutamate and ammonia (Magasanik and Kaiser, 2002). The amino acids glutamate and glutamine are nitrogen donors for other cellular nitrogen compounds and can be directly metabolised (Magasanik, 1992; ter Schure et al., 2000). Other nitrogen sources are degraded to glutamate and/or ammonium which is subsequently converted to glutamate or glutamine. Thus, ammonium acts as an important intermediate and regulator which connects and controls degradation and biosynthesis pathways of nitrogen compounds. It was suggested that the metric by which cells evaluate the quality of nitrogen molecules is the cytoplasmic levels of glutamate, glutamine or ammonium (ter Schure et al., 2000; Zaman et al., 2008). However, the actual sensor has not been identified yet but the cytoplasmic anchor protein Ure2p (see below) might play a central role.

The presence of preferred nitrogen sources results in repression of pathways for the utilisation of less preferred nitrogen sources. This process is known as nitrogen catabolite repression and operates at different levels (Cooper and Sumrada, 1983). Transcriptional regulation is mediated by the interplay of four GATA-type zinc-finger transcription factors (Hofman-Bang, 1999). Gln3p and Gat1p (alias Nil1p) are positive regulators that can enter the nucleus upon deprivation of rich nitrogen sources. Dal80p and Deh1p (alias Gzf3p/ Nil2p) are negative regulators affecting Gln3p- or Gat1p-dependent transcription by negative feedback loops. The fifth player, Ure2p, serves as a cytoplasmic anchor for Gln3p and Gat1p and sequesters both nuclear activators in the presence of rich nitrogen sources (Beck and Hall, 1999; Blinder et al., 1996; Cunningham et al., 2000).

The initial step in the use of nitrogen compounds – and in corresponding regulation – is their uptake by specific or general permeases. Ammonium uptake for instance involves at least three permeases (Mep1p, Mep2p and Mep3p) as well as the GATA-family activator Gln3p (Marini et al., 1997, 1994). Expression of the permeases is stimulated by low ammonium concentrations. Gnp1p, the specific and high-affinity permease for glutamine, is expressed on both rich and poor nitrogen sources but the expression level is higher on rich nitrogen sources (Zhu et al., 1996). The general amino acid permease Gap1p exhibits

a broad specificity for L-isomers of most amino acids (Chen and Kaiser, 2002; Jauniaux and Grenson, 1990). It is regulated at the transcriptional level by the consortium of the four GATA-type regulators mentioned above resulting in higher expression on less preferred nitrogen sources (Coffman et al., 1997). Moreover, Gap1p activity is regulated at the post-transcriptional level by phosphorylation, intracellular sorting and ubiquitin-dependent degradation (Chen and Kaiser, 2002; Craene et al., 2001; Springael and André, 1998).

1.2.3 Phosphorus regulation

In comparison to nitrogen and sulphur, phosphorus requirements of *S. cerevisiae* are met by a very limited selection of compounds: inorganic phosphate[3] and glycerophosphoinositol which is subsequently catabolised to yield inositol and inorganic phosphate (Almaguer et al., 2004; Persson et al., 2003). The intracellular concentration of free phosphate is usually maintained low. The bulk of intracellular phosphate is stored as polyphosphates that are important both for phosphorus and energy supply. Inorganic phosphate is required for the synthesis of nucleic acids, proteins, phospholipids and for transphosphorylation reactions.

Accordingly, the cellular phosphorus homeostasis involves a number of transporters, enzymes, etc. They are coordinately regulated in the phosphatase (*PHO*) system which consists of at least 22 related genes and five regulators (Oshima, 1997; Persson et al., 2003). The positive regulators Pho2p and Pho4p are DNA binding proteins that can interact with two consensus motifs in the promoters of *PHO* genes and recruit the transcription machinery. Upon limitation, interplay of the regulators activates (or better derepresses) for instance *PHO84* and *GIT1* that encode the major, high-affinity transporters for inorganic phosphate and glycerophosphoinositol, respectively (Bun-Ya et al., 1992; Patton-Vogt and Henry, 1998). Other activated genes encode for acid or alkaline phosphatases (*PHO3*, *PHO5*, *PHO8*, *PHO11*) and proteins involved in polyphosphate metabolism (Persson et al., 2003). Most likely, cells mobilise intracellular polyphosphate pools as an early response to phosphorus limitation in order to maintain cellular structures and functions (Kulaev et al., 1999; Vagabov et al., 2000).

Although the actual sensor remains obscure, inorganic phosphate and inositol are the major signal molecules that induce uptake of extracellular phosphorus compounds by yeast or their scavenge from intracellular pools under phosphorus limitation. Pho84p might play a particular role in sensing inorganic phosphate (Martinez et al., 1998; Wykoff and O'Shea, 2001). However, the discussion stays controversial whether cells sense extracellular or intracellular levels of phosphorus in order to adjust their cellular response via the *PHO* regulon (Mouillon and Persson, 2006).

[3] Also referred to as orthophosphate (P_i)

1.2.4 Sulphur regulation

The unique sulphur metabolism of *S. cerevisiae* comprises a battery of metabolic and regulatory pathways excellently reviewed by Thomas and Surdin-Kerjan (1997). *S. cerevisiae* can metabolise nearly all inorganic sulphur sources including elemental sulphur, sulphates, sulphites, sulphides, thiosulphates and polythionates. The sulphur demand of yeast is generally met by uptake of sulphate minerals that are assimilated through reduction into sulphur amino acids cysteine and methionine or S-adenosylmethionine, an important metabolic intermediate. Yeast is also one of the rare organisms that can grow on all three organic sulphur compounds as the solitary source of sulphur. Whether synthesised *de novo* or taken up, these sulphur compounds are valuable constituents of proteins, cofactors and prosthetic groups or function as antioxidants.

Methionine and cysteine are solely taken up by specific high-affinity permeases in the presence of ammonium as the general amino acid permease Gap1p is not active (see Section 1.2.2) (Thomas and Surdin-Kerjan, 1997). There are three transporters reported for methionine (Mup1p, Mup2p, Mup3p) and one for cysteine. There is also a transport system for S-adenosylmethionine in yeast but details about the mechanism are still unknown.

Sulphate uptake is mediated by two high-affinity permeases, Sul1p and Sul2p (Breton and Surdin-Kerjan, 1977; Cherest et al., 1997). Transcription of *SUL2* and a number of so-called *MET*[4] genes whose products are functionally or regulatively involved in sulphate assimilation is specifically activated under sulphur deficiency (Boer et al., 2003; Tai et al., 2005).

The pathway is thought to be regulated by the intracellular level of organic sulphur compounds (Cherest et al., 1973, 1971; Kaiser et al., 2000; Rouillon et al., 2000). Met4p is the key regulator of *MET* genes (Thomas and Surdin-Kerjan, 1997). The protein is unstable in the presence of high S-adenosylmethionine levels. Upon sulphate limitation, a heterotrimeric complex consisting of Met4p and two DNA-binding proteins, Cbf1p and Met28p, promotes the coordinated activation of *MET* genes by binding to a conserved promoter motif (Kuras et al., 1997). Additionally, *MET* promoters contain a conserved motif for binding of the Met31p/Met32p activator complex but their function is not restricted to the sulphate assimilation pathway (Blaiseau et al., 1997).

Met4p and its DNA-binding partners Cbf1p, Met28p, Met31p and Met32p are also involved in another interesting mechanism named 'sulphur sparing' (Cormier et al., 2010; Fauchon et al., 2002). During stress response, yeasts convert the majority of assimilated sulphur into glutathione for detoxification. In order to save sulphur, some abundant, sulphur-rich enzymes of the carbohydrate metabolism are replaced by their

[4] This nomenclature is a consequence of the extraordinary property of *S. cerevisiae* to grow on methionine as the solitary sulphur source. The plurality of genes linked to the sulphur amino acid metabolism were identified as mutations that result in methionine auxotrophy and hence termed *MET* genes (Thomas and Surdin-Kerjan, 1997).

sulphur-depleted counterparts. Importantly, this response is also activated in other conditions in which Met4p is active, including sulphur limitation. A well-studied example is the activation of *PDC6* encoding pyruvate decarboxylase isozyme with low content in cysteine and methionine. Accordingly, numerous genes of the carbohydrate metabolism are down-regulated in response to sulphur deficiency (Boer et al., 2003; Tai et al., 2005). Other sulphur sparing strategies might have evolved by adaptation of transport routes. Sulphur limitation results in down-regulation of genes whose products might import stress-inducing metal ions and of *SSU1* which is required for sulphite export (Boer et al., 2003; Park and Bakalinsky, 2000). Repression of *SSU1* might benefit the conservation of intracellular sulphite which is both toxic but also an ordinary intermediate in reductive sulphur assimilation of yeast.

1.3 The mating pheromone system of *S. cerevisiae*

1.3.1 Mating of *S. cerevisiae*

S. cerevisiae is a unicellular organism but can exist in three particular cell types: haploids of mating type **a** or α, and **a**/α diploids (Herskowitz, 1988). Alone, haploid **a** or α cells proliferate asexually by budding. In addition, they may fuse efficiently with cells of the opposite mating type. The result is a diploid zygote (**a**/α cell) that can also proliferate by budding but is incapable to mate with further **a** or α cells. Meiosis is initiated under nutrient-limited conditions and yields four haploid spores (two **a** and two α cells) enclosed in an ascus. Every haploid progeny can initiate a new life cycle if environmental conditions improve.

The mating type is determined by a single locus on chromosome III named *MAT* (Dolan and Fields, 1991). Haploid cells that carry one of the two mating type alleles *MAT***a** and *MAT*α both constitutively express two regulatory proteins designated a1p and a2p or α1p and α2p, respectively. The function of a2p is not known but the interplay of the other transcription factors is responsible for the differential expression of numerous mating type-specific and haploid-specific genes in **a** or α cells. Diploid cells carry both alleles resulting in activation of all mating type-specific but not of haploid-specific genes.

Regulated genes comprise numerous members involved in the mating process. Mating is initiated by reciprocal activation of haploid cells that produce mating type-specific pheromones and display surface receptors to perceive the pheromone of cells of the opposite mating type (Sprague et al., 1983). In detail, **a** cells produce **a**-factor and perceive α-factor by the Ste2p receptor and α cells produce α-factor and perceive **a**-factor by the Ste3p receptor (Hagen et al., 1986; Jenness et al., 1983). Pheromone stimulation triggers various physiological changes in order to prepare cells for mating (Bardwell, 2005).

The α-factor-induced mating response in **a** cells has drawn attention of various disciplines ranging from fundamental biological research to mathematical modelling and is an extraordinarily well-studied signalling pathway in eukaryotes (Brent, 2009; Schwartz and Madhani, 2004). The following sections will give a brief overview about the pheromone molecules and the α-factor-induced mating response in *S. cerevisiae* with special emphasis on theory that is essential for the generation of a yeast cell-to-cell communication and signal amplification system.

1.3.2 Mating pheromone α-factor

The mating pheromones **a**-factor and α-factor are oligopeptides of similar function but of quite dissimilar structure and biogenesis. Mature **a**-factor is derived by expression from the two functionally redundant genes *MFa1* and *MFa2* and posttranslational modification by proteolytic cleavage, prenylation and methylation (Chen et al., 1997; Michaelis and Herskowitz, 1988). The dodecapeptide is finally exported by the ATP binding cassette transporter Ste6p (Kuchler et al., 1989).

The genes *MFα1* and *MFα2* encode precursor proteins of 165 and 120 amino acids that contain 4 and 2 tandem copies of the tridecapeptide WHWLQLKPGQPMY named α-factor (Kurjan and Herskowitz, 1982; Singh et al., 1983). The *MFα1* product, prepro-α-factor, enters the classical secretory pathway to undergo processing and release of mature α-factor molecules (Caplan et al., 1991; Julius et al., 1984; Waters et al., 1988). After translocation to the endoplasmic reticulum, a N-terminal signal sequence is cleaved and the nascent propeptide is glycosylated at three sites within the pro-region. Further endoproteolytic and exoproteolytic trimming in the Golgi and secretory vesicles results in removal of spacer peptides between the α-factor units as well as the pro-region. Subsequently released mature α-factor molecules have an estimated molecular mass of about 1,700 Daltons (Emter et al., 1983; Julius et al., 1984).

In the majority of published studies on the mating response of yeast, α-factor has been applied and its secretion mechanism has been unravelled much earlier than that of **a**-factor. Lower hydrophobicity and ease of chemical synthesis might have promoted the molecule's superior career. In order to generate a cellular communication and amplifier system in the present work, α-factor biogenesis appears more versatile for implementation in foreign cells (such as **a** cells) because it is based on the classical secretory pathway.

Haploid α cells continuously secrete α-factor and expression of *MFα1/MFα2* is increased in the presence of potential mating partners. Thus, cells perceive a spatial pheromone gradient and may localise mating partners with higher accuracy which is beneficial for mating (Arkowitz, 2009; Barkai et al., 1998). In addition, higher amounts of secreted pheromone increase the probability of mating (Jackson and Hartwell, 1990).

Under normal conditions α-factor is rapidly degraded by **a** cells (Finkelstein and Strausberg, 1979). This results in limited diffusion of the pheromone and recovery of

a cells from pheromone-induced arrest. Moreover it helps cells in accurate detection of mating partners (Barkai et al., 1998). The barrier aspartyl protease Bar1p (alias Sst1p[5]) recognises and cleaves α-factor between positions Leucine6 and Lysine7 (MacKay et al., 1991, 1988). *BAR1* expression and product release is under the control of *MAT*α*2* and α-factor (Manney, 1983). Like its target, Bar1p undergoes processing and secretion by the classical secretory pathway. Its final destination is the periplasm where it is retained and shows major activity (Moukadiri et al., 1999). However, Ballensiefen and Schmitt (1997) showed that the protease is already active in early compartments of the export system. Accordingly, deletion of *BAR1* might be beneficial both in α-factor secreting and perceiving **a** cells of a cellular communication and signal amplification system.

1.3.3 Mating response of *S. cerevisiae*

Stimulation of **a** cells with secreted or synthetic α-factor triggers sundry physiological and structural changes in order to prepare cells for mating. This can be observed on the cellular as well as the molecular level. It includes cell cycle arrest to switch from asexual to sexual mode of the life cycle, chemotropism in order to grow towards mating partners, display of necessary proteins for agglutination/fusion and changed expression of more than 350 genes (Bardwell, 2005; Marsh et al., 1991; Roberts et al., 2000).

The most apparent change is the formation of mating projections. Pheromone-treated cells show a typical pear-like shape also termed 'shmoo' after a homonymous cartoon character. This enables *S. cerevisiae* cells to stretch via cytoskeleton reorganisation (Chenevert, 1994). Studies by Moore et al. (2008) and Segall (1993) demonstrated that chemotropism is not random but typically aligns with the gradient. Interestingly, cells also produce a single but randomly oriented mating projection in an environment with uniform pheromone distribution (Dorer et al., 1995). In fact, shmoo tip formation follows internal positioning signals (Nern and Arkowitz, 2000).

All above mentioned processes are orchestrated by a mitogen-activated protein kinase (MAPK) pathway termed mating pheromone response pathway. The cascade is exhaustively studied and a widely used paradigm for eukaryotic signal transduction pathways (Bardwell, 2005; Brent, 2009; Dohlman and Thorner, 2001).[6] Some key components and events are depicted in Figure 1.1.

The mating pathway is activated by binding of α-factor to Ste2p, a G protein coupled receptor. Cells of mating type **a** display about 10,000 receptor molecules on their surface (Jenness et al., 1986). Pheromone-occupied Ste2p is internalised to a non-detectable level within 15 minutes and degraded via the lysosomal pathway (Hicke and

[5] These gene (product) standard names stand for 'barrier' and 'super sensitive' and refer to the phenotype of *bar1*Δ/*sst1*Δ deletion mutants that can not hinder α-factor diffusion and are hypersensitive to pheromone-induced cell cycle arrest.

[6] The majority of studies has been performed using α-factor and **a** cells (see Section 1.3.2).

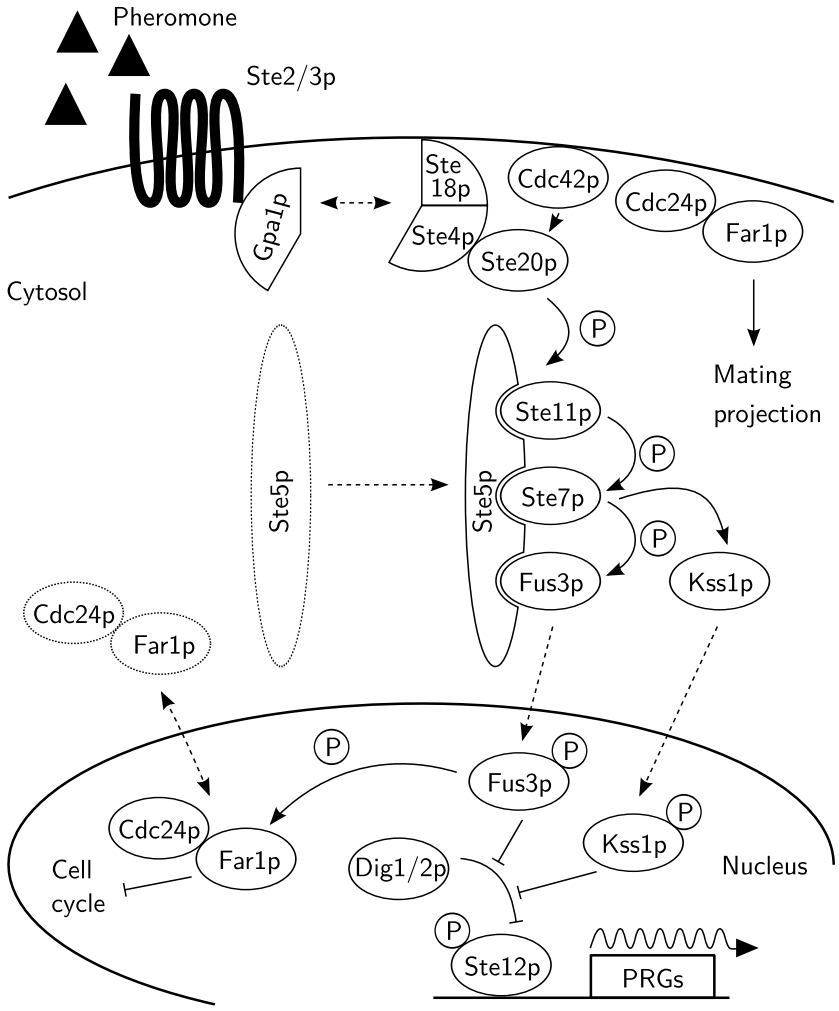

Figure 1.1: Key components and events of the *S. cerevisiae* mating pheromone response pathway (adapted from Yu et al., 2008b). Pheromones α-factor and **a**-factor bind to their receptors Ste2p or Ste3p, respectively. This triggers various molecular events such as formation of mating projections, cell cycle arrest and transcription of numerous pheromone-responsive genes (PRGs). See text in Section 1.3.3 for details. Proteins are illustrated by labelled ovals, phosphorylation steps by an encircled P, translocation processes by dotted lines, protein activation or inhibition by arrows or T-bars, respectively, and gene expression by a wavy line.

Riezman, 1996; Mulholland et al., 1999). Binding of α-factor causes dissociation of the attached heterotrimeric G protein into monomeric, GTP-bound Gpa1p (alias G_α) and a Ste4p/Ste18p dimer (alias $G_{\beta\gamma}$).[7] While Ste18p anchors the dimer to the membrane, Ste4p transmits the signal to three effectors: the Far1p/Cdc24p complex, Ste20p and the recruited MAPK scaffold protein Ste5p with the first of three MAP kinases, Ste11p.

The Far1p/Cdc24p complex is multifunctional and shuttles between the nucleus and the cytosol. In pheromone-treated cells, it assembles with the Ste4p/Ste18p complex and triggers the formation of mating projections. This is likely promoted by Cdc24p-mediated activation of Cdc42p, a small membrane-bound GTPase. Far1p also stimulates cell cycle arrest by a controversially discussed mechanism. Apparently, Far1p acts as a direct inhibitor of Cdc28p that drives cells through the G1 phase of the cell cycle. However, this requires nucleus-localised Far1p and phosphorylation by the MAP kinase Fus3p (see below).

Cdc42p is of fundamental role for the activation of the other aforementioned effectors. It recruits and activates the kinase Ste20p as a direct target. Brought in close contact, Ste20p phosphorylates Ste11p and triggers the actual MAPK cascade, i.e. sequential phosphorylation of recruited Ste7p and Fus3p. Phosphorylated Fus3p translocates to the nucleus and activates the DNA-binding, transcriptional regulator Ste12p by rescue from Dig1p/Dig2p-mediated repression. Ste12p finally activates expression of pheromone-responsive genes. In addition, activation of pheromone-responsive genes is triggered by sequential Ste7p/Kss1p phosphorylation.

Genome-wide transcript analysis revealed over 350 genes which upon α-factor stimulation were regulated (over 200 up-regulated genes) by the mating pathway and Ste12p (Roberts et al., 2000). Repressed genes are mainly cell cycle-related. The products of activated genes are key players of the MAPK cascade such as *STE2*, *FUS3* and *FAR1*, or regulators of negative feedback loops such as *SST2*. Other genes are correlated with the formation of mating projections and cell fusion (*FUS1*, *FIG1* and *PRM1*).

FIG1 (acronym for 'factor induced gene') and *PRM1* (acronym for 'pheromone-related membrane protein') have a similar expression pattern and transcription is considerably fast with about 100-fold and 10-fold up-regulation after 30 minutes stimulation with α-factor (Heiman and Walter, 2000; Roberts et al., 2000). Prm1p is a multi-spanning membrane protein that promotes membrane fusion of mating partners (Heiman and Walter, 2000; Olmo and Grote, 2010). The *FIG1* promoter region contains five putative binding sites for the transcriptional activator Ste12p (Erdman et al., 1998). The gene encodes an integral membrane-spanning protein that functions downstream of Fus1p and was originally characterised to be involved in low-affinity calcium ion influx (Muller et al., 2003). It is now suggested that Fig1p together with Prm1p stabilise the bilayer

[7] Reassociation of the G protein occurs by exchange of GTP to GDP at the Gpa1p subunit. This is promoted by the GTP-activating protein Sst2p.

membrane fusion zone in order to maintain membrane fusion fidelity (Aguilar et al., 2007). Calcium may be involved in membrane repair to counteract membrane disruption. Fig1p is also required for rapid cell death after exposure to high concentrations[8] of α-factor in the absence of an appropriate mating partner (Zhang et al., 2006).

In several studies, the promoters of *FUS1* and *PRM1* were exploited for expression of fluorescence reporter genes in order to follow downstream response of the MAPK cascade (Colman-Lerner et al., 2005; Ishii et al., 2006; Yu et al., 2008a). In this work, the *FIG1* promoter was used to generate a cellular communication and signal amplification system. It is particularly suitable and preferred because *FIG1* transcription undergoes the highest fold-induction during pheromone response.

[8] The applied α-factor concentration (60 μmol l^{-1}) was significantly higher than in other studies and the recent work.

Chapter 2

Materials and Methods

2.1 Laboratory equipment

Table 2.1: Special laboratory equipment used in this work

Description	Name	Manufacturer
Cell disruptor	Mixer Mill MM200	Retsch GmbH + Ko. KG (Haan, Germany)
Electroporation system	Gene Pulser II	Bio-Rad Laboratories GmbH (Munich, Germany)
Electrotransfer system	PerfectBlue Semi-Dry Electro Blotter Sedec M	Peqlab Biotechnologie GmbH (Erlangen, Germany)
Flow cytometer	CyFlow SL	Partec GmbH (Görlitz, Germany)
Fluorescence microscope	Axio Imager.1A	Carl Zeiss MicroImaging GmbH (Jena, Germany)
Fluorescence microscope	BZ-8100	Keyence Deutschland GmbH (Neu-Isenburg, Germany)
Fluorescence scanner	Typhoon Trio	GE Healthcare Europe GmbH (Munich, Germany)
Horizontal electrophoresis system	PerfectBlue Gel System Mini M/Midi S	Peqlab Biotechnologie GmbH (Erlangen, Germany)
Microplate nephelometer	NEPHELOstar	BMG Labtech GmbH (Ortenberg, Germany)
Microplate reader	Infinite M200	TECAN Group Ltd. (Männedorf, Switzerland)
Nano-Plotter	NP2.1	GeSiM GmbH (Rossendorf, Germany)
UV Transilluminator	AlphaImager HP Imaging System	Biozym Scientific GmbH (Hessisch Oldendorf, Germany)
UV/VIS Spectrophotometer	Nanodrop ND-1000	Peqlab Biotechnologie GmbH (Erlangen, Germany)
UV/VIS Spectrophotometer	Ultrospec 3000	Pharmacia Biotech (Munich, Germany)
Vertical electrophoresis system with Cast-It system	PerfectBlue Dual Gel System Twin ExW S	Peqlab Biotechnologie GmbH (Erlangen, Germany)

2.2 Laboratory materials

2.2.1 Antibodies

Table 2.2: Antibodies with applied dilutions for immunostaining. All antibodies were diluted in TBS–T containing 5% (w/v) non-fat dried milk powder (Section 2.8.2).

Antibody	Specificity	Dilution	Purchaser
Primary antibodies			
Anti-GFP (from mouse IgG)	ECFP, EGFP, EGFPpest, GFPuv	1:1,000	Roche Diagnostics GmbH (Mannheim, Germany)
Anti-PhiYFP (d) (from rabbit IgG)	TurboYFP, PhiYFP	1:10,000	Evrogen Joint Stock Company (Moscow, Russia)
Anti-tRFP (from rabbit IgG)	TurboRFP	1:5,000	Evrogen Joint Stock Company (Moscow, Russia)
Anti-TurboGFP (d) (from rabbit IgG)	TurboGFP	1:10,000	Evrogen Joint Stock Company (Moscow, Russia)
Secondary antibodies			
ECL Mouse IgG, HRP-conjugated Whole Ab (from sheep)	Mouse IgG	1:5,000	GE Healthcare Europe GmbH (Munich, Germany)
ECL Rabbit IgG, HRP-conjugated Whole Ab (from donkey)	Rabbit IgG	1:5,000	GE Healthcare Europe GmbH (Munich, Germany)

2.2.2 Chemicals

Laboratory chemicals not listed below were obtained from Merck KGaA (Darmstadt, Germany), Sigma–Aldrich Co. LLC. (Seelze, Germany), Carl Roth GmbH + Co. KG (Karlsruhe, Germany) or AppliChem GmbH (Darmstadt, Germany) in analytical quality. Media and solutions were prepared with distilled water and, if required, either heat-sterilised at 121°C for 20 min or filter-sterilised.

Table 2.3: Special and ultra-pure chemicals

Chemical	Supplier
Agar	ForMedium (Norfolk, United Kingdom)
Agarose (low gelling point)	Biozym Scientific GmbH (Hessisch Oldendorf, Germany)
Alginic acid sodium salt (medium viscosity)	Sigma–Aldrich Co. LLC. (Seelze, Germany)
α-Factor (yeast pheromone)	Zymo Research Corporation (Irvine, California)
Herring sperm DNA (ultra-pure)	Invitrogen GmbH (Darmstadt, Germany)
RedSafe DNA staining solution	HiSS Diagnostics GmbH (Freiburg, Germany)
Sheath fluid for flow systems	Partec GmbH (Görlitz, Germany)
Tryptone, yeast extract	ForMedium (Norfolk, United Kingdom)
Yeast nitrogen base w/o amino acids	ForMedium (Norfolk, United Kingdom)

2.2.3 Consumables

Table 2.4: Special consumables used in this work

Description	Specification/Brand	Supplier
Autoradiography films	Amersham Hyperfilm ECL	GE Healthcare Europe GmbH (Munich, Germany)
Blotting filter paper	Rotilabo, 0.36 mm	Carl Roth GmbH + Co. KG (Karlsruhe, Germany)
Dialysis membrane	Millipore 'V'-series membrane, 0.025 μm, ⌀ 25 mm	Millipore (Schwalbach/Ts, Germany)
Electroporation cuvettes	Gap distance 2 mm	Bio–Rad Laboratories GmbH (Munich, Germany)
Glass beads	⌀ 0.25–0.5 mm, acid-washed	Carl Roth GmbH + Co. KG (Karlsruhe, Germany)
Microscope slides for nanoprinting	Treated with 0.5% (v/v) Fixacol solution	GMBU e. V., Department Dresden (Dresden, Germany)
Needles	Sterican Gr. 14, 23G 1¼", ⌀ 0.6×30 mm	B. Braun Melsungen AG (Melsungen, Germany)
PVDF membranes	*Immobilon*–P 0.45 μm	Millipore (Schwalbach/Ts, Germany)
Quadratic petri dishes	PS, 12×12 cm^2	Carl Roth GmbH + Co. KG (Karlsruhe, Germany)
Sealing film for microplates	Breathe–Easy	Diversified Biotech (Dedham, Massachusetts)
Syringes	10 ml with Luer-Lok tip	Becton Dickinson GmbH (Heidelberg, Germany)
96-well microplates, black	BRAND*plates* pureGrade S #781668	BRAND GmbH + Ko. KG (Wertheim, Germany)
96-well microplates, transparent	#473–810	Dr. Ilona Schubert Laborfachhandel (Leipzig, Germany)
μ-Dishes	⌀ 35 mm, ibiTreat	ibidi GmbH (Martinsried, Germany)

2.2.4 Enzymes and size standards

Table 2.5: Enzymes for DNA restriction, amplification or modification, and size standards for DNA and protein electrophoresis. All enzymes were used with purchased buffers and additives according to the supplier's instructions.

Enzyme/size standard	Supplier
Antarctic Phosphatase	New England Biolabs GmbH (Frankfurt am Main, Germany)
DyNAzyme EXT DNA Polymerase	New England Biolabs GmbH (Frankfurt am Main, Germany)
Phusion High-Fidelity DNA Polymerase	New England Biolabs GmbH (Frankfurt am Main, Germany)

[Continued on Next Page]

Table 2.5: [Continued]

Enzyme/size standard	Supplier
Restriction endonucleases	New England Biolabs GmbH (Frankfurt am Main, Germany)
RNase A	Carl Roth GmbH + Co. KG (Karlsruhe, Germany)
Taq DNA Polymerase	New England Biolabs GmbH (Frankfurt am Main, Germany)
T4 DNA Ligase	New England Biolabs GmbH (Frankfurt am Main, Germany)
Zymolyase T20	AMS Biotechnology (Europe) Ltd. (Frankfurt am Main, Germany)
GeneRuler 1 kb Plus DNA Ladder	Fermentas GmbH (St. Leon-Rot, Germany)
Lambda (λ) DNA/*Pst*I Marker	Fermentas GmbH (St. Leon-Rot, Germany)
PageRuler Plus Prestained Protein Ladder	Fermentas GmbH (St. Leon-Rot, Germany)

2.2.5 Fluorescent proteins

Table 2.6: Properties of fluorescent proteins. Λ_{Ex} and Λ_{Em} are excitation and emission wavelength maxima in nm, respectively. QY is the quantum yield, defined as the ratio between the number of emitted and absorbed photons. EC is the molar extinction coefficient in 10^{-3} l mol^{-1} cm^{-1}. The computed relative brightness values (Br_r) were derived from the product of molar extinction coefficient and quantum yield, divided by the value for EGFP.

Protein (acronym)	$\Lambda_{Ex}/\Lambda_{Em}$	QY	EC	Br_r	Reference
AvGFP	397/509	0.80	25.0	0.6	Patterson et al. (1997)
ECFP	434/477	0.40	26.0	0.3	Patterson et al. (2001)
GFPuv	395/509	0.79	30.5	0.7	Crameri et al. (1996)
EGFP	488/509	0.60	55.0	1.0	Cormack et al. (1996)
EGFPpest	488/509	0.60	55.0	1.0	Mateus and Avery (2000)
TurboGFP	482/502	0.53	70.0	1.1	Evdokimov et al. (2006)
TurboYFP	525/538	0.60	105.0	1.7	Shagin et al. (2004)
PhiYFP	525/537	0.40	130.0	1.6	Shagin et al. (2004)
TurboRFP	553/574	0.67	92.0	1.9	Merzlyak et al. (2007)
DsRedT4	555/586	0.44	30.3	0.4	Bevis and Glick (2002)

2.2.6 DNA oligonucleotides

DNA oligonucleotides (Tabs. 2.7–2.11) were purchased from biomers.net GmbH (Ulm, Germany) or Eurofins MWG Operon (Ebersberg, Germany). Numbers in tables denote personal oligonucleotide identifiers.

Table 2.7: Oligonucleotides for PCR amplification of signature promoters (P_x). Sequences complementary to the target DNA sequence are written in capital letters. Cleavage sites for restriction enzymes are written in italics.

P_x	Nos.	Forward primer (5'→3')	Reverse primer (5'→3')	Product size	Cleavage sites
P_{BDS1}	101/102	ta*gagctc*CGTATCTCGGTAATCCTCCT	cg*actagt*ATCCGGTTGTTTAGTGAGAC	923 bp	*Sac*I, *Spe*I
P_{DAL5}	85/86	at*gagctc*ATCTACCCGCTAATTGTGAT	gc*actagt*CTTGAATTTTTTTTTTTTACACTATTT	954 bp	*Sac*I, *Spe*I
P_{DAL80}	45/46	tg*gagctc*CTTGGAATAGAGG	gcc*ggatcc*TCTCTTATATATAATATGATAT	1,391 bp	*Sac*I, *Bam*HI
P_{DIP5}	126/127	ag*gagctc*TCTTATCAATTATGTAAGTGCT	at*actagt*TACTTAGAGTTAGTTCTTTTTTTCCTGTG	977 bp	*Sac*I, *Spe*I
P_{GAP1}	83/84	at*gagctc*GTTGTACTATTACGAAGCACTA	ta*ggatcc*TTTTTATTTCTTTTTTTTGTTTCTTAT	981 bp	*Sac*I, *Bam*HI
P_{GNP1}	87/88	ta*gagctc*ACTGAACTGGGTCCTTCTGT	at*actagt*AATGTGCAATATTTGATATTATATAAGC	943 bp	*Sac*I, *Spe*I
P_{HPF1}	89/90	ta*gagctc*ATATGCTTCAATGGCCTGCT	at*actagt*CTCTTTGACAGGCGAGATCTTA	926 bp	*Sac*I, *Spe*I
P_{JLP1}	91/92	ta*cccggg*ACGAACAGGATGGTATTGAT	ag*ggatcc*ATTTTAACTGGGTTACTGTGCTA	960 bp	*Sma*I, *Bam*HI
P_{NSR1}	19/20	tattat*cccggg*GAGATTCCAAACTGGTTCATTGAAATAGGC	tattat*ggatcc*CTTATTTTATCCTGCCTGGGTTGAGTGAT	1,024 bp	*Sma*I, *Bam*HI
P_{PDC6}	119/120	at*gagctc*TCTCGCAACTAATGCTACCC	GCGC*actagt*TTTGTTGGCAATATGTTTTT	1,032 bp	*Sac*I, *Spe*I
P_{RPS22B}	23/24	tattat*cccggg*ACTGCAACTATTCTTACAATCTTTCATTTAC	tattat*ggatcc*TTTTTACCTAATTACTATGTTTTGAAACGTTAG	1,024 bp	*Sma*I, *Bam*HI
P_{SCS3}	93/94	ta*cccggg*GGGTCCTGTATTTGCGTTTA	gc*ggatcc*TGTTGTAATATGCCGTGCTT	1,001 bp	*Sma*I, *Bam*HI
P_{SOL1}	122/123	aa*gagctc*AAGATGAAACGCCTCCAGTT	gcgt*actagt*CTTGCAAAAAATTATTCCAGTTAAA	1,269 bp	*Sac*I, *Spe*I
P_{SSU1}	48/49	*cccggg*GCCACGTTCTAAACTAACTA	at*ggatcc*TTTTTTCTTGTACTTGTCTTCTC	1,273 bp	*Sma*I, *Bam*HI
P_{TMA10}	128/129	tt*gagctc*ATTTGCGCATTCCTATATCC	cg*actagt*GTTTGAATTGTGTTTGTGTTAG	918 bp	*Sac*I, *Spe*I

Table 2.8: Oligonucleotides for PCR amplification of fluorescence reporter genes (FP). Sequences complementary to the target DNA sequence are written in capital letters. Cleavage sites for restriction enzymes are written in italics.

FP	Nos.	Forward primer (5'→3')	Reverse primer (5'→3')	Product size	Cleavage sites
ECFP	25/26	tattat*gaattc*ATGGTGA-GCAAGGGCGAGGAG	tattat*gtcgac*TTACTTG-TACAGCTCGTCCAT-GCCG	744 bp	*Eco*RI, *Sal*I
GFPuv	151/152	agcg*actagt*ATGAGTAA-AGGAGAAGAACTTT	ttatat*aagctt*TTATTTG-TAGAGCTCATCCA	739 bp	*Spe*I, *Hin*dIII
EGFP	25/26	tattat*gaattc*ATGGTGA-GCAAGGGCGAGGAG	tattat*gtcgac*TTACTTG-TACAGCTCGTCCAT-GCCG	744 bp	*Eco*RI, *Sal*I
EGFPpest	33/31	tattat*gaattc*ATGTCTAA-AGGTGAAGAATTATT-CACTGGT	tattat*gtcgac*CTATATTA-CTTGGGTATTGCCC-ATACC	1,275 bp	*Eco*RI, *Sal*I
TurboGFP	42/43	ta*gaattc*ATGGAGAGC-GACGAGAG	tata*gtcgac*TTATTCTTC-ACCGGCATC	717 bp	*Eco*RI, *Sal*I
TurboYFP	–/–	tattat*actagt*ATGAGCA-GCGGCGCCCTGCT	tattat*gtcgac*TTAGCTT-GTATCTCCGGAAC	756 bp	*Spe*I, *Sal*I
PhiYFP	59/60	tata*gaattc*ATGAGAGG-ATCGGGATCC	tattat*gtcgac*TCACAGG-TAGGTCTTGCG	765 bp	*Eco*RI, *Sal*I
TurboRFP	138/139	tattat*actagt*ATGAGCG-AGCTGATCAAGG	tattat*gtcgac*TCATCTG-TGCCCCAGTTTG	630 bp	*Spe*I, *Sal*I
DsRedT4	77/78	tattat*gaattc*ATGGCCTC-CTCCGAGGACGTCAT	tattat*gtcgac*CTACAGG-AACAGGTGGTGGCG	726 bp	*Eco*RI, *Sal*I

Table 2.9: Oligonucleotides assigned for sequencing. An 'x' indicates applicability of this oligonucleotide for sequencing of numerous vectors/plasmids. For details about nomenclature see Figure 2.1 (Section 2.2.7) and Figure B.1 (Appendix B.1).

Primer name	No.	Sequence (5'→3')	Template(s)
ADHprom_seq	H	CTCGTTCCCTTTCTTCCTTG	p426ADH–FP
CYC1_seq	F	TCGGTTAGAGCGGATGTG	p42xP$_x$–FP
CYCtermrev	–	GCGTGAATGTAAGCGTGAC	p42xP$_x$
EGFP_chk	41	GAACTTCAGGGTCAGCTTGC	p426P$_x$–EGFP
EGFPpest_chk	40	GACTAAGGTTGGCCATGGAA	p42xP$_x$–EGFPpest
FIG1prom_seq	K	CTCAGGTTCTTGCTTGTCTTTGG	p426FIG1–FP
GNP1seq	99	AAACTATCGCTTTCTCAAGTAGC	p424GNP1–EGFPpest
GPDprom_seq	G	GACGGTAGGTATTGATTGTAATTCTG	p426GPD–FP
HPF1seq	100	CCCATCGTTGATTCTTTTTG	p424HPF1–EGFPpest
NSR1seq	47	ACCAATTTCGGATCACTCAAC	p424NSR1–EGFPpest
pRS_seq	I	GACCATGATTACGCCAAGC	p42xProm, p42xP$_x$

[Continued on Next Page]

Table 2.9: [Continued]

Primer name	No.	Sequence (5'→3')	Template(s)
p42x_seq	A	TTCCGGCTCCTATGTTGTGT	p42xProm, p42xP_x–FP
RPS22Bseq	44	CGAGAGCTCGAAGCATAAGT	p424RPS22B–EGFPpest
SCS3seq	98	TCCACTGAAACCAGCTATAAAG	p424SCS3–EGFPpest
SSU1seq	61	AGTGTAAGAGAAGACAAGTACAAGAAA	p424SSU1–EGFPpest
TurboGFP_chk	95	GATGCGGCACTCGATCTC	p426P_x–TurboGFP

Table 2.10: Oligonucleotides for the generation and verification of a nitrogen sensor strain with genome-integrated detection construct. Sequences complementary to the target DNA sequence are written in capital letters. Cleavage sites for restriction enzymes are written in italics. Primers labelled with 'check-PCR' were applied to confirm the correct insertion of the reporter cassette into the chromosomal *TYR1* locus of *S. cerevisiae* W303–1A.

Primer name	No.	Sequence (5'→3')	Features
F100_AG	130	tta*gatatcgcatgc*AGGGCTGTAAGCGGTGTAGA	*Eco*RV, *Sph*I
R100_AG	131	tta*gatatcgcatgc*ACGAACGATAATCGCGGTAG	*Eco*RV, *Sph*I
TRP1-ka-for	132	ggg*c**aggcct*AATTCGGTCGAAAAAAGAAA	*Stu*I
TRP1-Li-rev	133	taat*aggcctgagctcccgggtacc*GGCAAGTGCACAAACAA	*Stu*I, *Sac*I, *Sma*I, *Kpn*I
TYR1_F_chk	140	CCCAGGATGGCACTCAAAAA	Check-PCR
TRP1ka_chk	141	TTCACCTGTCCCACCTGCTT	Check-PCR
GAP1prom_chk	142	AGGGGCAAGACACCATCTGA	Check-PCR
TYR1_R_chk	143	ATGCGCCATCCTGAGAAGAC	Check-PCR

Table 2.11: Oligonucleotides for the generation and verification of BY4742 *matα*Δ. Sequences complementary to the target DNA sequence are written in capital letters. Italic letters in oligonucleotides assigned for deletion indicate sequences that are homologous to the denoted chromosomal locus.

Primer name	No.	Sequence (5'→3')	Features
MFalp1_F2	51	*aagaagattacaaactatcaatttcatacacaatataaacgattaaaaga*CG-GATCCCCGGGTTAATTAA	*MFα1* deletion *mfα1*Δ::*natMX6*
MFalp1_R1	52	*tgggaacaaagtcgactttgttacatctacactgttgttatcagtcgggc*GAAT-TCGAGCTCGTTTAAAC	*MFα1* deletion *mfα1*Δ::*natMX6*

[Continued on Next Page]

Table 2.11: [Continued]

Primer name	No.	Sequence (5'→3')	Features
MFalp2_F2	53	*ttactaccatcacctgcatcaaattccagtaaattcacatattggagaaa*CGGATCCCCGGGTTAATTAA	*MFα2* deletion *mfα2*Δ::*hphMX6*
MFalp2_R1	54	*atgaacgtgaaagaaatcgagagggtttagaagtagtttagggtcatttt*GAATTCGAGCTCGTTTAAAC	*MFα2* deletion *mfα2*Δ::*hphMX6*
R1	50	GAATTCGAGCTCGTTTAAACTG	Check-PCR
Alp1chk5	55	TGCAAGAAAACCAAAAAGCA	Check-PCR
Alp1chk3	56	GTTGGTAACGGAACGAAAAA	Check-PCR
Alp2chk5	57	CTTTACAGCGCAGAGACGAG	Check-PCR
Alp2chk3	58	TCGCATCATTTGAGAGAATACTT	Check-PCR

2.2.7 Plasmids and vectors

Two types of vectors were used to generate fluorescent yeast sensor and reporter cells. Based on the p42x series of expression vectors by Mumberg et al. (1995) (Fig. 2.1 and Tab. 2.12), plasmids for constitutive or conditional expression of target genes in recombinant *S. cerevisiae* sensor and reporter strains were constructed (Tab. 2.13). Vector pUC18 (Yanisch-Perron et al. (1985), Fig. 2.2) was used to generate a vector-borne genome integration cassette for *S. cerevisiae* using a one-step gene replacement strategy adapted from Mirisola et al. (2007) (Tab. 2.14). Further vectors given in Table 2.12 were used as DNA templates for PCR amplification of fluorescence reporter genes or antibiotic markers.

Table 2.12: Basic vectors. Important features of bacterial and shuttle vectors assigned for controlled expression of reporter genes in *S. cerevisiae*, construction of a genome integration cassette, or for PCR-amplification of target sequences are given.

Vector name	Relevant characteristics	Reference
p423ADH	Amp^R, *ColE1* origin, *HIS3*, 2μ origin, P_{ADH}, T_{CYC1}	Mumberg et al. (1995)
p424GPD	Amp^R, *ColE1* origin, *TRP1*, 2μ origin, P_{GPD}, T_{CYC1}	Mumberg et al. (1995)
p426ADH	Amp^R, *ColE1* origin, *URA3*, 2μ origin, P_{ADH}, T_{CYC1}	Mumberg et al. (1995)
p426ADH–DsRed	*DsRedT4*	Groba (2007)

[Continued on Next Page]

Table 2.12: [Continued]

Vector name	Relevant characteristics	Reference
p426FIG1	*Amp*^{R}, *ColE1* origin, *URA3*, 2μ origin, P_{FIG1}, T_{CYC1}	Groba (2007)
p426GPD	*Amp*^{R}, *ColE1* origin, *URA3*, 2μ origin, P_{GPD}, T_{CYC1}	Mumberg et al. (1995)
pFA6a–ECFP–natMX6	*ECFP*	Driessche et al. (2005)
pFA6a–hphMX6	*hphMX6*	Hentges et al. (2005)
pFA6a–natMX6	*natMX6*	Hentges et al. (2005)
pFA6a–yEGFP3–CLN2$_{PEST}$–natMX6	*EGFPpest*	Driessche et al. (2005)
pGFPuv	*GFPuv*	Clontech (Saint-Germain-en-Laye, France)
pPhi–Yellow–B	*PhiYFP*	Evrogen (Moscow, Russia)
pTurboGFP–N	*TurboGFP*	Evrogen (Moscow, Russia)
pTurboRFP–N	*TurboRFP*	Evrogen (Moscow, Russia)
pTurboYFP–N	*TurboYFP*	Evrogen (Moscow, Russia)
pUC18	*Amp*^{R}, *ColE1* origin, *lacZ*' adjacent to *Pvu*II cleavage sites	Yanisch-Perron et al. (1985)

Table 2.13: Plasmids for constitutive or conditional expression of target genes in yeast. All plasmids are based on the p42x shuttle vector series by Mumberg et al. (1995) featuring an ampicillin resistance cassette, a *ColE1* and 2μ origin, a selection marker for complementation of amino acid or nucleobase auxotrophy and the *CYC1* terminator (see Figure 2.1 and Table 2.12). Other relevant characteristics are listed. General plasmid maps and cloning strategies are illustrated in Figures B.1 and B.2 (Appendix B).

Vector name	Relevant characteristics	Reference
p423ADH–TurboRFP	P_{ADH}, *TurboRFP*	This work
p424GNP1–EGFPpest	P_{GNP1}, *EGFPpest*	This work
p424HPF1–EGFPpest	P_{HPF1}, *EGFPpest*	This work
p424NSR1–EGFPpest	P_{NSR1}, *EGFPpest*	This work
p424RPS22B–EGFPpest	P_{RPS22B}, *EGFPpest*	This work
p424SCS3–EGFPpest	P_{SCS3}, *EGFPpest*	This work
p424SOL1–EGFPpest	P_{SOL1}, *EGFPpest*	This work
p424SSU1–EGFPpest	P_{SSU1}, *EGFPpest*	This work

[Continued on Next Page]

Table 2.13: [Continued]

Vector name	Relevant characteristics	Reference
p426ADH–EGFP	P_{ADH}, *EGFP*	Pham (2008)
p426ADH–MFα1	P_{ADH}, *MFα1*	Groba (2007)
p426ADH–TurboGFP	P_{ADH}, *TurboGFP*	This work
p426ADH–TurboRFP	P_{ADH}, *TurboRFP*	S. Thierfelder (IfG, 2010)
p426BDS1–EGFP	P_{BDS1}, *EGFP*	This work
p426DAL4–EGFP	P_{DAL4}, *EGFP*	Pham (2008)
p426DAL5–EGFPpest	P_{DAL5}, *EGFPpest*	This work
p426DAL5–TurboGFP	P_{DAL5}, *TurboGFP*	This work
p426DAL80–EGFP	P_{DAL80}, *EGFP*	This work
p426DAL80–TurboGFP	P_{DAL80}, *TurboGFP*	This work
p426DIP5–EGFPpest	P_{DIP5}, *EGFPpest*	This work
p426FIG1–EGFP	P_{FIG1}, *EGFP*	Groba (2007)
p426FIG1–GFPuv	P_{FIG1}, *GFPuv*	This work
p426FIG1–MFα1	P_{FIG1}, *MFα1*	Groba (2007)
p426FIG1–TurboRFP	P_{FIG1}, *TurboRFP*	This work
p426GAP1–EGFPpest	P_{GAP1}, *EGFPpest*	This work
p426GAP1–TurboGFP	P_{GAP1}, *TurboGFP*	This work
p426GPD–DsRedT4	P_{GPD}, *DsRedT4*	This work
p426GPD–ECFP	P_{GPD}, *ECFP*	This work
p426GPD–EGFP	P_{GPD}, *EGFP*	This work
p426GPD–EGFPpest	P_{GPD}, *EGFPpest*	This work
p426GPD–GFPuv	P_{GPD}, *GFPuv*	This work
p426GPD–PhiYFP	P_{GPD}, *PhiYFP*	This work
p426GPD–TurboGFP	P_{GPD}, *TurboGFP*	This work
p426GPD–TurboRFP	P_{GPD}, *TurboRFP*	This work
p426GPD–TurboYFP	P_{GPD}, *TurboYFP*	S. Thierfelder (IfG, 2010)
p426JLP1–TurboGFP	P_{JLP1}, *TurboGFP*	This work
p426PDC6–EGFP	P_{PDC6}, *EGFP*	This work
p426PHO11–EGFP	P_{PHO11}, *EGFP*	Pham (2008)
p426PHO11–MFα1	P_{PHO11}, *MFα1*	This work
p426PRM2–TurboRFP	P_{PRM2}, *TurboRFP*	K. Zarschler (IfG, 2010)
p426TMA10–EGFPpest	P_{TMA10}, *EGFPpest*	This work

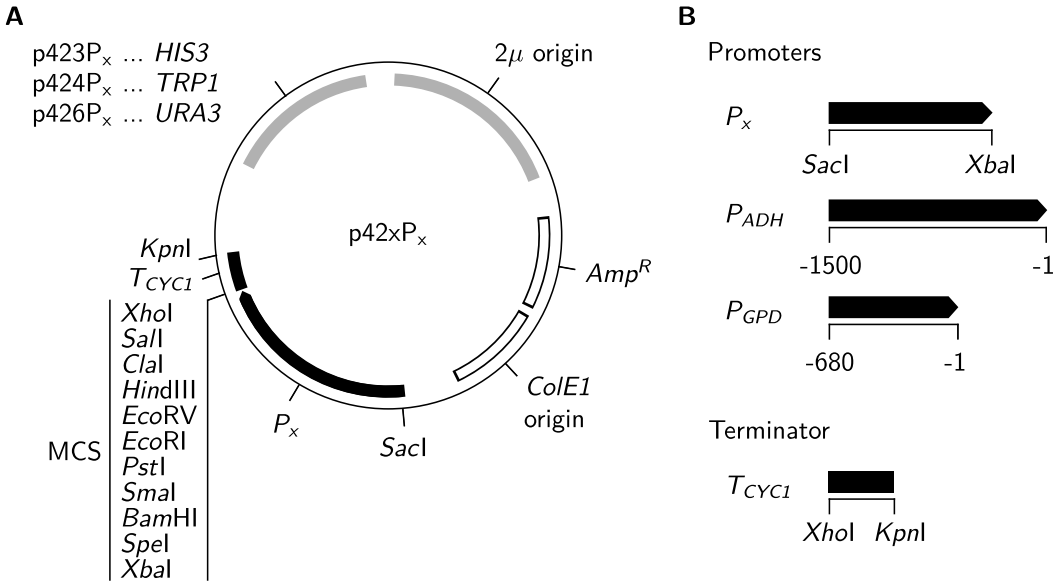

Figure 2.1: Structure of 2 μ-based vectors for heterologous gene expression in recombinant *S. cerevisiae* created by Mumberg et al. (1995), figure adapted from article. **A** Schematic map of expression vectors. Each shuttle vector carries a 2μ origin for vector replication in *S. cerevisiae* and one selection marker for complementation of either histidine (*HIS3*), tryptophan (*TRP1*), or uracil (*URA3*) auxotrophy. An ampicillin resistance cassette (Amp^R) and *ColE1* replication origin are enclosed for selection and vector propagation in *E. coli*. Restriction sites of the multiple cloning site (MCS) between the promoter (P_x) and the *CYC1* terminator (T_{CYC1}) are shown. **B** Schematic maps of promoters and *CYC1* terminator. The *ADH* and *GPD* promoters (P_{ADH} and P_{GPD}, respectively) mediate moderate and strong expression. Numbers below promoters give positions relative to the first nucleotide of the encoded ATG start codon of the corresponding gene (+1). Drawings not to scale.

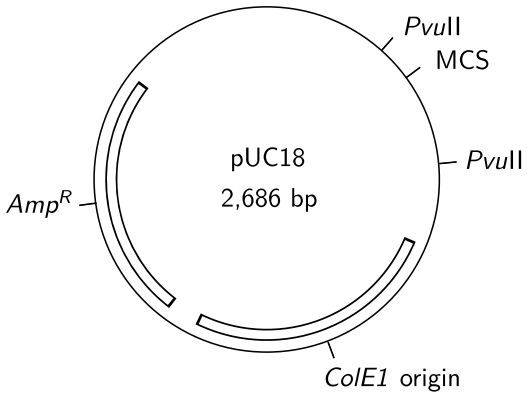

Figure 2.2: Vector map of pUC18. Relevant features are shown, comprising an ampicillin resistance cassette (Amp^R), a *ColE1* replication origin and the multiple cloning site (MCS) which is flanked by *Pvu*II cleavage sites.

Table 2.14: Plasmids for the construction of a genome integration cassette. The cloning strategy and plasmid maps are illustrated in Figure B.3 (Appendix B.3).

Vector name	Relevant characteristics	Reference
pTYR1	Like pUC18, 1,872-bp *TYR1* fragment (chromosome II region 571,506–569,636 including *YBR166C*)	This work
pTT	Derived from pTYR1, *tyr1*Δ::*TRP1*+MCS (838-bp fragment)	This work
pTT–GAP1	Like pTT, P_{GAP1}, *TurboGFP*, T_{CYC1}	This work

2.3 Microorganisms

2.3.1 *Escherichia* (*E.*) *coli*

E. coli strain TOP10F' (Invitrogen GmbH; Darmstadt, Germany) was employed for standard cloning procedures and propagation of plasmid vectors (Tab. 2.15).

Table 2.15: Genotype of *E. coli* strain TOP10F'

Strain	Genotype	Reference
TOP10F'	*F'* [$lacI^q$ *Tn10*(Tet^R)] *mcrA* Δ(*mrr–hsdRMS–mcrBC*) *φ80lacZ*Δ*M15* Δ*lacX74 deoR nupG recA*1 *ara*D139 Δ(*ara leu*)*7697 galU galK rpsL*(Str^R) *endA1* λ^-	Invitrogen GmbH (Darmstadt, Germany)

2.3.2 *Saccharomyces* (*S.*) *cerevisiae*

S. cerevisiae strains used in this work are listed in Table 2.16.

Table 2.16: Genotypes of *S. cerevisiae* strains

Strain	Genotype	Reference
BY4741	*MAT***a**, *his3*Δ*1*, *leu2*Δ*0*, *met15*Δ*0*, *ura3*Δ*0*	EUROSCARF (Frankfurt, Germany)
BY4741 *bar1*Δ	Like BY4741, *bar1*Δ::*kanMX4*	EUROSCARF (Frankfurt, Germany)
BY4742	*MAT*α, *his3*Δ*1*, *leu2*Δ*0*, *lys2*Δ*0*, *ura3*Δ*0*	EUROSCARF (Frankfurt, Germany)
BY4742 *mat*αΔ	Like BY4742, *mf*α*1*Δ::*natMX6*, *mf*α*2*Δ::*hphMX6*	This work
BY4742 *mat*αΔ *bar1*Δ	*mat*αΔ, *his3*Δ*1*, *leu2*Δ*0*, *met15*Δ*0*, *ura3*Δ*0*, *mf*α*1*Δ::*natMX6*, *mf*α*2*Δ::*hphMX6*, *bar1*Δ::*kanMX4*	This work
W303–1A	*MAT***a**, *leu2–3,112*, *ura3–1*, *trp1–1*, *his3–11,15*, *ade2–1*, *can1–100*	Thomas and Rothstein (1989)
W303–1A GAP1	Like W303–1A, *tyr1*Δ::*TRP1*+P_{GAP1}–*TurboGFP*–T_{CYC1}	This work

2.4 Cultivation and storage of microorganisms

2.4.1 Cultivation of *E. coli*

Routine growth of *E. coli* cells was carried out in LB-Miller medium with required antibiotics at 37°C and constant shaking (180 rpm). After transformation of *E. coli* with plasmid DNA, cells were cultivated first in SOC medium at 37°C without shaking for 1 h. Subsequently, cells were plated onto solid LB-Miller medium with ampicillin and incubated at 37°C for 16 h.

LB-Miller medium	10 g l^{-1} Tryptone
	5 g l^{-1} Yeast extract
	10 g l^{-1} NaCl
	15 g l^{-1} Agar (solid medium only)
Antibiotics	100/150 μg ml^{-1} Ampicillin
Liquid/solid medium	30/50 μg ml^{-1} Streptomycin
SOC medium	20 g l^{-1} Tryptone
	5 g l^{-1} Yeast extract
	10 mmol l^{-1} NaCl
	2.5 mmol l^{-1} KCl
	10 mmol l^{-1} $MgCl_2$
	10 mmol l^{-1} $MgSO_4$
	20 mmol l^{-1} Glucose

2.4.2 Cultivation of *S. cerevisiae*

Cultivation of *S. cerevisiae* was performed at 30°C and constant shaking (180 rpm) for liquid cultures. YPD was used for routine growth of untransformed yeast cells.

YPD medium	20 g l^{-1} Tryptone
	10 g l^{-1} Yeast extract
	20 g l^{-1} Glucose
	20 g l^{-1} Agar (solid medium only)

Meiosis and formation of spores was induced by starvation of diploid cells for nitrogen and carbon. The sporulation process was performed in liquid sporulation medium.

Sporulation medium	10 g l^{-1} Potassium acetate
	1 g l^{-1} Yeast extract
	0.5 g l^{-1} Glucose

Transformants were cultivated in synthetic minimal medium with glucose (SD medium), mineral medium (MM) or a nutrient limitation medium (N-lim, P-lim or S-lim), each supplemented with required amino acids and nucleobases for growth of auxotrophic yeast strains.

SD medium	1.7 g l^{-1} Yeast nitrogen base w/o amino acids
	5 g l^{-1} $(NH_4)_2SO_4$
	20 g l^{-1} Glucose
	20 g l^{-1} Agar (solid medium only)
Constituents	20 mg l^{-1} Adenine sulphate
	60 mg l^{-1} L-Histidine
	80 mg l^{-1} L-Leucine
	30 mg l^{-1} L-Lysine
	20 mg l^{-1} L-Methionine
	20 mg l^{-1} L-Tryptophan
	30 mg l^{-1} L-Tyrosine
	20 mg l^{-1} Uracil

The defined mineral medium composition was based on the formulation by Verduyn et al. (1992). Composition of nutrient limitation media was based on formulations by Boer et al. (2003) with few changes. Glucose levels were adapted[1] to standard levels used in SD and YPD media for batch cultivation. Respective concentrations of the limiting macronutrient were lowered since original concentrations for chemostat cultivation yielded poor response of sensor cells during batch cultivation. The magnitude of change and final concentrations were in line with that in other reported nutrient-limited batch cultivation experiments (Klosinska et al., 2011; Saldanha et al., 2004).

Mineral medium (MM) adapted from Verduyn et al. (1992)	Macronutrients	30 g l^{-1} Glucose
		5 g l^{-1} $(NH_4)_2SO_4$
		1 g l^{-1} KH_2PO_4
		0.5 g l^{-1} $MgSO_4 \cdot 7\ H_2O$
	Trace minerals	15 mg l^{-1} EDTA–Na_2
		4.5 mg l^{-1} $ZnSO_4 \cdot 7\ H_2O$
		0.3 mg l^{-1} $CoCl_2 \cdot 6\ H_2O$
		1 mg l^{-1} $MnCl_2 \cdot 4\ H_2O$
		0.3 mg l^{-1} $CuSO_4 \cdot 5\ H_2O$
		4.5 mg l^{-1} $CaCl_2 \cdot 2\ H_2O$
		3 mg l^{-1} $FeSO_4 \cdot 7\ H_2O$

[1] Glucose concentrations of 3% (w/v) were applied. This yielded higher fluorescence of sensor cells but does not induce osmotic shock in yeast.

	0.4 mg l^{-1} $NaMoO_4 \cdot 2\ H_2O$
	1 mg l^{-1} H_3BO_3
	0.1 mg l^{-1} KI
Vitamins	0.05 mg l^{-1} Biotin
	1 mg l^{-1} Calcium pantothenate
	1 mg l^{-1} Nicotinic acid
	25 mg l^{-1} Inositol
	1 mg l^{-1} Thiamine HCl
	1 mg l^{-1} Pyridoxine HCl
	0.2 mg l^{-1} *p*-Aminobenzoic acid

Macronutrient formulations of nutrient limitation media (adapted from Boer et al., 2003) were as follows.

Nitrogen limitation medium (N-lim)	30 g l^{-1} Glucose
	50 mg l^{-1} $(NH_4)_2SO_4$
	5.3 g l^{-1} K_2SO_4
	1 g l^{-1} KH_2PO_4
	0.5 g l^{-1} $MgSO_4 \cdot 7\ H_2O$
Phosphorus limitation medium (P-lim)	30 g l^{-1} Glucose
	5 g l^{-1} $(NH_4)_2SO_4$
	10 mg l^{-1} KH_2PO_4
	0.5 g l^{-1} $MgSO_4 \cdot 7\ H_2O$
Sulphur limitation medium (S-lim)	30 g l^{-1} Glucose
	5 mg l^{-1} $(NH_4)_2SO_4$
	1 g l^{-1} KH_2PO_4
	4 g l^{-1} NH_4Cl
	0.4 g l^{-1} $MgCl_2$

In few experiments, recombinant yeast nutrient sensor cells were cultivated in microalgae media. Their formulations are listed in Appendix C.3. Three percent (w/v) glucose and required constituents (amino acids, nucleobases) were added.

2.4.3 Storage of microorganisms

Bacterial and yeast cells were stored on solid medium at 4°C for 4 weeks in maximum before being replica-plated onto fresh medium. For long-term storage, glycerol stocks were prepared. Cells from 2 ml stationary liquid culture were harvested by centrifugation (3500×g, RT, 5 min). The supernatant was removed and the cell pellet was resuspended

in fresh medium with all required additives and 40% (v/v) glycerol. This mixture was incubated at RT for 30 min to guarantee equilibration of cells to the glycerol. Then, vials were stored at –70°C.

2.5 Molecular cloning

2.5.1 Isolation of plasmid DNA from bacterial cells

Standard preparation of plasmid DNA from *E. coli* was based on the method by Birnboim and Doly (1979). Cells from 2 ml stationary *E. coli* culture were collected by centrifugation at 12,000×g and 4°C for 1 min. The supernatant was discarded and the cell pellet was resuspended in 100 μl Doly solution I. A volume of 200 μl Doly solution II was added, followed by gentle mixing and addition of 150 μl Doly solution III. The mixture was centrifuged at 12,000×g and 4°C for 10 min to precipitate cell debris and chromosomal DNA. The supernatant was transferred to a new reaction tube. To remove proteins, 120 μl of phenol:chloroform:isoamyl alcohol (25:24:1 (v/v/v)) was added. The phases were mixed properly by vortexing for 20 s and separated again by centrifugation at 3,500×g and RT for 5 min. The upper, aqueous phase was carefully transferred into a new reaction tube and mixed with the same volume of absolute 2-propanol. Nucleic acids were precipitated by centrifugation at 12,000×g and 4°C for 15 min. The pellet was carefully washed with 400 μl of ice-cold absolute ethanol, dried at RT and solved in 50 μl TE/RNase buffer. For RNA degradation, isolated plasmid DNA was incubated at 37°C for 30 min prior to restriction, transformation or storage at –20°C.

Isolation of ultra-pure plasmid DNA from *E. coli* for sequencing was performed using the Invisorb Spin Plasmid Mini *Two*-kit (STRATEC Molecular GmbH; Berlin, Germany) following the manufacturer's instructions.

Doly solution I	50 mmol l^{-1} Glucose 20 mmol l^{-1} Tris base 10 mmol l^{-1} EDTA–Na_2 pH 8.0
Doly solution II	10 g l^{-1} SDS 0.2 mol l^{-1}NaOH
Doly solution III	5 mol l^{-1} Potassium acetate pH 5.2
TE/RNase	10 mmol l^{-1} Tris base 1 mmol l^{-1} EDTA 20 mg l^{-1} RNase A[2] pH 8.0

2.5.2 Isolation of genomic DNA from yeast cells

DNA of *S. cerevisiae* was isolated according to the method by Hoffman and Winston (1987). Yeast cells from 5 ml stationary YPD cultures were harvested by centrifugation at 3,500×g and RT for 5 min. The pellet was washed once with 1 ml sterile water and resuspended in 500 μl yeast lysis buffer. An equal volume of acid-washed glass beads was added and the mixture was shaken for 5 min in a cell disrupter with a frequency of 30 s^{-1}. The liquid phase was recovered, mixed with 275 μl of 7 mol l^{-1} ammonium acetate (pH 7.0) and incubated at 65°C for 5 min. After chilling for another 5 min on ice, 500 μl chloroform were added. The phases were properly mixed for 30 s by vortexing and separated again by centrifugation. The upper aqueous phase was transferred into a new reaction tube. The DNA was precipitated by addition of 1 ml absolute 2-propanol, incubated for 5 min at RT and subsequently centrifuged at 14,000×g and 4°C for 15 min. The DNA pellet was washed with 70% (v/v) ethanol, air-dried and dissolved in 200 μl sterile water.

Yeast lysis buffer	100 mmol l^{-1} Tris–HCl (pH 8.0)
	50 mmol l^{-1} EDTA–Na_2
	10 g l^{-1} SDS

2.5.3 DNA amplification

For PCR amplification of DNA fragments targeted for cloning, DNA polymerases with proofreading activity were used in 50 μl reactions. Routine PCR was carried out with 1 unit DyNAzyme EXT DNA Polymerase and 2 mmol l^{-1} $MgCl_2$ in the final reaction volume. GC-rich templates were amplified with 1 unit Phusion High-Fidelity DNA Polymerase, the provided GC buffer and 3% (v/v) DMSO in the final reaction volume. Template DNA concentration per reaction was about 10 ng for plasmids or 100 ng for genomic DNA. All required ingredients were mixed on ice in a 200 μl reaction tube according to the pipetting instructions of the DNA polymerase supplier. The composition of a typical PCR mixture is given in Table 2.17. Amplification according to the supplier's cycling instructions featured either 30 cycles with the same temperature during the annealing step or sequentially 10 cycles with a lower and 20 cycles with a higher annealing temperature (Tab. 2.18). The latter strategy was used to meet the needs of elevating melting temperatures of primers with restriction-site overhangs. Annealing temperatures were determined using the Finnzymes Tm calculator (Tab. 2.24).

Diagnostic check-PCR was performed in a 20 μl reaction volume with 1 unit *Taq* DNA Polymerase. Other ingredients and the cycling procedure were applied accordingly to instructions for DyNAzyme EXT DNA Polymerase.

[2] Final concentration is given. It is important to boil RNase A stock solution (10 mg ml^{-1}) prior to use.

Table 2.17: Composition of PCR mixtures. DNA polymerases were applied in an appropriate buffer and with further additives if required. The amount of used DNA template depended on its complexity. Typically, 10 ng were used for plasmid DNA (low complexity) and 100 ng for genomic DNA (high complexity). Standard PCR was carried out in 50 μl reaction volumes. For diagnostic check-PCR, the volume of all ingredients was scaled down to 20 μl reactions.

Component	**Final concentration/amount**
ddH_2O	add to 50 μl (20 μl)
DNA polymerase buffer	1×
$MgCl_2$	1.5–2 mmol l^{-1}
dNTPs	0.2 mmol l^{-1}
Forward primer	0.5 μmol l^{-1}
Reverse primer	0.5 μmol l^{-1}
Template DNA	10–100 ng
DMSO (optional)	(3% (v/v))
DNA polymerase	1 unit

Table 2.18: Cycling procedure for PCR amplification of DNA fragments. For each cycle step, temperature and duration are listed. Parameters for denaturation and extension steps depend on polymerase and template properties (see instructions of supplier). T_{A1} and T_{A2} are different annealing temperatures. Alternatively, 30 cycles with the same annealing temperatures were carried out.

Cycle step	**Temperature**	**Time**	**Cycles**
Initial denaturation	94/98°C	0.5–2 min	1
Denaturation	94/98°C	10–30 s	
Annealing	T_{A1}	15–30 s	10
Extension	72°C	0.5–1 min kb^{-1}	
Denaturation	94/98°C	10–30 s	
Annealing	T_{A2}	15–30 s	20
Extension	72°C	0.5–1 min kb^{-1}	
Final extension	72°C	10 min	1
	10°C	Hold	

2.5.4 DNA quantification

DNA concentration/purity for sequencing or PCR reactions was determined with a NanoDrop ND-1000 Spectrophotometer using the 'Nucleic Acid' application mode. For ligation reactions, the DNA concentration was estimated via agarose gel electrophoresis by comparing the signal intensity of DNA samples with that of Lambda (λ) DNA/*Pst*I Marker.

2.5.5 DNA cleavage

Up to 1 μg of DNA was cleaved in a 50 μl reaction volume with 10 units restriction endonuclease(s). For simultaneous digestion with two restriction enzymes, the buffer with maximum activity for both enzymes was used. If activity of one enzyme was below 75% in the selected buffer, restriction was carried out sequentially with an intermediate purification step (Section 2.5.8). Five microlitres of 10× reaction buffer and, if necessary, BSA to a final concentration of 0.1 mg ml^{-1} was added to DNA. The restriction enzyme was the last component added. The reaction was incubated at the recommended temperature (usually 37°C) for 3 h. Finally, restriction endonucleases were heat-inactivated if possible (usually at 65°C for 20 min) and DNA was purified (Section 2.5.8) for further processing.

2.5.6 Vector dephosphorylation

After cleavage of vector DNA with a restriction endonuclease producing blunt ends, it was dephosphorylated with Antarctic Phosphatase according to the supplier's instructions prior to purification (Section 2.5.8) for further processing.

2.5.7 Agarose gel electrophoresis

DNA fragments were separated by agarose gel electrophoresis. TBE buffer containing 1% (w/v) agarose was boiled until completely melted. Before solidification, 10 μl of 4,000× RedSafe DNA staining solution per 40 ml gel solution was added and quickly poured into a casting tray containing a sample comb. The solidified gel was placed into a horizontal electrophoresis chamber and just covered with TBE buffer. Samples containing DNA mixed with 1× DNA loading buffer were pipetted into sample wells. Another well was filled with 500 ng DNA size marker to estimate length and concentration of DNA samples. Fragments were separated at a current of 8 V cm^{-1} until the bromophenol blue dye has migrated to the endmost quarter of the gel. DNA was visualised on a UV Transilluminator at a wavelength of 365 nm. If required, fragments were excised using a sterile scalpel and purified (Section 2.5.8) for further processing.

TBE buffer	108 g l^{-1} Tris base
	55 g l^{-1} Boric acid
	7.5 g l^{-1} EDTA–Na_2
DNA loading buffer (6×)	3.3 ml Glycerol
	25 mg Bromophenol blue
	ddH_2O to 10 ml

2.5.8 DNA purification

To purify DNA after PCR amplification and cleavage with restriction enzymes or to extract fragments from agarose slices, the Invisorb Fragment CleanUp-kit (STRATEC Molecular GmbH; Berlin, Germany) was used according to the manufacturer's instructions except for the elution step. Depending on the desired concentration, DNA was eluted with 20–50 μl double-distilled water.

2.5.9 DNA ligation

For ligation of cohesive ends, linearised vector was mixed with a threefold molar excess of insert to total amount of about 400 ng. For ligation of blunt ends, 0.5 μl of 50% (w/v) polyethylene glycol 4,000 was added. The volume was adjusted to 20 μl with double-distilled water containing 1× concentrated ligase reaction buffer and 10 units of corresponding T4 DNA Ligase in the total volume. The reaction was carefully mixed and incubated overnight at 16°C. T4 DNA Ligase was heat-inactivated at 70°C for 10 min.

2.5.10 Bacterial transformation with plasmid DNA

Preparation of cells for electroporation

A fresh colony of the *E. coli* host strain (Tab. 2.15) was grown to stationary phase in 10 ml LB-Miller medium with streptomycin. Five millilitres of this cell suspension were added to 500 ml fresh LB-Miller medium without antibiotics. Cells were grown to an OD_{600} of 0.6–0.8 and chilled on ice for 30 min. The cells were harvested by centrifugation (3,500×g, 4°C, 15 min) and washed twice with 100 ml cold distilled water and once with 10% (v/v) cold glycerol. Each washing step was followed by centrifugation and discard of the wash. Finally, the pellet was carefully resuspended in 10% (v/v) glycerol to a final volume of 3–4 ml. Aliquots of 40 μl were submerged in liquid nitrogen and stored until use at –70°C (for up to 6 months).

Drop dialysis

To remove excess salts from ligation reactions before transformation, DNA solution was placed onto a Millipore 'V'-series membrane and dialysed for 45 min against double-distilled water.

Electroporation

E. coli cells were transformed with plasmid DNA by electroporation. An aliquot of electrocompetent cells was thawed on ice and mixed with 0.1–1 μg DNA targeted for transformation. The mixture was pipetted into a pre-cooled electroporation cuvette and a short pulse (25 μF, 200 Ω, 2.5 kV) was applied. Then cells were immediately transferred to 1 ml sterile SOC medium and incubated at 37°C without shaking for 1 h. Two different concentrations (usually 10 μl and 100 μl) were spread on LB-Miller medium with ampicillin. Transformants were obtained after 16 h incubation at 37°C.

2.5.11 DNA sequencing

Ultra-pure plasmid DNA (Section 2.5.1) and sequencing primers (Tab. 2.9, Section 2.2.6) were mixed for standard sequencing ('Value Read Tube') at Eurofins MWG Operon (Ebersberg, Germany) following the service's instructions.

2.5.12 Yeast transformation

Yeast transformation with plasmid DNA

A rapid method adapted from Gietz and Woods (2002) was employed to transform *S. cerevisiae* with plasmid DNA. A single colony of the strain targeted for transformation was grown in 10 ml YPD medium to stationary phase. Per transformation, cells from 2 ml suspension were harvested by centrifugation (3,500×g, RT, 5 min), resuspended in 1 ml double-distilled water and centrifuged again. Sequentially, 10 μl carrier DNA, 1 μg plasmid DNA in a total volume of 10 μl and 500 μl PEG/lithium acetate solution were added and carefully mixed by pipetting. The mixture was incubated without shaking at 30°C for 30 min and then heat-shocked at 42°C for another 15 min. Cells were spun down, resuspended in 200 μl distilled water and spread on selective SD minimal medium. Transformants were obtained after 3 days of incubation at 30°C and replica-plated on fresh medium for further use or storage.

In order to generate dual-colour yeast strains, cells were sequentially transformed with plasmid DNA. For the second transformation step, cells were grown in SD medium with required amino acids/nucleobases instead of YPD.

PEG/lithium acetate solution	40% (w/v) Polyethylene glycol 4,000 100 mmol l^{-1} Lithium acetate 10 mmol l^{-1} Tris–HCl (pH 7.5) 1 mmol l^{-1} EDTA (pH 8.0)
Carrier DNA	10 mg ml^{-1} Herring sperm DNA boiled for 10 min, then chilled on ice

Yeast transformation for genomic integration

A DMSO-enhanced transformation method (Bähler et al., 1998) was used for transformation of *S. cerevisiae* with DNA fragments for genomic integration by an one-step gene replacement strategy. A stationary YPD culture of cells targeted for transformation was used to inoculate 60 ml fresh YPD medium with an OD_{600} of 0.5 and grown to an OD_{600} of 2. Per transformation, cells from 10 ml suspension were collected by centrifugation (3,500×g, RT, 5 min). The pellet was washed once with 1 ml double-distilled water and once with 1 ml 100 mmol l^{-1} lithium acetate. After discarding the second wash, cells were resuspended in another 50 μl lithium acetate and carefully mixed with 10 μl carrier DNA, 5 μg of DNA targeted for transformation and 300 μl PEG/lithium acetate solution by pipetting (for solutions see previous paragraph). The mixture was incubated without shaking at 30°C for 60 min before 43 μl DMSO was added. The contents were mixed by inverting the tube and then heat-shocked at 42°C for 15 min. Cells were collected by centrifugation (12,000×g, RT, 10 s), washed with 1 ml double-distilled water and resuspended in 3 ml YPD medium for another 3-h incubation step at 30°C. Finally, cells were harvested by centrifugation (3,500×g, RT, 5 min), and spread on the desired selective medium. In case of transformation with antibiotic resistance cassettes, YPD medium was supplemented with 100 μg ml^{-1} nourseothricin or 400 μg ml^{-1} hygromycin B, dependent upon the given resistance cassette inserted. Transformants were obtained after 3 days of incubation at 30°C and replica-plated on fresh medium for further analysis.

2.5.13 Generation of a BY4742 *mat*$\alpha\Delta$ *bar1*Δ double deletion strain

Generation of diploids

Diploids were constructed by patch mating. To this end, freshly grown colonies of both haploid parents, BY4741 *bar1*Δ and BY4742 *mat*$\alpha\Delta$, were mixed in 40 μl YPD medium and pipetted onto solid YPD medium containing 1 μmol l^{-1} synthetic α-factor. Mating was allowed to proceed for 16 h before spreading the mating mixture onto selective minimal medium supplemented with histidine, leucine and uracil to select for the diploid genotype. Diploids were obtained after 48 h of incubation at 30°C.

Sporulation and tetrad dissection

A single colony of diploid clones was grown in 10 ml sporulation medium with all required amino acids and uracil at 30°C. The occurrence of tetrads was verified under a transmission light microscope at a magnification of 400×. Cells from 100 μl sporulation medium were harvested by centrifugation (10,000×g, RT, 10 s), yielding a barely visible pellet (diameter of about 1.5 mm). Cells were washed once with double-distilled water, spun down again and resuspended in 20 μl zymolyase solution. The mixture was incubated at 30°C for 10 min, gently mixed with 200 μl double-distilled water and placed on ice. Approximately 30 tetrads were dissected under a MSM System dissecting microscope (Singer Instrument Co. Ltd.; Somerset, United Kingdom). For this purpose, respectively 15 μl of the zymolyase-treated suspension was spread in a line on one side of a YPD plate and let to soak in prior to mounting on the microscope. Completed plates with dissected tetrads were incubated overnight at 30°C. The line of zymolyase-treated cells was removed using a sterile scalpel and plates were incubated for another 3 days to obtain outgrown haploids from individual spores.

Zymolyase solution	0.5 mg ml^{-1} Zymolyase T20
	1 mol l^{-1} Sorbitol

Tetrad analysis

Colonies from outgrown tetrads were replica-plated onto YPD plates with either 100 μg ml^{-1} nourseothricin, 400 μg ml^{-1} hygromycin B, or 500 μg ml^{-1} G418 in order to identify haploids featuring resistance to all three antibiotics and, therefore, deletion of all designated loci. The mating type of such clones was determined indirectly by exposing haploids to 1 μmol l^{-1} synthetic α-factor for 4 h followed by microscopic examination.[3] Clones displaying no mating projections were supposed to be desired BY4742 *mat*$\alpha\Delta$ *bar1*Δ cells. Finally, nutritional requirements were tested by replica-plating cells on selective minimal medium with all drop-out conditions for relevant amino acids/uracil.

2.6 Preparation of yeast cells for assays or before immobilisation procedures

For growth and fluorescence analysis experiments or before immobilisation of yeast cells, five single colonies from an agar plate were transferred to 10 ml SD medium or mineral medium with required supplements and allowed to grow at 30°C under constant shaking for 16 h. For cell growth under nutrient limitation previous to an assay, cells were first

[3] Typically, the progeny of an ascus was analysed completely in order to confirm that precisely two haploids (the **a** cell progeny) display mating projections.

grown in mineral medium as described, then washed with 5 ml of the respective nutrient limitation medium and subsequently cultivated in 20 ml limitation medium for another 20 h. The OD_{600} of the cell suspension was determined in a UV/VIS spectrophotometer (typically using a 1:10 dilution) and a culture volume equivalent to the desired cell density was centrifuged (3,500×g, RT, 5 min). As an example, to inoculate 20 ml medium for an assay with cells to an OD_{600} of 0.5, 10 OD units (equals 10 ml culture with an OD_{600} of 1 and about 10^7 cells ml^{-1}) were prepared. The cell pellet was washed with 1 ml sterile water, spun down again and finally resuspended in fresh medium for an assay or for immobilisation. Batch cultures for fluorescence analysis assays were typically started with an OD_{600} of 0.5 in a volume of 20 ml. For experiments with cells of a cellular communication and signal amplification system, 20 ml cultures with an initial OD_{600} of 1 were used.

2.7 Growth analysis by nephelometry

Growth of yeast sensor cells in microalgae media and supernatants was monitored in 96-well microplates. As described in Section 2.6, cells were grown in mineral medium, washed and adjusted to an OD_{600} of 0.5 with respective media for the growth analysis. Per medium, 3 compartments of a transparent 96-well microplate were filled with 200 μl cell suspension. The microplate was sealed with a gas-permeable sealing film and incubated in a BMG microplate nephelometer at 30°C under orbital shaking (140 rpm). Scattered light was monitored in 30-min intervals using the settings listed in Table 2.19.

Table 2.19: Performance values of nephelometry

Parameter/setting	Specification/value
Light source	Laser diode, 1 mW
Wavelength/bandwidth	635/10 nm
Laser beam width	2 mm
Gain	80
Measurement time per well	0.1 s
Position delay	0.2 s

2.8 Fluorescence assays with batch-cultivated cells

2.8.1 Microplate reader-based fluorometry

Twenty millilitres medium with required additives were inoculated with washed yeast cells to the desired density ($OD_{600} = 0.5$ or 1, see Section 2.6). Samples (2–4 ml) were harvested at indicated time points, washed once with double-distilled water and adjusted to an

OD_{600} of 1. Three aliquots of 100 μl were pipetted into a black 96-well plate. Fluorescence was determined as arbitrary units (A. U.) using a TECAN Infinite M200 microplate reader with the parameters and settings listed in Table 2.20. Excitation/emission wavelength and the gain depended on the fluorophore to be detected but were kept constant during one experiment.

Table 2.20: Performance values of microplate reader-based fluorometry. Wavelength for excitation/emission and gain depended on the fluorophore targeted for detection. Due to excitation/emission bandwidth, applied values were set at least 30 nm apart from each other. Typical measurements for GFP fluorophores were performed with excitation/emission at 490/520 nm and a gain of 100.

Parameter/setting	**Specification**
Light source	UV xenon flash lamp
Excitation wavelength/bandwidth	434–555/9 nm
Emission wavelength/bandwidth	485–585/20 nm
Gain	Manual, 80–203
Number of reads per well	50
Integration time	40 μs
Multiple reads per well (MRW)	Enabled, 2×2 alignment
MRW border function	Enabled, 1,000 μm distance

2.8.2 Western blot analysis

Sample preparation

One millilitre-aliquots from samples of microplate reader-based assays with an OD_{600} of 1 (Section 2.8.1) were concentrated by centrifugation (3,500×g, 4°C, 5 min) and adjusted to a final volume of 24 μl containing 1× concentrated protein sample buffer. Cells were disintegrated by boiling for 5 min. Samples were stored one ice before separation by electrophoresis.

Protein sample buffer	125 mmol l^{-1} Tris–HCl (pH 6.8)
(2×)	20% (v/v) Glycerol
	4% (w/v) SDS
	0.04% (w/v) Bromophenol blue
	200 mmol l^{-1} DTT

Separation by electrophoresis

Proteins of disintegrated cells were separated by SDS-PAGE in a discontinuous buffer system based on the procedure by Laemmli (1970). A vertical sandwich cassette (glass plates and 0.8 mm spacers) was assembled. Enough resolving gel solution to fill the

sandwich cassette completely and 1/3 that volume of stacking gel solution were prepared on ice. The sandwich cassette was filled with resolving gel solution to a level that allows for the insertion of a comb with a 1 cm gap between the bottom of the comb wells and the top of the resolving gel. After 30 min of polymerisation, the cassette's top was filled with stacking gel solution and a comb inserted. The gel was allowed to polymerise at least for another 30 min. Samples (see previous paragraph) and 5 μl PageRuler Plus Prestained Protein Ladder were loaded onto the gel and separated by electrophoresis in a vertical electrophoresis system filled with running buffer. The current was set to 30 mA per gel and a maximum voltage of 120 V was applied.

Resolving gel solution	15% (v/v) Acrylamide/Bis solution (37.5:1) 375 mmol l^{-1} Tris–HCl (pH 8.8) 0.1% (w/v) SDS 0.05% (w/v) Ammonium persulphate 0.005% (v/v) TEMED
Stacking gel solution	4% (v/v) Acrylamide/Bis solution (37.5:1) 125 mmol l^{-1} Tris–HCl (pH 6.8) 0.1% (w/v) SDS 0.05% (w/v) Ammonium persulphate 0.01% (v/v) TEMED
Running buffer	25 mmol l^{-1} Tris base 192 mmol l^{-1} Glycine 0.1% (w/v) SDS

Electrotransfer (semi-dry blotting)

By electrophoresis separated proteins were transferred from a SDS/polyacrylamid gel onto a PVDF membrane by a semi-dry blotting procedure. One piece of PVDF membrane and 6 sheets of blotting filter paper were cut to the dimension of the gel and equilibrated together with the gel in transfer buffer for 15 min. The transfer stack was assembled according to the 'Instruction Manual PerfectBlue Semi-Dry Electro Blotter' (Peqlab, v0211E). The electrotransfer was performed with a current of 1.5 mA cm^{-2} and a maximum voltage of 25 V for 1 h. The membrane was air-dried prior to immunostaining and chemiluminescent detection (see next paragraph).

Transfer buffer	25 mmol l^{-1} Tris base 192 mmol l^{-1} Glycine 20% (v/v) Methanol 0.01% (w/v) SDS

Immunostaining and chemiluminescent detection

After electrotransfer to a PVDF membrane, fluorescent proteins were immunostained with specific antibodies (Tab. 2.2, Section 2.2.1) and detected with a chemiluminescent detection reagent following the instructions of the 'ECL Plus Western Blotting Detection Reagents' product booklet (GE Healthcare Life Sciences, RPN2132PL AE 02-2011). Washing steps were performed in TBS–T. For blocking the membrane and dilution of primary/secondary antibodies, TBS–T was supplemented with 5% (w/v) non-fat dried milk powder. The exposure time of an autoradiography film during chemiluminescent detection depended on the samples and varied between 15 s and 45 min. For samples from one experiment, an identical exposure time was applied.

TBS–T	20 mmol l^{-1} Tris–HCl (pH 7.6)
	137 mmol l^{-1} NaCl
	0.1% (v/v) Tween 20

Protein transfer control

After electrotransfer, SDS/polyacrylamid gels were incubated in Coomassie staining solution for 3 h. To visualise proteins, gels were washed with destaining solution to the desired contrast. Uniform protein transfer on a PVDF membrane was confirmed by staining with Ponceau S. Membranes were incubated in Ponceau S solution for 1 h and subsequently rinsed with distilled water until the desired contrast was achieved.

Coomassie staining solution	40% (v/v) Methanol
	10% (v/v) Acetic acid
	0.1% (w/v) Coomassie brilliant blue R–250
Destaining solution	40% (v/v) Methanol
	10% (v/v) Acetic acid
Ponceau S solution	3% (w/v) Trichloroacetic acid
	0.2% (w/v) Ponceau S

2.8.3 Flow cytometry

Yeast cells from 100 μl samples of batch cultures (Section 2.6) were collected by centrifugation (3,500×g, RT, 5 min) and resuspended in 1.5 ml sheath fluid for flow systems. Flow cytometric analysis was performed in a Partec CyFlow SL system with excitation from an argon ion laser operating at 488 nm and 20 mW. Optical parameters from forward and side scatter channel (FSC, SSC) and green fluorescence channel (FL1, 530/30 nm band pass filter) were collected at a flow rate of 750–1,000 events s^{-1} with

a total accumulation of 40,000 counts per run. The actual settings depended on the physiological conditions of the cells but were kept constant during one experiment. Typical performance values are given in Table 2.21. Raw data were exported from the FloMax software and further processed with R.

Table 2.21: Typical performance values of flow cytometry analyses

Channel	Gain	Log	L–L	U–L
FSC	185	log3	50	999.9
SSC	180	log3	10	999.9
FL1	415	log4	10	999.9

2.8.4 Fluorescence microscopy

For microscopy of yeast cells from batch cultures (Section 2.6), cells from 1 ml samples were washed and concentrated in double-distilled water. Twenty microlitres cell suspension were mixed with an equal volume of 0.5% (w/v) agarose solution equilibrated to 50°C and mounted on a microscopy slide with cover slip. Microscope slides with nano-printed cells were directly covered with a cover slip. For microscopy of yeast cells in calcium-alginate beads, 10 beads were placed into a μ-dish and covered with 1.5 ml agarose solution. Microscopic images were acquired with a Keyence BZ-8100 or Zeiss Axio Imager.1A fluorescence microscope using the objectives and filters for fluorescence detection listed in Table 2.22. When examining samples with the BZ-8100 microscope, ten z-stack images of 0.1 μm (100× objective) or 4 μm (4× objective) distance were taken. Image overlays and z-stack merge were performed with the BZ Analyzer software.

Table 2.22: Objectives and filters for fluorescence microscopy

Parameter	Specification
Keyence BZ-8100	
Objectives	CFI Plan Apochromat 100× (NA1.4 WD0.13 oil immersion)
	CFI Plan Apochromat 4× (NA0.2 WD20)
Filters	GFP BP (Excitation = 472.5/30 nm, Emission = 520/35 nm)
	TxRed (Excitation = 562/40 nm, Emission = 624/40 nm)
Zeiss Axio Imager.1A	
Objective	Epiplan-Neofluar 100× (NA1.3 oil pol WD0.31)
Filter	Fs44 (Excitation = 475/40 nm, Emission = 530/50 nm)

2.9 Software-assisted microscopy image analysis

Green and red fluorescence of dual-colour sensor cells was quantified in microscope images (Section 2.8.4) using the program CellProfiler. The procedure was based on a previously described approach (Jahn, 2011). Briefly, a pipeline of modules was created that allowed for the identification of cells as individual objects by their size, shape and edges in bright field images and subsequent measurement of each object's overall fluorescence intensity in according images taken from green and red fluorescence channels (converted to grey scale). The overall fluorescence intensity of an object was defined as the mean brightness values of all pixels within the object's area. Values ranged from 0 (black, no fluorescence) to 1 (fluorescence saturation).

2.10 Fluorescence assays with immobilised cells

2.10.1 Fluorescence assay with cells in calcium-alginate beads

Harvested and washed cells (Section 2.6) were adjusted to an OD_{600} of 2 in 5 ml medium and mixed with an equal volume of 2% (w/v) sodium-alginate. This mixture was extruded from a syringe with needle into 100 mmol l^{-1} $CaCl_2$ solution. The resulting beads with an average diameter of 3 mm were washed and cured in medium containing 10 mmol l^{-1} $CaCl_2$ for at least 16 h at 4°C. All further steps were performed in medium with 10 mmol l^{-1} $CaCl_2$. For the fluorometry assay, 6 wells of a black 96-well microplate were filled with 10 beads each and covered with 200 μl medium. Microplates were incubated at 30°C without shaking and fluorescence was determined in a TECAN Infinite M200 microplate reader as described in Section 2.8.1.

2.10.2 Fluorescence assay with nano-printed cells

Nano-printing/immobilisation was done at the Institute of Materials Science/TU Dresden. Harvested and washed cells (Section 2.6) were mixed with 4 ml medium containing 1.5% (w/v) sodium-alginate to the desired OD_{600} (≤ 4) and filled into the Delo-Dot dosage head connected to the Nano-Plotter NP2.1 instrument. Under RT with an air humidity over 70%, 7-nl spots were deposited on Fixacol-treated microscope slides in arrays with a dimension of about 5 mm^2. Microscope slides were incubated in 100 mmol l^{-1} $CaCl_2$ solution for 5 min in order to precipitate the alginate and entrap cells within the gel. The microscope slides were stored at 4°C in medium containing 10 mmol l^{-1} $CaCl_2$ for equilibration. For an assay, microscope slides were covered with fresh medium, incubated as described and fluorescence-scanned in face-down position with the Typhoon Trio instrument (Section 2.10.4) at indicated time points. The mean fluorescence intensity of scan images was calculated using the 'Measure' function of ImageJ.

2.10.3 Fluorescence assay with agarose-embedded cells

Yeast cells and/or α-factor were adjusted to the desired density or concentration in pre-warmed SD medium containing 1% agarose (w/v) and filled into $5\times5\times5$ mm^3 cavities in a prepared petri dish with quadratic profile as described previously (Jahn, 2011). Cells were set to an OD_{600} of 0.1–2 and α-factor to a concentration of 0.01–10 μmol l^{-1}. The plates were fluorescence-scanned every two hours with the Typhoon Trio instrument (Section 2.10.4) with interim incubation at 30°C. Fluorescence profiles of compartments filled with pheromone-responsive reporter cells were analysed using the 'Plot Profile' tool of ImageJ.

2.10.4 Fluorescence scanning

Face-down-positioned microscope slides or quadratic petri dishes with immobilised yeast cells (Sections 2.10.2 and 2.10.3) were scanned with the Typhoon Trio instrument using the blue- or green-excited mode for fluorescence scans. Required settings and filters depended on the samples but were kept constant during one experiment. Important parameters and settings are listed in Table 2.23. Acquired raw images were exported from ImageQuant TL for further processing. Fluorescence was quantified with ImageJ.

Table 2.23: Performance values of fluorescence scans with the Typhoon Trio instrument

Parameter/setting	**Specification**
Excitation mode	Solid-state argon ion laser (blue, 488 nm, 20 mW)
	Double frequency SYAG laser (green, 532 nm, 20 mW)
Emission filters	520 BP 40 (for GFP fluorophores)
	580 BP 30 (for RFP fluorophores)
PMT voltage	400–500 V
Spatial resolution	25–100 μm pixel size
Focal plane (optional)	(+3 mm)

2.11 Statistics and reproducibility

All experiments were carried out at least in triplicates to assure reproducibility. For fluorescence quantification experiments, mean values and standard deviation (sd) were calculated and depicted in plots produced with R. For qualitative studies, representative data are shown.

2.12 Software and databases

Table 2.24: Software and databases. URLs were last accessed on 28 September 2011.

Name	Application	Reference
ApE (v 1.17)	Plasmid/vector maps, *in silico* DNA manipulation, sequence alignments	`http://biologylabs.utah.edu/jorgensen/wayned/ape/`
BLAST (v 2.2.25)	Sequence alignments (blastn)	`http://www.ncbi.nlm.nih.gov/blast/Blast.cgi?CMD=Web&PAGE_TYPE=BlastHome`
BZ Analyzer (v 2.5)	Microscope image overlays, *z*-stack merge	Keyence Deutschland GmbH (Neu-Isenburg, Germany)
CellProfiler (v 2.0)	Automated cell recognition, fluorescence intensity calculation in microscope images	Carpenter et al. (2006)
ExPASy – Compute pI/Mw tool	Estimation of the size (i.e. molecular mass) of proteins	`http://web.expasy.org/compute_pi/`
Finnzymes Tm calculator	Determination of annealing temperature for PCR reactions	`https://www.finnzymes.fi/tm_determination.html`
FloMax (v 2.4)	Flow cytometer instrument control, data acquisition	Partec GmbH (Münster, Germany)
i-Control (v 1.1)	Microplate reader instrument control, data acquisition	TECAN Group Ltd. (Männedorf, Switzerland)
ImageJ (v 1.44)	Fluorescence intensity calculation in fluorescence scan images	Girish and Vijayalakshmi (2004)
ImageQuant TL (v 5.2)	Typhoon Trio scan image export	Amersham Biosciences (Freiburg, Germany)
NEPHELOstar-control (v 4.30-0)	Nephelometer instrument control, data acquisition	BMG Labtech GmbH (Ortenberg, Germany)
Primer3 (v 0.4.0)	PCR primer design	`http://frodo.wi.mit.edu/primer3/`
PubMed Central	Literature research	`http://www.ncbi.nlm.nih.gov/pubmed/`
R (v 2.9.2)	Plot artwork	`http://cran.r-project.org/`
Saccharomyces genome database	Gene sequence resources, protein information	`http://www.yeastgenome.org/`
SPELL (v 2.0.2)	Search for expression profiles of query genes in microarray data sets	`http://spell.yeastgenome.org/`

Chapter 3

Results

3.1 Development of fluorescent yeast reporter cells

In this section, requirements for the development of fluorescent *S. cerevisiae* sensor cells with prospective operation in microbial biosensor systems were examined. Generation of convenient fluorescence signal output in respective sensor cells relies on implementation of appropriate fluorescent reporters and an efficient expression strategy.

Enhanced expression of (heterologous) genes in yeast is typically conducted by the use of a strong promoter in conjunction with a multicopy 2μ-based plasmid. Mumberg et al. (1995) created a set of such 2μ-based expression vectors that obtain mitotic stability and can be maintained in yeast cells due to complementation capacity of amino acid or nucleobase auxotrophy.

Selection criteria considering the fluorescent reporter are its spectral properties (i.e. excitation/emission peaks, quantum yield), brightness and protein stability. Accessibility to various qualitative and quantitative analytical methods is important for evaluation of generated yeast sensor strains as well as for implementation of a transducer technology. In this work, the expression of fluorescence reporter genes was monitored both on cell population and single-cell level using diverse qualitative and quantitative detection methods. This included fluorescence microscopy, microplate reader-based fluorometry, flow cytometry and Western blot analysis.

3.1.1 Plasmid-based expression of fluorescence reporter genes

Generation of yeast reporter cells with strong and constitutive expression of fluorescence reporter genes

The ability of *S. cerevisiae* to express a set of nine genes encoding fluorescent proteins from different metazoa was examined. A summary of the fluorescent reporter proteins including important features is presented in Table 2.6. The selected reporter's spectral emission profiles cover almost the entire visible spectrum, i.e. they emit blue (ECFP),

green (GFPuv, EGFP, EGFPpest and TurboGFP), yellow (PhiYFP, TurboYFP) or red (TurboRFP, DsRedT4) light.

Coding sequences of respective fluorescent proteins were cloned into the multiple cloning site of yeast expression vector p426GPD. To this end, PCR-amplified fragments with flanking restriction sites were inserted into the multiple cloning site of the vector. Figure B.1 (Appendix B.1) illustrates the basic map of generated reporter plasmids. Sequence accuracy of inserted fluorescence reporter genes was confirmed by sequencing.

Cells of strain *S. cerevisiae* BY4741 were transformed with respective reporter plasmids. As a control, cells were transformed with p426GPD, the 'parental' vector without an insert. Recombinant yeast reporter cells were grown in selective minimal medium for 24 hours before analysis.

Initially, expression of all nine fluorescence reporters was checked by fluorescence microscopy (Fig. 3.1, upper panels). Equipped with a reporter plasmid, fluorescent cells could be detected for all reporter constructs using the available GFP BP or TxRed filters. Fluorescence was uniformly distributed in respective cells, suggesting cytosolic localisation of the reporter protein. Cells harbouring the parental vector p426GPD emitted no significant fluorescence signal if identical exposure times were applied. It was observed that all yeast reporter strains displayed high cell-to-cell variance regarding brightness. This might be caused by unequal plasmid copy number per cell, loss of plasmid over time or diverse expression capacity of individual cells due to their growth stage. Interestingly, reporter cells displayed best fluorescence signals after they were freshly transformed (data not shown). Moreover, gathered fluorescence signals from different reporter strains varied with regard to the required exposure time for imaging of reporters. Of the four green fluorescence reporters, GFPuv and EGFPpest featured high signal intensity and photo-bleaching stability while EGFP and TurboGFP yielded moderate signals. Surprisingly, GFPuv worked best although excitation was not optimal with the GFP BP filter. GFPuv is an enhanced derivative of AvGFP with improved performance for eukaryotic cells (Crameri et al., 1996). This may account for its excellent brightness despite suboptimal excitation. In contrast, blue fluorescent ECFP was poorly detectable due to inappropriate excitation/emission and its low quantum yield and brightness. Neither the GFP BP nor the TxRed filter were optimal for detection of yellow fluorescence. However, both TurboYFP and PhiYFP reporters were detectable with a similar signal intensity to each other using the GFP BP filter. Regarding the two red fluorescent reporters, signal intensity of TurboRFP was excellent and superior to performance of DsRedT4.

Expression of reporter gene was confirmed on the molecular level by immunodetection. For all reporter proteins except DsRedT4, specific antibodies were available (Tab. 2.2). Signals of expected sizes were detectable in soluble protein fractions of reporter cells but not in cells harbouring the parental vector (Fig. 3.1, bottom panels). The majority

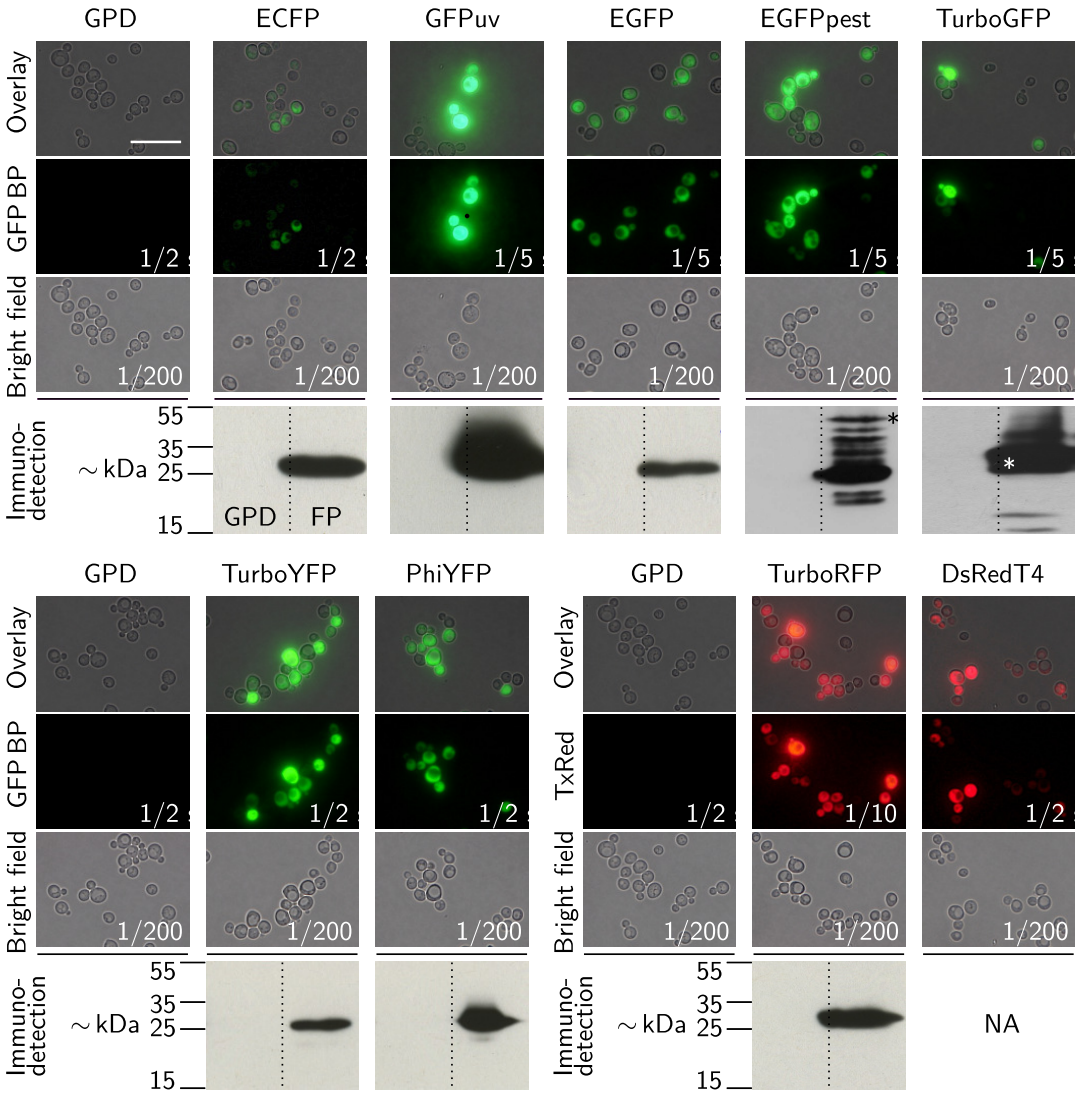

Figure 3.1: Microscopy and Western blot analysis of recombinant *S. cerevisiae* reporter strains with strong and constitutive fluorescence reporter gene expression. Vector p426GPD was exploited for expression of genes encoding blue (ECFP), green (GFPuv, EGFP, EGFPpest, TurboGFP), yellow (TurboYFP, PhiYFP) or red (TurboRFP, DsRedT4) fluorescent proteins in yeast strain BY4741. As a control, yeast cells were transformed with the parental vector (GPD). Cells were monitored using a Keyence BZ-8100 fluorescence microscope with 1,000× magnification, given exposure times in each channel and GFP BP or TxRed filters for fluorescence monitoring. Each vertical microscopic image block shows the overlay (scale bar = 20 μm) and corresponding fluorescence and bright field images. In the bottom row, immunodetection signals from soluble fractions of about 10^7 reporter cells (FP, right) and cells harbouring the parental vector (GPD, left), respectively, are shown. Single immunostained bands were obtained for strains with ECFP (~26.9 kDa), GFPuv (~26.8 kDa), EGFP (~26.9 kDa), TurboYFP (~28.8 kDa), PhiYFP (~28.8 kDa) and TurboRFP (~28.8 kDa). For EGFPpest (~45.8 kDa) and TurboGFP (~25.7 kDa) multiple signals were detected. The band of expected size is marked with an asterisk. All fluorescent proteins unless DsRedT4 were tracked with specific antibodies targeted to the respective reporter (Tab. 2.2). For DsRedT4 no specific antibody was available (NA). Migration positions of reference proteins are given on the left.

of reporter cell lysates displayed a unique band in line with the calculated molecular mass of fluorescent protein monomers. For EGFPpest, a destabilised EGFP variant, additional degradation products were visible. One abundant signal of the size of EGFP was obviously more resistant to proteolysis. Detection of TurboGFP using high antibody concentration yielded multiple signals, but a signal in line with the size of the reporter protein monomer was dominant.

To probe fluorescence of reporter strains quantitatively, yeast cells were prepared for microplate reader-based fluorometry using customised excitation and emission wavelengths and optimal gain adjustment for each fluorescent protein (Fig. 3.2). In line with the microscopy results for green fluorescent reporter strains, brightness of cells with GFPuv or EGFPpest was superior to that of cells with EGFP or TurboGFP. Regarding the signal yield, application of a lower gain was sufficient for an equal output signal in case of GFPuv and EGFPpest. Again, no significant fluorescence signal was detected in control cells harbouring the parental vector. Although optimised excitation and emission wavelengths were applied in ECFP detection, fluorescence was hardly five times higher than in control cells transformed with the parental vector. Additionally, a higher gain was necessary to yield a comparable signal to green fluorescent reporter strains. All strains expressing genes encoding yellow fluorescent proteins TurboYFP and PhiYFP or red fluorescent protein TurboRFP exhibited excellent fluorescence yield. Control cells displayed almost no fluorescence with the applied excitation/emission setup. In agreement with microscopy results, both yellow fluorescent reporter strains yielded a comparable signal output. The red fluorescent reporter strain with DsRedT4 showed weak fluorescence as expected. The signal was significantly below fluorescence of bright yeast cells displaying TurboRFP.

In summary, nine genes encoding GFP-like proteins which emit light in the visible spectrum ranging from cyan to red were successfully expressed in *S. cerevisiae* BY4741. Detection of these reporter proteins is possible *in vivo* using qualitative analysis by microscopy or quantification by microplate reader-based fluorometry. Besides high cell-to-cell variance in expression of a single fluorescence reporter gene, the tested reporters differed in brightness and signal yield. Best results were obtained from GFP variants and TurboRFP. GFPuv exhibited the best signal yield and highest brightness among the green fluorescent markers but has only become available at a later stage of the experimental work. Consequently, the other three GFP variants (EGFP, TurboGFP and EGFPpest) were applied to engineer prototype yeast reporter and sensor cells (Sections 3.2 and 3.3). All three reporter proteins share comparable excitation and emission spectra and can be optimally detected with available analysis methods/instruments. Brightness of TurboRFP was superior to brightness of green fluorescent reporters. In addition, the signal-to-background fluorescence was better. Thus, TurboRFP was considered to be useful in advanced studies such as the development of dual-colour yeast

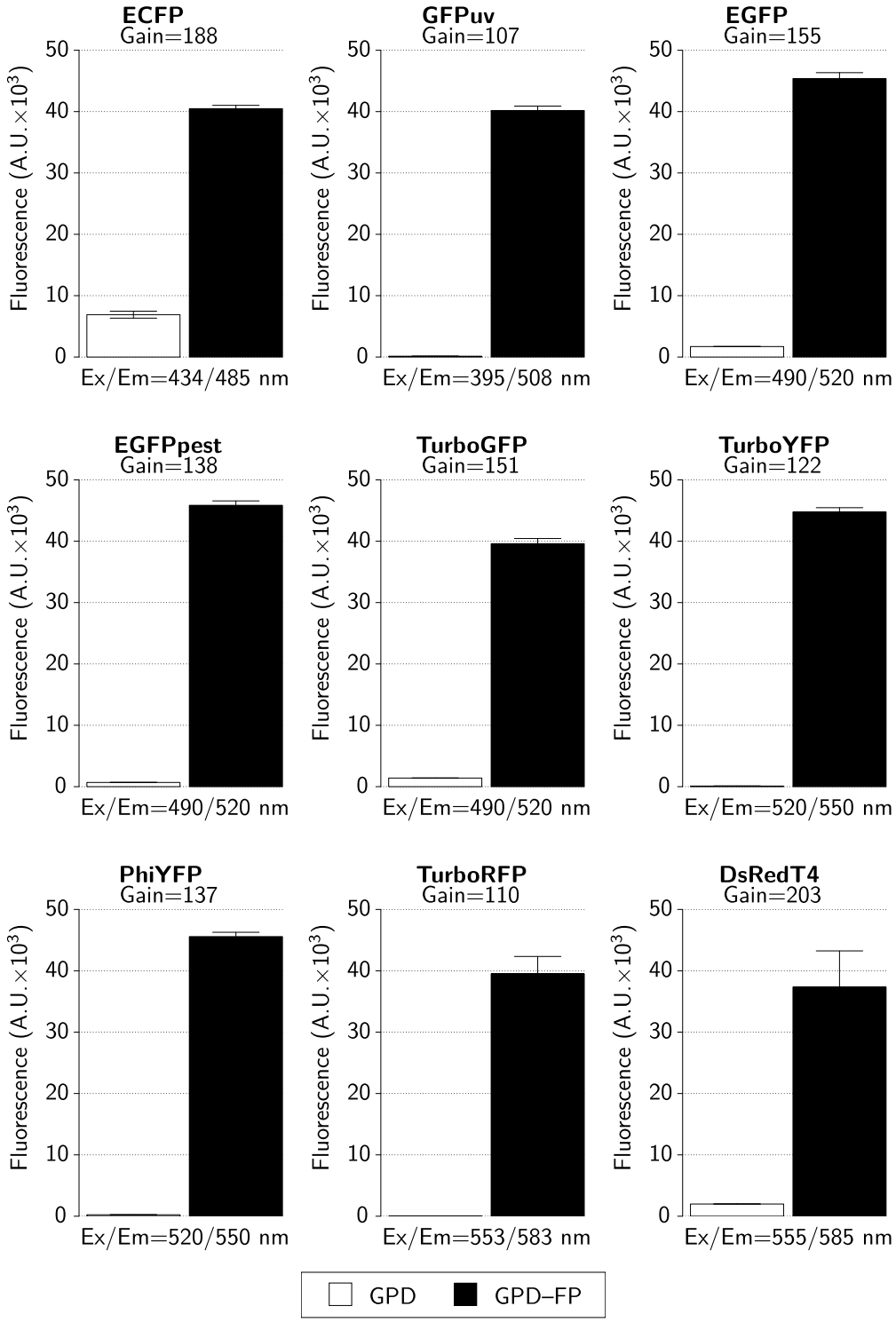

Figure 3.2: Fluorometric analysis of recombinant *S. cerevisiae* reporter strains with strong and constitutive fluorescence reporter gene expression. Vector p426GPD was exploited for expression of genes encoding blue (ECFP), green (GFPuv, EGFP, EGFPpest, TurboGFP), yellow (TurboYFP, PhiYFP) or red (TurboRFP, DsRedT4) fluorescent proteins in yeast strain BY4741 (GPD–FP, black bars). As a control, cells were transformed with the parental vector (GPD, white bars). For each strain, total fluorescence of about 10^6 cells was detected using a TECAN Infinite microplate reader with given excitation/emission wavelength (Ex/Em) and gain. Mean values ± sd of triple measurements are shown.

sensor strains (Section 3.2.10) or experiments aiming at improved signal yield of the cellular communication and signal amplification system (Sections 3.3.4 and 3.3.7) which were also performed at a later stage of this work.

Generation of yeast reporter cells with constitutive expression of fluorescent reporter genes at different levels

Plasmid-based expression of various fluorescence reporter genes from the constitutive *GPD* promoter in *S. cerevisiae* was successfully shown. Green fluorescent reporter strains displayed sufficient signal levels and exhibit optimal accessibility for available detection methods. However, reporter gene expression was solely examined using this strong promoter but putative detection constructs might contain weaker promoters that mediate lower fluorescence. To this end, the expression of green fluorescent marker proteins EGFP and TurboGFP from the constitutive promoters of *GPD* (strong expression level) and *ADH* (intermediate expression level) was compared. Coding sequences of EGFP and TurboGFP were cloned into yeast expression vector p426ADH as described for the set of p426GPD–FP plasmids (see above) and transformed into *S. cerevisiae* strain BY4741. Control cells were transformed with the according parental vector p426ADH.

Recombinant yeast cells were cultivated in selective minimal medium for 24 hours and analysed subsequently by microplate reader-based fluorometry using identical settings for all samples. The result is depicted in Figure 3.3. The fluorescence level of cells expressing reporter genes *EGFP* or *TurboGFP* were comparable if the same promoter was used for expression. For *GPD* promoter-driven expression, fluorescence was approximately 23-fold higher than in control cells harbouring the parental vector. Cells with expression from the moderate *ADH* promoter still displayed fourfold higher fluorescence than respective control cells. This demonstrates that expression of intermediate reporter levels is still detectable *in vivo* by microplate reader-based fluorometry.

Reporter and control strains were also examined on single-cell level (Figs. C.1 and C.2, Appendix C.1). Recombinant cells were grown in selective minimal medium for 20 hours, shifted to fresh medium for four hours and analysed subsequently by flow cytometry. Figure C.1A shows the scatter plot of reporter cells harbouring plasmid p426ADH–TurboGFP. Such a scatter plot was obtained for all strains, irrespective of the particular expression profile. In detail, forward scatter channel and side scatter channel intensities roughly equate particle's size and granular content, respectively, and were in similar linear correlation for all strains. This implied that heterologous gene expression apparently did not affect growth or morphology of reporter cells. Fluorescence histograms of cells with moderate expression of *EGFP* and *TurboGFP* reporter genes from the *ADH* promoter were comparable. They exhibited a similar shape and peak at a value of 200 (Fig. C.1B,C). Curves were clearly distinguishable from the histogram of non-fluorescent control cells harbouring the parental vector (Fig. C.1D). Cells expressing high reporter

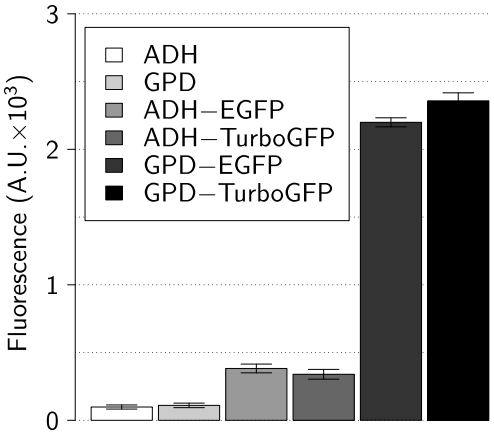

Figure 3.3: Comparison of fluorescence reporter gene expression levels in *S. cerevisiae* BY4741 reporter cells. Yeast expression vectors p426ADH and p426GPD were exploited for constitutive expression of intermediate and high levels, respectively, of *EGFP* and *TurboGFP*. As a control, yeast cells were transformed with the parental vectors (labelled with 'ADH' and 'GPD'). Total fluorescence of about 10^6 cells was determined with a TECAN Infinite microplate reader using excitation/emission wavelength of 490/520 nm and a gain of 100. Mean values ± sd of triple measurements are shown.

levels from the strong GPD promoter displayed higher average fluorescence (Fig. C.2). Again, fluorescence profiles of reporter strains expressing *EGFP* and *TurboGFP* were similar in shape but clearly different from the profile of non-fluorescent cells harbouring the parental vector. The profile resembled a broad plateau with extensive distribution of counted particles around a value of 300. The highest average signal was obtained from GPD–EGFPpest reporter cells. Moreover, the cell population exhibited a bimodal distribution with two peaks at signal intensities of 100 (low fluorescence) and 400 (high fluorescence).

In summary, results of fluorescence analysis on the level of single cells and total cell population were in good agreement regarding tendency of obtained signal patterns.

3.1.2 Time trend analysis of constitutively expressed fluorescence reporter genes

So far, recombinant reporter strains with strong and moderate fluorescence were successfully evaluated whereupon fluorescence was monitored at single time points (endpoint detection). Following experiments were consistently based on batch cultivation of yeast sensor cells and repeated measurements over an average time period of eight hours (Sections 3.2 and 3.3). To test whether fluorescence of reporter strains producing EGFP, EGFPpest or TurboGFP from the *GPD* and *ADH* promoter is constant over an eight-hour interval, fluorescence time trends of reporter cells were probed. Respective reporter cells were grown in selective minimal medium overnight and shifted to fresh medium. Fluorescence was detected after shift by hourly repeated microplate reader-based fluorometry (Fig. 3.4).

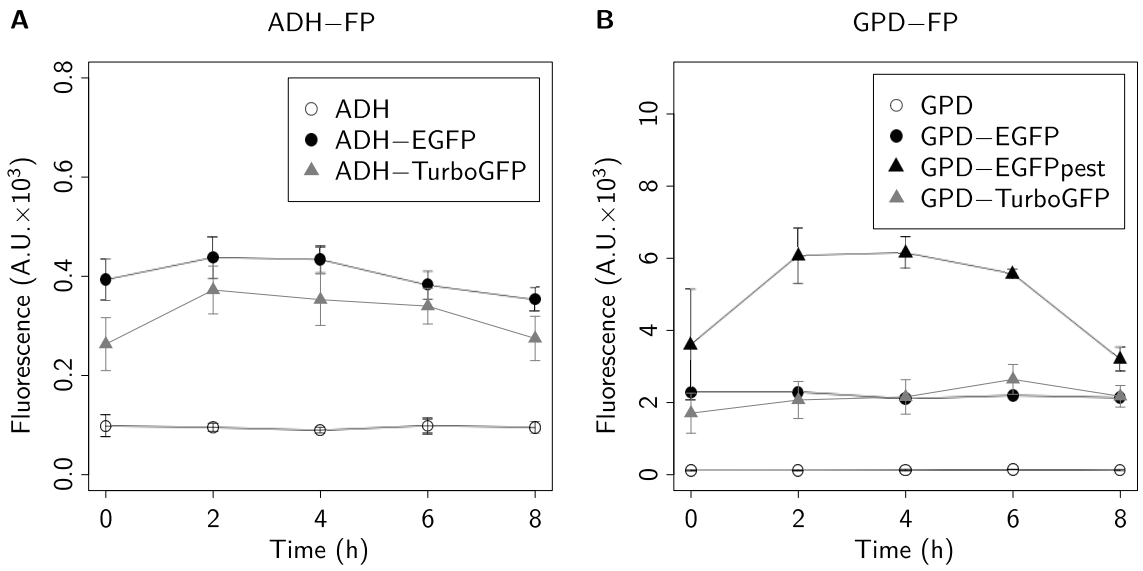

Figure 3.4: Time trend analysis of *S. cerevisiae* BY4741 reporter cells with intermediate or strong fluorescence. Yeast expression vectors p426ADH (**A**) and p426GPD (**B**) were exploited for constitutive expression of genes encoding EGFP, TurboGFP, or EGFPpest. As a control, yeast cells were transformed with parental vectors (labelled with 'ADH' and 'GPD', respectively). Total fluorescence of about 10^6 cells was determined with a TECAN Infinite microplate reader using excitation/emission wavelength of 490/520 nm and a gain of 100. Mean values ± sd of triple measurements are shown.

The obtained fluorescence signals of cells with EGFP and TurboGFP were comparable for each promoter and stable over time. Cells with the GDP–EGFPpest reporter construct displayed two- to threefold higher fluorescence than respective EGFP or TurboGFP reporter cells, but that was accompanied by higher signal fluctuation over time. In fact, a significant increase in fluorescence yield was obtained in case of EGFPpest after shift of reporter cells to fresh medium. Beginning after six hours, the initial level of fluorescence was almost restored after eight hours. Rapid fluctuation in fluorescence of reporter cells could be a consequence of EGFPpest instability. While stable EGFP or TurboGFP generated steady fluorescence, EGFPpest appeared more susceptible to degradation during prolonged batch cultivation of expressing cells.

Time trends of EGFP, TurboGFP and EGFPpest levels in reporter cells were also probed by immunodetection (Fig. 3.5). Immunoreactive signals in soluble protein fractions of reporter cells producing EGFP or TurboGFP were uniform over time as expected. This confirmed the maintenance of constant protein levels. For EGFPpest, a distinct signal in line with the molecular mass of the reporter protein (about 45 kDa) was only detectable between two and six hours. Degradation bands were detected at all time points of observation. A signal in line with the size of EGFP (about 27 kDa) was apparently more resistant to degradation. Thus, residual EGFP may lead to fluorescence of long-run batch-cultivated EGFPpest reporter cells.

The time trend for fluorescence of reporter cells with the GPD–EGFP and GPD–EGFPpest reporter construct was examined on the level of single cells (Fig. 3.6). Flow

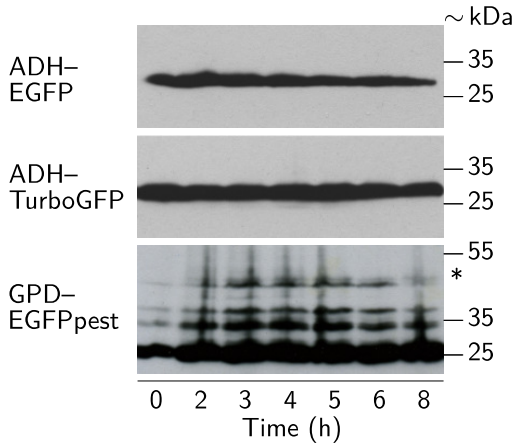

Figure 3.5: Time trend Western blot analysis of *S. cerevisiae* BY4741 reporter strains with moderate or strong fluorescence. Soluble protein fractions of about 10^7 reporter cells expressing genes encoding EGFP (∼ 26.9 kDa), TurboGFP (∼ 25.7 kDa) or EGFPpest (∼ 45.8 kDa, marked with an asterisk) were used for Western blot analysis. Fluorescent proteins were tracked with specific antibodies targeted to respective reporter proteins (Tab. 2.2). Migration positions of reference proteins are given on the right.

cytometry was conducted directly after shift of reporter cells to fresh medium as a reference and after four as well as eight hours. For reference, control cells carrying the parental vector were analysed. Similar scatter plots for all three strains and sampling time points indicated that there occurred no significant change in reporter cell morphology during batch cultivation (data not shown). Both reporter cell populations expressing *EGFP* or *TurboRFP* displayed their characteristic fluorescence profile. Fluorescence histograms of EGFP reporter cells were consistent over time while significant fluctuation of fluorescence was observed for EGFPpest reporter cells between the three sampling time points. The double-peaked shape was definitive after four hours.

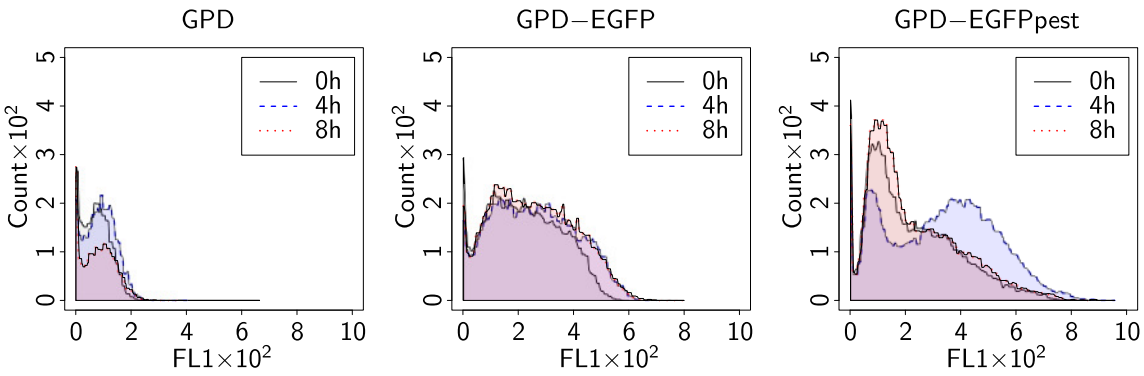

Figure 3.6: Time trend flow cytometry analysis of *S. cerevisiae* reporter cells with strong fluorescence. Cells of strain BY4741 harbouring plasmids p426GPD–EGFP or p426GPD–EGFPpest were examined after zero, four and eight hours. Cells that carry the parental vector p426GPD (no fluorescence) were used as a control. For each strain, 40,000 cells were analysed using a Partec CyFlow SL flow cytometer with identical settings. Fluorescence distribution over time is depicted as green fluorescence histogram overlays (FL1).

3.2 Development of yeast sensor cells for the detection of nutrient limitation

3.2.1 Aims and strategy

The utilisation of yeast cells in order to detect the biological availability of three macronutrients was tested as a proof of concept. Based on the set of yeast expression vectors developed by Mumberg et al. (1995), plasmids for the monitoring of nitrogen, phosphorus and sulphur in *S. cerevisiae* were generated. The promoter[1] fragments in vectors p426ADH or p424GPD were replaced by approximately 1-kb promoter fragments of 'signature' genes that indicate limitation of one of the macronutrients above in *S. cerevisiae*. To follow the activity of selected signature promoters, they were fused to GFP-like reporter genes. All detection plasmids were evaluated in common laboratory yeast strains B4741 or W303–1A.

The extensive and systematic survey of engineered sensor strains is summarised in the following sections. This includes the evaluation of general features with a particular focus on prospective practical application, i.e. their ability to near-line monitor nutrient deficiency during fermentation processes in white biotechnology.

3.2.2 Selection of nutrient-responsive signature promoters

Based on microarray analyses, Boer et al. (2003) and Tai et al. (2005) proposed signature genes indicating limitation of either glucose, nitrogen, phosphorus or sulphur.[2] These genes were specifically up-regulated or down-regulated under one particular nutrient limitation. Published transcript abundance data were carefully examined in order to identify promising promoter candidates for the generation of nutrient sensor strains. One criterion for selection was an abundant microarray signal, either under the limited nutrient condition of interest for up-regulated genes or under control conditions for down-regulated genes. It was assumed that the signal intensity is proportional to the expression level and can be used as a surrogate for fluorescent reporter protein yield that is expected. Signature genes were also selected because of a high average fold-change of signal abundance in the limitation condition of interest in comparison to all three other conditions (including glucose). A high fold-change in signal between different conditions implies that expression in the condition of interest is distinct and highly specific. The three to four most convenient candidates from each regulatory profile are summarised in Table C.1 (Appendix C.2). Signature genes whose promoters were finally evaluated in

[1] In the context of this work, the term 'promoter' is used synonymously to describe the (regulatory) region immediately adjacent to the 5'-end of the referring gene.

[2] Indicative signature genes were categorised as significantly changed at a 99% confidence level if expression in the respective limited condition was changed at least twofold in comparison to its expression in all three other conditions.

the present work are given in Table 3.1. Boer et al. (2003) and Tai et al. (2005) also identified over-represented sequences (putative regulatory motifs) in some clusters of co-regulated genes. As such motifs might indicate affiliation to a common regulon, the presence of these motifs was also examined for selected signature promoters.

3.2.3 Generation of detection plasmids and yeast sensor strains for the monitoring of nutrient availability

It was shown that the multicopy expression vectors p426ADH and p426GPD can be applied for moderate and strong expression of fluorescence reporter genes in *S. cerevisiae*. Yeast detection plasmids for the monitoring of nutrient availability were engineered using this vector series and a two-step cloning strategy (Fig. B.2, Appendix B.2). In addition to p426ADH, featuring a *URA3* cassette for complementation of uracil auxotrophic yeast strains, vector p424GPD was used. It carries a *TRP1* selection marker for complementation of tryptophan auxotrophic yeast strains like W303–1A.

Approximately 1-kb promoter fragments of signature genes which are either up-regulated or down-regulated under one specific nutrient limitation were used to replace the promoter fragments in vectors p426ADH or p424GPD. Sequence accuracy was checked by sequencing. For the majority of promoters, a fragment with the correct sequence was identified. The promoter region of *PHO11* was cloned in a previous work and contained four nucleotide aberrations located 600–700 bp upstream of the start codon (Pham, 2008). Promoter fragments of *DAL80*, *DIP5*, *TMA10*, *RPS22B* and *SOL1* contained one single nucleotide substitution each (see Appendix A). In case of the first three fragments, point mutations were located more than 500 bp upstream of the translational start site. The C→A transversion in the *RPS22B* promoter fragment and the T→C transition in the *SOL1* promoter fragment were located at positions –267 and –236, respectively. Mutations were not expected to impair promoter activity as they were located in the non-coding region and outside the typical binding region[3] of transcription factors of common yeast promoters (Tirosh et al., 2007; Zhu and Zhang, 1999).

In the second step, PCR-amplified genes encoding reporters EGFP or TurboGFP were fused to promoters that are up-regulated under one specific nutrient limitation and reporter EGFPpest to promoters that are down-regulated under one specific nutrient limitation. Sequences of all inserted fragments were again confirmed by sequencing, and products without mutations were obtained for all constructs.

All detection plasmids were transformed into *S. cerevisiae* strains BY4741 or W303–1A. Respective sensor cells were batch-cultivated in selective medium with defined concentrations of particular macronutrients. Results of detailed nutrient sensor strain examination is presented in the following sections.

[3] Typically 100–200 bp upstream of the start codon

Table 3.1: List of signature genes whose promoters were selected for the generation of *S. cerevisiae* nutrient sensor strains. Information about gene functions are according to the *Saccharomyces* genome database*. The presence of promoter motifs was examined manually by sequence alignment. Motif sequence strings are taken from Boer et al. (2003) and Tai et al. (2005). If modes of expression in own experiments diverged from published data, this is commented in the last column.

Gene name	Gene function	Promoter motif† (quantity)	Discrepancy own experiments/literature
Higher in nitrogen limitation			
GAP1	General amino acid permease	wGATAAs (5), dnCAGCAA (2), CAATGA (1)	
DAL5	Allantoate permease	wGATAAs (5), dnCAGCAA (3)	
DAL80	Repressor of genes in multiple nitrogen degradation pathways	wGATAAs (4), dnCAGCAA (2), CAATGA (1)	Not up-regulated
DAL4	Allantoin permease	wGATAAs (2), dnCAGCAA (1), CAATGA (3)	Not up-regulated
Lower in nitrogen limitation			
HPF1	Haze-protective mannoprotein	NS‡	Not down-regulated
NSR1	Nucleolar protein	NS	Not down-regulated
GNP1	Glutamine permease	NS	
Higher in phosphorus limitation			
PHO11	Acid phosphatase	mACGTGb (3), GCAGCAnndd (1), sdTGGAdnh (1)	
Lower in phosphorus limitation			
TMA10	Unknown, ribosome-associated	NS	Up-regulated
DIP5	Amino acid permease	NS	Transiently up-regulated
RPS22B	Protein component of 40S ribosomal subunit	NS	
Higher in sulphur limitation			
JLP1	Fe(II)-dependent sulphonate/ α-ketoglutarate dioxygenase	GCCACA (2), hACAGwk (1)	Not up-regulated
PDC6	Pyruvate decarboxylase isoform	GCCACA (2), hACAGwk (2)	
BDS1	Bacterially-derived sulphatase	hACAGwk (1)	
Lower in sulphur limitation			
SOL1	Possible role in tRNA export	AGGGG (4), GGmACm (1)	Not down-regulated
SCS3	Required for inositol prototrophy	AGGGG (2)	Partially down-regulated
SSU1	Plasma membrane sulphite pump	AGGGG (2), GGmACm (2)	

* `http://www.yeastgenome.org` [URL was last accessed on 28 September 2011.]
† Redundant nucleotides are given, s = C or G, w = A or T, k = G or T, m = A or C, b = C, G or T, d = A, G or T, h = A, C or T, n = A, C, G or T.
‡ NS, no significant motifs identified

3.2.4 Evaluation of nitrogen sensor strains

Ammonium is an important intermediate of yeast's nitrogen metabolism and the preferred nitrogen source of common laboratory strains. Detection plasmids for monitoring of nitrogen availability were transformed into *S. cerevisiae* strains BY4741 or W303–1A. Respective nitrogen sensor cells were batch-cultivated in mineral medium containing 5 g l^{-1} ammonium sulphate (non-limited medium) or nitrogen limitation medium containing 50 mg l^{-1} ammonium sulphate as nitrogen source (Section 2.4.2). Total fluorescence of sensor strains was initially probed on cell population level by microplate reader-based fluorometry and Western blot analysis.

Sensor strains with higher fluorescence in nitrogen limitation

Four promoters of signature genes that are specifically higher expressed in nitrogen deficiency were evaluated using *S. cerevisiae* BY4741. The *DAL4* promoter was also evaluated previously (Pham, 2008). Within eight hours no expression of reporter gene *EGFP* from this promoter was detectable. Similarly, sensor cells with expression of *EGFP* and *TurboGFP* from the *DAL80* promoter displayed no significant fluorescence (data not shown).

Fluorescence of the other two sensor strains featuring *TurboGFP* reporter gene expression from *GAP1* and *DAL5* promoters was strongly triggered within eight hours of cultivation in nitrogen limitation medium while fluorescence remained constantly low over time in mineral medium (Fig. 3.7). The GAP1 sensor strain was superior in terms of response time, total signal yield and fold-change of signal intensity. Fluorescence of DAL5 sensor cells started to increase four hours after the shift to nitrogen limitation medium and yielded sixfold higher fluorescence than cells in mineral medium after eight hours. Elevated fluorescence of nitrogen-limited GAP1 sensor cells was observed already after two hours and was about eightfold increased after seven hours. However, the *GAP1* promoter was leaky since basic fluorescence of non-limited cells was equal to fluorescence of reporter cells with p426ADH–TurboGFP (see Section 3.1.1).

It was tested whether the use of reporter EGFPpest has an impact on total signal yield like it was shown for constitutively expressed reporters in Section 3.1.2. Fluorescence of respective nitrogen sensor strains was indeed higher regarding total signal intensity and fold-change in fluorescence of limited versus non-limited cells (Fig. 3.8). The maximum fold-change in fluorescence observed with EGFPpest was about twelvefold after seven hours under the control of the *GAP1* promoter and even 37-fold under the *DAL5* promoter. Fluorescence of sensor cells with destabilised EGFPpest was steadily increasing in nitrogen limitation medium implying that continuous expression of the reporter gene is possible even during batch cultivation and lack of nitrogen. The nitrogen sensor strain with the GAP1–TurboGFP detection construct was used in further investigations

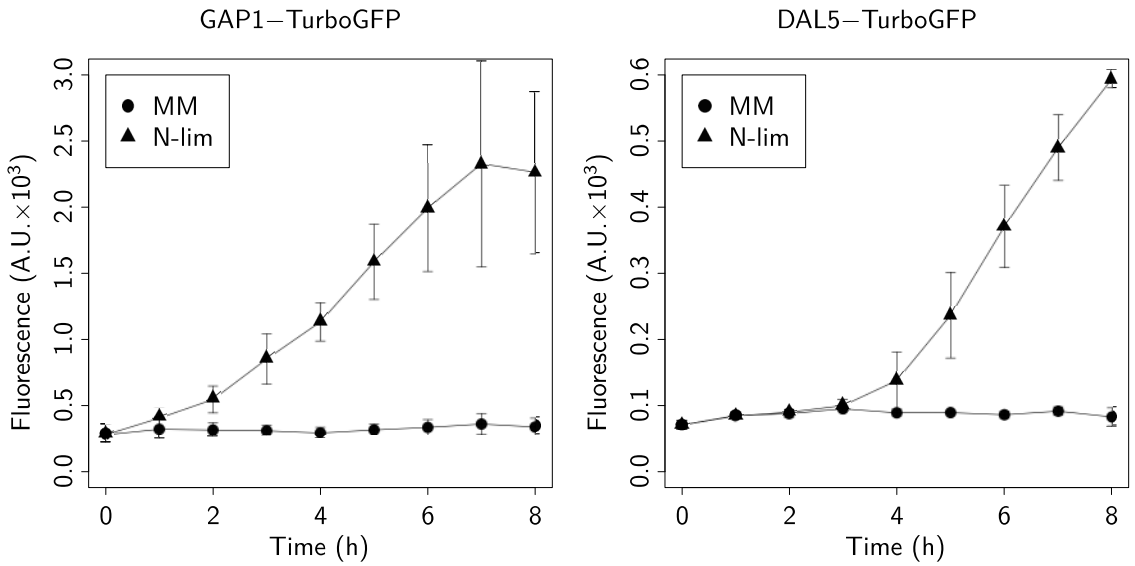

Figure 3.7: Fluorometric analysis of nitrogen sensor strains with higher fluorescence in nitrogen limitation. Cells of BY4741 were transformed with detection plasmids p426GAP1–TurboGFP or p426DAL5–TurboGFP. For each strain, total fluorescence of about 10^6 cells cultivated in mineral medium (MM) and nitrogen limitation medium (N-lim) was determined using a TECAN Infinite microplate reader with excitation/emission wavelength of 490/520 nm and a gain of 100. Mean values ± sd from three independent measurements are shown.

because of sufficient signal yield and reporter stability.

Expression of the detection construct GAP1–TurboGFP was compared between *S. cerevisiae* strains BY4741 and W303–1A (Fig. 3.9). Both laboratory strains were exploited for sensor purposes in this work but have diverse genetic backgrounds. Growth media for both recombinant sensor strains are also supplemented with different amino acids which are a minor pool of biologically available nitrogen for yeast (histidine, leucine, methionine and tryptophan) as well as nucleobases (adenine and uracil). The basic fluorescence of non-limited W303–1A GAP1 sensor cells was higher than basic fluorescence of BY4741 GAP1 sensor cells. Higher autofluorescence of strain W303–1A is reported in literature (Schofield et al., 2007). In addition, different supplementation of selective media with amino acids and nucleotide bases may influence basic fluorescence of both strains. Irrespective of this observation, both sensor strains displayed similar fluorescence expression patterns after shift to nitrogen limitation medium. This suggests that both strains can be used equally for nitrogen monitoring purposes.

Sensor strains with lower fluorescence in nitrogen limitation

Three promoters of signature genes that are down-regulated under nitrogen limitation were evaluated in yeast strain W303–1A. Cells were transformed with detection plasmids that drive expression of reporter *EGFPpest* from the promoters of *NSR1*, *HPF1* or *GNP1*. The results are summarised in Figure 3.10.

Distinct fluorescence of respective nitrogen sensor strains which were cultivated

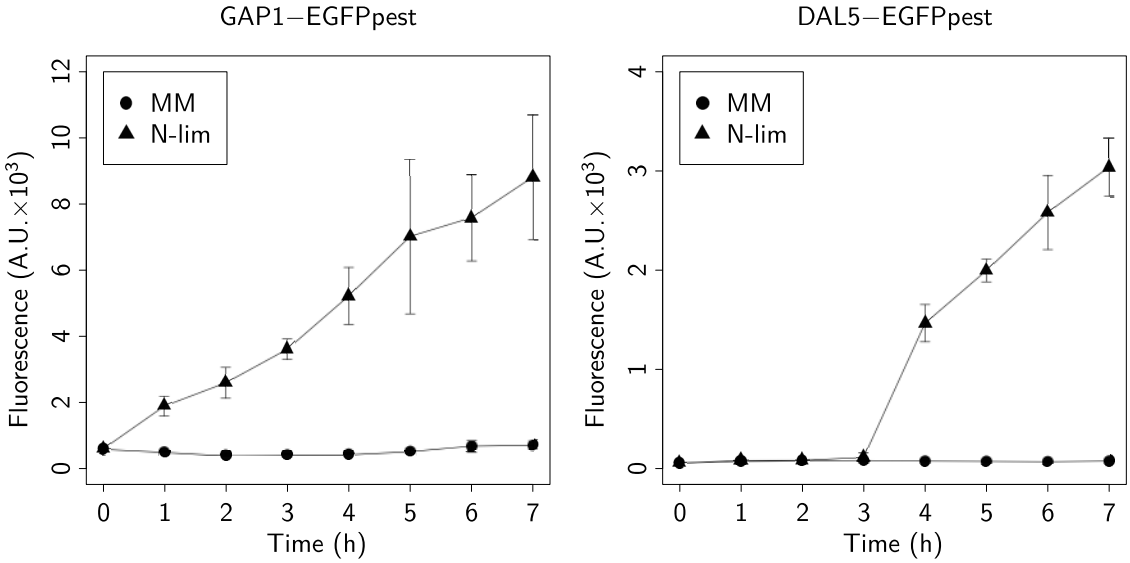

Figure 3.8: Fluorometric analysis of nitrogen sensor strains with higher fluorescence in nitrogen limitation and destabilised fluorescent reporters. Cells of BY4741 were transformed with detection plasmids p426GAP1–EGFPpest or p426DAL5–EGFPpest. For each strain, total fluorescence of about 10^6 cells cultivated in mineral medium (MM) and nitrogen limitation medium (N-lim) was determined using a TECAN Infinite microplate reader with excitation/emission wavelength of 490/520 nm and a gain of 100. Mean values ± sd from three independent measurements are shown.

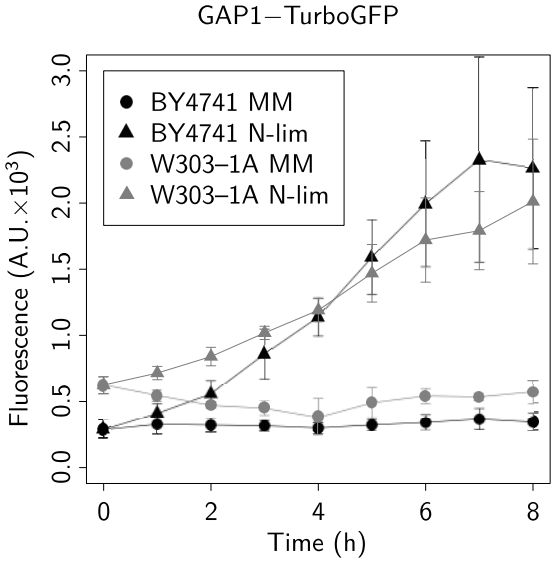

Figure 3.9: Fluorometric analysis of BY4741 and W303–1A nitrogen sensor strains with higher fluorescence in nitrogen limitation. Cells were transformed with detection plasmid p426GAP1–TurboGFP. For each strain, total fluorescence of about 10^6 cells cultivated in mineral medium (MM) and nitrogen-limited medium (N-lim) was determined using a TECAN Infinite microplate reader with excitation/emission wavelength of 490/520 nm and a gain of 100. Mean values ± sd from three independent measurements are shown.

in mineral medium was expected but cells harbouring the NSR1–EGFPpest construct displayed no significant fluorescence, neither in mineral medium nor in nitrogen limitation medium. Beginning after five hours, a weak decrease in fluorescence of nitrogen-limited NSR1 sensor cells was detectable. Basic fluorescence of *HPF1* sensor cells in the presence of nitrogen was higher. But after shift to nitrogen limitation medium, sensor cells exhibited slightly higher fluorescence than in mineral medium.

Only results for nitrogen sensor cells with the *GNP1* detection construct were roughly conform with assumptions. Explicit fluorescence was detected for non-limited sensor cells but the signal was not stable as expected. Within five hours the fluorescence of GNP1 sensor cells increased steadily in mineral medium, followed by a rapid decrease to the initial level. Transfer of sensor cells to fresh medium might lead to transient regeneration of sensor cells' fluorescence until reporter expression is changed again because of anew limitation in the fresh batch culture. However, steadily decreased fluorescence was detected for GNP1 sensor cells which were cultivated in nitrogen limitation medium. They, therefore, displayed lower fluorescence at all time points of examination after shift to nitrogen limitation medium. The difference was clearly visible after two hours and maximum fourfold signal difference was observed after five hours.

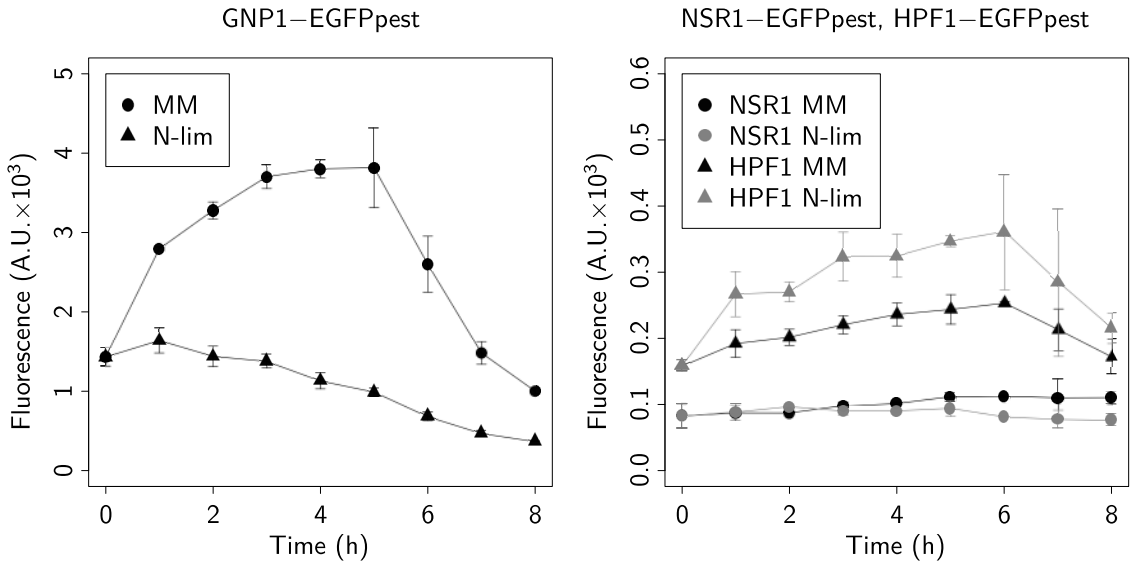

Figure 3.10: Fluorometric analysis of nitrogen sensor strains with lower fluorescence in nitrogen limitation. Cells of W303–1A were transformed with detection plasmids p424GNP1–EGFPpest, p424NSR1–EGFPpest or p424HPF1–EGFPpest. For each strain, total fluorescence of about 10^6 cells cultivated in mineral medium (MM) and nitrogen-limited medium (N-lim) was determined using a TECAN Infinite microplate reader with excitation/emission wavelength of 490/520 nm and a gain of 100. Mean values ± sd from three independent measurements are shown.

Western blot analysis of nitrogen sensor strains

Time trends of GFP-like reporter gene expression for sensor strains with sufficient response to nitrogen limitation were verified by Western blot analysis (Fig. 3.11). All

data were in good agreement with the results from fluorometric analysis. In line with the data for GAP1 sensor cells, basic levels of TurboGFP and EGFPpest (degraded) were even detectable without nitrogen limitation and steadily stronger signals were observed for nitrogen-limited cells. No TurboGFP was detectable in non-limited DAL5 sensor cells but distinct signals were observed in nitrogen-limited cells after four hours with subsequently increasing signal strength. For the GNP1 nitrogen sensor strain, distinct signals in the size range of full-length EGFPpest were observed only two to six hours after the shift of sensor cells to fresh mineral medium. In nitrogen-limited sensor cells, only degradation bands of lower intensity were detected.

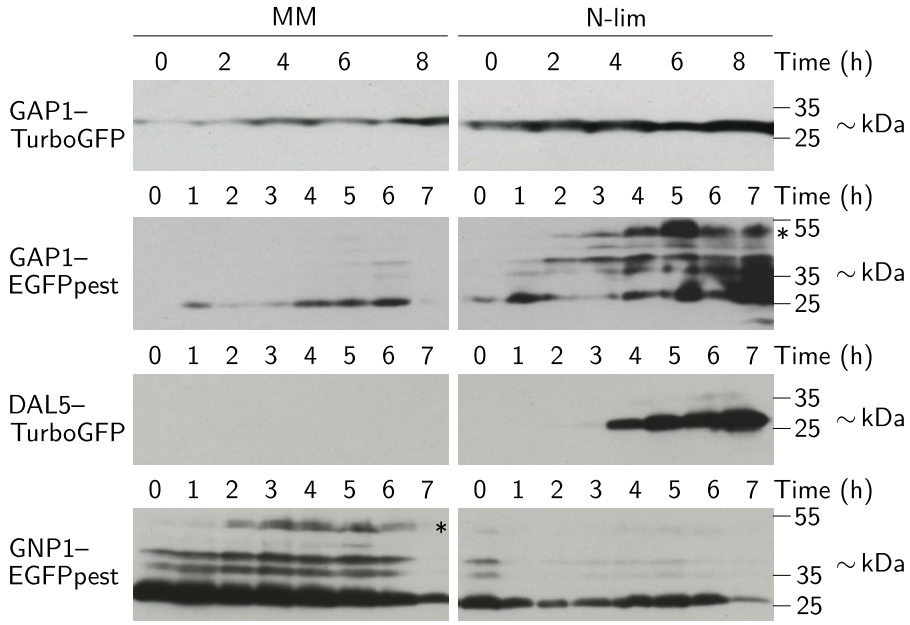

Figure 3.11: Western blot analysis of nitrogen sensor strains. Cells of BY4741 with p426GAP1–TurboGFP, p426GAP1–EGFPpest or DAL5–TurboGFP and W303–1A with p424GNP1–EGFPpest were cultivated in mineral medium (MM) or nitrogen limitation medium (N-lim). Total protein fractions of about 10^7 cells harvested at indicated time points were subjected to analysis by protein immunoblotting. Fluorescent proteins were tracked with specific antibodies targeted to respective reporter proteins (Tab. 2.2). Expected sizes of proteins are ~25.7 kDa for TurboGFP and ~45.8 kDa for EGFPpest (marked with an asterisk). Migration positions of reference proteins are given on the right.

3.2.5 Evaluation of phosphorus sensor strains

Here, the evaluation of four phosphorus sensor strains is reported. Phosphorus demand of yeast is primarily met by minerals containing inorganic phosphate. The applicability of the *PHO11* promoter for sensor purposes was already validated by Pham (2008). Recombinant BY4741 cells with the PHO11–EGFP construct displayed elevated fluorescence in phosphorus limitation medium and a clear difference in fluorescence of limited and non-limited sensor cells was observed after five hours. Thus, no further promoters of up-regulated signature genes were probed in this work. Instead, promoters of signature

genes *TMA10*, *DIP5* and *RPS22B* with lower expression in phosphorus deprivation were fused to reporter gene encoding EGFPpest and evaluated in yeast strain W303–1A. Total fluorescence of all four phosphorus sensor strains was analysed by microplate reader-based fluorometry like for the nitrogen sensor strains (see Section 3.2.4). Cells were again batch-cultivated in either mineral medium that contains 1 g l^{-1} potassium phosphate, or in limitation medium with 10 mg l^{-1} potassium phosphate to simulate phosphorus deficiency (Section 2.4.2). The result is shown in Figure 3.12.

Fluorescence of PHO11 sensor cells was triggered in phosphorus limitation medium after four hours while low and constant signals were detected for non-limited sensor cells. After eight hours, the fluorescence level of phosphorus-limited sensor cells was threefold higher than the level of non-limited sensor cells. In contrast to the data of Boer et al. (2003) and Tai et al. (2005), fluorescence of phosphorus-limited TMA10 sensor cells was higher rather than lower in phosphorus limitation. After shift from mineral medium to phosphorus-deficient medium, steadily increasing fluorescence signals were detectable over time and an approximately fivefold higher signal strength was observable after eight hours. Basic fluorescence of TMA10 sensor cells in mineral medium was around tenfold higher than of PHO11 sensor cells suggesting promoter-leakiness in the presence of phosphorus like that observed with the GAP1 sensor strain accompanied by adequate nitrogen availability (Section 3.2.4). After transfer to fresh mineral medium, fluorescence of non-limited TMA10 sensor cells was slightly decreased for approximately four hours indicating minor fluctuation of the EGFPpest level.

Fluorescence of DIP5 and RPS22B sensor strains was lower in phosphorus-deficient medium which was in line with the reference literature. The two strains yielded 3.5-fold and twelvefold lower fluorescence after three and five hours of cultivation in phosphorus limitation medium, respectively. However, fluorescence decline of limited DIP5 sensor was only transient. After transfer of DIP5 sensor cells to fresh mineral medium, fluorescence regeneration was detectable for a time range of four hours before fluorescence yielded a lower level than immediately after the transfer. DIP5 sensor cells that were shifted to phosphorus limitation medium exhibited oscillating fluorescence with abrupt but transient decline, rise and a second decline. This indicates that *DIP5* promoter activity is possibly not solely affected by phosphorus deficiency. Dip5p is an amino acid permease rather than directly involved in phosphorus metabolism (Regenberg et al., 1998). A shift to fresh medium with new nitrogen resources might influence promoter activity and interfere with global down-regulation of *DIP5* in phosphorus limitation. Additionally, a correlation of lower fluorescence and glucose exhaustion may exist. Fluorescence of phosphorus-limited RPS22B sensor cells decreased within four hours from intermediate to low and constant level while fluorescence of sensor cells increased within five hours after transfer to fresh mineral medium. This pattern was already observed for GNP1 nitrogen sensor cells in adequate nitrogen availability (Section 3.2.4).

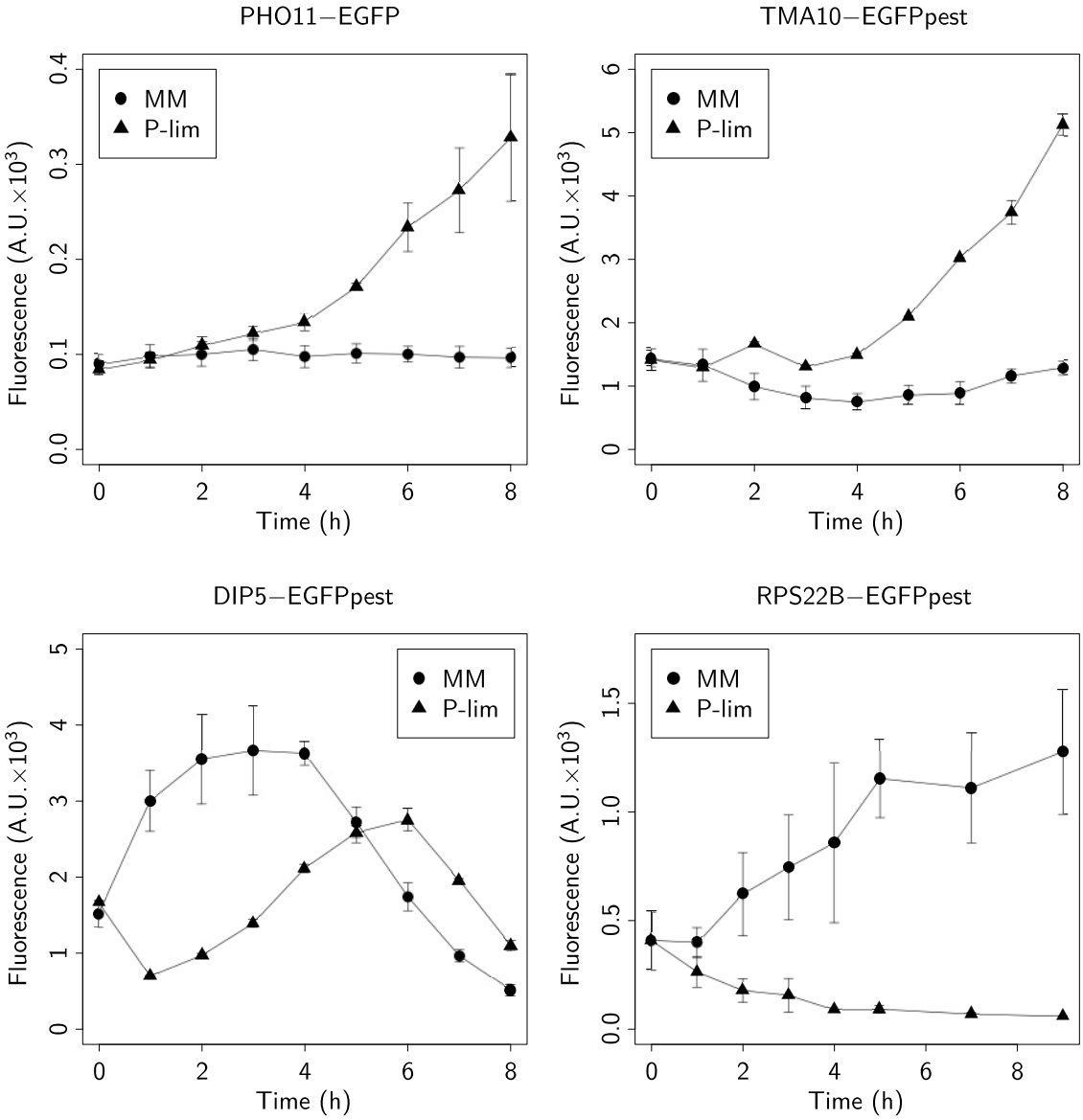

Figure 3.12: Fluorometric analysis of phosphorus sensor strains. Detection plasmid p426PHO11–EGFP was evaluated in BY4741 and detection plasmids p426TMA–EGFPpest, p426DIP5–EGFPpest and p424RPS22B–EGFPpest were evaluated in W303–1A. For each strain, total fluorescence of about 10^6 cells cultivated in mineral medium (MM) and phosphorus limitation medium (P-lim) was determined using a TECAN Infinite microplate reader with excitation/emission wavelength of 490/520 nm and a gain of 100. Mean values ± sd from three independent measurements are shown.

In conclusion, three out of the four tested phosphorus sensor strains showed a clear change of fluorescence in response to phosphorus deficiency. Time trends of GFP-like reporter gene expression for phosphorus sensor strain with the PHO11 (higher in limitation) and RPS22B (lower in limitation) detection construct were additionally probed by Western blot analysis. The result confirmed the observations of microplate reader-based fluorometry (Fig. 3.13). Immunoactive EGFP in PHO11 sensor cells was only detectable in phosphorus-limited cells with the earliest but weak signal after two hours and a distinct signal after five hours. Strong signals of full-length EGFPpest and its characteristic degradation pattern were solely detectable in non-limited RPS22B sensor cells while signals in phosphorus-limited sensor cells were weaker and bands referring to degraded reporter protein were abundant.

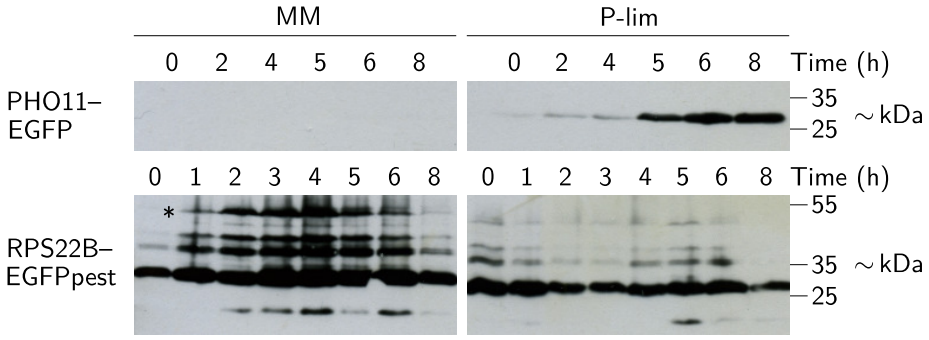

Figure 3.13: Western blot analysis of phosphorus sensor strains. Cells of BY4741 with p426PHO11–EGFP and W303–1A with p424RPS22B–EGFPpest were cultivated in mineral medium (MM) or phosphorus limitation medium (P-lim). Total protein fractions of about 10^7 cells harvested at indicated time points were subjected to analysis by protein immunoblotting. Fluorescent proteins were tracked with anti-GFP (Tab. 2.2). Expected sizes of proteins are ~26.9 kDa for EGFP and ~45.8 kDa for EGFPpest (marked with an asterisk). Migration positions of reference proteins are given on the right.

3.2.6 Evaluation of sulphur sensor strains

Three promoters of signature genes which are specifically up-regulated or down-regulated under sulphur limitation were evaluated for sensor purposes by microplate reader-based fluorometry and Western blot analysis. Although yeast may uptake and metabolise a broad spectrum of sulphur compounds, ammonium sulphate is typically used to feed laboratory strains. Sulphur sensor cells were either batch-cultivated in mineral medium that contains 5 g l^{-1} ammonium sulphate as a control or in sulphur limitation medium with a trace concentration of only 5 mg l^{-1} (Section 2.4.2).

Furthermore, addition of methionine is required for selective growth of BY4741 sensor cells due to the strain's methionine auxotrophy. The potential impact of methionine as an additional sulphur source on the functionality of yeast sensor strains was examined. The *JLP1* promoter was chosen for initial analysis because the according signature gene is specifically up-regulated under sulphur limitation with superior signal abundance and

high fold-change rate apparent in transcript analysis data (Tab. C.1, Appendix C.2). The respective detection construct JLP1-TurboGFP was transformed into strains BY4741 and W303–1A and fluorescence of JLP sensor cells was probed after transfer to fresh mineral medium or shift to sulphur-deficient medium (Fig. 3.14). Specific induction of fluorescence in sulphur limitation medium was uniquely obtained in W303–1A sensor cells yielding 1.2- and 3.3-fold induction after five and 24 hours, respectively. Thus, all sulphur detection plasmids were evaluated in W303–1A in the following experiments.

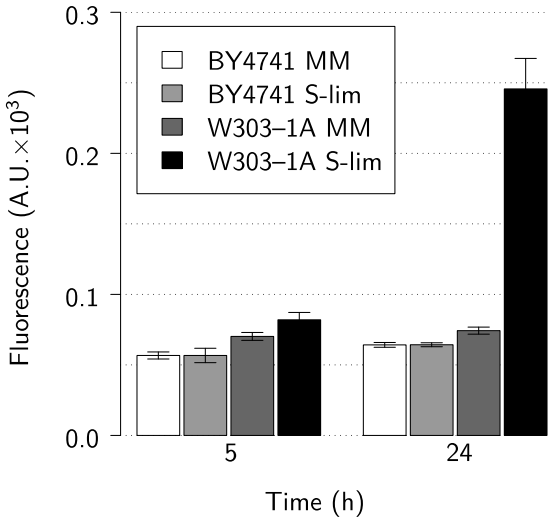

Figure 3.14: Comparison of strains BY4741 and W303–1A as a host for sulphur detection plasmids. Cells of both strains were transformed with plasmid p426JLP1–TurboGFP. For each sensor strain, total fluorescence of about 10^6 cells cultivated in mineral medium (MM) or sulphur-limited medium (S-lim) was detected after five and 24 hours using a TECAN Infinite microplate reader with excitation/emission wavelength of 490/520 nm and a gain of 100. Mean values ± sd of triple measurements are shown.

Functionality of further W303–1A-based sulphur sensor strains was probed by time trend fluorometric analysis (Fig. 3.15). Basic fluorescence of non-limited sensor cells with GFP-like reporter gene expression from the promoters of *PDC6*, *BDS1* and *JLP1* was constantly low and comparable to levels of control cells that harbour the parental vector p426ADH (see Section 3.1.2). Distinct fluorescence signals in response to sulphur limitation were obtained after five hours. Within eight hours, sulphur-deficient PDC6 sensor cells yielded about threefold higher fluorescence than non-limited sensor cells. Sulphur-limited BDS1 as well as JLP1 sensor cells reached at least twofold higher fluorescence levels than non-limited cells. Promoters of genes *SCS3*, *SOL1* and *SSU1* were predicted to be down-regulated under sulphur limitation. Distinct fluorescence of sensor cells producing EGFPpest as a reporter in non-limited mineral medium was expected but not observed. All three sensor strains displayed a different response after shift to sulphur limitation medium. After transfer, fluorescence of SSU1 sensor cells was triggered in both media over time but was lower in sulphur limitation medium at any time point of observation. After seven hours, fluorescence of sulphur-limited SSU1 sensor cells was approximately three times lower than of non-limited cells. Transiently higher

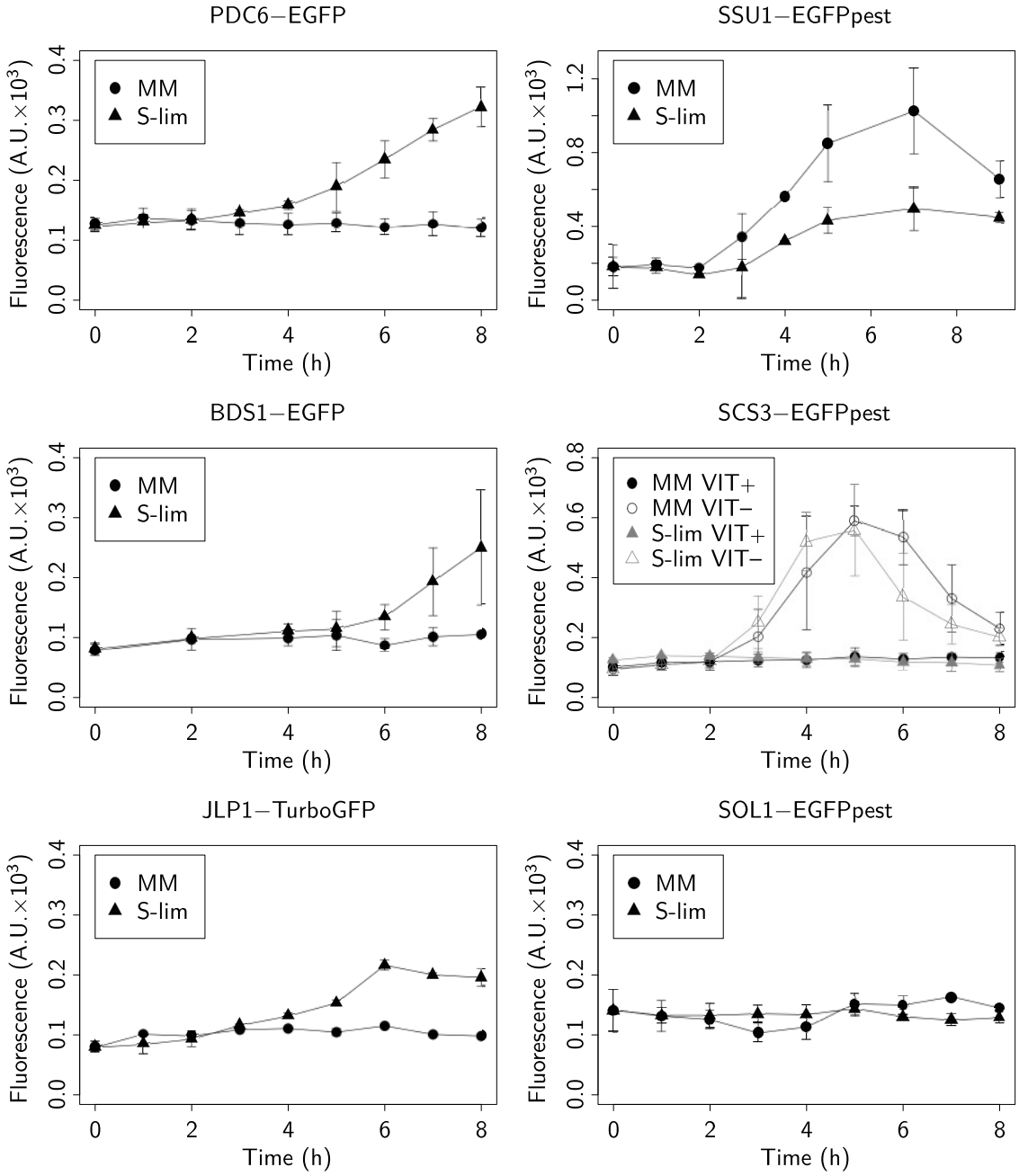

Figure 3.15: Fluorometric analysis of sulphur sensor strains. Cells of W303–1A were transformed with detection plasmids p426PDC–EGFP, p426BDS1–EGFP and p426JLP1–TurboGFP (higher fluorescence in sulphur-limited conditions) or p424SSU1–EGFPpest, p424SCS3–EGFPpest and p424SOL1–EGFPpest (lower fluorescence in sulphur-limited conditions). For each strain, total fluorescence of about 10^6 cells cultivated in mineral medium (MM) and sulphur limitation medium (S-lim) was determined using a TECAN Infinite microplate reader with excitation/emission wavelength of 490/520 nm and a gain of 100. SCS3 sensor cells were cultivated in media with vitamin solution (VIT+) or vitamin-free media (VIT–). Mean values ± sd from three independent measurements are shown.

fluorescence of SCS3 sensor cells was solely detected in growth media lacking vitamins but irrespective whether sulphur was in surplus or deficient. This indicates that *SCS3* promoter activity is probably influenced by vitamin components. The added vitamin solution contains for instance inositol and *SCS3* is involved in inositol phospholipid biosynthesis (Hosaka et al., 1994). Fluorescence of SCS3 sensor cells was at maximum sixfold increased after five hours of cultivation in media lacking vitamin additives. Fluorescence of SOL1 sensor cells was rather unaffected in both media over time strongly suggesting that this sensor strain is not convenient for sulphur monitoring purposes.

PDC6 and SSU1 sensor strains displayed sufficient response to sulphur limitation which was in line with the expected tendency. Respective production of reporter proteins EGFP and EGFPpest was examined by Western blot analysis. The results are depicted in Figure 3.16 and were in agreement with microplate reader-based fluorometric analysis. Distinct EGFP signals were solely detected in sulphur-deficient PDC6 sensor cells six hours after shift to limitation medium. Before, only a faint signal was observed. Full-length EGFPpest was clearly detectable in non-limited SSU1 sensor cells between four and seven hours after shift to fresh medium. At later time points, only low levels and abundant degradation bands were detected fitting the fluorescence decline after seven hours. Weak signals for full-length EGFPpest and abundant signals of degraded EGFPpest were mainly visible in sulphur-limited SSU1 sensor cells after five to seven hours which was also in line with measurement of increased fluorescence for sulphur-limited SSU1 sensor cells.

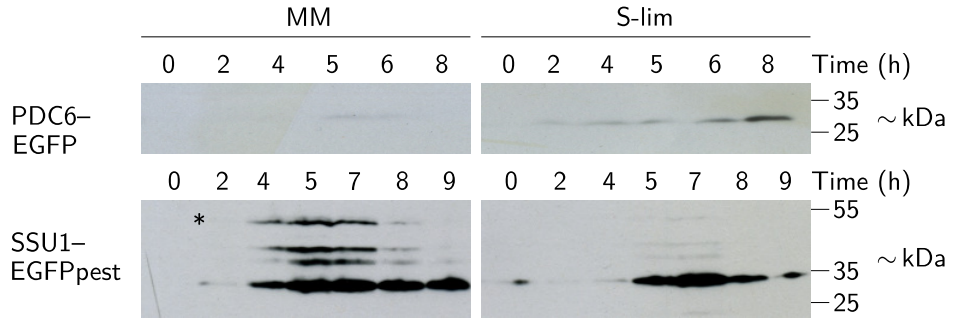

Figure 3.16: Western blot analysis of sulphur sensor strains. Sulphur sensor cells W303–1A with p426PDC6–EGFP or p424SSU1–EGFPpest were cultivated in mineral medium (MM) or sulphur limitation medium (S-lim). Total protein fractions of about 10^7 cells harvested at indicated time points were subjected to analysis by protein immunoblotting. Fluorescent proteins were tracked with anti-GFP (Tab. 2.2). Expected sizes of proteins are ~26.9 kDa for EGFP and ~45.8 kDa for EGFPpest (marked with an asterisk). Migration positions of reference proteins are given on the right.

3.2.7 Analysis of nutrient sensor strains on single-cell level

Initial evaluation of sensor strains that monitor availability of ammonium, inorganic phosphate or sulphate in yeast media was probed by determining total fluorescence or

reporter protein production on cell population level. For each nutrient limitation, at least one sensor strain with at least threefold induced or reduced fluorescence in response to nutrient-deficiency was identified (see Table 3.2). Here, the impact of nutrient limitation on batch-cultivated sensor cells was analysed on the level of single cells. Sensor cells were cultivated in mineral medium or respective limitation medium. At time points of strong fluorescence yield in one of the two media (concluded from microplate reader-based fluorometric analysis), cells were analysed by microscopy and flow cytometry.

Table 3.2: *S. cerevisiae* sensor strains displaying significant fluorescence fluctuation after shift to nutrient limitation medium. Acronyms refer to implemented promoter fragments.

Nutrient limitation	**Higher fluorescence**	**Lower fluorescence**
Nitrogen	DAL5, GAP1	GNP1
Phosphorus	PHO11, TMA10	DIP5, RPS22B
Sulphur	BDS6, JLP1, PDC6	SCS3, SSU1

Fluorescence microscopy of nutrient sensor strains

Sensor strains with distinct change of fluorescence in limitation medium were analysed using fluorescence microscopy. For each strain, identical exposure times were applied to compare brightness of non-limited and nutrient-limited cells.

GAP1 and GNP1 nitrogen sensor strains with higher and lower fluorescence under nitrogen limitation, respectively, were examined six hours after transfer to fresh mineral medium or nitrogen-deficient medium (Fig. 3.17). BY4741 and W303–1A sensor cells differed slightly in size as reported previously (Petrezselyova et al., 2010). More importantly, cell morphology of each strain was similar in mineral medium and nitrogen limitation medium. Fluorescence of plasmid-based sensor cells was clearly detectable but not uniform within one sensor cell population. This was already observed for reporter strains with constitutive expression of fluorescence reporter genes (Section 3.1.1). Thus, both brightness of individual sensor cells and the proportion of fluorescent sensor cells was affected by nitrogen availability. GAP1 sensor cells displayed zero to moderate fluorescence in mineral medium and predominantly strong fluorescence in nitrogen limitation medium along with a remaining fraction of cells exhibiting no or low fluorescence. The majority of GNP1 sensor cells exhibited particular fluorescence in mineral medium while only a small fraction of sensor cells exhibited weak fluorescence in nitrogen limitation medium. With regard to the results of fluorometric analysis, fluorescence of nitrogen-limited GNP1 sensor cells was decreasing further after six hours indicating that either down-regulation of the *GNP1* promoter or degradation of EGFPpest was yet incomplete at the time point of microscopic analysis.

PHO11 and TMA10 sensor cells, both exhibiting higher fluorescence in phosphorus limitation, and RPS22B sensor cells with lower fluorescence under limitation were

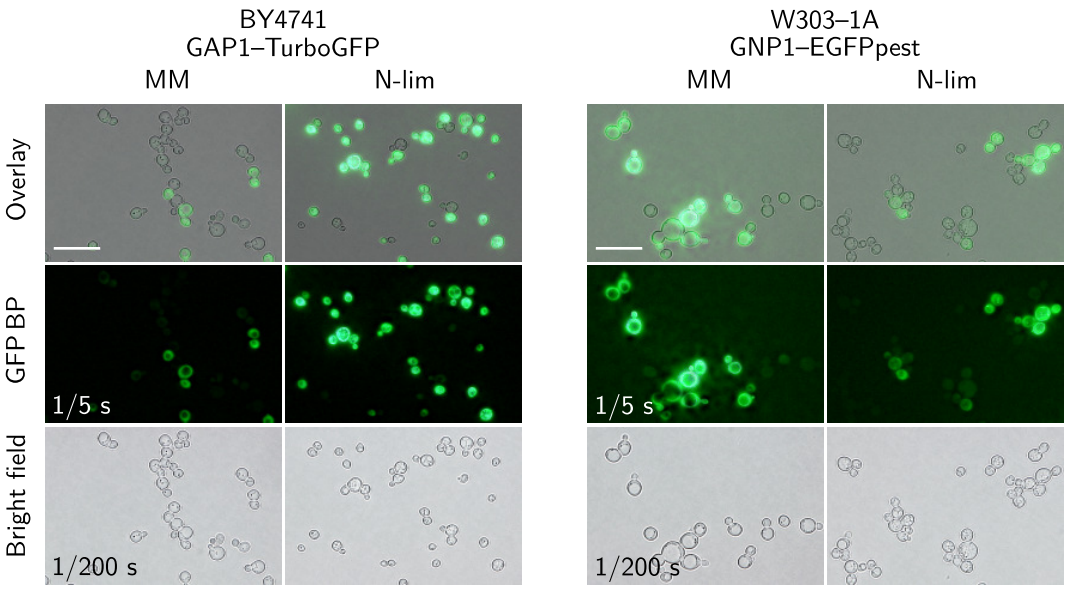

Figure 3.17: Microscopic analysis of nitrogen sensor strains. Sensor cells with detection plasmids p426GAP1–TurboGFP and p424GNP1–EGFPpest were imaged after cultivation in mineral medium (MM) or nitrogen limitation medium (N-lim) using a Keyence BZ-8100 fluorescence microscope with 1,000× magnification, GFP BP filter for fluorescence monitoring and given exposure times for each channel. Each image block shows the overlay (scale bar = 20 μm) and respective fluorescence and bright field images.

analysed seven hours after shift to fresh media. DIP5 sensor cells with transiently lower fluorescence in phosphorus limitation were imaged already after three hours. Cell morphology of non-limited and phosphorus-limited sensor cells was comparable with slightly different vacuoles which was more apparent after seven hours (Fig. 3.18). Similar fractions of PHO11 and TMA10 sensor cells exhibited higher fluorescence in phosphorus limitation medium. In line with results of microplate reader-based fluorometry, brightness of EGFPpest in TMA10 sensor cells was stronger but some sensor cells displayed only moderate fluorescence in mineral medium too. As judged by eye, about 50% of DIP5 and RPS22B sensor cells displayed bright fluorescence in mineral medium. Fluorescence under phosphorus limitation was observed in a smaller fraction of sensor cells suggesting incomplete down-regulation of promoters or residual EGFPpest.

All sensor strains with higher (PDC6, JLP1), conditionally higher (SCS3) or lower (SSU1) fluorescence in sulphur limitation were monitored six hours after shift to fresh medium (Fig. 3.19). Sulphur-limited cells exhibited a slightly changed morphology regarding size and appearance of vacuoles. Longer exposure time was required to detect sufficient fluorescence of sulphur sensor strains. Besides lower brightness, the fraction of fluorescent cells appeared smaller than for nitrogen and phosphorus sensor strains resulting in both reduced signal-to-background ratio and image quality. Fractions of PDC6 and JLP1 sensor cells exhibited elevated fluorescence in sulphur limitation medium while non-limited cells displayed no significant signals as expected. In line with fluorometric analysis, signal yield was slightly better within PDC6 sensor cells. Fluorescence of few

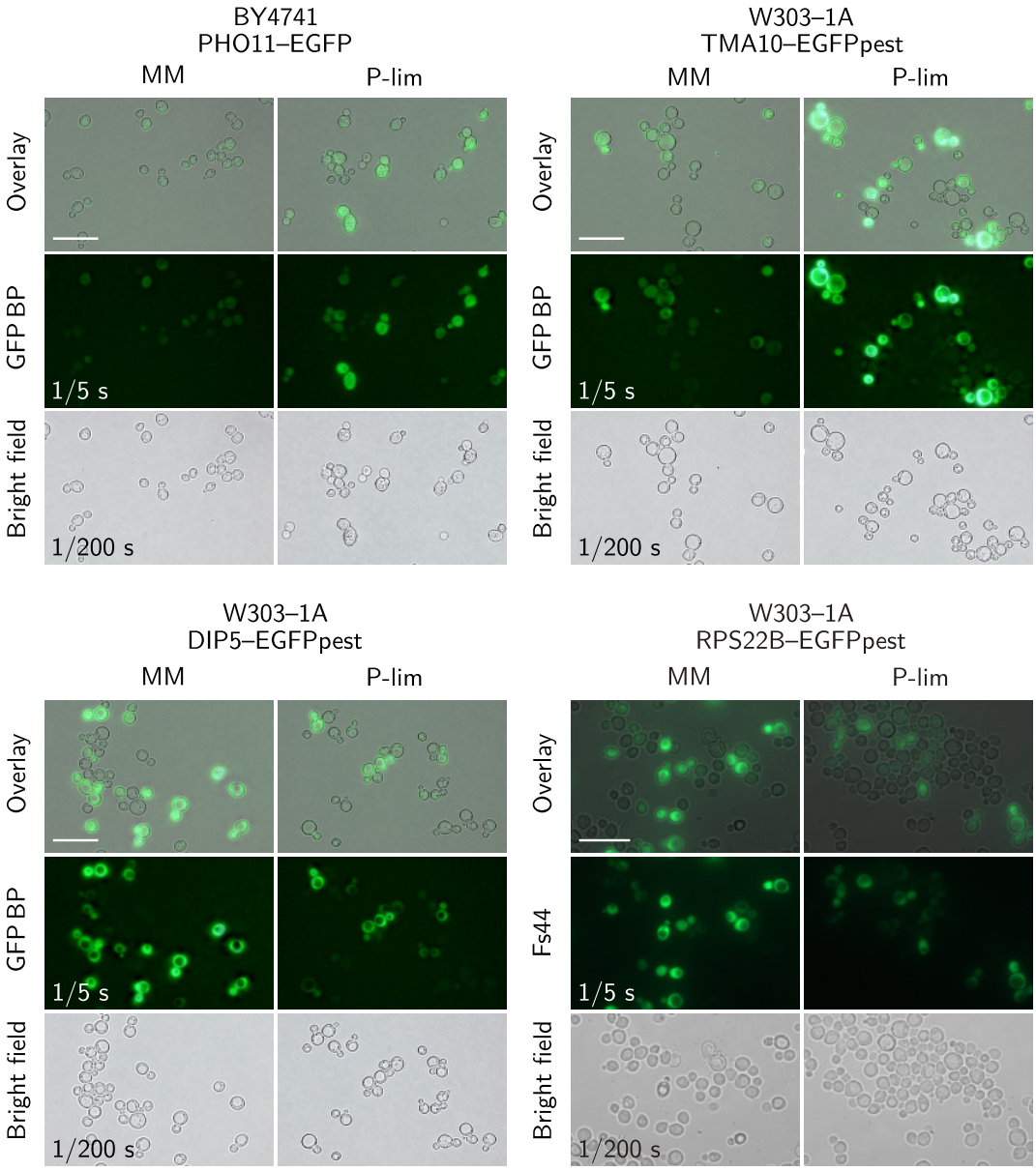

Figure 3.18: Microscopic analysis of phosphorus sensor strains. Cells with detection plasmids p426PHO11–EGFP, p426TMA10–EGFPpest, p426DIP5–EGFPpest and p424RPS22B–EGFPpest were imaged after cultivation in mineral medium (MM) or phosphorus limitation medium (P-lim) using a Keyence BZ-8100 or Zeiss Axio Imager.1A fluorescence microscope with 1,000× magnification, GFP BP or Fs44 filter for fluorescence monitoring and given exposure times for each channel. Each image block shows the overlay (scale bar = 20 μm) and respective fluorescence and bright field images.

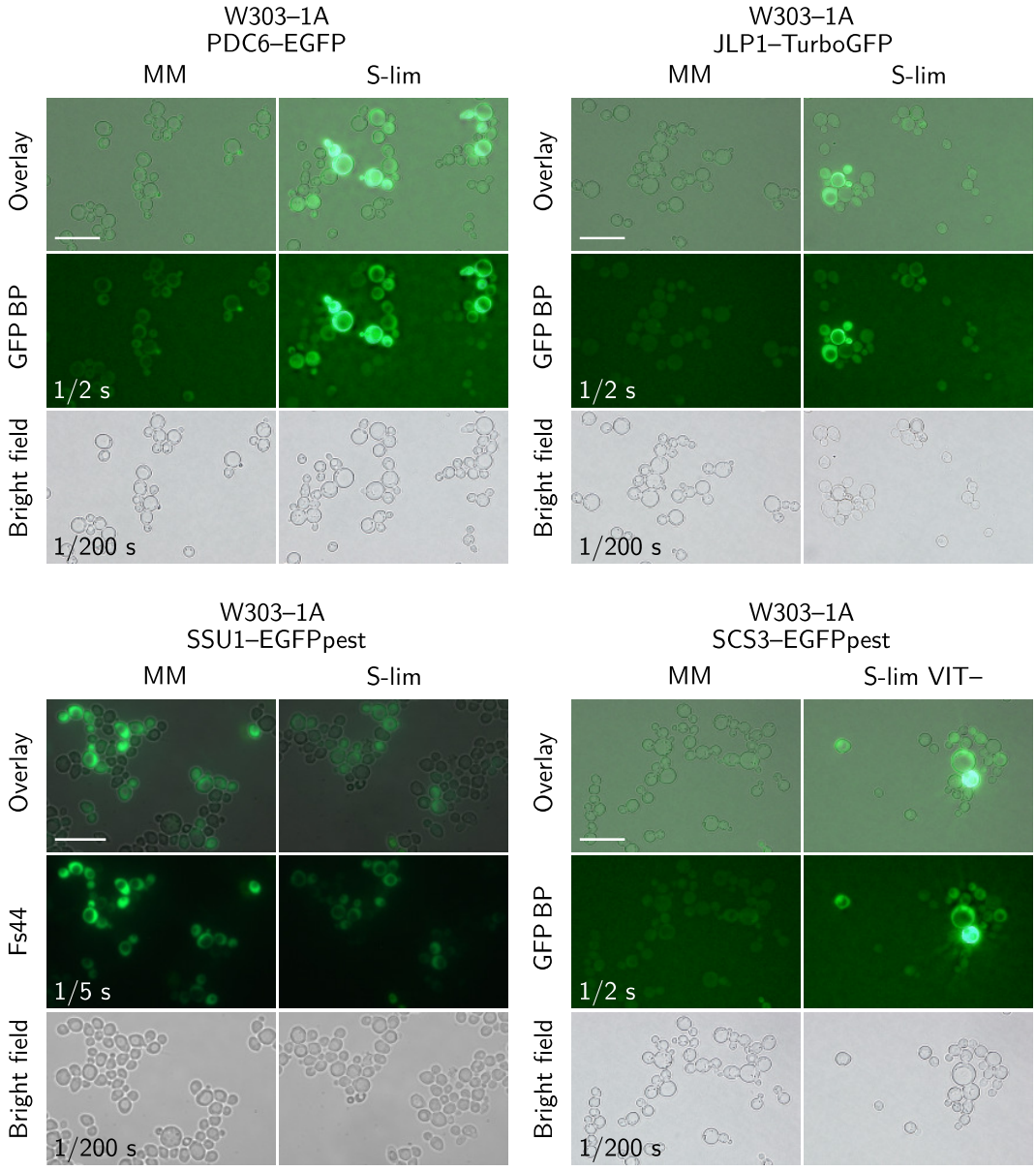

Figure 3.19: Microscopic analysis of sulphur sensor strains. Cells with detection plasmids p426PDC6–EGFP, p426JLP1–TurboGFP, p424SSU1–EGFPpest and p424SCS3–EGFPpest were imaged after cultivation in mineral medium (MM), sulphur limitation medium (S-lim) or sulphur limitation medium without vitamins (S-lim VIT–) using a Keyence BZ-8100 or Zeiss Axio Imager.1A fluorescence microscope with 1,000× magnification, GFP BP or Fs44 filter for fluorescence monitoring and given exposure times for each channel. Each image block shows the overlay (scale bar = 20 μm) and respective fluorescence and bright field images.

SCS3 sensor cells was only observed in the absence of vitamins with high cell-to-cell variation in brightness. Of all sulphur sensor strains, SSU1 sensor cells displayed the strongest fluorescence signal. About 30% of SSU1 sensor cells displayed moderate or high fluorescence in mineral medium and weak fluorescence in sulphur limitation medium.

Evaluation of nutrient sensor strains by flow cytometry

Fluorescence microscopy only allowed for rough estimation and qualitative analysis of sensor cells' fluorescence and morphology. Moreover, only limited amounts of cells can be analysed per set of images by this method. Flow cytometry was conducted in order to analyse nutrient sensor cells with a quantitative single-cell analysis method. GAP1, PHO11 and PDC6 sensor cells, all featuring higher fluorescence under nutrient deficiency, were cultivated in mineral medium or respective nutrient limitation medium for eight hours. This confers to the maximum exposure time of fluorometric analysis and yielded distinct fluorescence induction. Then, 40,000 sensor cells per strain and cultivation condition were analysed with regard to fluorescence and morphology (i.e. forward- and side-scattered light).

Results for the GAP1 sensor strain with moderate fluorescence in mineral medium and high fluorescence in nitrogen limitation medium is shown in Figure 3.20. Scatter plots of nitrogen-deficient and non-limited GAP1 sensor cells were similar. Both plots indicated a linear correlation between cell size and granular content of sensor cells. The fluorescence histogram of non-limited sensor cells featured a right-skewed distribution and, therefore, numerous cells with moderate fluorescence but also a scattered fraction of cells with bright fluorescence. Nitrogen deficiency resulted in particular right-shift of the fluorescence peak and a bell-shaped curve suggesting higher total fluorescence with widespread but symmetric distribution of bright and dim cells.

Results of single-cell analysis of PHO11 phosphorus sensor cells and PDC6 sulphur sensor cells are presented in Figures C.3 and C.4 (Appendix C.1). As observed for GAP1 sensor cells, scatter plots of non-limited and nutrient-deficient cells were comparable for every strain. A linear correlation between cell size and granular content was evident with slightly higher size distribution for nutrient-limited cells. Both strains exhibited lower basic fluorescence in mineral medium or triggered fluorescence in nutrient limitation than respective GAP1 nitrogen sensor cells which was expected regarding the data of microplate reader-based fluorometric analysis. In fact, non-limited sensor cells of both strains were detectable as a slim bell-shaped peak in the range of low fluorescence. Fluorescence curves of both cell populations were right-shifted in nutrient limitation medium because of promoter activation. The right-skewed shape with a tail indicated moderate fluorescence with a particular fraction of bright fluorescent cells. In both cases, fluorescence profiles were comparable to the histogram of non-limited GAP1 nitrogen sensor cells in mineral medium that equates moderate fluorescence.

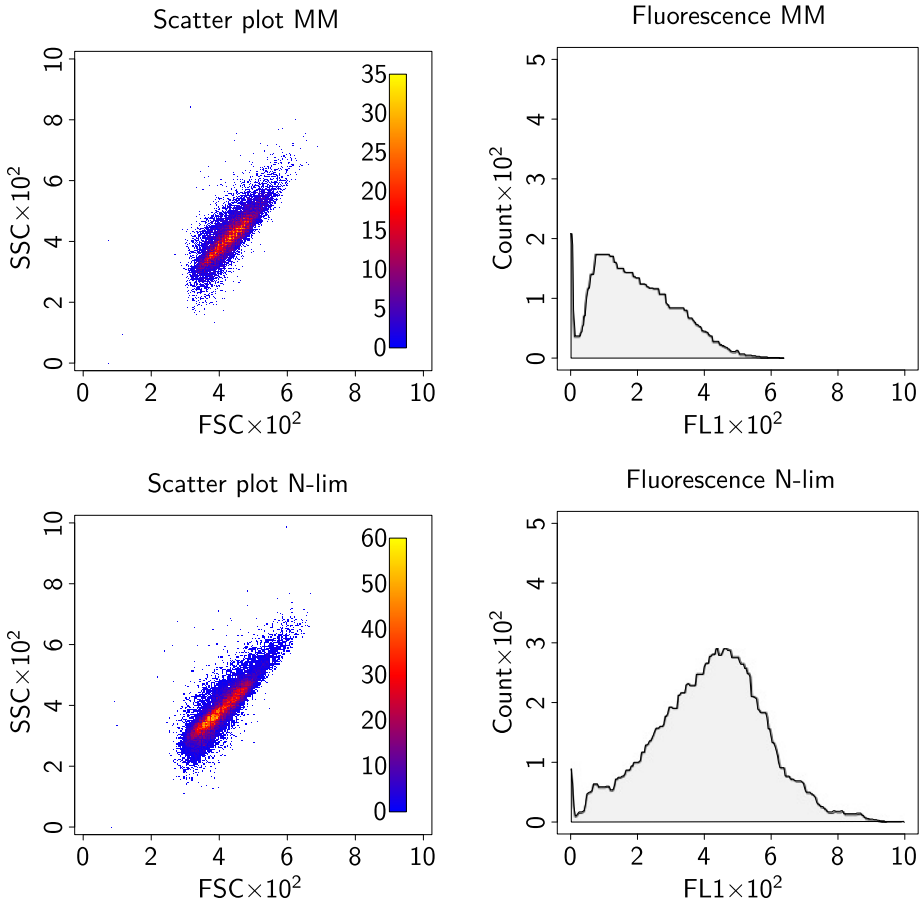

Figure 3.20: Flow cytometry analysis of GAP1 nitrogen sensor cells by flow cytometry. Cells of BY4741 harbouring sensor plasmid p426GAP1–TurboGFP were cultivated in mineral medium and then shifted to fresh mineral medium (upper panels) or nitrogen limitation medium (lower panels) for eight hours. For each condition, 40,000 cells were analysed using a Partec CyFlow SL flow cytometer with identical settings. Scatter plots of FSC (forward scatter channel) and SSC (side scatter channel) intensities which provide information about cell size and granular content, respectively, and green fluorescence histograms (FL1) are shown. Coloured legends in scatter plots specify the count of cells at given positions in plots.

3.2.8 Evaluation of specificity, sensitivity and selectivity of nutrient sensor strains

So far, functionality of nutrient-responsive yeast sensor strains was probed after shift from definite high to definite low concentrations of ammonium sulphate as the source of nitrogen and sulphur, or potassium phosphate as the source of phosphorus. Only one particular nutrient deficiency was considered for each sensor strain. Cross-reactivity of sensor cells in response to other nutrient limitations, the impact of variable nutrient concentrations as well as the influence of the nutrient source is documented for a selection of sensor strains in the following paragraphs.

Specificity of nutrient sensor strains

Transcription of signature genes *GAP1*, *PHO11* and *PDC6* is specifically induced upon limitation to nitrogen, phosphorus and sulphur, respectively (Tab. C.1, Appendix C.2). Specificity of the derived yeast sensor strains was confirmed by comparing fluorescence of sensor cells in non-limited mineral medium and all three limitation media (Fig. 3.21). Fluorescence was determined by microplate reader-based fluorometry and none of the sensor strains exhibited cross-reactivity. However, PDC6 sensor cells displayed slightly higher fluorescence in nitrogen and phosphorus limitation medium than in mineral medium after eight hours but fluorescence in response to sulphur limitation was significantly higher.

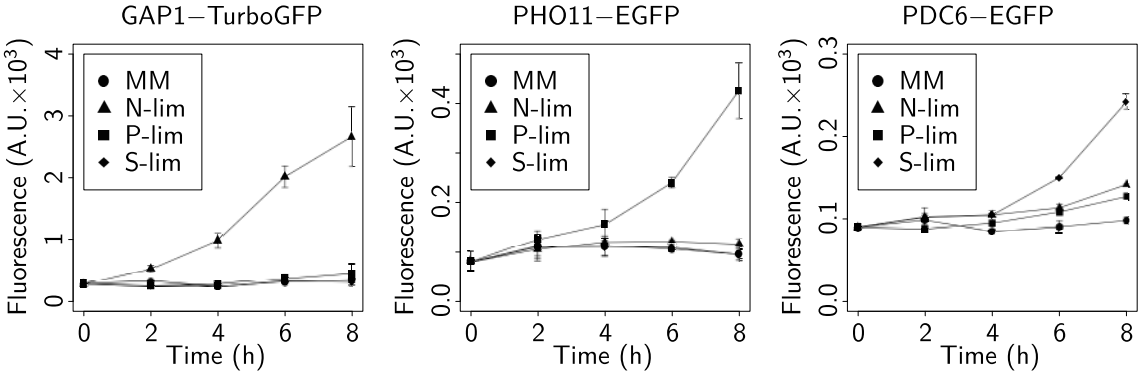

Figure 3.21: Cross-reactivity analysis of nutrient sensor strains. Cells of BY4741 harbouring detection plasmids p426GAP1–TurboGFP or p426PHO11–EGFP and W303–1A harbouring detection plasmid p426PDC6–EGFP were cultivated in mineral medium (MM) or medium limited in nitrogen (N-lim), phosphorus (P-lim) or sulphur (S-lim). For each condition, about 10^6 cells were analysed using a TECAN Infinite microplate reader with excitation/emission wavelength of 490/520 nm and a gain of 100. Mean values ± sd of triple measurements are shown.

Sensitivity of nutrient sensor strains

The GAP1 and GNP1 nitrogen sensor strains displayed a distinct change of fluorescence levels after shift from 5 to 0.05 g l^{-1} ammonium sulphate, i.e. from mineral medium to

nitrogen limitation medium. Variation in fluorescence as a function of different ammonium concentrations was tested for both sensor strains. The result is shown in Figure 3.22. Fluorescence values are given as difference of the observed fluorescence intensity in the presence of indicated ammonium sulphate concentrations to fluorescence intensity in mineral medium as the reference condition. Importantly, time trend fluorescence curves for sensor cells that were batch-cultivated in the presence of 5 g l^{-1} and 50 mg l^{-1} ammonium sulphate (corresponding to mineral medium and nitrogen limitation medium, respectively) were in agreement with the curves depicted in Figure 3.7 and Figure 3.10 (Section 3.2.4).

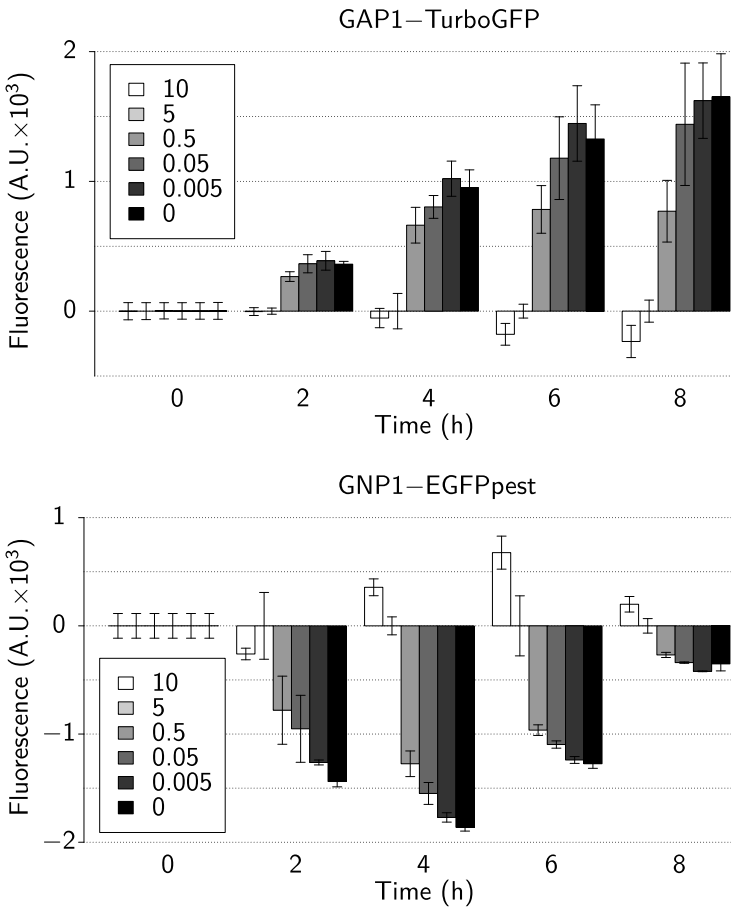

Figure 3.22: Fluorescence of nitrogen sensor strains as a function of nitrogen concentration. Strains BY4741 and W303–1A were transformed with detection plasmids p426GAP1–TurboGFP and p424GNP1–EGFPpest, respectively, and grown in mineral medium with the given ammonium sulphate concentrations (in g l^{-1}). Total fluorescence of about 10^6 cells was determined at indicated time points using a TECAN Infinite microplate reader with excitation/emission wavelength of 490/520 nm and a gain of 100. Fluorescence is given as the signal difference to fluorescence of cells that were grown in mineral medium containing 5 g l^{-1} ammonium as a reference (depicted as the base line). Mean values ± sd from three independent measurements are shown.

All concentrations below 5 g l^{-1} ammonium sulphate triggered higher fluorescence in GAP1 sensor cells and lower fluorescence in GNP1 sensor cells. Response of sensor cells was graded if the ammonium concentration was stepwise changed in intervals of one order of magnitude. Changes were observed already after two hours. The highest fluorescence

yield was observed after eight hours for GAP1 sensor cells mediating fluorescence of stable TurboGFP, and after four hours for GNP1 sensor cells producing destabilised EGFPpest. Strong fluorescence of GAP1 sensor cells was even triggered in complete absence of ammonium suggesting certain robustness of heterologous gene expression to nitrogen deficiency. Cells may mobilise intracellular, stored nitrogen resources for protein synthesis for a limited period of time. Interestingly, fluorescence of non-limited cells was slightly affected if ammonium sulphate was in surplus (10 g l^{-1}). In detail, GAP1 and GNP1 cells displayed lower and higher fluorescence than in 'standard' mineral medium, respectively. These data prove excellent capability of both nitrogen sensor strains to monitor short-term and long-term variation in ammonium availability.

The ability of TMA10 and PDC6 sensor cells to monitor different concentrations of phosphorus and sulphur, respectively, was probed (Fig. 3.23). Again, time trend fluorescence curves of non-limited sensor cells in mineral medium containing 1 g l^{-1} potassium phosphate and 5 g l^{-1} ammonium sulphate were in line with corresponding curves depicted in Figure 3.12 (Section 3.2.5) and Figure 3.15 (Section 3.2.6). TMA10 phosphorus sensor cells displayed only slightly higher fluorescence if the potassium phosphate concentration was reduced to 0.1 g l^{-1}. The signal level was steady after two hours. Concentrations of 0.01 g l^{-1} phosphate (equates limitation medium) and 0 g l^{-1} phosphate induced graded fluorescence signals although cells featured the destabilised fluorescent reporter EGFPpest. Distinct signals were observed after four to six hours. Response of PDC6 sensor cells was graded too but yielded lower and delayed fluorescence. Concentrations of 0.5 and 0.05 g l^{-1} ammonium sulphate that strongly affected fluorescence of nitrogen sensor strains, triggered only weak fluorescence of PDC6 sulphur sensor cells after four hours. Lower tested concentrations induced graded, moderate fluorescence after six hours. In conclusion, TMA10 and PDC6 sensor cells displayed only sufficient fluorescence in the presence of nutrient concentrations which correspond to the levels in respective nutrient limitation medium. Activation of PDC6 sulphur sensor cells required a low sulphur threshold and long time indicating a generally low sulphur demand of yeast cells and/or delayed activation of the *PDC6* promoter.

Evaluation of nitrogen sensor strain response to different nitrogen sources

The ability of GAP1 and GNP1 nitrogen sensor strains to monitor variable ammonium levels in mineral medium was successfully shown. Ammonium is a preferred nitrogen source but yeast can also uptake and metabolise a palette of other nitrogen sources from its environment. As a proof of concept, response of GAP1 and GNP1 nitrogen sensor strains to amino acids as the sole nitrogen source was analysed. To this end, sensor cells were batch-cultivated in mineral medium with 5 g l^{-1} ammonium sulphate and shifted to fresh medium with 5 and 0.05 g l^{-1} ammonium sulphate both as a reference, or with equal molar amounts of amino acids L-glutamine or L-alanine. Both nitrogen compounds

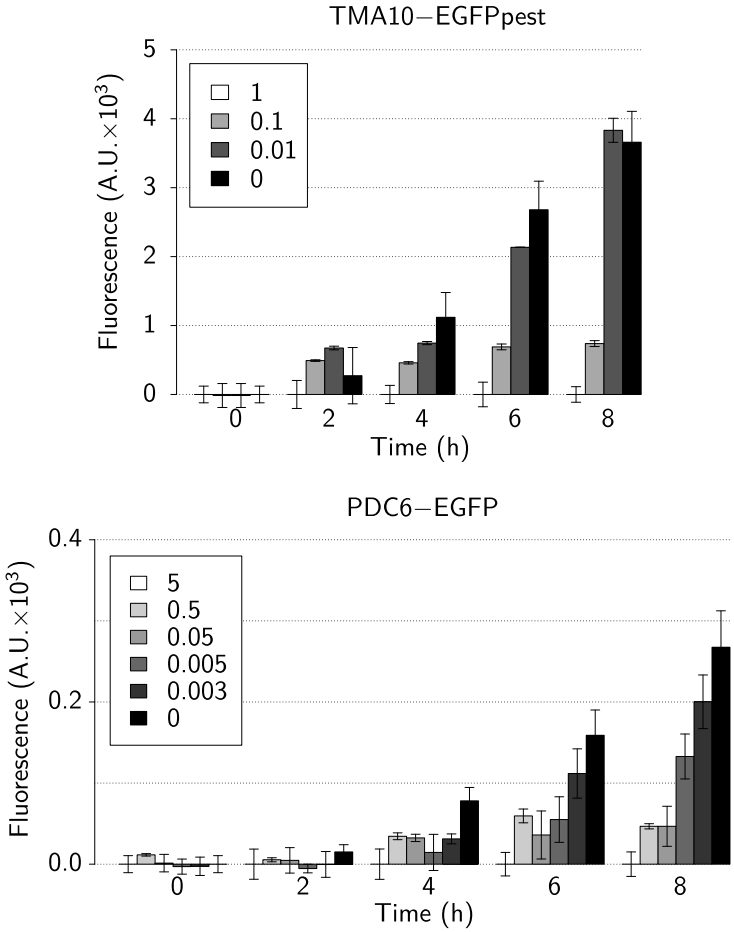

Figure 3.23: Fluorescence of phosphorus and sulphur sensor strains as a function of nutrient concentration. Cells of phosphorus sensor strain BY4741 with detection plasmid p426TMA10–EGFPpest and sulphur sensor strain W303–1A with detection plasmid p426PDC6–EGFP were cultivated in mineral medium with the given concentrations of potassium phosphate or ammonium sulphate (in g l^{-1}). Total fluorescence of about 10^6 cells was determined at indicated time points using a TECAN Infinite microplate reader with excitation/emission wavelength of 490/520 nm and a gain of 100. Fluorescence is given as the signal difference to fluorescence of cells that were grown in mineral medium containing 5 g l^{-1} ammonium sulphate and 1 g l^{-1} potassium phosphate as a reference (depicted as the base line). Mean values ± sd from three independent measurements are shown.

enter the nitrogen metabolism of yeast via different pathways and may therefore trigger differential response of the two nitrogen sensor strains. Glutamine is a preferred nitrogen source and a direct nitrogen donor for other nitrogen compounds in yeast. L-alanine is a poor nitrogen source that enters the pathway by degradation to α-ketoglutarate and subsequent conversion to glutamate or glutamine.

Fluorescence of GAP1 and GNP1 sensor cells was monitored by microplate reader-based fluorometry in a time-dependent manner (Fig. 3.24). GAP1 sensor cells showed a similar response to ammonium and amino acid L-glutamine. Fluorescence of sensor cells was constantly low in mineral medium with excess of ammonium or L-glutamine, and triggered in a similar manner in respective limitation media. In the presence of low and high L-alanine concentrations however, a threefold stronger fluorescence was observed in GAP1 sensor cells. A significant difference in fluorescence of GNP1 sensor cells was only observed in media containing ammonium as nitrogen source. Fluorescence of sensor cells was steadily decreasing in the presence of high and low concentrations of both amino acids. Differential response of GAP1 and GNP1 nitrogen sensor strains to the same nitrogen source indicates different regulation of both the *GAP1* and *GNP1* promoter in the presence of preferable and less preferable nitrogen sources. Thus, applicability of sensor strains may be limited and has to be evaluated for other sensor strains as well.

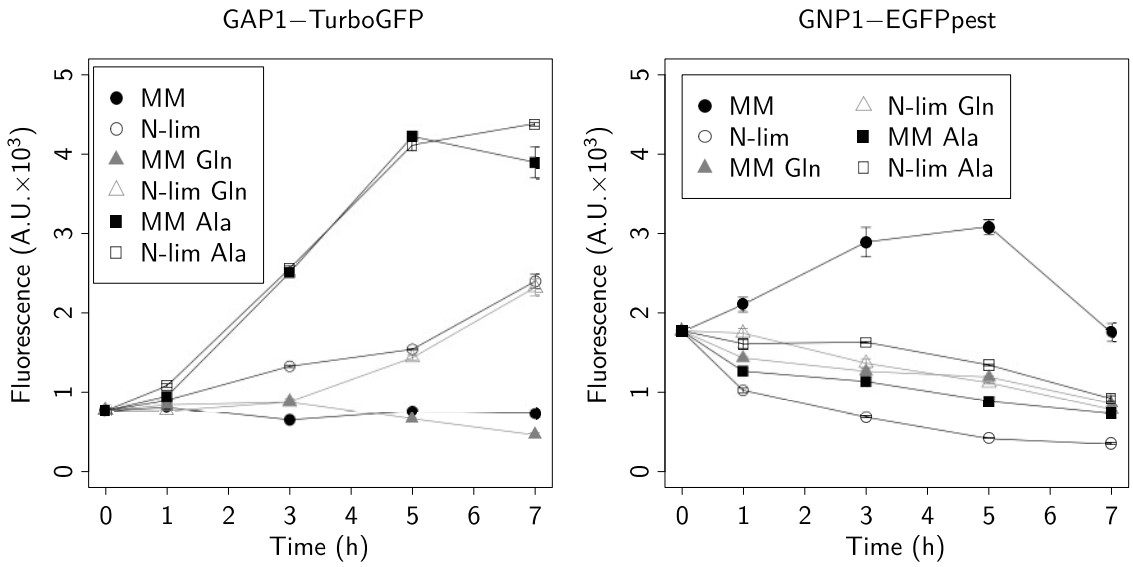

Figure 3.24: Fluorescence of nitrogen sensor strains in response to different nitrogen sources. Strains BY4741 with detection plasmid p426GAP1–TurboGFP and W303–1A with detection plasmid p424GNP1–EGFPpest were cultivated in mineral medium (MM) or nitrogen limitation medium (N-lim) using ammonium sulphate as the nitrogen source or equimolar amounts of L-glutamine (Gln) or L-alanine (Ala). Total fluorescence of about 10^6 cells was determined using a TECAN Infinite microplate reader with excitation/emission wavelength of 490/520 nm and a gain of 100. Mean values $\pm$ sd from three measurements are shown.

3.2.9 Regeneration of basic fluorescence of nutrient sensor strains

In all previously described experiments, fluorescence of nutrient sensor strains was examined after shift of cells from high to low concentrations of a certain nutrient to follow expression of reporter genes after exposure to particular nutrient limitation. Sensor strains with higher fluorescence in limitation to nitrogen (GAP1), phosphorus (PHO11, TMA10) and sulphur (PDC6) displayed steadily increasing fluorescence within eight hours after shifting cells to respective nutrient-deficient medium. Fluorescence of GNP1 nitrogen sensor cells was decreasing in nitrogen limitation but strong fluorescence fluctuation was also observed in mineral medium. This probably resulted from instability of employed EGFPpest reporter protein.

It was examined whether the above mentioned sensor strains were able to restore the basic fluorescence level if sensor cells were shifted from nutrient limitation medium with low nutrient availability to mineral medium with high nutrient availability (regeneration). Since expression of fluorescence reporter genes from signature promoters should reach their basic levels in non-limited medium, a distinct fluorescence decline was expected for all strains except GNP1 sensor cells. Sensor cells were grown in respective nutrient limitation media for 20 hours and either cultivated further in nutrient deficiency as a control or shifted to mineral medium for regeneration. Fluorescence was monitored over eight hours by microplate reader-based fluorometry (Fig. 3.25)

Observed fluorescence of sensor strains with detection plasmids p426GAP1–TurboGFP (nitrogen), p426PHO11–EGFP (phosphorus) and p426PDC6–EGFP (sulphur) was in good agreement with expectations. High signals with a shallow depression after the shift were detected for nutrient-limited sensor cells while a distinct and steady signal decline was observed after shift to mineral medium for regeneration. Within eight hours the basic level of non-limited sensor cells was not reached. TMA10 sensor cells featuring destabilised EGFPpest yielded poor fluorescence after 20 hours of growth in nitrogen limitation medium. Instead of fluorescence decline after shift to mineral medium, regeneration of fluorescence after shift to fresh limitation was observed. Destabilised reporter EGFPpest was therefore not suitable to monitor fluorescence of sensor cells after long pre-cultivation in batch cultures. GNP1 sensor cells displayed low fluorescence after overnight cultivation in nitrogen limitation medium as expected. This may result from both down-regulation of the *GNP1* promoter and EGFPpest instability. Fluorescence was constantly low at subsequent cultivation in limited medium and steadily increasing after shift to mineral medium. Interestingly, the signal curves of cells that were primarily addressed to limitation and regeneration, respectively, were not congruent.

Persistent fluorescence of sensor strains with EGFP and TurboGFP after eight hours of regeneration may result from stability of reporter proteins. So far, fluorescence decline was observed on cell population level. Results of flow cytometry analysis for GAP1,

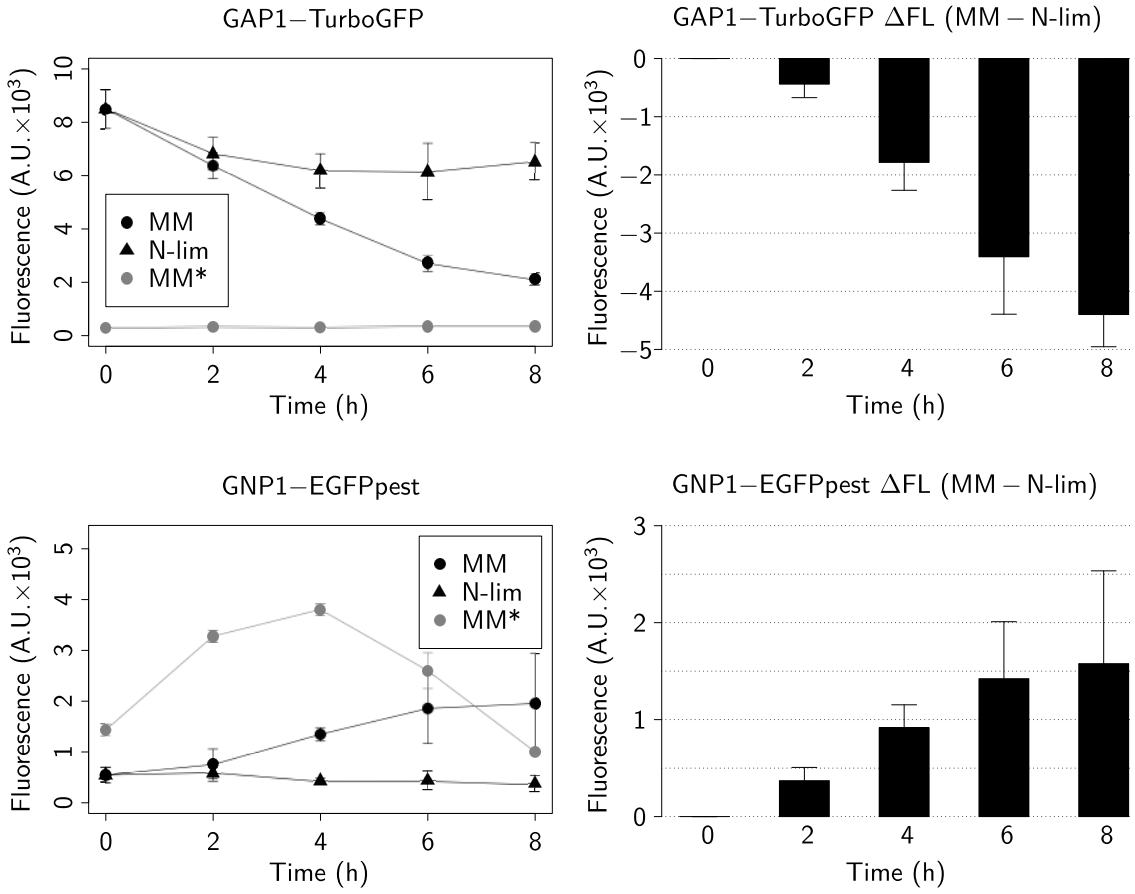

Figure 3.25: Fluorescence regeneration of nutrient sensor strains after pre-cultivation in limitation medium [Continued on Next Page]. Cells of BY4741 harbouring detection plasmids p426GAP1–TurboGFP, p426PHO11–EGFP or p426TMA10–EGFPpest and W303–1A harbouring detection plasmids p424GNP1–EGFPpest or p426PDC6–EGFP were shifted to mineral medium (MM) for regeneration or to medium limited in nitrogen (N-lim), phosphorus (P-lim) or sulphur (S-lim) after pre-cultivation in respective limitation medium. MM* gives the basic fluorescence of sensor cells in mineral medium. Total fluorescence of about 10^6 cells was analysed using a TECAN Infinite microplate reader with excitation/emission wavelength of 490/520 nm and a gain of 100. Time trend curves (left) and difference in fluorescence of sensor cells in mineral medium and nutrient limitation medium (right) are depicted. Mean values ± sd from three independent measurements are shown.

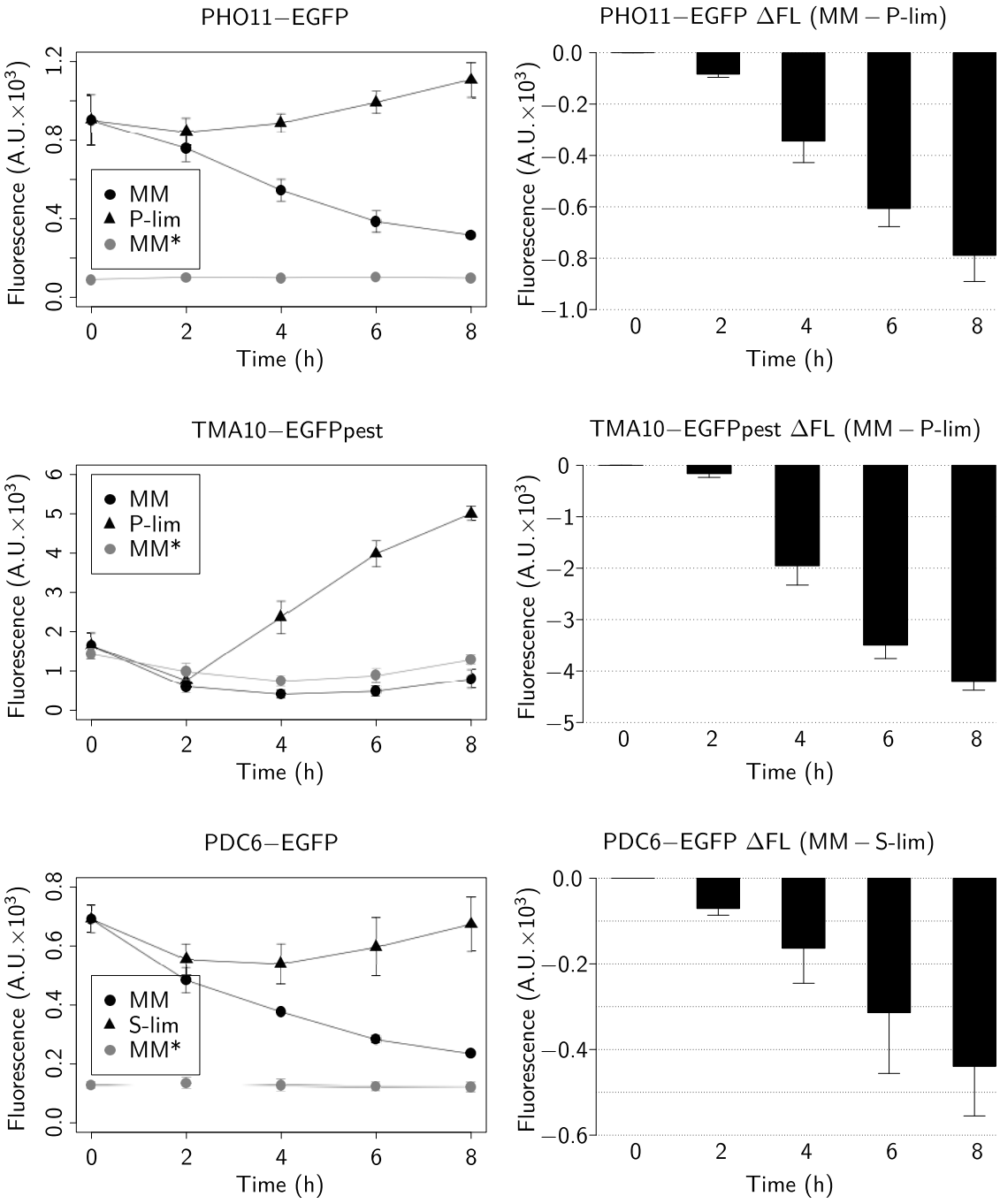

Figure 3.25: [Continued]

PHO11 and PDC6 sensor cells indicates that fluorescence decreases on the level of single cells over time in a similar manner (Figs. C.5–C.7, Appendix C.1). After eight hours, a left-shift of fluorescence peaks towards lower fluorescence was observed for all regenerated sensor cell populations. Besides a lower value of the fluorescence peak, the fluorescence profile typically changed from a right-skewed curve with a broad right shoulder to a bell-shaped curve with a truncated right shoulder.

3.2.10 Evaluation of a dual-colour nitrogen sensor strain

A set of yeast sensor strains for the monitoring of macronutrient availability was recently evaluated. Each sensor strain harbours one detection construct and all detection plasmids feature expression of reporter genes encoding green fluorescent reporter proteins. Advanced sensor cells with multiple detection constructs are convenient in order to double-check limitation occurrence or to sense multiple parameters. However this requires the implementation of two fluorescent reporters which can be detected simultaneously. It was earlier shown in this work that TurboRFP yields bright fluorescence in yeast reporter cells (Section 3.1.1), and detection of green and red fluorescent proteins can be mainly resolved with appropriate filters and excitation/emission settings.

Performance of dual-colour yeast sensor cells with simultaneous expression of reporter genes encoding green and red fluorescent proteins was examined as a proof of concept. GAP1 nitrogen sensor cells that exhibit bright green fluorescence in nitrogen-deficient medium were transformed with a second plasmid for moderate red fluorescence. Plasmid p423ADH–TurboRFP was engineered by cloning the PCR-amplified open reading frame of TurboRFP into yeast expression vector p423ADH. This vector contains a selection marker to complement histidine auxotrophy of BY4741. For control, GAP1 sensor cells were transformed with the parental vector p423ADH. Since selection of the sensor plasmid p426GAP1–TurboGFP was based on uracil, propagation of both plasmids in dual-colour sensor cells is ensured.

GAP1 dual-colour sensor cells were examined by microplate reader-based fluorometry. Cells were grown in mineral medium and then transferred to fresh mineral medium or to nitrogen limitation medium to trigger green fluorescence that was mediated by the GAP1–TurboGFP detection construct. Green and red fluorescence of GAP1 dual-colour sensor cells was monitored over eight hours (Fig. 3.26A). Expression of TurboRFP from the *ADH* promoter was comparable for non-limited and nitrogen-deficient cells. After four hours, a slight decline of red fluorescence was observed in nitrogen limitation medium. Shift of GAP1 dual-colour sensor cells to nitrogen limitation medium induced green fluorescence as expected.

Green and red fluorescence of GAP1 control sensor cells and dual-colour sensor cells was compared with regard to fluorescence signal yield and specificity of both fluorescent reporters in their dedicated channels. In addition, reporter cells harbouring

the plasmid p423ADH–TurboRFP (no GFP) were examined. Cells were cultivated in mineral medium or nitrogen limitation medium for eight hours and hourly analysed by microplate reader-based fluorometry (Fig. 3.26B). Red fluorescence was not detectable for GAP1 control sensor cells. GAP1 dual-colour sensor cells displayed comparable red fluorescence in both media as observed in the time trend analysis. The signal level was notably lower than in reporter cells expressing only TurboRFP. One reason may be that overexpression of two reporter genes causes limitation of transcription factors (Weber et al., 1992). This could result in lower signal yield. Interestingly, expression of TurboRFP was detectable in the green fluorescence channel since a distinct signal was observed for reporter cells with plasmid p426ADH–TurboRFP. This 'bleed-through effect' still allowed for the monitoring of changes in nitrogen availability. A threefold induction of green fluorescence was detectable in nitrogen limitation medium with both GAP1 control and dual-colour sensor cells.

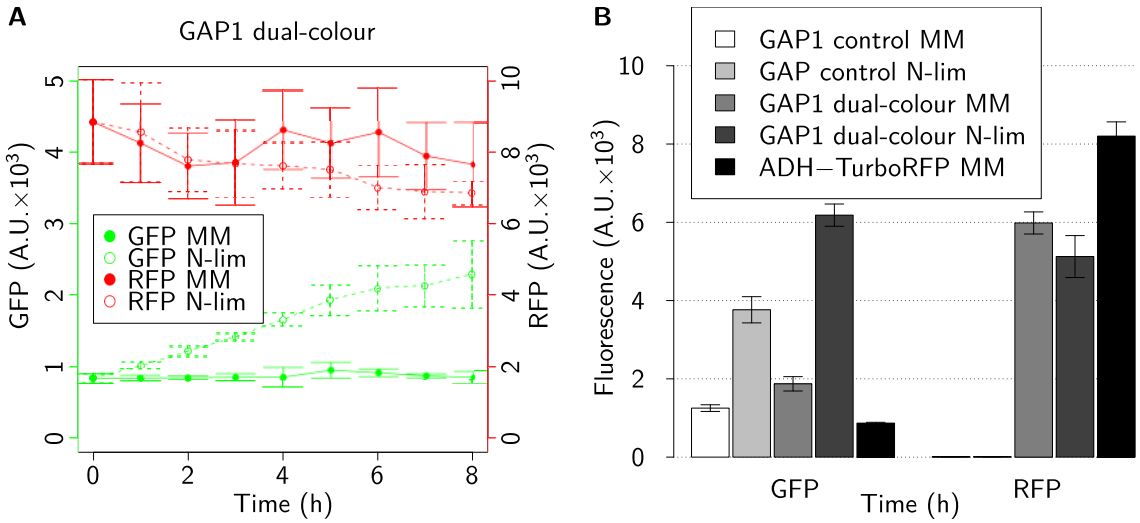

Figure 3.26: Evaluation of a dual-colour nitrogen sensor strain. Nitrogen sensor strain BY4741 harbouring detection plasmid p426GAP1–TurboGFP was transformed with plasmid p423ADH–TurboRFP for moderate red fluorescence yielding GAP1 dual-colour sensor cells, or with parental vector p423ADH as a control. **A** Time trends of green and red fluorescence of the GAP1 dual-colour sensor strain in mineral medium (MM, solid line) or after shift to nitrogen limitation medium (N-lim, dashed line) are shown in green and red curves. Total fluorescence of about 10^6 cells was determined using a TECAN Infinite microplate reader. GFP and RFP were tracked with excitation/emission wavelength of 490/520 nm and 550/580 nm, respectively, and a gain of 100. Mean ± sd from three independent measurements are shown. **B** Green and red fluorescence of GAP1 control and GAP1 dual-colour sensor strain as well as cells of BY4741 harbouring only p423ADH–TurboRFP was determined in respective media as described above.

Fluorescence of GAP1 control and dual-colour sensor strains was also examined on the level of single cells by fluorescence microscopy (Fig. 3.27). Again, cells were batch-cultivated in mineral medium or nitrogen limitation medium for six hours before analysis. In line with the results for GAP1 nitrogen sensor cells in Section 3.2.7 and the fluorometry data above, GAP1 control sensor cells displayed moderate and high green

fluorescence in mineral medium and nitrogen limitation medium, respectively, but no red fluorescence. Basic green fluorescence of GAP1 dual-colour sensor cells was particularly higher than of GAP1 control sensor cells but increased under nitrogen limitation too. In contrast, moderate red fluorescence was observed in both cultivation media. This resulted in a visible shift from red to yellow appearance of cells in the image overlays. Within the cell populations, single cell fluorescence signals varied which was observed before for other plasmid-based sensor strains. This phenomenon was even more apparent and complex since four fractions of cells displaying only green or only red, both green and red, or no fluorescence at all were found.

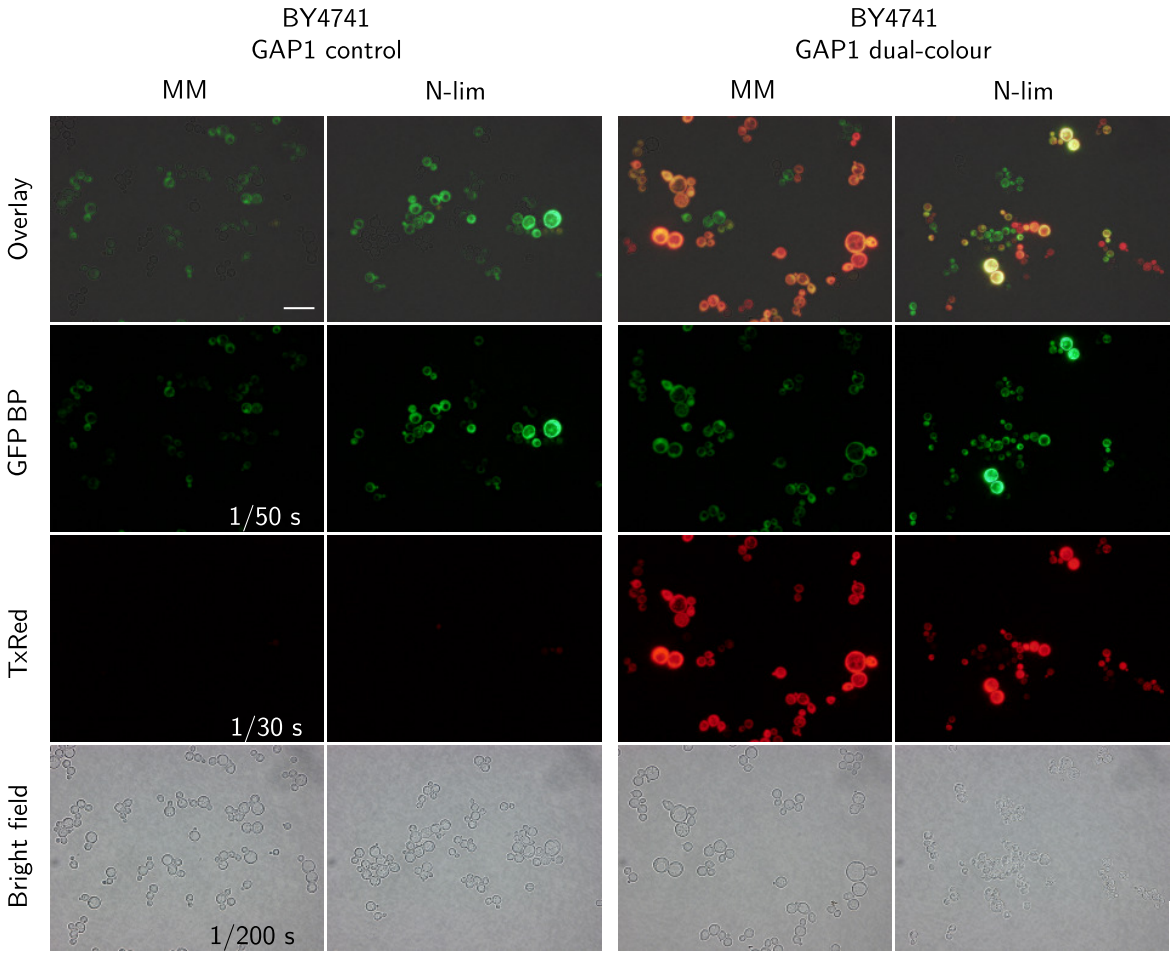

Figure 3.27: Microscopic analysis of a dual-colour nitrogen sensor strain. Cells of nitrogen sensor strain BY4741 harbouring detection plasmid p426GAP1–TurboGFP were transformed with vector p423ADH as control or p423ADH–TurboRFP for moderate red fluorescence (GAP1 dual-colour). Cells were imaged six hours after shift to mineral medium (MM) or nitrogen limitation medium (N-lim) using a Keyence BZ-8100 fluorescence microscope with 1,000x magnification, GFP BP or TxRed filters for green and red fluorescence tracking, and given exposure times in each channel. Each image block shows overlay (scale bar = 20 μm) of green and red channel and bright field images.

In another attempt, brightness and fluorescence variance of GAP1 control and dual-colour sensor cells under non-limited and nitrogen-limited cultivation conditions were quantified on the level of single cells by software-assisted, semi-automated microscopy

image analysis. To this end, three to four microscopic images were taken with identical settings for all strains and cultivation conditions (see Figure 3.27). Per strain and condition, green and red fluorescence of 114–177 individual cells was analysed with the software CellProfiler. Values ranged from zero (black, no fluorescence) to one (white, saturated fluorescence) in their dedicated channel. The result is shown in Figure 3.28. Observations considering the signal yield were in good agreement with data of microplate reader-based fluorometry. Nitrogen-deficient GAP1 sensor cells exhibited slightly lower median fluorescence than non-limited sensor cells. This was partially compensated by a higher maximum fluorescence value. Variation in green fluorescence of GAP1 control and dual-colour sensor strains was comparable for each cultivation condition. In mineral medium, variation was moderate. After shift to nitrogen limitation medium, higher variation rather than higher median fluorescence was observed. Thus, higher total fluorescence results from a fraction of sensor cells with extraordinary brightness.

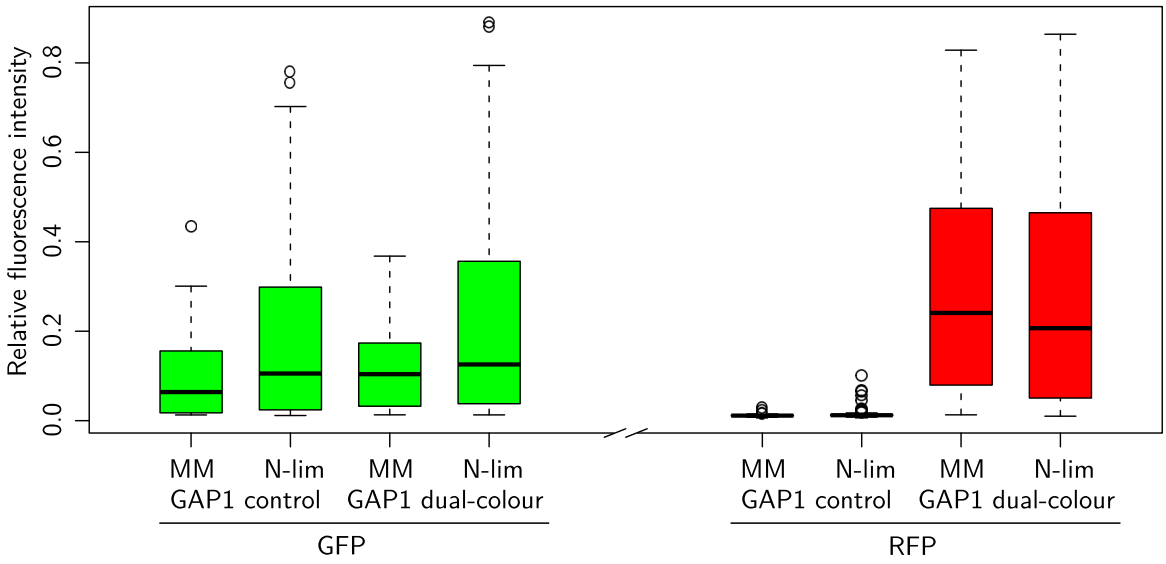

Figure 3.28: Fluorescence variation of nitrogen sensor strains. Cells of nitrogen sensor strain BY4741 harbouring detection plasmid p426GAP1–TurboGFP were transformed with vector p423ADH as a control or p423ADH–TurboRFP for moderate red fluorescence (GAP1 dual-colour). Variation in green (TurboGFP) and red (TurboRFP) fluorescence for both strains in mineral medium (MM) and nitrogen limitation medium (N-lim) is shown, given as relative values in a range from zero (no fluorescence) to one (saturated fluorescence). GAP1 control cells exhibited no red fluorescence since values were below 0.1. Boxes visualise the interquartile range (IQR) with median (black line). Whiskers show the minima/maxima and circles suspected outliers ($>1.5\times$IQR).

3.2.11 Nitrogen sensor strain with a genome-integrated detection construct

Aims and strategy

So far, comprehensive evaluation of fluorescent reporter and nutrient sensor strains in this work was carried out using a set of tailored multicopy detection plasmids. However, the plasmid-based expression strategy posed problems regarding cell-to-cell variance of signal intensity and loss of fluorescence yield during extended storage of sensor strains. As a countermeasure, a sensor strain with a genome-integrated detection construct as an alternative expression strategy was engineered. Lowering the number of detection constructs to one copy per cell was expected to reduce signal yield significantly. Nitrogen detection construct GAP1–TurboGFP was selected for these studies because of the excellent plasmid-based fluorescence yield.

Based on the work of Mirisola et al. (2007), an integration vector was generated. It allows for the expression of the GAP1–TurboGFP detection construct from a disrupted chromosomal *TYR1* locus. Furthermore the vector can be easily used to clone a multitude of other detection cassettes for other integration purposes. The cloning strategy is illustrated in Figure B.3 (Appendix B.3). The replacement cassette includes a *TRP1* marker for complementation of tryptophan auxotrophy of yeast strain W303–1A and the GAP1–TurboGFP detection construct comprising the *GAP1* promoter, the coding sequence of fluorescent reporter TurboGFP and the *CYC1* terminator. The cassette was recovered from the confirmed integration vector and transformed into yeast strain W303–1A. Clones were double-selected for tyrosine auxotrophy and tryptophan prototrophy. Additionally, the correct integration was verified by diagnostic PCR (data not shown).

Evaluation of the genome-integrated nitrogen detection construct

The initial motivation to generate a nitrogen sensor strain with genome-integrated detection construct was to improve fluorescence uniformity of sensor cells. Genomic GAP1 sensor cells were thus examined first on the level of single cells. Cells were monitored by fluorescence microscopy after six hours of cultivation in mineral medium or after shift to nitrogen limitation medium (Fig. 3.29). In clear contrast to the plasmid-based GAP1 sensor strain (see Figure 3.17, Section 3.2.7), cells with the genome-integrated construct displayed weak but uniform fluorescence with low cell-to-cell variance. In addition, all cells were fluorescent demonstrating uniform response of sensor cells.

Three to five microscopic images of non-limited and nitrogen-limited GAP1 sensor cells (plasmid-based and genome-integration) were analysed with the software CellProfiler to determine fluorescence intensity of 87–254 single cells per strain and cultivation condition. Cells of the same strain were imaged with identical settings under both cultivation conditions. Intensity ranged from zero (no fluorescence, black) to one (saturated

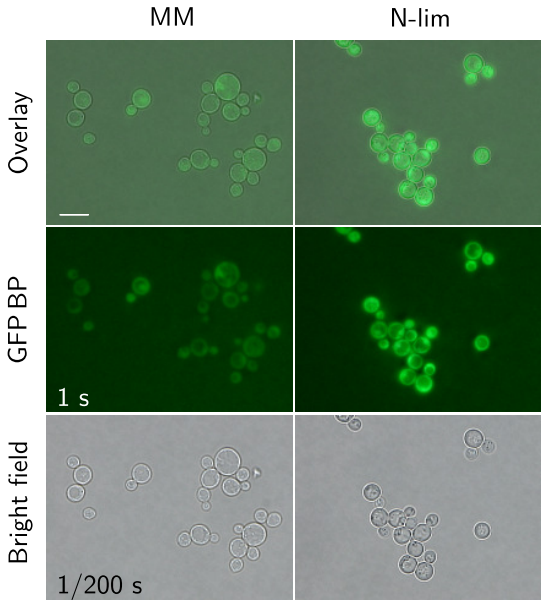

Figure 3.29: Microscopic analysis of genome-integration yeast sensor cells for monitoring of nitrogen availability. For yeast strain W303–1A with expression of TurboGFP from the *TYR1* locus representative images of sensor cells in mineral medium (MM) or nitrogen limitation medium (N-lim) are shown. Each microscopic image block shows the overlay (scale bar = 20 μm) and respective fluorescence and bright field images. Cells were monitored using a Keyence BZ-8100 fluorescence microscope with 1,000x magnification, GFP BP filter for fluorescence monitoring and given exposure times for each channel.

fluorescence, white). In line with qualitative evaluation by eye, 100% of both cells populations harbouring the genome-integrated GAP1 detection construct displayed detectable fluorescence with significantly low cell-to-cell variance and a clear shift in response to nitrogen limitation (Fig. 3.30). This resulted in only a minor fraction of non-limited and nitrogen-limited genomic GAP1 sensor cells with overlapping fluorescence intensity values. In contrast, plasmid-based GAP1 sensor cells in mineral medium possessed nearly 100% overlapping fluorescence with nitrogen-limited cells.

Fluorescence was double-checked on the single-cell level by flow cytometry. Using the same measurement settings for each strain, 40,000 cells of both GAP1 sensor strains were analysed after overnight cultivation in mineral medium and nitrogen limitation (Fig. 3.31). Sensor strain populations exhibited a similar morphology, i.e. distribution in size and surface properties, but visibly different fluorescence profiles. Non-limited and nitrogen-limited cells with the genome-integrated GAP1 detection construct were displayed both in narrow, bell-shaped fluorescence histograms with symmetric shoulders and barely overlapping areas. The population of nitrogen-limited cells was significantly right-shifted indicating brighter fluorescence. Fluorescence profiles of plasmid-based sensor cells were right-skewed or bell-shaped with widespread shoulders (see Figure 3.20, Section 3.2.7). Here, signal values of the majority of cells were overlapping.

Uniform fluorescence of genome-integration GAP1 sensor cells was accompanied by reduced signal yield. In single-cell analysis, each strain was analysed with separately

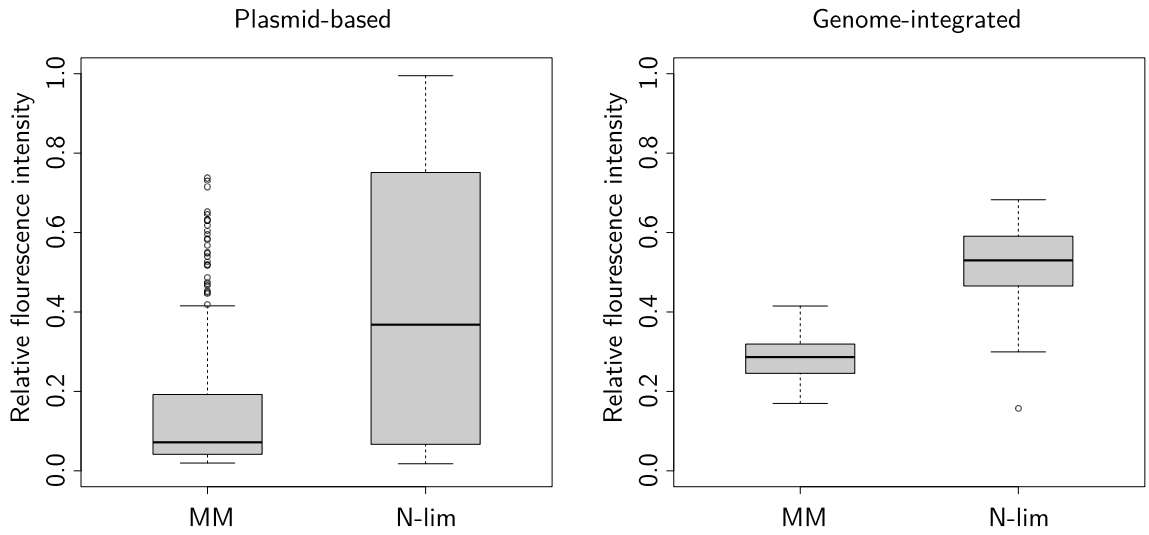

Figure 3.30: Fluorescence variation in plasmid-based and genome-integration nitrogen sensor cells. Nitrogen sensor strains with either detection plasmid p426GAP1–TurboGFP or genome-integrated GAP1–TurboGFP detection construct were cultivated in mineral medium (MM) and nitrogen limitation medium (N-lim). Variation in green fluorescence is displayed, given as relative values in the range from zero (no fluorescence) to one (saturated fluorescence). Boxes visualise interquartile range (IQR) with median (black line). Whiskers show minima/maxima and circles suspected outliers ($>1.5\times$IQR).

adapted settings to obtain optimum resolution. Now, total fluorescence was directly compared on the cell population level by microplate reader-based fluorometry with identical settings for plasmid-based and genome-integrated GAP1 sensor cells after six hours of cultivation in non-limited and nitrogen-limited conditions (Fig. 3.32A). Plasmid-based sensor cells displayed fivefold higher fluorescence in nitrogen limitation medium. Cells with the genome-integrated GAP1 detection construct yielded less than twofold induction and hardly reached the basic fluorescence signal level of plasmid-based GAP1 sensor cells.

To follow the dynamics of fluorescence display in genome-integration GAP1 sensor cells, total fluorescence was probed after shift from high to low nitrogen availability (induction) and *vice versa* (regeneration). Results of microplate reader-based fluorometry are depicted in Figure 3.32B. After shift of cells from mineral medium to nitrogen limitation medium, the signal increased steadily and reached a 1.6-fold higher level than in non-limited cells after eight hours. Phosphorus and sulphur limitations did not affect fluorescence which was expected from the data with the plasmid-based detection construct (see Figure 3.21, Section 3.2.8). Accordingly, fluorescence of pre-limited cells was higher than fluorescence after shift to nitrogen-deficient medium for eight hours. Regeneration of cells was fast and yielded 1.3-fold of the basic fluorescence signal of non-limited cells.

In conclusion, the genome-integrated GAP1 nitrogen sensor strain was superior to its plasmid-based counterpart in terms of signal uniformity and reliability of expression. However, severe loss of total signal yield was a major drawback.

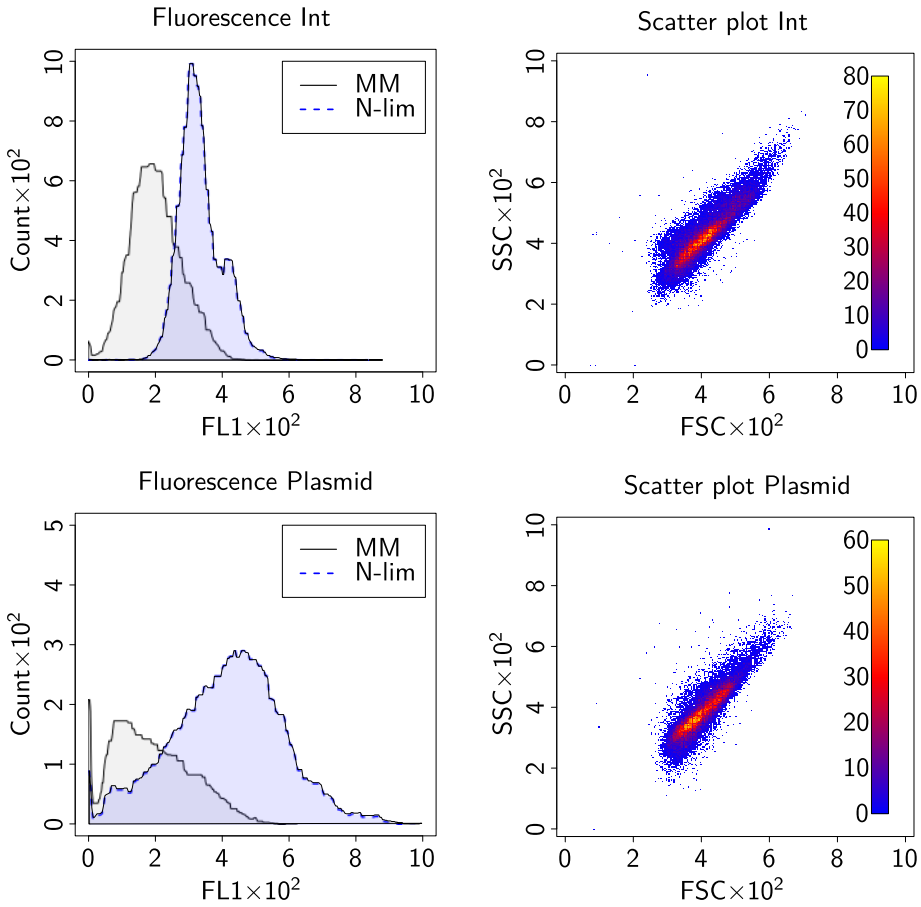

Figure 3.31: Flow cytometry analysis of plasmid-based and genome-integration (labelled with 'Int') nitrogen sensor strains. Cells were monitored after overnight cultivation in mineral medium (MM) or nitrogen limitation medium (N-lim). Per analysis, 40,000 cells were monitored using a Partec CyFlow SL flow cytometer. Settings were adjusted separately for each strain but applied consistently. Green fluorescence histograms (FL1) of all samples and scatter plots of nitrogen-limited cells are shown. Coloured legends in scatter plots specify the count of cells at given positions in plots. FSC (forward scatter channel) and SSC (side scatter channel) intensities which provide information about cell size and granular content, respectively, were similar for all samples.

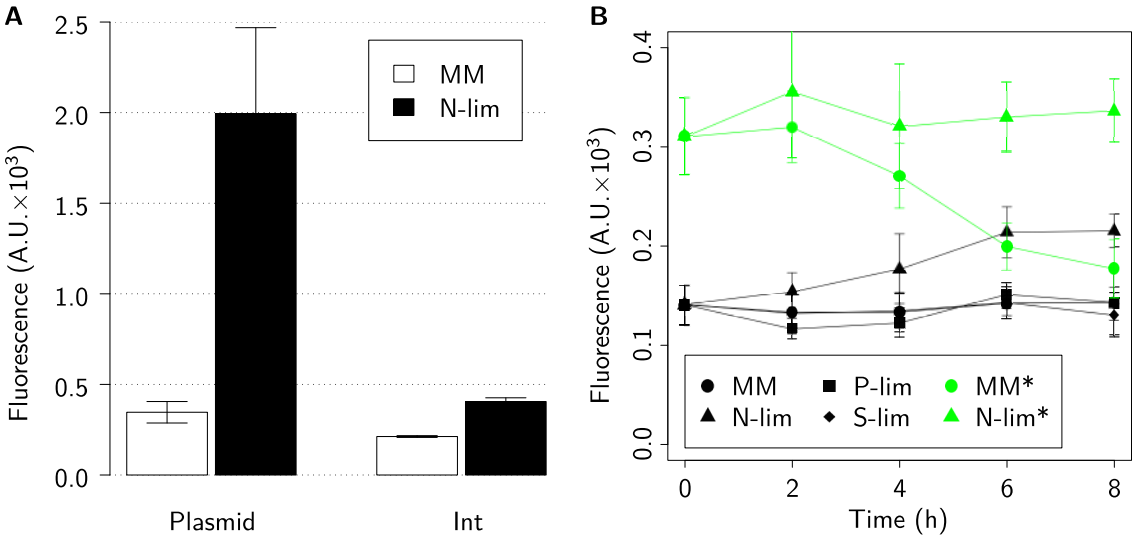

Figure 3.32: A Comparison of fluorescence signal yield between plasmid-based and genome-integration nitrogen sensor strains. Cells of BY4741 harbouring detection plasmid p426GAP1–TurboGFP ('plasmid') and W303–1A with genome-integrated GAP1–TurboGFP ('Int') were cultivated in mineral medium (MM) and nitrogen limitation medium (N-lim). Total fluorescence of about 10^6 cells was detected using a TECAN Infinite microplate reader with excitation/emission wavelength of 490/520 nm and a gain of 100. Mean values ± sd from three independent measurements are shown. **B** Fluorescence of the genome-integration nitrogen sensor strain after transfer from mineral medium (black curves) or nitrogen limitation medium (∗, green curves) to fresh mineral medium or shift to medium limited in nitrogen, phosphorus (P-lim) or sulphur (S-lim). Measurements were performed as described in A.

3.2.12 Evaluation of nutrient sensor cells in microalgae media

Aims and strategy

It was hypothesised that *S. cerevisiae* can grow on a broad range of media and can be useful for sensor purposes in white biotechnology, e.g. for the monitoring of macronutrient availability during fermentation processes. A set of yeast nutrient sensor strains was recently generated and evaluated. Sensor cells exploiting the promoters of signature genes *GAP1*, *PHO11* and *PDC6* displayed specifically higher fluorescence if sensor cells have limited access to ammonium, inorganic phosphate or sulphate, respectively. A systematic survey in terms of specificity, sensitivity and selectivity was performed but conditional triggering of fluorescence was followed exclusively in media that were optimised for growth of baker's yeast. In this section, implementation of the above mentioned nutrient sensor strains in media that are not primarily used for growth of yeast was probed.

In the framework of the MBC project FOBIO, media and supernatants of batch fermentation studies with microalgae were kindly provided by the cooperation partner GMBU e. V., Department Dresden (Tab. 3.3). Cultivation of GAP1, PHO11 and PDC6 sensor cells in microalgae media/supernatants and response of sensor cells to the nutrient composition in these liquids was evaluated as a proof of concept.

Table 3.3: Microalgae media and supernatants for the evaluation of yeast sensor strains for the monitoring of nitrogen, phosphor and sulphur availability. For each medium, the cultivated microalgae species and supernatant declaration is given. Media and samples were kindly provided by G. Rode from GMBU e. V., Department Dresden.

Medium	Microalgae species	Supernatant declaration
BG11	*Botryococcus braunii*	BG11 + *B. b.*
OHM	*Haematococcus pluvialis*	OHM + *H. p.*
Tamiya	*Chlorella vulgaris*	Tamiya + *C. v.*

Growth of nutrient sensor strains in microalgae media

Growth of yeast sensor cells with the PHO11–EGFP detection construct was compared between microalgae media/supernatants and yeast-optimised media. Algae are phototrophs and neither media nor supernatants contained glucose as determined by glucose assay (data not shown). For growth and activity of yeast sensor strains, 3% (w/v) glucose and required amino acids or nucleobases were added. The result is shown in Figure 3.33.

In spite of additives, growth of PHO11 sensor cells was delayed in microalgae media and respective supernatants in comparison to growth in yeast-optimised media, i.e. mineral medium or phosphorus-deficient medium. While growth curves were similar for PHO11 sensor cells in media BG11 or Tamiya and respective supernatants, cells grew faster in *Haematococcus pluvialis* supernatant than in pure OHM medium.

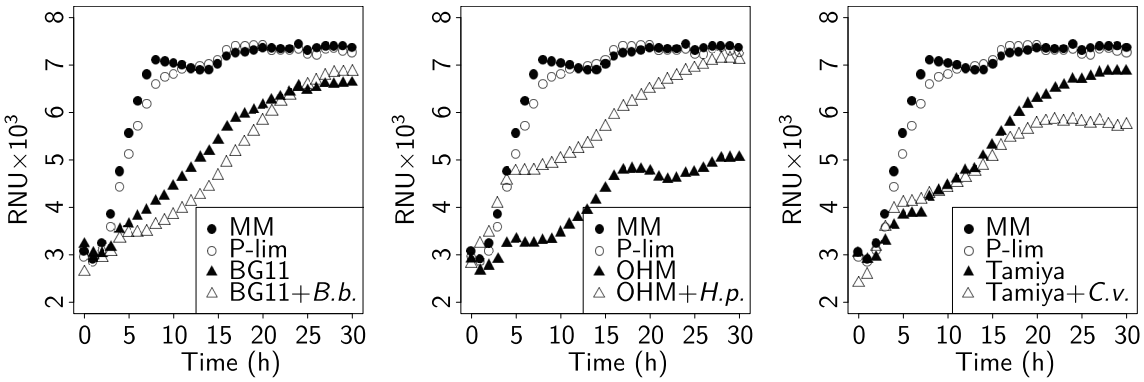

Figure 3.33: Growth analysis of phosphorus sensor cells in microalgae media and supernatants. Cells of BY4741 harbouring detection plasmid p426PHO11–EGFP were adjusted to an OD_{600} of 0.5 in microalgae media/supernatants (Tab. 3.3), or yeast-optimised mineral medium (MM) and phosphor limitation medium (P-lim) as a reference. Growth was monitored for 30 hours using a BMG microplate nephelometer. Scattered light measurements were performed in triplicates, mean values (RNU, relative nephelometer units) are shown.

Response of nutrient sensor cells GAP1–TurboGFP (higher in nitrogen limitation), PHO11–EGFP (higher in phosphorus limitation) and PDC6–EGFP (higher in sulphur limitation) to nutrient availability in microalgae media and supernatants was examined by microplate reader-based fluorometry. Sensor cells were grown in yeast-optimised mineral medium that triggers no fluorescence. Cells were subsequently shifted to fresh

yeast-optimised or algae media, respectively. Time trends of basic fluorescence of nutrient sensor strains in algae media were first compared to signals in yeast-optimised media (non-limited and nutrient-deficient). Fluorescence curves are shown in Figure 3.34. It was further analysed whether batch fermentation of microalgae in respective media affected nutrient composition in a detectable manner. Thus, fluorescence yield of nutrient sensor cells after eight hours cultivation in microalgae supernatants was compared to yield in pure media and evaluated (Tabs. C.2–C.4, Appendix C.4).

GAP1 nitrogen sensor cells yielded particularly higher fluorescence in all microalgae media than in yeast-optimised nitrogen limitation medium after eight hours. Reasons can be easily identified by comparing the composition of media. BG11, OHM and Tamiya contain no ammonium but nitrate, which is a poor nitrogen source for *S. cerevisiae*. As a consequence of this strong difference in nitrogen metabolism between microalgae and yeast, the generated sensor strains can not be used for nitrogen monitoring purposes in algae media if nitrate is used for feeding. Fluorescence of GAP1 sensor cells was slightly lower in algae supernatants. This might indicate accumulation or release of preferable nitrogen sources for yeast by algae during fermentation. However, this phenomenon was not examined further due to limited sample volumes and lack of time.

All algae media contain intermediate amounts of inorganic phosphate, and PHO11 sensor cells displayed slightly higher fluorescence in OHM and Tamiya medium than in yeast-optimised mineral medium. In microalgae medium BG11, the twofold fluorescence level was detectable suggesting weak phosphorus limitation. However, in all cases fluorescence was significantly lower than in phosphorus limitation medium. Like for nitrogen sensor strains, fluorescence decline was observed for PHO11 sensor cells that were cultivated in microalgae supernatants.

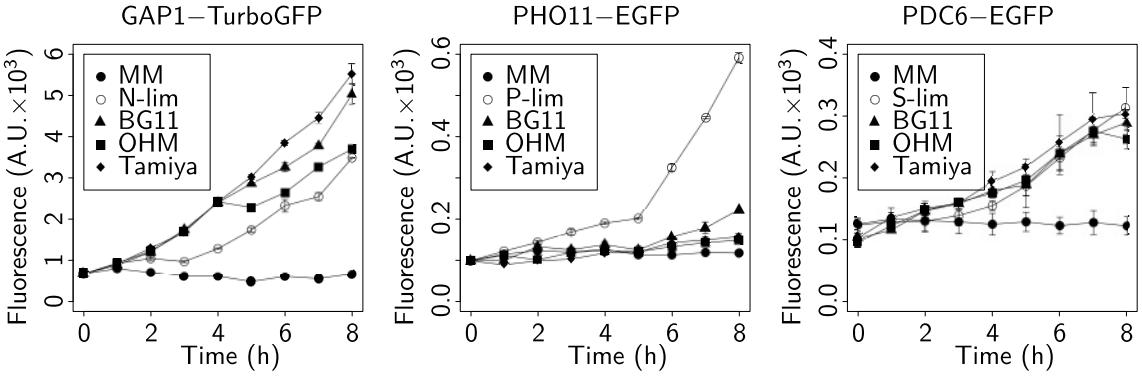

Figure 3.34: Fluorometric analysis of nutrient sensor strains in microalgae media. Cells of BY4741 were transformed with detection plasmids p426GAP1–TurboGFP or p426PHO11–EGFP and cells of W303–1A with p426PDC–EGFP. Sensor cells were cultivated in microalgae media (Tab. 3.3) or yeast-optimised media, i.e. mineral medium (MM) or medium limited in nitrogen (N-lim), phosphorus (P-lim) or sulphur (S-lim), as a reference. Total fluorescence of about 10^6 cells was determined using a TECAN Infinite microplate reader with excitation/emission wavelength of 490/520 nm and a gain of 100. Mean values ± sd of triple measurements are shown.

PDC6 sulphur sensor cells displayed moderate fluorescence in all three microalgae media. Brightness of sensor cells was always comparable to that of cells in yeast-optimised sulphur limitation medium. This was surprising as the concentration of sulphate minerals was higher than in sulphur limitation medium according to media formulations. The main difference is that sulphur is supplied as magnesium salt rather than ammonium sulphate. Again, fluorescence was recovered in respective algae supernatants suggesting accumulation or release of biologically available sulphur sources for yeast sensor cells during fermentation.

In conclusion, yeast nutrient sensor cells can be grown in microalgae media supplemented with glucose and required constituents for the particular auxotrophic strain. Observed fluctuations in fluorescence in algae media and respective supernatants demonstrate varying activity of sensor cells as a proof of concept. It must be emphasised that these experiments neither qualify sensor cells to monitor nutrient availability in microalgae media in a concentration-dependent manner nor exclude them from such purposes. Most importantly, nitrogen, phosphorus and sulphur concentrations were estimated from media composition rather than quantified by physical off-line methods. Comparison – for instance by commercially available colourimetric tests – is strongly recommended for further examinations. There was no capacity for such analyses in this work because of limited sample volumes and insufficient time for establishment of these methods.

3.2.13 Immobilisation of nutrient sensor strains

Aims and strategy

Immobilisation of cells in transparent hydrogel matrices like calcium-alginate could be beneficial in biosensor applications with an optical output signal. Neither the development of advanced immobilisation techniques nor the systematic survey of the impact on sensor cell activity and vitality was in the focus of this work. This section focuses on the performance evaluation of entrapped sensor and reporter cells with regard to signal yield, the possibility to trigger conditional fluorescence and accessibility of immobilised cells to different fluorescence detection methods.

Cells were entrapped in 3 mm beads to evaluate the general suitability of calcium-alginate for immobilisation of sensor cells and to detect fluorescence within the matrix. Spherical shape and given bead size were expected to allow for maximum interaction of cells with their environment and dense packaging of sensor cells to generate sufficient signals. Moreover, beads were facile to generate, store and handle during experimental procedures. Cells were mixed with sterile sodium-alginate solution and extruded from a syringe with needle into calcium chloride solution for gelation and cross-linking. Fluorescence performance was qualitatively checked by fluorescence microscopy. Additionally, a microplate reader-based assay was performed to monitor fluorescence time trend.

Secondly, sensor and reporter cells were immobilised in planar arrays on microscope slides by nanoplotting. Fluorescence scanning was tested as a new method to detect total fluorescence.

Evaluation of sensor and reporter cells after immobilisation in calcium-alginate hydrogel beads

The ability to monitor fluorescence after entrapment of sensor cells was first tested using BY4741 reporter cells featuring moderate fluorescence and non-fluorescent cells as a control. Cells harbouring reporter plasmid p426ADH–TurboGFP or parental vector p426ADH were immobilised in calcium-alginate beads. TurboGFP-mediated fluorescence was both detectable by microscopy and microplate reader-based fluorometry (Fig. 3.35). In contrast to fluorometric analyses of cell suspensions, the number of cells could not be adjusted and beads displayed increasing fluorescence signals over time. Total fluorescence of beads with reporter cells was significantly higher and was rising faster than of beads with control cells. Over time, more cells contribute to the total signal. The shift to fresh medium may also affect *TurboGFP* expression in reporter cells.

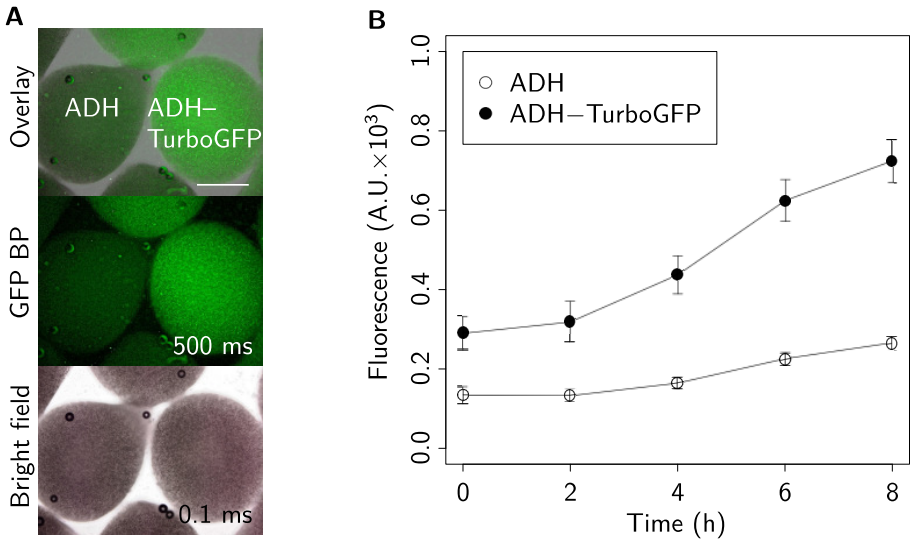

Figure 3.35: Fluorescence analysis of immobilised reporter cells with moderate fluorescence. Cells of BY4741 harbouring reporter plasmids p426ADH (control, no fluorescence) or p426ADH–TurboGFP (constitutive fluorescence) were monitored in calcium-alginate beads. **A** Fluorescence microscopy of cells after entrapment. Panel shows overlay image (scale bar = 1 mm) and images of GFP BP and bright field channels with 8× magnification. **B** Fluorescence time-lapse of entrapped reporter and control cells. Total fluorescence of beads was measured using a TECAN Infinite microplate reader with excitation/emission wavelength of 490/520 nm and a gain of 100. Mean values ± sd of three independent measurements are shown.

GAP1 sensor cells with strong fluorescence induction in nitrogen deficiency were immobilised to test whether triggered fluctuations in fluorescence can be detected after immobilisation as well. Sensor cells were immobilised in calcium-alginate beads after growth in non-limited and nitrogen-deficient medium to obtain low and high fluorescence

or to monitor induction and regeneration of sensor cells, respectively. Beads with entrapped cells were washed with equilibration medium and cultivated in mineral medium or medium limited in nitrogen, phosphorus or sulphur. Subsequently, fluorescence was analysed by fluorescence microscopy and microplate reader-based fluorometry (Fig. 3.36). First, immobilised cells were monitored after shift from non-limited mineral medium. Beads were bright fluorescent after six hours after transfer to nitrogen limitation medium and displayed dim fluorescence if nitrogen was in surplus (Fig. 3.36A). Like observed for immobilised reporter cells in the time trend analysis, fluorescence of non-limited GAP1 nitrogen sensor beads increased over time (Fig. 3.36B) yielding twofold higher signals after eight hours. Total fluorescence of nitrogen-limited beads was higher but not as distinct as expected from microscopy or fluorometry using cells in suspension. One important difference in both experiments was the volume of medium beads were shifted to. Beads were transferred to 20 ml of fresh medium for microscopy but only 200 μl for the fluorometry assay. Therefore, fluorescence of sensor cells may be affected by retained mineral medium within the beads. Monitoring the time trend of fluorescence regeneration within beads was troublesome. Bright fluorescent GAP1 sensor cells were immobilised after induction in nitrogen limitation medium and transferred to mineral medium for regeneration or continued cultivation in nitrogen-deficient medium as a reference. Distinctly lower fluorescence was detectable by microscopy after shift of beads to mineral medium (Fig. 3.36C), but total fluorescence of regenerated beads still increased over time (Fig. 3.36D). From the smoother slope of the respective signal curve in comparison to that of control beads – steadily grown in mineral medium – it was assumed that fluorescence of individual cells within regenerated beads was indeed decreasing over time (Fig. 3.36E).

Evaluation of sensor and reporter cells after immobilisation in calcium-alginate by nano-printing

Immobilisation of GAP1 sensor cells in calcium-alginate beads was useful to prove the concept of induction and fluorescence detection of entrapped nutrient sensor cells in response to variable nitrogen availability. Simultaneously, drawbacks were discerned. Sensor cell entrapment in beads allowed for dense packaging of sensor cells and sufficient signal yield. However, the signal was inhomogeneous within the measured area. Signal loss was assumed from overlapping cells and quenching effects and beads retain much medium which results in an indefinite environment after shift to fresh medium. Thus, response of sensor cells and signal yield was examined in thin, planar calcium-alginate layers. To this end, cells were mixed with sodium-alginate and spotted on microscope slides by piezoelectric printing technology by R. Liebschner at the Institute of Materials Science/TU Dresden. The Fixacol coating ensured adhesion of alginate on the glass surface and was developed by GMBU e. V., Department Dresden. Microscope slides

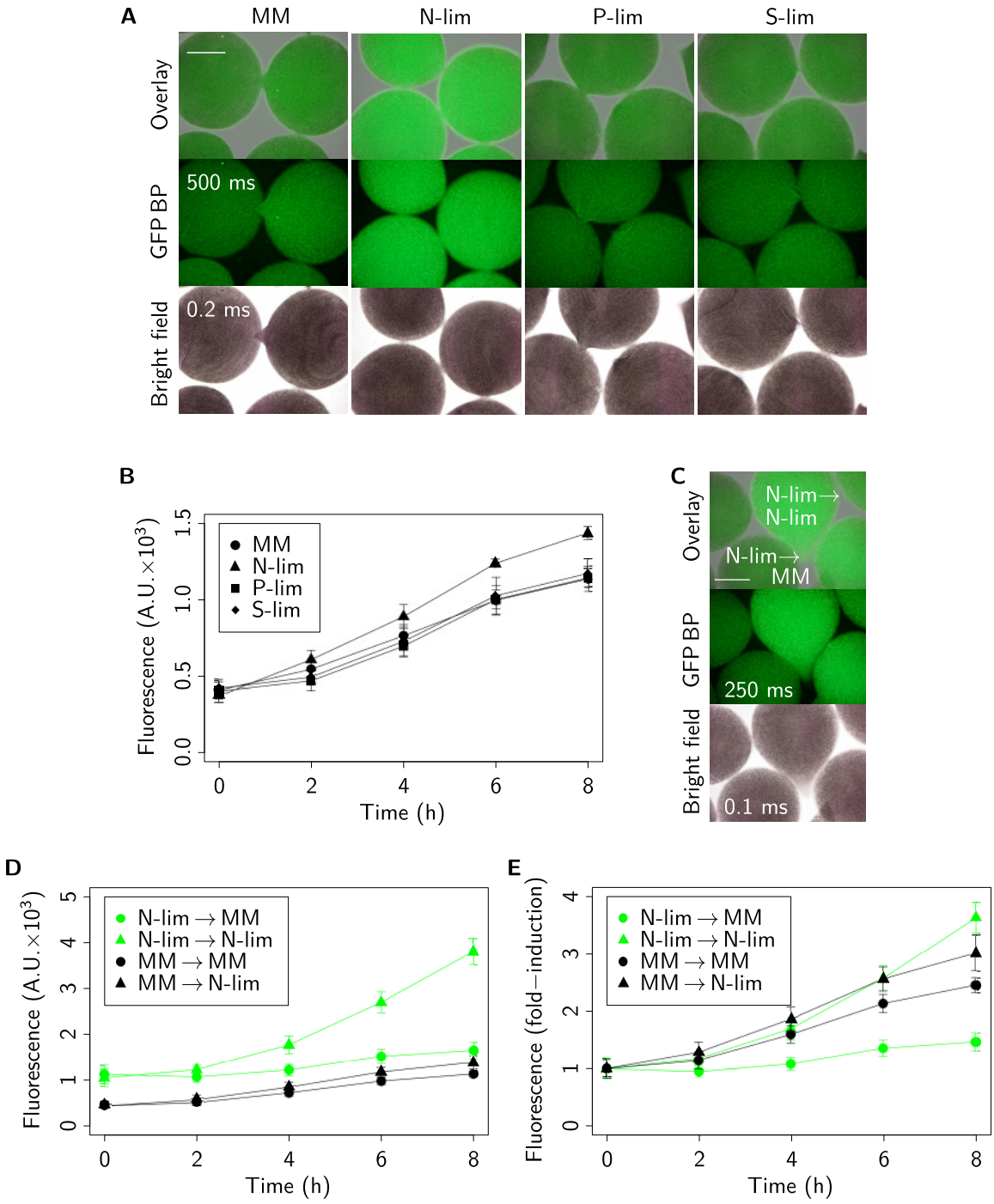

Figure 3.36: Evaluation of immobilised nitrogen sensor cells. Cells of BY4741 harbouring detection plasmid p426GAP1–TurboGFP were grown in mineral medium (MM) or nitrogen limitation medium (N-lim) before immobilisation in calcium-alginate hydrogel. **A** Fluorescence microscopy of beads six hours after shift from mineral medium to fresh mineral medium or medium limited in nitrogen, phosphorus (P-lim) or sulphur (S-lim). Panel shows overlay image (scale bar = 1 mm) and images from GFP BP and bright field channel with 8× magnification. **B** Time-lapse fluorometric analysis of entrapped sensor cells after shift from mineral medium. Total fluorescence of beads was measured using a TECAN Infinite microplate reader with excitation/emission wavelength of 490/520 nm and a gain of 100. Mean values ± sd from three independent measurements are shown. **C** Fluorescence microscopy of beads six hours after shift from nitrogen limitation medium to indicated media. See A for details. **D, E** Fluorescence time trends after indicated shifts were acquired as described in B. Shown are total signal intensities (D) or relative fluorescence in comparison to bead's fluorescence at zero hours (E).

were dipped into calcium chloride solution to precipitate the alginate and entrap cells within the matrix. Instead of microplate reader-based fluorometry, fluorescence of areas with immobilised cells was scanned using the Typhoon Trio instrument and fluorescence intensity was quantified using ImageJ.

First, different concentrations of reporter cells BY4741 harbouring the plasmid p426GPD–TurboGFP with strong, constitutive fluorescence were nano-printed in square arrays of 5×5 mm^2 with 20×20 spots of 7 nl volume to determine necessary amounts of cells to acquire a sufficient signal by fluorescence scanning. The result is depicted in Figure 3.37. Arrays were scanned after immobilisation and overnight incubation at 4°C in selective mineral medium with calcium chloride for equilibration of sensor cells and calcium-alginate layers. Cells or cell clusters were visible as dot-like structured pattern of higher signal intensity and in clear contrast to the microscope slide background. Mean image intensities of the plotted array areas were measured with the software ImageJ and displayed a distinct correlation between the amount of plotted cells and fluorescence signal yield. Vitality of cells after nano-printing was confirmed by incubating the array with initially 1,500 cells at 30°C in selective medium with calcium chloride. Swelling of the calcium-alginate hydrogel layer and brighter fluorescence was observed which indicated cell proliferation and further reporter gene expression. However, prolonged incubation caused particular release and disintegration of array patches.

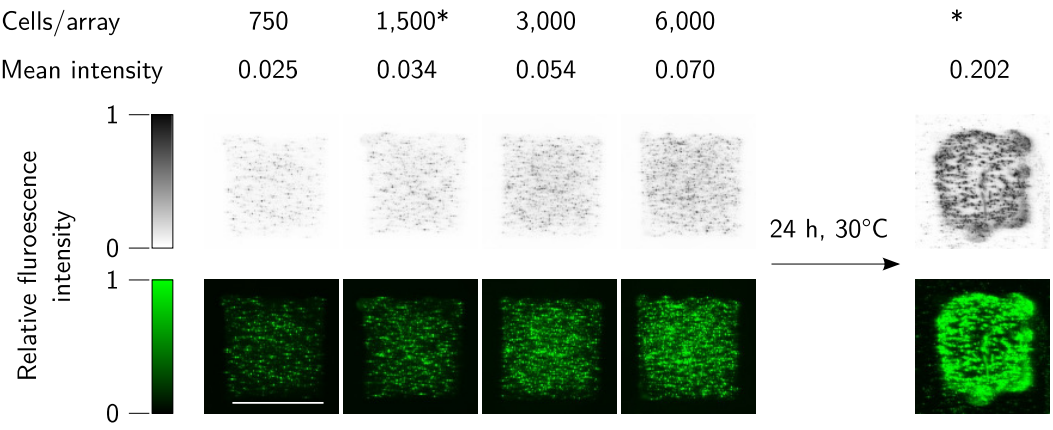

Figure 3.37: Fluorescence analysis of nano-printed reporter cell arrays with strong fluorescence. Cells of BY4741 harbouring reporter plasmid p426GPD–TurboGFP were mixed with sodium-alginate, nano-printed (20×20 spots of 7 nl) on Fixacol-coated microscope slides in 5×5 mm^2 arrays with approximately 750–6,000 cells and dipped into calcium chloride solution for alginate cross-linking. Fluorescence of arrays was detected using a Typhoon Trio fluorescence scanner with excitation/emission wavelength of 488/520 nm, a PMT voltage of 500 V and a resolution of 25 μm. Scan images are depicted unmodified (top) and pseudo-coloured (bottom) respectively. Scale bar = 5 mm. Detected intensities range from zero (no fluorescence) to one (fluorescence saturation). The array with 1,500 cells was incubated for 24 h at 30°C and scanned again (∗). Mean intensity of scan images was determined with software ImageJ.

To test whether inducible fluorescence is detectable, nitrogen-responsive GAP1 sensor cells were again immobilised by nano-printing technology at the Institute of Materials

Science/TU Dresden. Cells were adjusted to an optical density of 1 in sodium-alginate and spotted (10×10 spots of 7 nl) on Fixacol-treated microscope slides. Each 4×4 mm^2 array contained about 7,000 cells. Immobilised cells were cultivated at 30°C for seven hours in mineral medium or media limited in either nitrogen, phosphorus or sulphur. Arrays were subsequently examined by fluorescence scanning and microscopy. Figure 3.38 shows the result. Higher fluorescence was uniquely observable for the GAP1 array that was incubated in nitrogen-deficient medium. The difference in fluorescence intensity was confirmed by fluorescence microscopy. Moreover, cell vitality was concluded from growth of cells to clusters.

In summary, immobilisation of sensor cells in thin, planar arrays and subsequent fluorescence detection by scanning was shown as a proof of concept. Here, this method only worked with cells that feature strong green fluorescence like GAP1 nitrogen sensor cells. PHO11 and PDC6 sensor cells that respond to phosphorus and sulphur deficiency, respectively, were immobilised in nano-printed arrays but no significant fluorescence was detectable by scanning (data not shown). Thus, signal amplification of weak signals might be beneficial or even essential. Section 3.3 reports on the development of an amplifier circuit to gain enhanced signal yield.

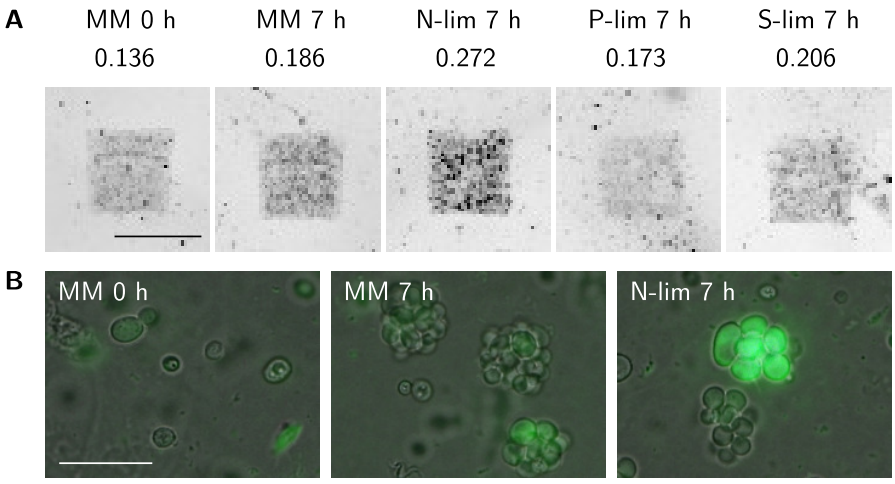

Figure 3.38: Fluorescence of nano-printed nitrogen sensor cells. Cells of BY4741 harbouring detection plasmid p426GAP–TurboGFP were mixed with sodium-alginate solution, nano-printed (10×10 spots of 7 nl) on Fixacol-coated microscope slides in 4×4 mm^2 arrays with about 7,000 cells and dipped into calcium chloride solution for alginate cross-linking. Arrays were incubated in mineral medium (MM) or medium limited in nitrogen (N-lim), phosphorus (P-lim) or sulphur (S-lim) for seven hours at 30°C. **A** Fluorescence was detected using a Typhoon Trio fluorescence scanner with excitation/emission wavelength of 488/520 nm, a PMT voltage of 450 V and a resolution of 50 μm. Unmodified scan images are depicted, scale bar = 4 mm. Mean intensity of scan images was determined with software ImageJ. **B** Cells were imaged within arrays using a Keyence BZ-8100 fluorescence microscope with 1,000× magnification and a GFP BP filter. Overlay images of green fluorescence (exposure time 500 ms) and bright field channel (exposure time 5 ms) are shown, scale bar = 20 μm.

3.3 Development of a yeast pheromone-based cellular communication and signal amplification system

3.3.1 Findings from preliminary studies

An innovative cellular communication and signal amplification system inspired by pheromone signalling of *S. cerevisiae* was characterised and evaluated for versatile application in yeast cell-based biosensor systems. It features the pheromone α-factor as a trigger and the pheromone-responsive *FIG1* promoter to drive expression of a fluorescence reporter gene as an exemplary target product. The described system relies on gene expression from 2μ-based multicopy plasmids that were engineered and initially characterised in a previous work (Groba, 2007). Briefly, reporter plasmid p426FIG1–EGFP features expression of reporter gene *EGFP* from the pheromone-inducible *FIG1* promoter. Plasmids for the generation of yeast cells with constitutive or inducible α-factor production and secretion feature the *MFα1*-ORF under the control of the *ADH* promoter (moderate expression level), the *GPD* promoter (high expression level) or the *FIG1* promoter (α-factor-responsive expression). The system was initially tested in yeast strain BY4741, i.e. **a** cells which naturally produce no α-factor but can perceive and respond to the pheromone. It was assumed that α-factor production may be implemented in **a** cells without any difficulties, since maturation and secretion of α-factor is based on the classical secretory pathway. Furthermore, laborious modification of α cells by deletion of the α-factor-encoding genes *MFα1* and *MFα2* can be circumvented. The results of the preliminary work showed that EGFP was detectable in BY4741 reporter cells that were transformed with the plasmid p426FIG1–EGFP and treated with 20 μmol l^{-1} synthetic α-factor after three hours. Importantly, pheromone-secreting BY4741 cells were not able to induce noticeable fluorescence in BY4741 reporter cells with the p426FIG1–EGFP detection plasmid. This was true for both intermediate and high levels of secreted α-factor. Thus, optimisation of the cellular communication and signal amplification system was absolutely essential in the present work.

3.3.2 Evaluation of pheromone-responsive reporter cells using synthetic α-factor

Yeast cells of mating type **a** that lack the α-factor protease Bar1p are hypersensitive to the pheromone (MacKay et al., 1988). In order to compare their performance, cells of strains BY4741 and BY4741 *bar1*Δ were transformed with plasmid p426FIG1–EGFP (equivalent to 'reporter' or the acronym 'FE' in following text and figures). Cells of both reporter strains were incubated with different concentrations of synthetic α-factor and

analysed by microplate reader-based fluorometry (Fig. 3.39). After four hours, a strong increase in fluorescence was detectable after treatment with 10 μmol l^{-1} α-factor in both reporter strains. While fluorescence in BY4741 reporter cells was only observed from this concentration, concentrations of 0.1 μmol l^{-1} were sufficient to induce a distinct signal in reporter cells deleted for *BAR1*. Induction of fluorescence was accompanied by the formation of mating projections, which proved pheromone-induced mating response (data not shown). These observations confirmed the functionality of the p426FIG1–EGFP detection plasmid and α-factor signalling. The excellent response of hypersensitive strain BY4741 *bar1*Δ to low α-factor concentrations strengthened the intention to establish the cellular communication and signal amplification system on this deletion strain.

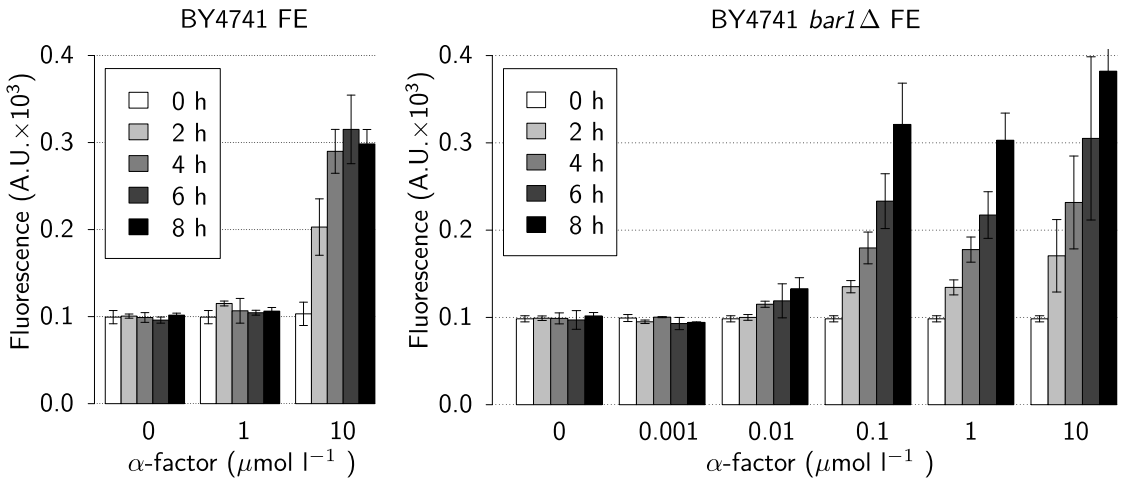

Figure 3.39: Fluorometric analysis of pheromone-inducible BY4741 and BY4741 *bar1*Δ reporter cells harbouring reporter plasmid p426FIG1–EGFP (FE) after stimulation with given concentrations of synthetic α-factor. Total fluorescence of about 10^6 cells was determined at indicated time points using a TECAN Infinite microplate reader with excitation/emission wavelength of 490/520 nm and a gain of 100. Mean values $\pm$ sd from three independent measurements are shown.

3.3.3 Evaluation of pheromone-responsive reporter cells using cell-secreted α-factor

As mentioned in Section 3.3.1, BY4741 cells harbouring the reporter plasmid p426FIG1–EGFP did not respond to BY4741 cells harbouring plasmid p426ADH–MFα1 or p426GPD–MFα1 for production and secretion of α-factor (Groba, 2007). The use of hypersensitive BY4741 *bar1*Δ reporter cells which were inducible with low concentrations of synthetic α-factor was expected to be beneficial for both cell-based pheromone secretion and sensing. It was found indeed that deletion of the *BAR1* locus was essential to induce fluorescence in cocultivation experiments of α-factor-secreting cells (termed 'AM' cells in figures) with reporter cells (Fig. 3.40). If one of both cell types still carried an intact *BAR1* gene, no significant fluorescence signal was visible and only a fraction of cells exhibited intermediate mating projections. In cocultures with both cell types lacking

Bar1p, mating projections and fluorescence were triggered even if the intermediate *ADH* promoter was used for *MFα1* gene expression.

Cocultivation of different ratios of α-factor-secreting to reporter cells revealed a 1:20 ratio to be sufficient for a distinct fluorescence increase within four hours while a ratio of 1:100 or 1:50 was not (Fig. 3.41A). In Western blot analysis, distinct EGFP signals were detectable for a 1:10 and 1:20 ratio of pheromone-secreting to reporter cells after four hours but not for a 1:50 ratio (Fig. 3.41D).

It was tested whether the implementation of a third type of cells that express *MFα1* under the control of the *FIG1* promoter can increase fluorescence in cocultivation experiments with pheromone-secreting and reporter cells. These 'amplifier' cells (termed 'FM' in figures) harbouring the plasmid p426FIG1–MFα1 displayed no mating projections (Fig. 3.40B). In line with this observation, they did not trigger fluorescence in sole cocultivation with reporter cells (Fig. 3.41B). Interestingly, distinct fluorescence was observed in cocultivation experiments of pheromone-secreting, reporter and amplifier cells in a 1:50:1 ratio (3.41C,D). The effect was even more pronounced if a 1:50:5 ratio of α-factor-secreting to reporter to amplifier cells was used. These findings strongly suggest that the presented cellular pheromone-driven expression system can be used as an amplification circuit.

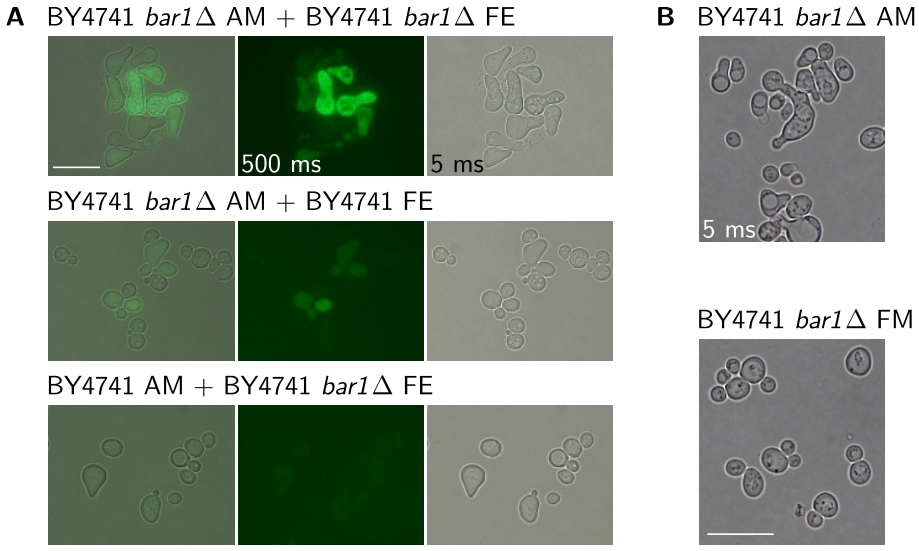

Figure 3.40: Microscopic analysis of recombinant yeast strains for a cellular communication and signal amplification system. Cells were imaged using a Keyence BZ-8100 fluorescence microscope with 1,000× magnification (scale bar = 20 μm), GFP BP filter for green fluorescence monitoring and given exposure times in each channel. **A** Cells of BY4741 and BY4741 *bar1*Δ were transformed with plasmids p426ADH–MFα1 (AM) for constitutive production and secretion of α-factor, or p426FIG1–EGFP (FE) for pheromone-inducible expression of reporter gene *EGFP*. AM- and FE-harbouring cells were cocultivated in a 1:1 ratio for six hours. Each image block shows the overlay and respective green fluorescence and bright field images. **B** Phenotype of BY4741 *bar1*Δ cells with constitutive (AM) or α-factor-inducible (p426FIG1–MFα1, FM) expression. AM cells display mating projections while FM cells do not because of the absence of α-factor as an initial trigger.

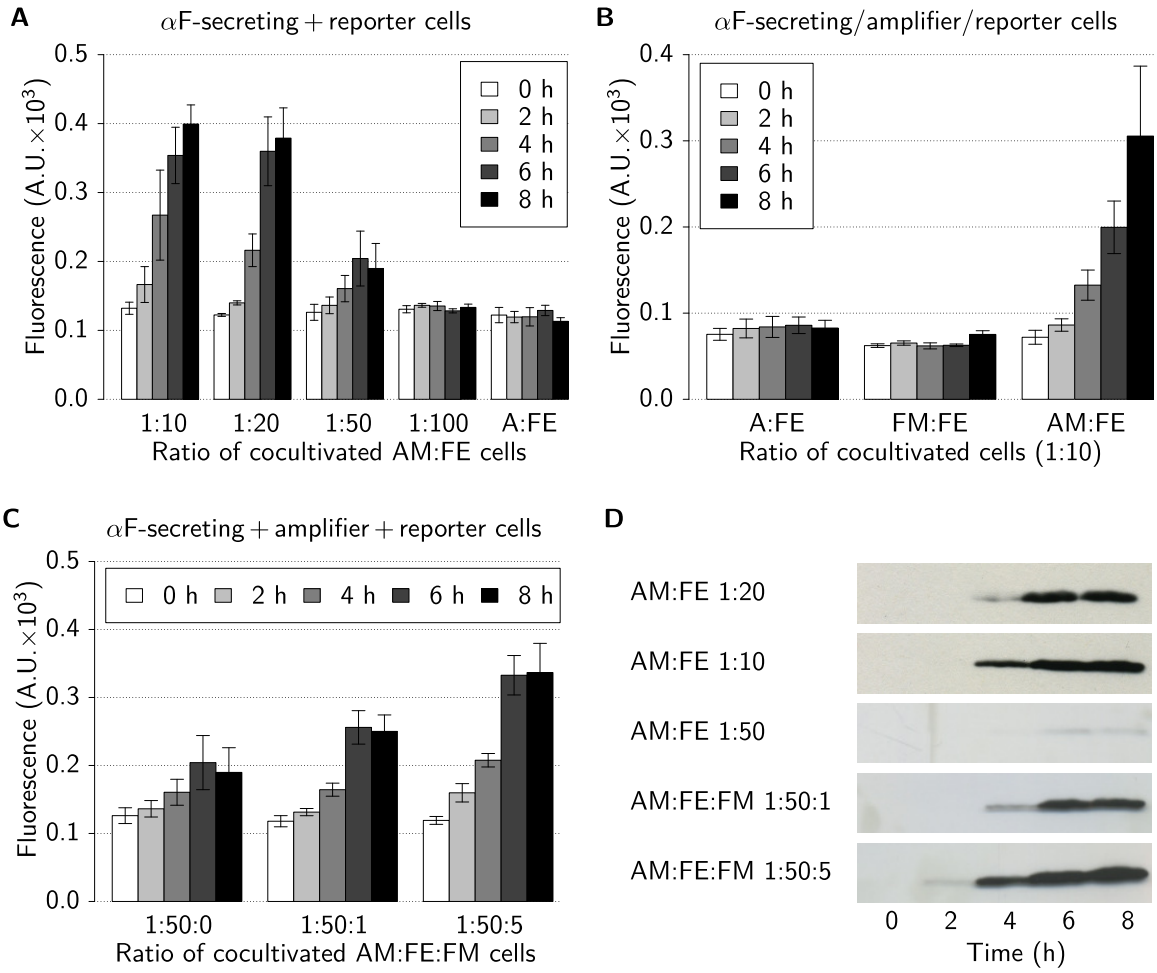

Figure 3.41: Fluorometric and Western blot analysis of recombinant yeast strains for a cellular communication and signal amplification system. Cells of BY4741 *bar1*Δ were transformed with plasmids p426ADH–MFα1 (AM) or p426FIG1–MFα1 (FM) for moderate or pheromone-inducible production and secretion of α-factor (αF). Reporter cells harbour plasmid p426FIG1–EGFP (FE), control cells the parental vector p426ADH (A). Indicated cell types were cocultivated in a 1:10 ratio unless otherwise stated. **A**–**C** Fluorometric analysis of cocultivated cells. Total fluorescence of about 10^6 cells was determined for given time points using a TECAN Infinite microplate reader with excitation/emission wavelength of 490/520 nm and a gain of 100. Mean values ± sd from three independent measurements are shown. **D** Western blot analysis of EGFP (∼26.9 kDa) in soluble protein fractions of about 10^7 cells from indicated cocultures. EGFP was tracked with anti-GFP (Tab. 2.2).

3.3.4 Implementation of immobilisation methods

Immobilisation in calcium-alginate beads

Immobilisation of yeast sensor cells in calcium-alginate beads and the ability to detect fluorescence of entrapped nitrogen sensor cells was already demonstrated (Section 3.2.13). Convenience of this immobilisation method was probed for the established cellular communication and signal amplification system. Initially, BY4741 and BY4741 *bar1*Δ cells that carry the p426FIG1–EGFP reporter plasmid were immobilised in calcium-alginate beads. Fluorescence of beads that were incubated in selective minimal medium containing different concentrations of synthetic α-factor was probed by microplate reader-based fluorometry. The result is depicted in Figure 3.42. Consistent with data from batch culture experiments, fluorescence of BY4741 reporter cells was exclusively induced after addition of 10 μmol l^{-1} synthetic α-factor. Although BY4741 *bar1*Δ reporter cells were not induced with 0.1 μmol l^{-1} α-factor as expected from preliminary results (Fig. 3.39, Section 3.3.2), fluorescence was observed with 1 μmol l^{-1} (Fig. 3.42B).

BY4741 *bar1*Δ reporter cells were also monitored in calcium-alginate beads by microscopy (Fig. 3.43). Cells displayed distinct fluorescence and mating projections in the presence of 1 μmol l^{-1} α-factor. Cells were also impaired in cell division by α-factor-induced cell cycle arrest while clusters of budding cells were observable in the absence of α-factor. This resulted in higher cell density and darker shading of respective calcium-alginate beads, but still poor fluorescence. Long-time incubation of beads at 30°C allowed for steady growth of immobilised cells and resulted in massive cell leakage accompanied by disintegration of the calcium-alginate matrix (data not shown).

To determine the threshold concentration for pheromone-induced response of hypersensitive BY4741 *bar1*Δ reporter cells after immobilisation more precisely, measurements were repeated with finer graduation between 0.1 and 1 μmol l^{-1} α-factor (Fig. 3.42C). Induction of fluorescence was already observed with 0.25 μmol l^{-1} α-factor. Thus it was assumed that slightly lower sensitivity after immobilisation was caused by dilution of applied α-factor through the liquid content of calcium-alginate beads rather than direct interference of α-factor with the hydrogel or its function as a diffusion barrier.

Finally, response of immobilised reporter cells to cell-secreted α-factor was examined in order to prove cellular communication via α-factor. BY4741 *bar1*Δ cells with plasmid p426ADH–MFα1 for production and secretion of moderate α-factor levels and BY4741 *bar1*Δ cells with the reporter plasmid p426FIG1–EGFP were embedded together in a 1:10 ratio. Induction of fluorescence was comparable to stimulation of reporter cells with 1 μmol l^{-1} α-factor (Fig. 3.42D).

To conclude, the presented results demonstrated effective α-factor-based signalling of calcium-alginate-immobilised reporter cells. Although lower in sensitivity with synthetic α-factor, the system was well-working with cell-secreted α-factor.

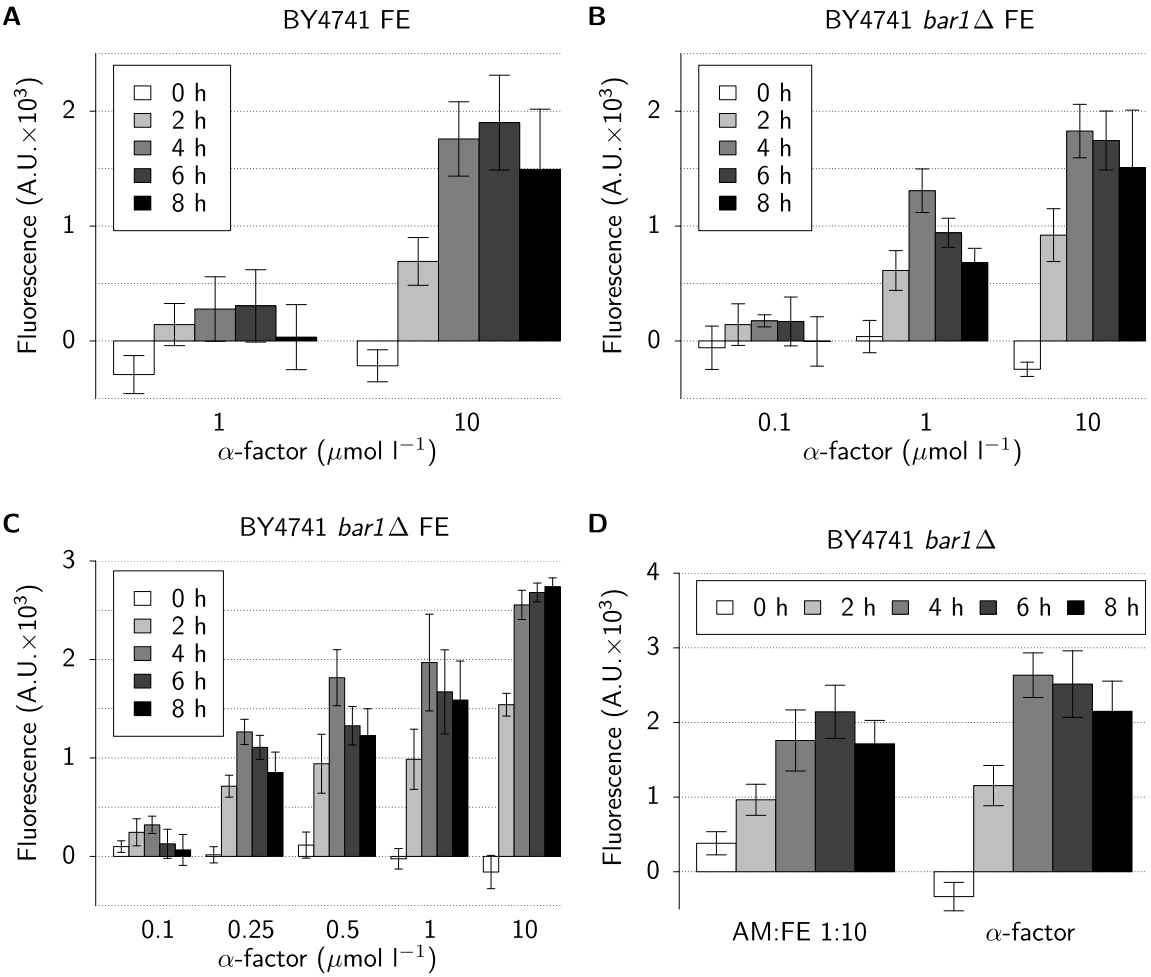

Figure 3.42: Fluorometric analysis of recombinant yeast strains for a cellular communication and signal amplification system after immobilisation in calcium-alginate beads. **A**–**C** Reporter cells BY4741 and BY4747 *bar1*Δ harbouring plasmid p426FIG1–EGFP (FE), respectively, were immobilised and incubated at 30°C with given concentrations of synthetic α-factor. Total fluorescence of beads was measured using a TECAN Infinite microplate reader with excitation/emission wavelength of 490/520 nm and a gain of 100. Shown fluorescence values (mean ± sd of three independent measurements) equate the signal difference to beads with the same reporter strain but treated without α-factor (base line). **D** Fluorometric analysis of calcium-alginate beads with FE reporter cells, either mixed with pheromone-secreting cells harbouring plasmid p426ADH–MFα1 (AM), or 1 μmol l^{-1} synthetic α-factor. Measurements were performed as described above. Fluorescence values of beads with FE reporter cells but no α-factor were used as a reference (base line).

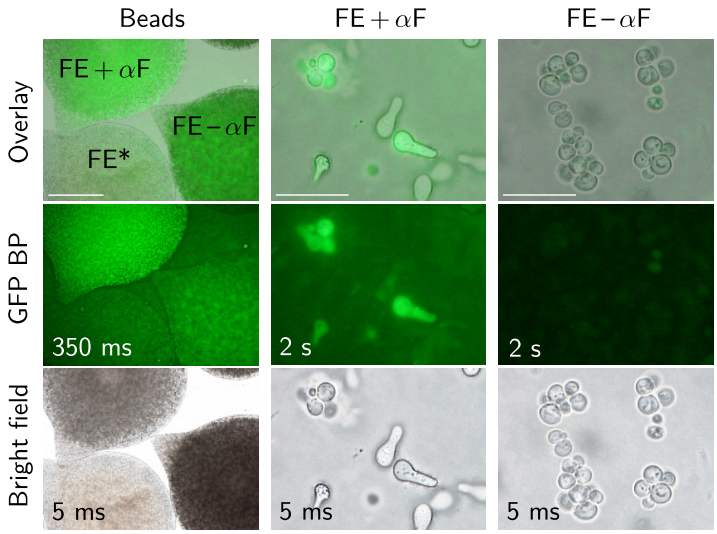

Figure 3.43: Microscopy of yeast reporter cells for a cellular communication and signal amplification system in calcium-alginate beads. Reporter cells BY4741 *bar1*Δ harbouring plasmid p426FIG1–EGFP were immobilised and incubated for six hours at 30°C with 1 μmol l^{-1} α-factor (FE + αF) or without (FE − αF) α-factor. Beads stored at 4°C (FE*) were used as another reference. Images were acquired using a Keyence BZ-8100 fluorescence microscope with 8× (beads) or 1,000× magnification (cell-tracking within beads), GFP BP filter for green fluorescence monitoring and given exposure times in each channel. Each vertical image block shows the overlay (scale bar = 1 mm for beads and 20 μm for cells) and respective green fluorescence and bright field images.

Immobilisation in agarose

So far, α-factor-secreting and α-factor-responsive reporter cells for a cellular communication and signal amplification system were coimmobilised in spherical calcium-alginate beads. The setup with cell mixtures minimises diffusion distances of α-factor and allows rapid activation of reporter cells but has disadvantages considering monitoring purposes. If α-factor-secreting and reporter cells are immobilised together, respective beads contain a fair proportion of cells that can not fluoresce, yielding in 'dilution' and fluorescence signal loss. Separation of the pheromone source (synthetic α-factor or secreting cells) allows for the immobilisation of pheromone-responsive reporter cells at maximum density. To realise this, a setup comprising planar, cube-shaped compartments that share a sharp boundary was recently established by Jahn (2011). Monitoring of planar areas is also preferable to analysis of spherical beads with respect to signal uniformity. Cells were immobilised in agarose rather than calcium-alginate to create accurate compartments without a cross-linking step by calcium chloride.

In a first attempt, response of BY4741 *bar1*Δ reporter cells to synthetic α-factor was examined in this two-compartment setup based on agarose. Adjacent compartments in an agarose grid matrix were filled with pheromone-responsive reporter cells BY4741 *bar1*Δ harbouring plasmid p426FIG1–TurboRFP (termed 'FR' in figures; see Section 3.3.6) and different concentrations of α-factor (0.01–10 μmol l^{-1}). Fluorescence intensity of reporter cell compartments was monitored over six hours using a Typhoon Trio fluorescence

scanner. The image analysis software ImageJ was applied for fluorescence quantification in terms of intensity distribution within the compartments. The result is depicted in Figure 3.44. Cells of BY4741 *bar1*Δ harbouring plasmid p426ADH–TurboRFP (alias 'AR') and displaying intermediate, uniform red fluorescence served as a reference. In control conditions with pheromone-inducible reporter cells, they exhibited no fluorescence in the absence of α-factor but were uniformly activated after direct mixing with 1 μmol l^{-1} α-factor. A slight increase was observed after two hours, followed by escalation after four and six hours. If α-factor diffused from the neighbouring compartment, reporter cells were activated in a concentration-dependent pattern. Interestingly, a minimal effect was observed even with the lowest concentration of 0.01 μmol l^{-1}. Concentrations from 0.1 μmol l^{-1} α-factor induced distinct fluorescence of reporter cells over a variable distance from the compartment boundary. Remarkably, this threshold was in line with the observations in batch cultivation experiments with pheromone-responsive reporter cells, confirming functional signalling in agarose. Higher concentrations of α-factor could diffuse over longer distances from the α-factor compartment, which was already described for the initially developed setup using a reporter strain with a genome-integrated FIG1–TurboRFP detection construct (Jahn, 2011).

The previously described two-compartment setup was modified by replacing α-factor with pheromone-secreting cells. To this end, cells of strain BY4741 *bar1*Δ harbouring plasmid p426ADH–MFα1 as the source of α-factor were immobilised with a cell density ranging from 0.1 to 2 adjacent to pheromone-responsive reporter cells. Like in the experiment described above, reporter cells and α-factor-secreting cells were directly mixed in one compartment as a positive control for immediate and uniform fluorescence induction. As a negative control, the compartment next to the reporter cell compartment was filled with cells BY4741 *bar1*Δ transformed with the parental vector p426ADH which trigger no fluorescence. As a reference, strain BY4741 *bar1*Δ harbouring plasmid p426ADH–TurboRFP and featuring constitutive, intermediate red fluorescence was used again. The result of the RFP-fluorescence scan with the Typhoon Trio is shown in Figure 3.45. Fluorescence of the reference strain and in negative and positive control experiments was similar to respective setups using α-factor as a trigger. The monitored compartments displayed constitutively intermediate, no or induced levels of fluorescence over time respective to the given promoter and stimulation. Activation of α-factor-responsive reporter cells correlated with the cell density of applied α-factor-secreting cells in the adjacent compartment regarding signal yield and activated distance from the compartment boundary. In detail, by using higher densities of α-factor-secreting cells, fluorescence was detectable in longer distances from the compartment boundary over time, accompanied by a stronger increase of the total fluorescence level. This was in contrast to data of Jahn (2011) using the genome-integrated reporter strain, where a variation in the occupied area but not in total fluorescence yield was observed. Interestingly,

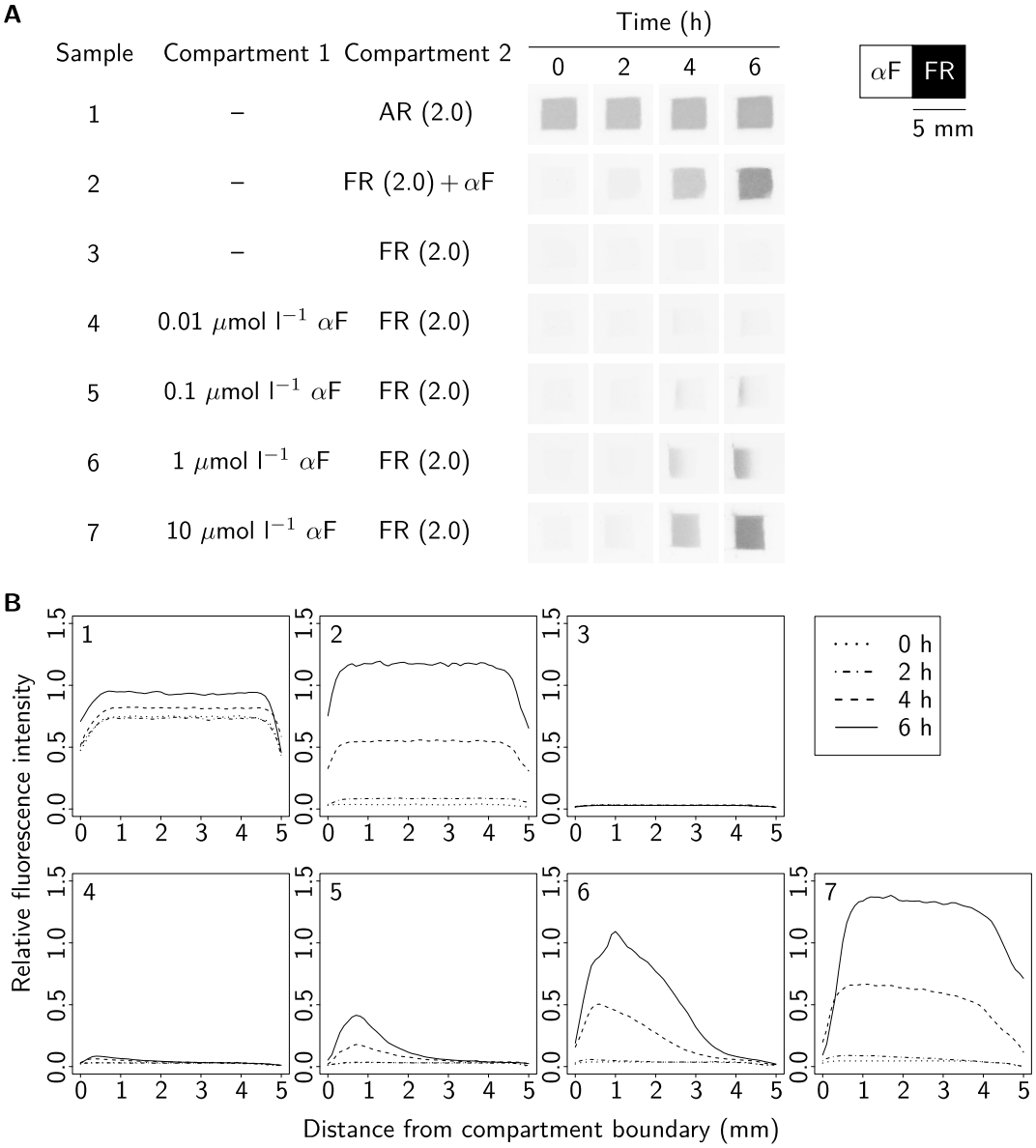

Figure 3.44: Analysis of immobilised yeasts for a plasmid-based cellular communication and signal amplification system using a two-compartment setup and synthetic α-factor as a trigger. **A** Two adjacent compartments of 5×5 mm^2 size in an agarose matrix were filled with 1% (w/v) agarose containing either yeast cells BY4741 *bar1*Δ (OD_{600} of 2) or α-factor (αF). Red fluorescence of compartment 2 was detected using a Typhoon Trio fluorescence scanner with excitation/emission wavelength of 532/580 nm, PMT voltage of 400 V, resolution of 100 μm and focal plane of +3 mm. **1** Compartment 2 was filled with cells harbouring plasmid p426ADH–TurboRFP (AR) that display constitutive fluorescence. **2** Reporter cells with plasmid p426FIG1–TurboRFP (FR) that were directly mixed with 1 μmol l^{-1} α-factor in compartment 2 displayed uniformly activated fluorescence. **3** FR cells without α-factor displayed no fluorescence. **4**–**7** Different α-factor concentrations yielded different fluorescence profiles of FR cells in compartment 2. **B** Fluorescence profiles of compartment 2 for samples 1–7 were analysed with software ImageJ. A value of 1.0 equates the fluorescence intensity of AR cells after six hours.

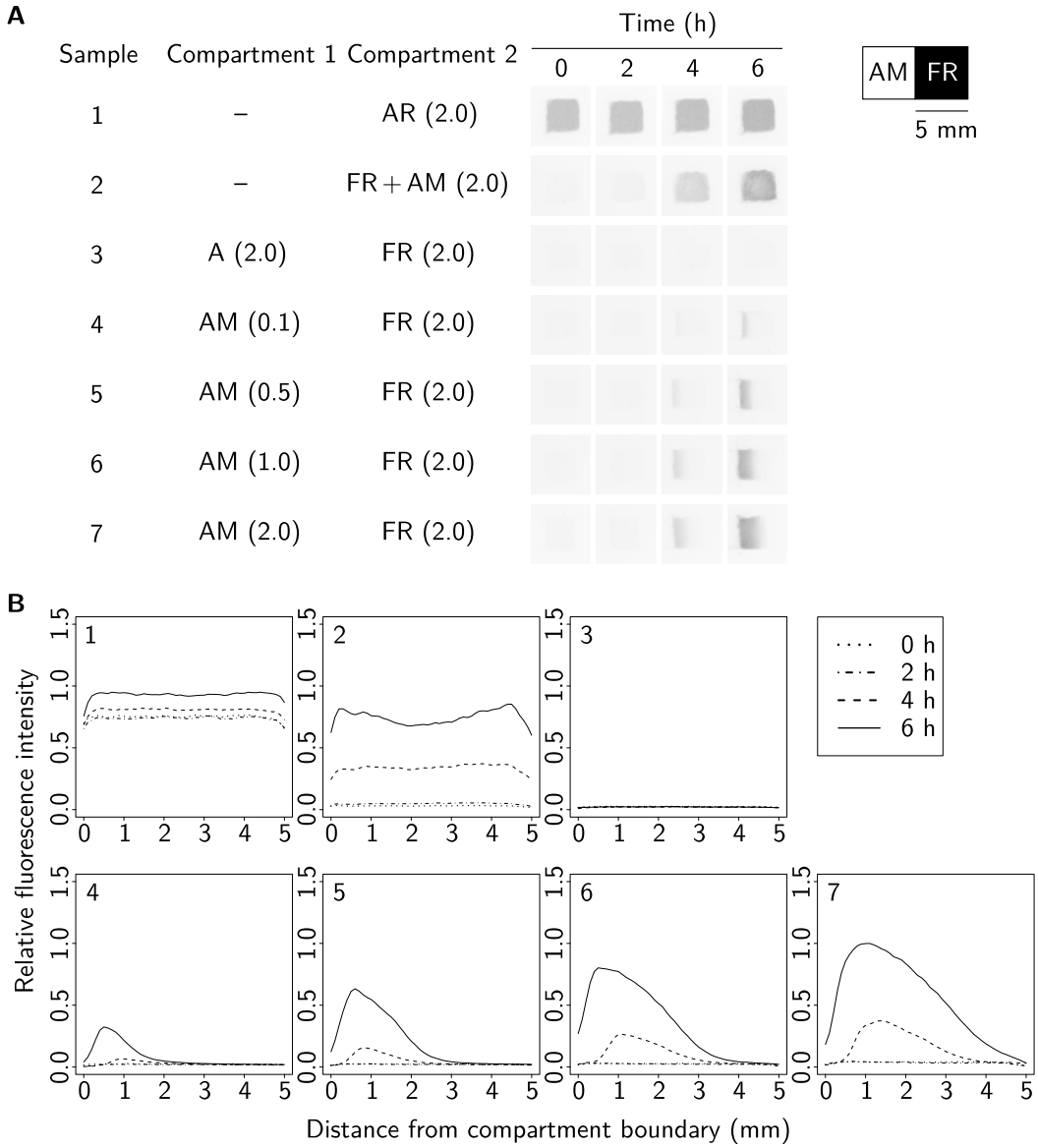

Figure 3.45: Analysis of immobilised yeasts for a plasmid-based cellular communication and signal amplification system using a two-compartment setup and α-factor-secreting cells as a trigger. **A** Two adjacent compartments of 5×5 mm^2 size in an agarose matrix were filled with yeast cells BY4741 *bar1*Δ (OD_{600} of 0.1–2) in 1% (w/v) agarose. Red fluorescence of compartment 2 was detected using a Typhoon Trio fluorescence scanner with excitation/ emission wavelength of 532/580 nm, PMT voltage of 400 V, resolution of 100 μm and focal plane of +3 mm. **1** Only compartment 2 was filled with cells harbouring plasmid p426ADH–TurboRFP (AR) that display constitutive fluorescence. **2** Reporter cells with plasmid p426FIG1–TurboRFP (FR) were mixed directly with α-factor-secreting cells harbouring p426ADH-MFα1 in compartment 2. **3** Compartment 1 was filled with cells carrying the parental vector p426ADH and do not trigger fluorescence of FR cells in compartment 2. **4**–**7** Different cell densities of AM cells in compartment 1 yielded different fluorescence profiles of FR cells in compartment 2. **B** Fluorescence profiles of compartment 2 for samples 1–7 were analysed with software ImageJ. A value of 1.0 equates the fluorescence intensity of AR cells after six hours.

even pheromone-secreting cells with an optical density of 0.1 were able to stimulate reporter cells with an optical density of 2 in a distance below 1.5 mm. This supports previous batch cultivation data which showed that a cocultivation of pheromone-secreting and pheromone-responsive cells in a ratio of 1:20 is sufficient to induce a detectable signal (Fig. 3.41A, Section 3.3.3). Moreover it favours the two-compartment setup for immobilisation purposes of the α-factor-based cellular communication and signal amplification system.

3.3.5 Implementation of the cellular communication and signal amplification system in nutrient sensor strains

The proof of concept for a cellular communication and signal amplification system based on α-factor was shown. It was found that induction of fluorescence can be triggered by cells that secrete intermediate levels of α-factor. Since expression of *MFα1* was driven from the constitutive *ADH1* promoter, reporter cells were exposed to mature pheromone immediately after mixing reporter with pheromone-secreting cells. This is an important difference to the conventional principle of a cell-based sensor which relies on conditional rather than continuous triggering of signals.

Yeast sensor strains for the monitoring of nutrient availability were extensively evaluated in Section 3.2. They feature discriminable expression of fluorescence reporter genes in the presence and absence of a particular nutrient. However, the majority of introduced signature promoters mediated moderate or low expression of reporter genes. The use of α-factor as a converter molecule as well as amplifier cells may increase signal yield if direct response is weak. Implementation of the cellular communication and signal amplification system in nutrient monitoring was tested with the *PHO11* promoter which is specifically up-regulated under phosphorus limitation. The promoter was chosen because fluorescence of non-limited and phosphorus-limited sensor cells BY4741 harbouring the p426PHO11–EGFP detection plasmid was comparable to signals of reporter cells BY4741 *bar1*Δ harbouring plasmid p426FIG1–EGFP that were exposed to 0 and 1 μmol l^{-1} α-factor, respectively.

Cells of strain BY4741 *bar1*Δ were transformed with plasmid p426PHO11–MFα1 (termed 'PM' in the figure below). This plasmid was generated by replacing the *EGFP*-fragment with the *MFα1* gene in plasmid p426PHO11–EGFP (alias 'PE'). Respective PHO11 'sender' cells carrying the plasmid thus produce and secrete α-factor after exposed to phosphorus limitation. Fluorescence of α-factor-responsive reporter cells BY4741 *bar1*Δ harbouring p426FIG1–EGFP was analysed in cocultivation with PHO11 sender cells. The result is depicted in Figure 3.46. In agreement with the data for sensor cells harbouring the 'direct' detection plasmid p426PHO11–EGFP, fluorescence of the two-component phosphorus sensor system was specifically induced in phosphorus limitation

medium but not in mineral medium. PHO11 sensor cells with the direct detection construct and α-factor-responsive FIG1 reporter cells displayed similar fluorescence levels after induction, either by phosphorus limitation (PHO11 sensor cells) or by α-factor-secreting cells (FIG1 reporter cells). This indicates that plasmid-based expression from both promoters follows similar kinetics and is of comparable strength. In contrast, signal yield with the two-component phosphorus sensor system (PHO11 sender and FIG1 reporter cells) was lower. An explanation is the longer time span required from expression of *MFα1* in PHO11 sender cells until α-factor perception by FIG1 reporter cells than for direct expression of *EGFP* from the *PHO11* promoter.

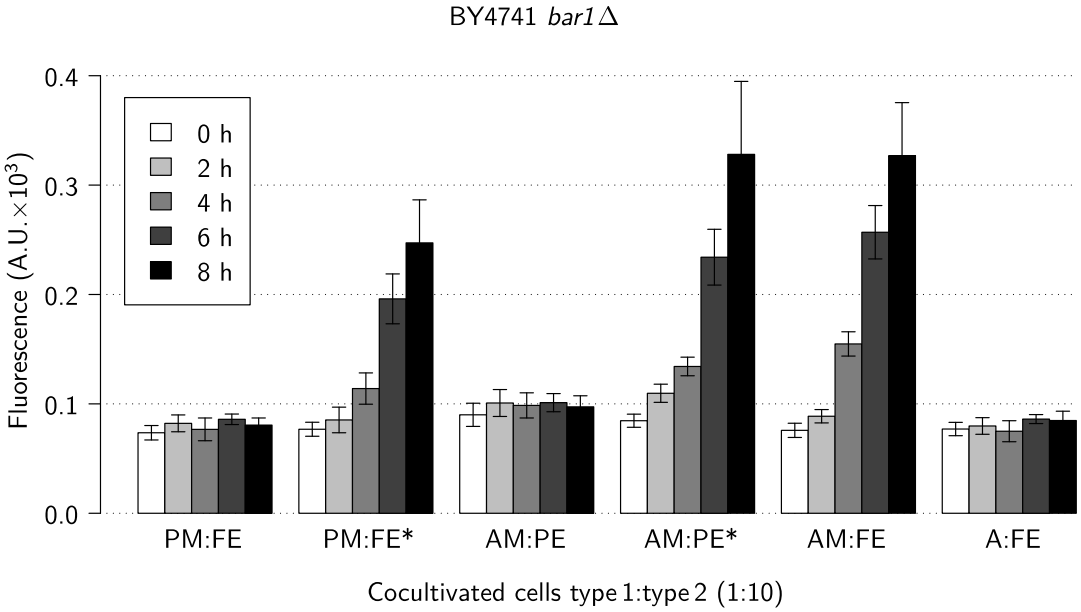

Figure 3.46: Implementation of a cellular communication and signal amplification system for monitoring of phosphorus availability. BY4741 *bar1*Δ cells of given types were cocultivated in a 1:10 ratio in mineral medium or phosphorus limitation medium (∗). Total fluorescence of about 10^6 cells was determined for given time points using a TECAN Infinite microplate reader with excitation/emission wavelength of 490/520 nm and a gain of 100. Mean values ± sd from three independent measurements are shown. Sender cells with plasmid p426PHO11–MFα1 (PM) express *MFα1* encoding α-factor under phosphorus limitation, and were cocultivated with α-factor-responsive reporter cells harbouring p426FIG1–EGFP (FE). For reference, phosphorus monitoring cells carrying the 'direct' detection plasmid p426PHO11–EGFP (PE) and FE reporter cells were each cocultivated with cells harbouring p426ADH–MFα1 (AM) for constitutive α-factor gene expression. As a negative control, FE reporter cells were cocultivated with cells carrying the parental vector p426ADH (A) which do not trigger fluorescence.

Nevertheless, the successful basis for integration of α-factor signalling in monitoring of nutrient availability with yeast sensor strains was demonstrated by using phosphorus as an analyte to proof the concept. Fluorescence yield in the two-component sensor system was hindered in comparison to the direct sensor construct regarding signal yield and time of response. In Section 3.3.3 it was shown, that the implementation of amplifier cells can increase sensitivity. Further studies may address the question whether the implementation of these amplifier is beneficial in order to increase signal yield. Moreover,

one single mixing ratio of sender and reporter cells was applied and the optimal ratio needs to be determined in future studies. In addition, the mixing ratio has to be adjusted individually for other detection as well.

3.3.6 Generation of novel FIG1 reporter strains for a cellular communication and signal amplification system

Two possibilities for the engineering of yeast pheromone-responsive reporter strains with improved fluorescence signal yield were examined. On the one hand, expression of genes encoding fluorescent proteins with higher brightness and signal-to-background ratio was tested. On the other hand, the use of another strong pheromone-responsive promoter for reporter gene expression was probed.

Expression of various fluorescence reporter genes from the *FIG1* promoter

Expression of genes encoding diverse GFP-like proteins with different spectral properties from the strong *GPD* promoter was described in Section 3.1.1. Brightness, signal yield and signal-to-background ratio of green fluorescent protein GFPuv and red fluorescent protein TurboRFP was superior to that of EGFP. Coding sequences of GFPuv and TurboRFP were recovered from respective p426GPD plasmids and cloned into p426FIG1 (Groba, 2007) to generate new reporter plasmids for the cellular communication and signal amplification system. Conditional expression of both reporters in the presence of α-factor was confirmed by fluorescence microscopy and Western blot analysis (Fig. 3.47). Pheromone-treated BY4741 *bar1*Δ reporter cells displayed mating projections and brilliant fluorescence that required only short exposure time. Like EGFP, reporters GFPuv and TurboRFP were only detectable by Western blot analysis in soluble protein fractions of induced cells.

Fluorescence of FIG1 reporter strains treated with and without α-factor was probed on the cell population level using microplate reader-based fluorometry (Fig. 3.48). Fluorescence of reporter strains expressing GFPuv and TurboRFP in the presence of 1 μmol l^{-1} α-factor was superior to fluorescence of the EGFP reporter strain in terms of signal yield and signal-to-background ratio. This was concluded from the lower gain that was applied to yield a comparable signal intensity and the higher fold-change in fluorescence of pheromone-treated versus untreated cells. Although kinetics of expression of both markers was not studied in detail here, it was expected to be comparable or even improved in comparison to EGFP. This hypothesis was strongly supported by examinations of Jahn (2011) comparing genome-integrated and plasmid-encoded TurboRFP reporter variants. In fact, for both BY4741 *bar1*Δ reporter strain expressing *EGFP* or *TurboRFP* first effects on the fluorescence level are visible after two hours, followed by steady signal increase at later time points of examination.

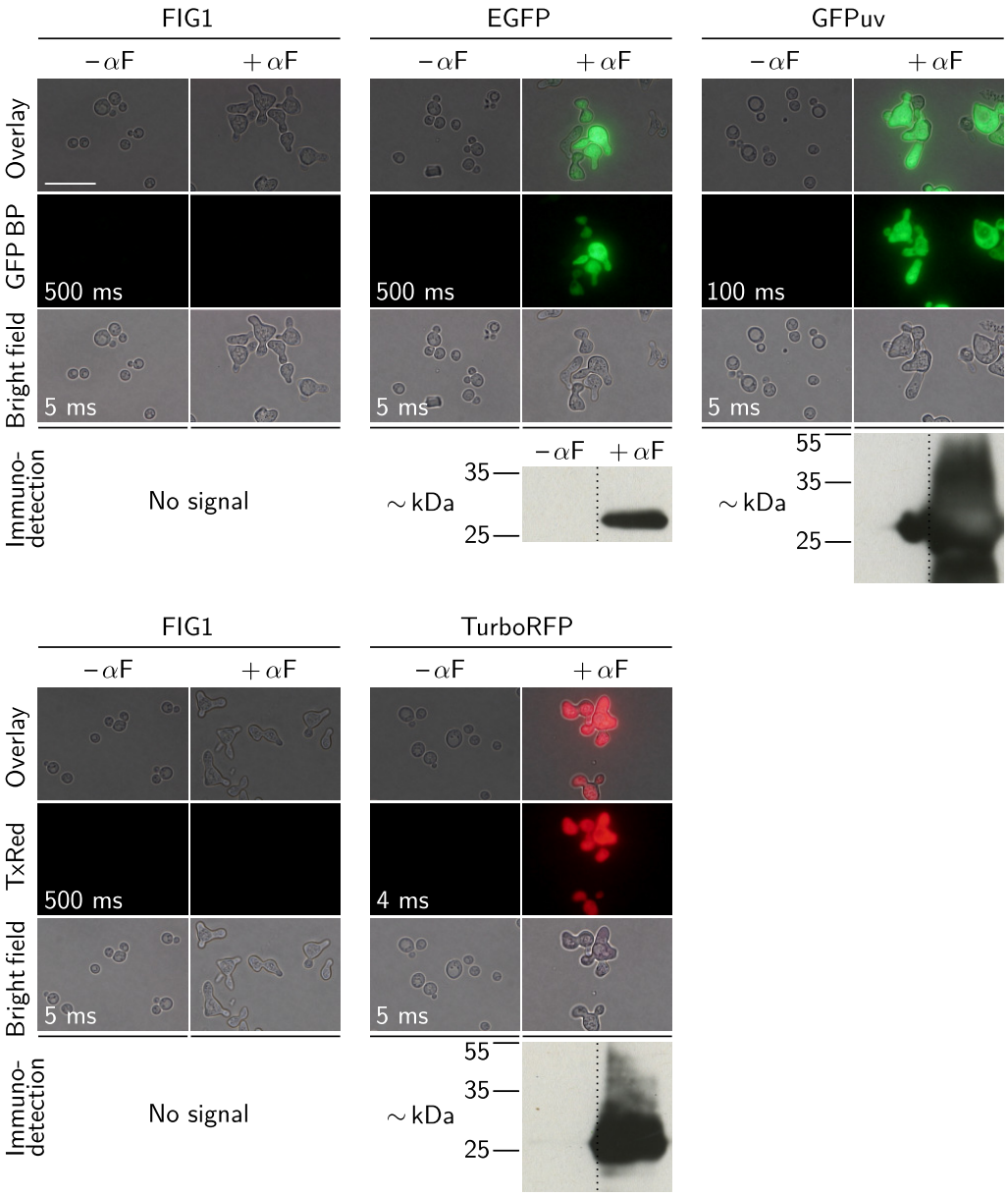

Figure 3.47: Microscopic and Western blot analysis of recombinant BY4741 *bar1*Δ strains with α-factor-inducible fluorescence reporter gene expression. Vector p426FIG1 (Groba, 2007) was exploited for expression of genes encoding green (GFPuv, EGFP) or red (TurboRFP) fluorescent proteins. As a control, cells were transformed with the parental vector (FIG1, no fluorescence). Cells were treated with 1 μmol l^{-1} α-factor (+αF) for 24 hours to induce fluorescence, accompanied by the formation of mating projections. In control experiments, reporter cells were grown without α-factor (−αF). Microscopic images (three upper panels in each image block) were taken with a Keyence BZ-8100 fluorescence microscope using 1,000× magnification, GFP BP and TxRed filters for green and red fluorescence monitoring, respectively, and given exposure times in each channel. Image blocks show the overlay (scale bar = 20 μm) and respective fluorescence and bright field images. In the bottom row, for each expression strain immunodetection signals from soluble protein fractions of about 10^7 cells treated with (right) and without α-factor (left) are shown. In the presence of α-factor, immunoreactive bands for EGFP (∼26.9 kDa), GFPuv (∼26.8 kDa) and TurboRFP (∼28.8 kDa) were obtained using specific antibodies targeted to the respective reporter protein (Tab. 2.2). Migration positions of reference proteins are given on the left. In control cells harbouring the parental vector, no signals were detectable.

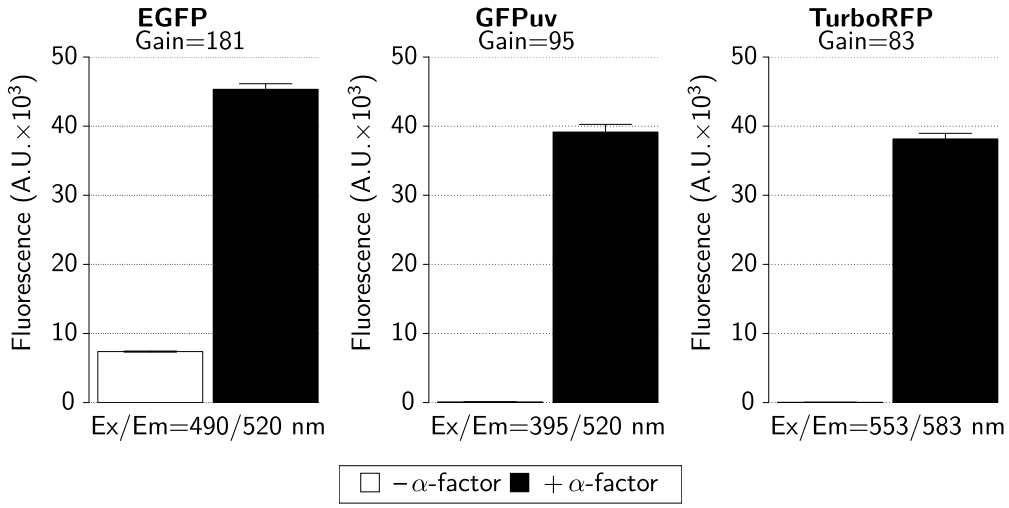

Figure 3.48: Fluorometric analysis of yeast reporter strains with α-factor-inducible expression of genes encoding green and red fluorescent proteins. Cells of BY4741 *bar1*Δ were transformed with reporter plasmids p426FIG1–EGFP, p426FIG1–GFPuv or p426FIG1–TurboRFP and cultivated in selective minimal medium without ($-\alpha$-factor) or with 1 μmol l^{-1} α-factor ($+\alpha$-factor). Total fluorescence of about 10^6 cells was detected after 24 hours using a TECAN Infinite microplate reader with given excitation/emission wavelength (Ex/Em) and gain. Mean values $\pm$ sd of triple measurements are shown.

Fluorescence reporter gene expression from different pheromone-responsive promoters

PRM2, encoding a pheromone-regulated membrane protein, and *FIG1* exhibit similar expression profiles. This was found by re-analysis of the data sets by Roberts et al. (2000) using the *Saccharomyces* Genome Database microarray analysis and query tool SPELL. The strength of both promoters was compared by examination of *TurboRFP* expression in strain BY4741 *bar1*Δ. The reporter plasmid p426PRM2–TurboRFP was kindly provided by K. Zarschler (Institute of Genetics/TU Dresden). It was derived from reporter plasmid p426FIG1–TurboRFP by replacement of the *FIG1* promoter fragment with a PCR-generated 1-kb fragment comprising the regulatory region of *PRM2*. Expression from the *FIG1* promoter was superior. Reporter cells harbouring the *PRM2* construct displayed no significant fluorescence in the absence of α-factor but after induction with α-factor, signal yield was four times lower than for cells harbouring the *FIG1* reporter construct (Fig. 3.49).

3.3.7 Generation of *mat*$\alpha\Delta$ deletion strains for the cellular communication and signal amplification system

Aims and strategy

The previously characterised cellular communication and signal amplification system based on the natural pheromone-system of *S. cerevisiae* used α-factor to trigger fluorescence of reporter cells with mating type **a**. In contrast to authentic yeast pheromone

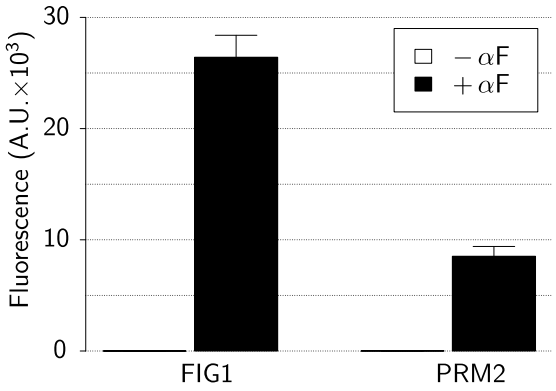

Figure 3.49: Comparison between *FIG1* and *PRM2* promoter-driven fluorescence reporter gene expression in *S. cerevisiae*. Reporter cells of BY4741 *bar1*Δ harbouring plasmid p426FIG1–TurboRFP or p426PRM2–TurboRFP were cultivated in selective minimal medium without (− αF) or with 1 μmol l^{-1} α-factor (+ αF) for six hours. Total fluorescence of about 10^6 cells was determined using a TECAN Infinite microplate reader with excitation/emission wavelength of 550/580 nm and a gain of 80. Mean values ± sd of triple measurements are shown.

signalling, **a** cells were also exploited for expression of *MFα1* – a sufficient but perhaps not optimal strategy. This was demonstrated for example by the strict requirement of deletion mutants lacking the α-factor protease Bar1p to obtain effective signalling. Other disadvantages of using **a** cells for α-factor expression and secretion are probably not so obvious.

For this reason, *S. cerevisiae mat*$\alpha\Delta$ deletion strains lacking α-factor gene expression were generated. The pheromone is encoded by two genes, *MFα1* and *MFα2*. Both loci were replaced in *S. cerevisiae* strain BY4742 (mating type α) by deletion cassettes mediating resistance to antibiotics nourseothricin and hygromycin B (Hentges et al., 2005). Briefly, the antibiotic resistance cassettes were PCR-amplified with primers linking 40-bp homologous regions of *MFα1* and *MFα2* to the ends of PCR fragments (Tab. 2.11). Fragments were sequentially transformed into BY4742. BY4742 *mat*$\alpha\Delta$ clones were successfully selected for antibiotic resistances and verified by diagnostic PCR (data not shown). Since *BAR1* expression is repressed by *MFα2* (lacking in the deletion strain) and activated by α-factor (Manney, 1983), a BY4742 *mat*$\alpha\Delta$ *bar1*Δ double-deletion strain was generated too. In fact, the afore generated BY4742 *mat*$\alpha\Delta$ and the BY4741 *bar1*Δ strains were mated, forced to sporulate, and the desired double-deletion strain was selected from their haploid progeny after tetrad dissection. Details can be found in Section 2.5.13.

Pheromone signalling of BY4742-based strains

The efficiency of the parental strain BY4742 and derived deletion strains to trigger fluorescence of BY4741 *bar1*Δ reporter cell harbouring plasmid p426FIG1–TurboRFP was tested and compared with the initially established BY4741 *bar1*Δ-based setup (Fig. 3.50). BY4742 cells feature authentic α-secretion and triggered fluorescence comparable to

BY4741 *bar1*Δ harbouring plasmid p426ADH–MFα1. Interestingly, both BY4742-derived deletion strains with plasmid-based *MFα1*-expression yielded equivalent signal levels. Here, BY4742 *matα*Δ *bar1*Δ exhibited a little higher efficiency which was probably due to deletion of *BAR1*. If both deletion strains were transformed with the vector p426ADH (no α-factor-production), however, they were incapable of fluorescence induction. This proved successful deletion of the *MFα1/2* loci on the cellular level.

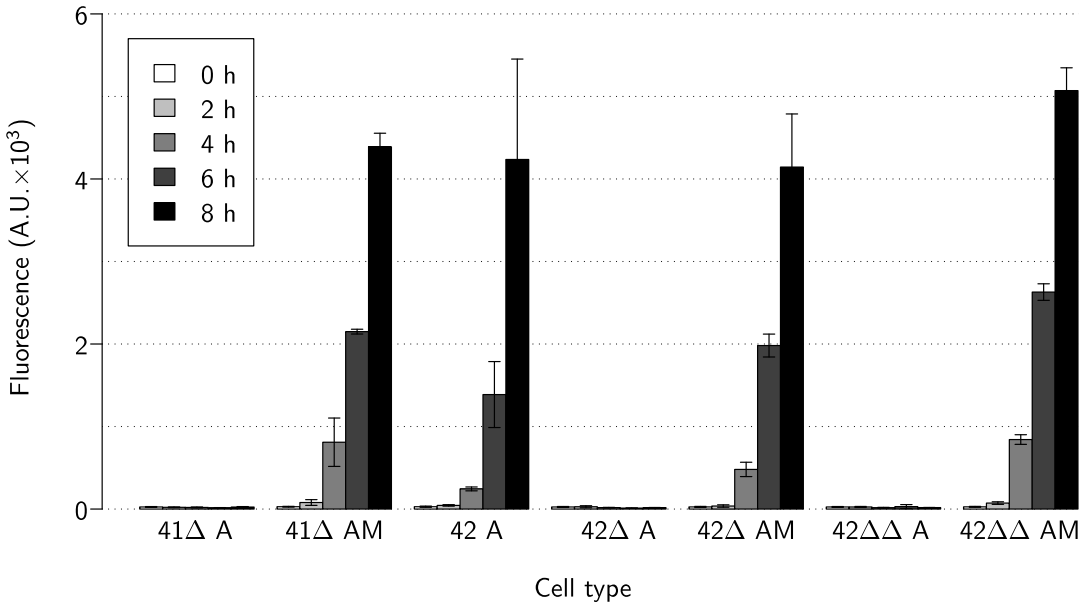

Figure 3.50: New *S. cerevisiae* BY4742 *matα*Δ strains for a cellular communication and signal amplification system. Reporter cells BY4741 *bar1*Δ harbouring plasmid p426FIG1–TurboRFP were cocultivated with indicated cell types in a 1:10 ratio. In detail, strains BY4741 *bar1*Δ (alias 41Δ), BY4742 (42), BY4742 *matα*Δ (42Δ) and BY4742 *matα*Δ *bar1*Δ (42ΔΔ) were transformed with plasmid p426ADH (A) or p426ADH–MFα1 (AM) for no or ectopic production/secretion of α-factor. Total fluorescence of about 10^6 cells was determined at given time points using a TECAN Infinite microplate reader with excitation/emission wavelength of 550/580 nm and a gain of 80. Mean values ± sd of triple measurements are shown.

In summary, the ability to exploit the yeast pheromone system for controlled cell-cell communication and as an amplifier circuit was extensively examined. The basic system comprises two cell types of *S. cerevisiae* with mating type **a**. Type 1 cells secrete the pheromone α-factor. Perception of the pheromone by type 2 cells with plasmid-encoded reporter gene expression triggers fluorescence in addition to native mating response. The system is functional both in batch cultivation and with immobilised cells. Applicability in biosensor approaches was successfully demonstrated by implementation into yeast cell-based monitoring of phosphorus availability. Furthermore, various detection constructs and yeast strains were generated that may improve signal yield and efficiency.

Chapter 4

Discussion

Based on the intentions of the two MBC projects FOBIO and MaBioS, fluorescent *S. cerevisiae* sensor and reporter cells were generated. Their performance was extensively probed in order to evaluate the suitability in optical cell-based biosensors or bioassays. A pilot set of yeast nutrient sensor strains was constructed following a classical plasmid-based approach with one type of tailored detection construct per cell (Section 3.2). All detection plasmids consistently carried a specific promoter (i.e. the 5'-regulatory region of adjacent genes with an expected expression profile) that drives expression of a foreign gene encoding a fluorescent protein reporter. It could be demonstrated that variation (genome-integration detection constructs) or extension (dual-colour sensor cells) of the concept may be beneficial with regard to signal fidelity or spectrum of functions. Since many yeast-based sensors may suffer from weak signal yield, the concept of a cellular communication and signal amplification system inspired by the natural yeast pheromone system and mating response was successfully tested (Section 3.3). However, particular advantages and drawbacks of the innovative approaches as well as the conclusions from the multitude of experimental observations need to be pointed out and discussed.

4.1 Strategies for expression of foreign genes

4.1.1 Plasmid-based and genome-integration strategies

The majority of fluorescence experiments in this work was conducted using a set of plasmid-based *S. cerevisiae* sensor and reporter strains. Like in most studies that aim at maximum foreign protein yield, multicopy 2μ-based plasmids were employed. Plasmid stability in recombinant yeast cells is affected by numerous genetic (intracellular) and environmental factors (Zhang et al., 1996). Genetic factors comprise the copy number, construct structure, expression level, conservation by a selection marker and properties of host cells, and can be governed by the experimenter. The cultivation medium or analyte solution and physical growth parameters also influence the expression rate but

as discussed later, only minimal alterations of a biosensor's monitored environment are desired. At the same time, yeast sensor and reporter cells must be viable and robust in respective conditions.

The hybrid (shuttle) vector series created by Mumberg et al. (1995) is a versatile tool for (over)expression of genes from constitutive promoters in three orders of magnitude. The vectors offer frequently used *URA3*, *TRP1* or *HIS3* markers for selection of auxotrophic mutant strains such as BY4741 or W303–1A. Importantly, they are also amenable to manipulation by means of reporter gene insertion and promoter replacement. In the course of single-cell analyses during recent experiments, some weaknesses became apparent. Transformants with a particular construct displayed a significant cell-to-cell variance in brightness and long-term storage of recombinant cells resulted in noticeable lower signal yield in microplate reader-based fluorometry measurements. The native 2μ plasmid itself is stably inherited with about 50–100 copies per cell (Clark-Walker and Miklos, 1974; Futcher and Cox, 1983). However, lower copy number and mitotic stability were obtained for artificial 2μ-based plasmids previously as well, even if they include auxotrophy selection markers (Christianson et al., 1992; Futcher and Cox, 1984). Fractions of 10–30% plasmid-free cells in suspension cultures and up to 60% in colonies on selective solid medium were observed in such studies and result presumably from crossfeeding. Moreover, individual transformants may also differ in productivity because of unequal plasmid copy number or variable fitness.

As a countermeasure, the genome-integrative strategy by Mirisola et al. (2007) was performed for transformation of cells with a stable detection construct. Cloning of the novel vector pTT allows for insertion of various promoter–reporter constructs into the *TYR1* locus and simple selection of transformants by double-checking for tyrosine auxotrophy and tryptophan prototrophy. The promoter–reporter construct GAP1–TurboGFP was selected as a first target because of the specific activation under limitation of rich nitrogen sources in yeast and superior brightness of plasmid-based GAP1 sensor cells. As expected, brightness of genome-integration sensor cells was multiple times lower than that of the plasmid-based counterpart. Despite significantly reduced maximum signal yield, fluorescence of non-limited and nitrogen-limited GAP1 sensor cells was distinguishable by qualitative and quantitative detection methods. Signal uniformity was impressive, given 100% of cells from each population displayed fluorescence at equal brightness.

Genome-based expression could be advantageous in the context of a microbial biosensor for several reasons. Next to highly dynamic changes in the expression profile at the population level, isogenic yeast cells also exhibit stochastic variation in expression levels (noise) at the single-cell level (Dong et al., 2011; Raser and O'Shea, 2004). A definite and stable copy number of the foreign promoter–reporter construct may lower fluorescence signal output noise and enhance fidelity of the reporter strains. Genome-

integrated detection constructs can be maintained without selection which is beneficial during long-term storage or application of yeast sensor and reporter cells in buffer solutions and monitoring environments. However, this conventional strategy is obviously limited to detection constructs employing strong promoters such as the *GAP1* promoter. Recently, a similar strategy allowed the generation of altogether ten integration constructs and a set of yeast reporter strains featuring three different fluorescent reporters: EGFP, TurboGFP and TurboRFP (Jahn, 2011). Remarkably, some clones with assumed random or another site-specific integration[1] displayed improved signal yield. There are probably loci other than *TYR1* in the genome of *S. cerevisiae* with better suitability for integration purposes. Alternatively, yeast sensor and reporter strains could be transformed with multiple or tandem-integrated detection constructs (Kudla and Nicolas, 1992; Plessis and Dujon, 1993). Ludwig et al. (1993) reported a strategy to deliver an expression cassette to the native 2μ plasmid. Insertion is carried out by a helper plasmid that is subsequently lost resulting in mitotic stable multicopy plasmids without selection markers. However, there has also been evidence that large 2μ plasmids are less stable.

4.1.2 Influence of the genomic background on the physiological activity

Experiments were performed with two common laboratory yeast strains, BY4741 and W303–1A. Both have mating type **a** and are reasonably isogenic to strain S288C[2] whose sequence is stored in the *Saccharomyces* genome database. With regard to the development of yeast biosensors for biotechnology application, both strains fulfil certain requirements. Of BY4741, a collection of deletion strains such as the *bar1*Δ mutant are directly available while the generation of respective W303–1A deletion strains takes additional effort. As BY4741 strains are licensed by the University of Basel (Switzerland) and are for scientific research purposes only, development of commercial products with these strains or their use in patented applications requires the purchase of further licences. No such claim is known for the popular strain W303–1A. In addition, W303–1A features five instead of four selection markers which may be advantageous for the generation of tailored multi-parameter sensor and reporter strains. Similar behaviour of BY4741 and W303–1A sensor cells in response to particular nutrient limitations was expected and verified for the nitrogen-responsive detection construct GAP1–TurboGFP for instance. Slightly higher basic fluorescence of W303–1A GAP1 sensor cells was observed and might be explained by higher autofluorescence of W303–1A which is reported in other studies

[1] Apart from the *TYR1* locus itself, few, however, not significant matches to the ends of the deletion cassette could be detected using BLAST.

[2] BY4741 was directly derived from S288C while the ancestral strain of W303–1A was mainly, but not exclusively, crossed with several S288C-like yeast strains (see Rogowska-Wrzesinska et al. (2001) and `http://wiki.yeastgenome.org/index.php/Commonly_used_strains` for details). [URL was last accessed on 28 September 2011.]

too (Schofield et al., 2007). Moreover, minor differences in the fluorescence reporter gene expression profile may result from cultivation in the presence of different amino acids and nucleobases that also form a minor nitrogen pool for yeast sensor cells. In contrast, a comparative study of BY4741 and W303–1A sulphur sensor strains showed that addition of supplements can be decisive for signal output. Methionine was required to grow auxotrophic BY4741 JLP1 sensor cells in selective medium but yeast has the rare ability to utilise methionine as a sulphur source (Thomas and Surdin-Kerjan, 1997). It was concluded that weak response of BY4741 JLP sensor cells to sulphur limitation was caused by methionine supplementation.

Selection of signature promoters in this study (see next section) was based on transcript analysis data of a member from the CEN.PK-family (Boer et al., 2003; Tai et al., 2005). The strain is not isogenic with BY4741 or W303–1A, and there could be crucial differences in response to nutrient limitation. A few other studies addressed this problem and showed that the genetic background may result in significant physiological differences such as phospholipid or amino acid metabolism (Daum et al., 1999; Rogowska-Wrzesinska et al., 2001). In their study, Rogowska-Wrzesinska et al. (2001) identified over 60 differently produced proteins in three yeast strains of the S288C-, W303- and CEN.PK-families. It should be noted that none was encoded by signature genes whose promoters were used in this study. In the theory chapter it was mentioned that ammonium is a preferred nitrogen source for yeast and a key component in the nitrogen metabolism. For S288C, in fact, ammonium can not be unambiguously classified as preferred nitrogen source but occupies an intermediate position (Magasanik and Kaiser, 2002). Thus, *GAP1* may be also expressed in the presence of ammonium which could explain moderate fluorescence of non-limited GAP1 sensor cells.

4.1.3 Selection of nutrient-responsive signature promoters

According to the central dogma of molecular biology, information runs from DNA to protein in a two-step process, i.e. transcription into mRNA and subsequent translation into protein[3] as the final product (Crick, 1958). In order to identify convenient signature promoters for the generation of nutrient-responsive sensor strains, transcript analysis data from the reports by Boer et al. (2003) and Tai et al. (2005) were used. Despite diligent data analysis of these studies, the identification of convenient promoters was virtually serendipitous. The mRNA abundance of signature genes was used as a surrogate to predict fluorescent protein production levels if the according signature promoter was used for reporter gene expression in yeast sensor cells. It was assumed that a high transcript abundance can be correlated with high protein levels. This is evident, for instance, for the amino acid metabolism of *S. cerevisiae* and suggests that yeast uses

[3] Disregarding the number of non-protein-encoding genes

common expression strategies to coordinate its metabolic and physiological functions (García-Martínez et al., 2007). Boer et al. (2003) and Tai et al. (2005) also detected some common regulatory motifs in promoters of genes belonging to the same regulatory cluster. They were also present in some signature promoters selected in this work. A possible reason for the lack of perfect correlation and an occasional failure of signature promoters could be ignorance of post-transcriptional regulation by this selection strategy (Beyer et al., 2004; Kolkman et al., 2006).

4.2 Performance of yeast nutrient sensor strains

4.2.1 Fidelity of signature promoters

In order to generate macronutrient-responsive detection constructs, about 1-kb fragments of the upstream regulatory region immediately adjacent to the start of translation of signature genes were cloned. Similar strategies for heterologous expression of fluorescence reporter genes were successfully applied in other studies (Park et al., 2007; Raser and O'Shea, 2004; Thierfelder et al., 2011). The sequences should include all relevant regulatory elements (Basehoar et al., 2004; Tirosh et al., 2007).

Despite careful selection criteria for signature promoters, successful regulation under a certain limitation was not guaranteed in every case. Some signature promoters yielded poor expression of fluorescence reporter genes (promoters of *HPF1*, *NSR1*, *SOL1*), or other responsiveness than expected (promoters of *DIP5*, *SCS3*, *TMA10*). All these promoters were predicted to feature lower expression under one particular nutrient limitation. The identification of reliable down-regulated promoters is probably more troublesome because of the lower number of existing signature genes and the absence of common regulatory motifs (Boer et al., 2003; Tai et al., 2005). Additionally, all down-regulated promoters were employed for expression of *EGFPpest* encoding a destabilised reporter protein with rapid turnover. With regard to distinct fluorescence fluctuations of yeast sensor and reporter cells employing this reporter after prolonged batch-cultivation, the fusion to a stable fluorescent reporter should be considered in future studies – at least for reference measurements. The suitability of fluorescence reporters is discussed in detail in Section 4.3. Other plausible explanations for inconsistent behaviour of sensor cells – the impact of genotype and cultivation of yeast on sensor cell performance – are discussed in Sections 4.1.2 and 4.2.2.

The observed expression levels from tested signature promoters mediating the desired expression trend were highly different with regard to signal yield and response time. Generally, nitrogen sensor cells yielded best brightness and fastest response while worst performance was observed for sulphur sensor cells. An explanation could be a difference in demand or storage capacity of the particular nutrient. Yeast takes up nitrogen in

concentrations one and two orders of magnitude higher than phosphorus and sulphur, respectively (Eide et al., 2005; Lange and Heijnen, 2001). This is in line with observed nutrient threshold concentrations in experiments presented in this work. From the abundance of known amino acid permeases it can be concluded that the cellular nitrogen demand is primarily met by uptake from the environment (Nelissen et al., 1997). In contrast, yeast can mobilise stored polyphosphates in response to phosphorus limitation or activate sulphur sparing mechanisms in response to sulphur deficiency (Fauchon et al., 2002; Kulaev et al., 1999). This could explain longer response time of yeast nutrient sensor cells after exogenous deprivation.

Fast and strong responses were obtained using promoters of genes encoding membrane-associated proteins such as amino acid permeases (*GAP1*, *GNP1*), an alkaline phosphatase (*PHO11*) and a sulphite pump (*SSU1*). Hence, the utilisation of promoters that regulate components of nutrient influx/efflux may be especially promising for sensor purposes. Raser and O'Shea (2004) successfully employed the *PHO84* promoter for genome-integrated fluorescence reporter gene expression in a yeast strain of the W303-family. *PHO84* encodes a high affinity inorganic phosphate transporter and is according to Tai et al. (2005) an up-regulated signature gene under phosphorus limitation too. Similarly, promoters of transporters *SUL2* (higher in sulphur limitation) or *HXT6* (lower in sulphur limitation) should be probed in order to generate new sulphur sensor strains with probably better performance in future studies.

In line with the transcript analysis data, GAP1 (nitrogen), PHO11 (phosphorus) and PDC6 (sulphur) sensor cells displayed no cross-reactivity in the presence of the other two macronutrient limitations, respectively. Different sources of one particular nutrient may trigger differential response of sensor cells though. This was evident, for instance, for GAP1 and GNP1 sensor cells that were cultivated in the presence of rich or poor nitrogen sources. Observed fluorescence levels of GAP1 sensor cells were in agreement with previously reported regulation of the general amino acid permease (Stanbrough and Magasanik, 1995). GAP1 is up-regulated in the presence of poor nitrogen sources (represented by L-alanine in current study's experiments) or in the absence of sufficient levels of rich nitrogen sources (represented by ammonium and L-glutamine). The response of GNP1 sensor cells in the presence of rich nitrogen sources was clearly different. *GNP1*, which is required for L-glutamine uptake, is about 1.6 fold lower expressed in the presence of glutamine than on ammonium and also weakly expressed on poor nitrogen sources (Zhu et al., 1996).

The *TMA10* promoter was expected to feature lower expression under phosphorus limitation (Boer et al., 2003), but TMA10 sensor cells displayed surprisingly higher fluorescence in experiments presented in this work. The related gene encodes a ribosome-associated protein of unknown function (Fleischer et al., 2006). Another ribosome-associated protein in yeast, Stm1p, plays an important role in protein translation under

nitrogen starvation although there is no evidence that its expression is nitrogen-regulated (Dyke et al., 2006). Accordingly, a particular function of Tma10p during phosphorus limitation could be hypothesised but its actual role and mode of expression could not be focused on in the context of this work. Highly interesting, the protein encoded by *RPS22B* is also ribosome-associated (Planta and Mager, 1998). Since expression is also affected by phosphorus levels, the hypothesis that phosphorus limitation may influence the expression of ribosomal proteins, is supported by another example. *DIP5* is listed as another signature gene that is down-regulated under phosphorus limitation (Boer et al., 2003). In experiments presented in this work, DIP5 sensor cells displayed only transiently lower fluorescence in phosphorus limitation medium compared to that observed in non-limited medium. This indicates that further factors influence its expression. Annotation of Dip5p as a high affinity amino acid permease strongly implies an impact of nitrogen sources on the performance of DIP5 sensor cells (Regenberg et al., 1998). Therefore, the strain is not convenient for unambiguous monitoring of phosphorus limitation. It should be noted that all three signature genes – *DIP5*, *RPS22B* and *TMA10*, – are less reliable under combinatorial limitation of phosphorus and oxygen (Tai et al., 2005). The authors proposed other phosphorus-responsive signature genes which function in transport and unambiguous regulation in both anaerobic and aerobic cultures, for example *PHO84* (see above). Such promoters should be primarily probed in future experiments.

PDC6 sensor cells displayed moderate but unambiguously higher fluorescence under sulphur limitation. The related gene encodes a pyruvate decarboxylase that is not directly involved in sulphur metabolism. In detail, Pdc6p is a sulphur-depleted enzyme isoform and up-regulation is in line with the hypothesis that yeast can remodel its protein composition in order to spare sulphur (Boer et al., 2003; Fauchon et al., 2002). However, *PDC6* transcription is also affected by levels of glucose and ethanol (Hohmann, 1991). This might be problematic during application in fermentation process control if glucose is exhausted or ethanol is produced. Probable occurrence of cross-reactivity should be examined in detail.

SCS3 sensor cells displayed transiently higher fluorescence in vitamin-deficient medium irrespective of the given sulphur concentration. Like in case of *PDC6*, there is no evidence for direct association of *SCS3* to yeast's sulphur metabolism. The gene encodes a protein with metabolic function in inositol prototrophy and phospholipid biogenesis (Hosaka et al., 1994). It is likely that lack of the vitamin solution containing inositol triggers activation of the *SCS3* promoter and thus fluorescence of respective sensor cells. The transient fluorescence is probably the consequence of cell death and cessation of metabolic activity upon inositol starvation which starts after four hours (Henry et al., 1977). Taking the required time for EGFPpest degradation (about 2 hours) into account, the observed fluorescence decay after five hours is in good agreement with this hypothesis. In conclusion, SCS3 sensor cell may be not appropriate to sense sulphur

limitation in general but their characteristic response towards lack of inositol could be beneficial for a (disposable) biosensor for qualitative diagnostic detection of inositol.[4]

4.2.2 Impact of the cultivation strategy

As mentioned before, signature promoters were selected from data acquired with a CEN.PK-type strain that is not isogenic with strains BY4741 and W303–1A which were used in the present work (Section 4.1.2). Essential differences in cultivation of sensor cells in own experiments and cells for mRNA analysis by Boer et al. (2003) and Tai et al. (2005) must be pointed out as a source of discrepancy in expression behaviour too. Yeast cells for transcript abundance measurements were grown in steady-state chemostats with accurate control of cultivation parameters and were non-recurrently analysed after 48 hours. However, if a change in expression is at the earliest detectable after a long time period as 48 hours, the signature promoter is evidently not suitable for near-line monitoring purposes anyway. In the presented experiments, sensor cells were batch-cultivated in shaking flasks and usually analysed repetitively over a time period of eight hours. Batch cultures represent a continuously changing environment and it is not possible to control or adjust a number of conditions during cultivation. Predominantly, the different growth rates[5] in batch- and chemostat operation can have a drastic impact on gene expression in *S. cerevisiae* (Diderich et al., 1999). On the other hand, there is also evidence that gene expression profiles of isogenic yeast cells in chemostats and batch cultures under phosphorus or sulphur limitation are comparable before complete nutrient exhaustion occurs (Saldanha et al., 2004).

It was observed that threshold concentrations for phosphorus and sulphur which trigger distinct response of respective sensor cells were one order of magnitude lower than they were used for microarray analyses in chemostat cultures by Boer et al. (2003) and Tai et al. (2005). The respective concentrations of the limiting macronutrient were, hence, lowered in limitation media for routine analysis experiments. Importantly, the magnitude of change and the final concentrations were in line with that in other nutrient-limited batch cultivation studies (Klosinska et al., 2011; Saldanha et al., 2004). A plausible explanation for a lower limiting nutrient threshold concentration in batch cultures is that sensor cells are probably able to compensate nutrient deficiency for a certain time period when shifted from non-limited medium. As mentioned before, yeast can remodel its structure and physiology to mobilise or spare intracellular nutrient resources. In addition, the biomass yield produced in a batch cultivation is lower than during chemostat cultivation (K. Kottmeier, Institute of Genetics/TU Dresden, pers. comm.).

[4] Inositol is a by-product from commercial yeast fermentation and could be utilised in feed additives for animals and aquaculture business (Henry and White, 1996).

[5] The specific growth rate (μ) in chemostats is constant and usually lower than in batch cultures where μ is maximum under the given environmental conditions.

With regard to the cell density, this results in an overall lower nutrient demand and slower consumption by batch-cultivated cells.

This touches another topic that needs to be discussed. The sequential utilisation of available nutrients during the course of batch cultivation, primarily glucose (required for energy supply) and nitrogen (required for protein biosynthesis), could result in exhaustion over time and subsequently fluctuating fluorescence reporter levels in sensor cells. Using a comparable experimental setup, Thierfelder et al. (2011) showed that glucose in synthetic mineral medium is reduced to non-detectable levels after four hours of batch cultivation. Despite the likely event of glucose and/or nitrogen starvation in own experiments, the generated yeast nutrient sensor cells mainly exhibited sufficient robustness against starvation for a certain time period. GAP1 nitrogen sensor cells, for instance, were still capable to produce and maintain high levels of stable (TurboGFP) and even destabilised (EGFPpest) fluorescence reporters under low nitrogen concentrations or poor nitrogen sources after up to eight hours of batch cultivation. Even nutrient sensor cells (GAP1, PHO11 and PDC6) that were fairly long-term cultivated in respective nutrient limitation medium for regeneration experiments (over 24 hours in total), displayed steady fluorescence. It could be hypothesised that cell viability is affected by prolonged starvation which could reduce sensor cell performance or durability. This was not examined by means of quantitative methods but differential response of sensor cells during regeneration experiments is rated as a clear indicator for viability.

It must be emphasised that there is certainly a discrepancy in the cultivation strategy of sensor cells for the presented evaluation studies and during perspective application in yeast biosensors. Industrial fermentation processes, for example, are primarily based on fed-batch cultivation strategies. Considering cultivation parameters, chemostats and fed-batch operation share more similarities with each other than both share with batch cultivation. Nevertheless, a batch cultivation mode can provide an informative basis for other yeast-based assays (Section 4.6.2). In order to near-line monitor certain processes, the generated sensor cells must be probed over a longer time period and continuous operation. However, this approach also requires another experimental setup with less manual labour, e.g. through immobilisation (Section 4.4). Experiments with oscillating nutrient concentrations may also be informative for durability. Next experiments must pursue these issues in detail.

4.2.3 Performance of nutrient sensor cells in microalgae media

The hypothesis saying the set of developed yeast nutrient sensor strains can be used for macronutrient monitoring purposes in white biotechnology was examined in a first attempt. To this end, selected sensor cells were cultivated in several microalgae media or supernatants after batch fermentation. This field of application is not randomly chosen. Controlled fermentation of microalgae in photobioreactors has drawn attention

of numerous industrial branches. Besides the use of microalgae biomass as a chemical feedstock, several attempts are taken to employ them for controlled production of valuable products (Pulz and Gross, 2004). For profitable production in an industrial scale with the objective of maximum yield and purity of end products, sufficient biological availability of nutrients during the fermentation process is essential. In the framework of the MBC project FOBIO that aims at the realisation of a new concept of photobioreactors with yeast cell-based near-line process analysis, media and supernatants of batch fermentation studies with microalgae were obtained from the project partner GMBU e. V., Department Dresden.

When comparing formulations of yeast-optimised mineral medium and microalgae media, yeast sensor cells have probably the best capacity for phosphorus monitoring purposes in the context of a biosensor for photobioreactors. Microalgae media contain intermediate concentrations of phosphorus in comparison to yeast-optimised mineral medium and phosphorus limitation medium. This substantiates that observed weak fluorescence levels of PHO11 sensor cells could result from the moderate concentration of inorganic phosphate sources. Observations by Sicko-Goad and Jensen (1976) strongly suggest that yeast and microalgae require identical sources and threshold concentrations of inorganic phosphate. Although the demand for sulphur by both species is primarily met by sulphate minerals, the difference in the main sulphur source in microalgae media (magnesium sulphate instead of ammonium sulphate) probably triggered fluorescence of PDC6 sensor cells. As noted before, *PDC6* is not directly connected to the sulphur metabolism of yeast. Although no cross-reactivity is observed in yeast-optimised media, unknown effects in foreign media could still have an impact on sensor cell performance. The actual reason must stay obscure in the context of this work as there was no available capacity to quantify nutrient concentrations. In future studies, nutrient concentrations could be determined by colourimetric methods. The most obvious difference in nutrient availability for yeast and microalgae has been observed with GAP1 nitrogen sensor cells. They were strongly fluorescent although all microalgae media contain intermediate concentrations of nitrogen compounds compared to yeast-optimised mineral medium and nitrogen limitation medium. But most importantly, nitrogen is provided in form of nitrate. This is the preferred nitrogen source for microalgae cultivation in photobioreactors but is not metabolised by yeast (Chen et al., 2011; Jin et al., 2006). In consequence, yeast sensor cells indicate nitrogen-limitation where there is none for microalgae.

When final signal levels of yeast nutrient sensor cells exposed to microalgae media and respective supernatants from batch cultivation were compared, small fluctuations were observed. Fluorescence in supernatants was typically lower than that in plain media. This probably resulted from release of biologically available nutrient sources for yeast in the course of the microalgae fermentation process, either by secretion or by lysis of microalgae. Utilisation of nitrate by algae requires its reduction to ammonium as well, and there

are likely intracellular resources of polyphosphates and sulphur metabolites (Giordano et al., 2008; Payne, 1973; Sicko-Goad and Jensen, 1976). However, further qualitative and quantitative examinations are necessary to evaluate which yeast sensor strains can be applied or are ineligible for monitoring of nutrient availability (in a concentration-dependent manner) during microalgae fermentation. Especially the capacity of yeast to sense broad spectra of sulphur[6] and nitrogen sources may be lucrative. Although the generated GAP1 nitrogen sensor strain failed to monitor nitrate in photobioreactors, it may be useful to monitor, for instance, the yield of (secreted) nitrogen products such as L-amino acids or proteins.

Yeast sensor strains may be also useful for nutrient monitoring purposes in fermentation processes with other microorganisms that share more similarities in demand of the nutrient source and the concentration. There are numerous processes already using *Pichia pastoris* or even *S. cerevisiae* (Li et al., 2007; Nevoigt, 2008). In the latter case, the producing host strain could be simultaneously exploited as a sensing element itself. Other potential fields of application for the generated nutrient sensor strains are discussed in the Outlook (Section 4.6.2).

It was demonstrated that yeast nutrient sensor cells may grow and can display varying fluorescence in microalgae media or supernatants if liquids were supplemented with glucose[7] as well as required amino acids and nucleobases. For the functionality of a perspective microbial biosensor, these additives could be either added directly to the fermentation process or solely to a separate containment including the microbial biosensor. The latter strategy avoids bulk glucose in the process and thereby reduces costs and danger of contamination of the photobioreactor with other microbes or germs.

4.3 Impact of fluorescent reporter proteins on the performance of sensor and reporter cells

4.3.1 General remarks

The measuring principle of all developed yeast sensor and reporter cells was based on fluorescence signal output. The production of fluorescent proteins is a popular reporter assay in order to examine and visualise particular promoter activity *in vivo*. This renders fluorescent proteins extremely useful for dynamic monitoring processes and biosensor purposes. From a technical point of view, signals can be directly collected from the sample with affordable equipment[8], and appropriate settings for excitation and signal de-

[6] The low threshold concentration for sulphur may counteract this attempt.

[7] Media for phototrophic microalgae contain no glucose and there was no detectable glucose enrichment in supernatants after fermentation of microalgae.

[8] A setup comprising a light-emitting diode and a coin-sized silicon photodetector may be sufficient for a microbial biosensor (Martineau et al., 2006).

tection/recording. Fluorescence can be monitored without cell disintegration or addition of exogenous substrates. If required, the signal can be measured repeatedly or continuously from the identical sample, which is an important criterion for the establishment of near-line process analysis. Most fluorescent reporters feature good thermal, pH and photostability allowing implementation in numerous processes and expression systems. Fluorescent proteins are usually considered as non-toxic and biologically compatible. However, DsRed-Express which is prone to oligomerisation and aggregation exhibits certain cytotoxicity in mammalian cells (Tao et al., 2007; Zhou et al., 2011). To current knowledge, such toxic effects have not been observed in yeast with the red fluorescent reporters used in this work, tetrameric DsRedT4 and dimeric TurboRFP.

Particular signal loss of an intracellular localised fluorescent reporter can be assumed because of shielding and light scattering effects by yeast's thick cell wall (Klis et al., 2002). As a countermeasure, the cell wall composition of sensor cells could be modified genetically, enzymatically or by growth conditions but this is expected to counteract their robust nature beneficial to biosensor applications. Alternatively, 'arming' sensor cells that display fluorescent reporters on the surface could be engineered (Kuroda and Ueda, 2011). Shibasaki et al. (2001) reported on the generation of yeast nutrient sensor cells that display ECFP or EYFP on the cell surface in response to low phosphate or ammonium ion concentrations, respectively. In another study, the heterologous expression of foreign proteins was followed by simultaneous display of an EGFP–α-agglutinin fusion protein (Shibasaki et al., 2003).

4.3.2 Suitability of fluorescent proteins for detection in sensor and reporter cells

The currently available palette of fluorescent proteins with over 100 members is impressive (Chudakov et al., 2010). A selection of nine members with emission maxima ranging from cyan to orange-red visible light was probed in this study. All reporters could be successfully expressed in yeast using the strong *GPD* promoter. Although the same promoter was applied for expression, there was a clear difference in performance of reporter cells regarding brightness and signal yield. Apart from weakly fluorescent ECFP reporter cells, at least one member of the examined green (GFPuv, EGFP, EGFPpest, TurboGFP), yellow (TurboYFP, PhiYFP) and red (TurboRFP, DsRedT4) fluorescent reporter cells displayed satisfying brightness. This can be mainly assigned to reporter protein's spectral characteristics (Tab. 2.6, Section 2.2.5). ECFP has a low relative brightness value in comparison to EGFP and hence features poor fluorescence of respective reporter cells. Green fluorescence-emitting EGFP and TurboGFP reporters cells gave a similar signal yield in line with comparable spectral properties of the two reporter proteins. The superior brightness of EGFPpest reporter cells was surprising

since the chromophore of EGFPpest is identical to that of EGFP. Higher brightness could result from yeast-optimised codon-usage in the encoding sequence. Cormack et al. (1997) also observed improved brightness of codon-optimised EGFP and suggested that higher translational efficiency as well as higher mRNA levels and stability may contribute to this increase. The brightness of EGFPpest reporter cells is even more impressive considering the fact that they can almost certainly not accumulate maximum concentrations of the fluorescent protein because of the destabilising PEST motif (Mateus and Avery, 2000). Codon-optimisation is, therefore, considerable for any reporter gene sequence in order to improve signal output. The enhanced GFP variant GFPuv proved to be a stable and bright reporter with particularly good performance in eukaryotes (Crameri et al., 1996). Here, brightness was even superior to that of EGFP if excitation was suboptimal. Unfortunately, GFPuv was not available prior to late stage of the experimental work and could not be used as a reporter in the pilot set of nutrient sensor strains and pheromone-responsive FIG1 reporter cells. The yellow reporters PhiYFP and TurboYFP mediated similar signal intensities given their kinship and similar spectral properties. However, close proximity of excitation and emission maxima of both reporters and their intermediate position around 530 nm made optimal detection difficult with available instruments.[9] TurboRFP was superior to DsRedT4 as a red fluorescent reporter. Besides its affiliation to the brightest (red-orange) fluorescent proteins known, fast maturation of the dimeric protein may be beneficial for tracking promoter activity (Chudakov et al., 2010; Day and Davidson, 2009). Nevertheless, a distinct bleed-through effect, i.e. noticeable green fluorescence of yeast cells expressing *TurboRFP*, was observed. As discussed in Section 4.3.4, this could be a crucial drawback for its application in dual-colour sensor cells. The optimised tetrameric DsRedT4 may serve such purposes better since it produces no detectable bleed-through into the GFP channel (Bevis and Glick, 2002). The poor brightness is still, however, hindering.

There is another advantage of yellow and red over green fluorescent reporter proteins. Longer wavelengths usually reduce problems associated with autofluorescence of cells and light scattering (Tsien, 1999). In line with this, background fluorescence was lower for yellow and red fluorescent reporter strains. The naturally abundant compounds NAD(P), FAD and FMN fluoresce in a wavelength range below or around 500 nm (Duchen and Biscoe, 1992; Weber, 1950). This is nearby the emission maxima of cyan (about 480 nm) and green (about 510 nm) fluorescent proteins and could obscure weak CFP/GFP fluorescence. In most microplate reader-based or fluorescence microscopy experiments the signal-to-background ratio for green fluorescent sensor and reporter cells was sufficient but implementation of red fluorescent reporter TurboRFP may significantly enhance the signal-to-background ratio. This is of special interest for measurements in immobilised

[9] For microplate reader-based fluorometry, excitation and emission wavelength needed to be set at least 30 nm apart from each other and filters for fluorescence microscopy were either optimal for detection of GFP or RFP.

state. In case of immobilised FIG1 reporter cells for a cellular communication and signal amplification system in conjunction with fluorescence scanning, an EGFP fluorescence signal of reporter cells was too weak for detection (data not shown). In contrast, even the lowest tested concentrations of pheromone sources (10 nmol l^{-1} synthetic α-factor and α-factor-secreting cells adjusted to an optical density of 0.1) were detectable with *TurboRFP*-expressing reporter cells.

In conclusion, qualification of a number of green, yellow and red fluorescent proteins for implementation in yeast sensor and reporter cells could be confirmed in this work but the selection of an appropriate reporter depends on the intended use. Presumably the most popular and well-studied fluorescent reporters for microbial biosensors are green fluorescent proteins as can be seen in Table 1.1 and reviews by Baronian (2004), Lei et al. (2006) and Su et al. (2011). They were primarily used in this work too because of their properties and optimal amenability to all available measurement devices.

4.3.3 Stability of fluorescent proteins

Most experiments were performed using one out of three green fluorescent reporters: EGFP, TurboGFP or EGFPpest. According to literature, these reporters possess similar spectral characteristics but rather differ in maturation time and stability. Primarily in order to generate stable signals like in reporter cells for a cellular communication and signal amplification system or nutrient sensor cells with higher fluorescence under nutrient limitation, up-regulated promoters were fused to genes encoding the stable GFP variants EGFP and TurboGFP (Cormack et al., 1996; Evdokimov et al., 2006). Although expression of both reporter genes was not directly compared for the same promoter, no significant difference in general performance of these two types of sensor cells was observed. Distinct changes in expression from a nutrient-responsive promoter, for instance, were detectable on protein level after a minimum of two hours after shift to respective nutrient limitation medium for both reporters. Therefore, superior chromophore maturation time for TurboGFP highlighted by Evdokimov et al. (2006) is irrelevant in comparison to the required time for transcription, translation and accumulation of detectable protein levels after promoter activation (Wulf et al., 2000). The results with GAP1 and DAL5 nitrogen sensor cells expressing codon-optimised *EGFPpest* yielded even higher cellular brightness. This supports the hypothesis that implementation of a reporter with host-adapted codon usage may benefit signal output and consequently sensor cell performance (Li et al., 1998; Mateus and Avery, 2000).

The destabilised EGFPpest reporter was primarily implemented in nutrient sensor cells that employ down-regulated signature promoters with the intent to ensure rapid reporter protein turnover during 'lights off' assays. According to Mateus and Avery (2000), EGFPpest has a remarkably lower half-life in yeast (about 30 minutes) than FACS- and codon-optimised stable EGFP (about seven hours). In line with the authors'

observation that EGFPpest levels significantly decrease within two hours of cell cycle progression, rapid fluorescence decline in a similar range of time was shown in own experiments. The instability of the reporter protein was particularly noticeable after prolonged batch cultivation of yeast sensor and reporter cells. GNP1 (nitrogen), RPS22B (phosphorus) and SSU1 (sulphur) sensor cells should display high basic fluorescence in non-limited medium. In contrast, overnight cultivated sensor cells displayed weak fluorescence that shortly recovered after shift to fresh medium before anew decline. In line with this observation, the fluorescence of EGFPpest reporter cells with expression from the strong constitutive *GPD* promoter showed a similar fluctuation. As marked earlier, this phenomenon could result from exhaustion of essential nutrients or a shifting expression behaviour of yeast reporter cells in the permanently changing environment of batch cultures (Section 4.2.2). Steadily increasing fluorescence of GAP1, DAL5 or TMA10 sensor cells with EGFPpest after shift to limitation medium partially disproves this hypothesis – at least for the time period of eight hours. TMA10 sensor cells displayed low fluorescence also after overnight cultivation in phosphorus limitation medium.

In Western blot analysis, a persistent signal matching the size of EGFP cells was observed in samples of EGFPpest reporter cells. Although the protein is tagged with the PEST motif, the GFP core could be resistant to degradation because of its stable tertiary structure or insufficient degradation capacity for abundant amounts of overexpressed protein. This phenomenon was apparently not observed in studies with weaker expression levels (Mateus and Avery, 2000; Thierfelder et al., 2011).

In conclusion, rapid protein turnover of EGFPpest theoretically renders the protein valuable for dynamic monitoring purposes but explicit fluctuations give a high uncertainty in total readout values and could make sensor strains less reliable in batch operations. The performance in continuous systems must be carefully probed in further studies. For next batch cultivation experiments, sensor cells could be equilibrated for two hours in fresh mineral medium prior to actual analysis in order to restore basic fluorescence levels.

Because of poor fluorescence of down-regulated sensor cells after overnight cultivation, sensor cells producing stable EGFP or TurboGFP reporters were used to examine basic fluorescence regeneration after shift from nutrient-limited to non-limited conditions. In detail, GAP1 (nitrogen), PHO11 (phosphorus) and PDC6 (sulphur) sensor cells were analysed. In batch cultures, a signal decline was observed on the population and single cell level but the basic fluorescence level of non-limited cells was never reached within eight hours. For glucose sensor cells and a similar experimental setup, particular regeneration of basic fluorescence was reported by Thierfelder et al. (2011). Because EGFP and TurboGFP are very stable, the observed fluorescence decline results most likely from signal dilution due to cell division (Wulf et al., 2000). Quantitative real-time RT-PCR could be conducted in order to follow and confirm the hypothesised changes in expression on the level of transcription.

4.3.4 Simultaneous detection of two fluorescent reporter proteins in dual-colour nitrogen sensor cells

Sensor cells with multiple detection constructs are of particular interest, for instance, to acquire several parameters simultaneously, to double-check occurrence of one limitation or for internal control of cell number and vitality. A 'next generation' bacterial biosensor for simultaneous detection of cytotoxicity and genotoxicity was described previously (Hever and Belkin, 2006). Combined expression of green/red fluorescent reporters in yeast was realised in some studies too (Kurischko et al., 2011; Malínská et al., 2003; Rodrigues et al., 2001). In order to test the concept of a dual-colour yeast sensor strain, nitrogen sensor cells with inducible green (TurboGFP) and moderate constitutive red (TurboRFP) fluorescence were generated. In good agreement with expectations, green fluorescence was triggered in nitrogen limitation medium while red fluorescence was basically unaffected by cultivation conditions or elapsed time. This opens the possibility to use the additional fluorescent reporter in this strain as a surrogate for cell number or cell density in prospective biosensor assays. Thinking further, *TurboRFP* could be fused to another inducible or repressible promoter in order to reaffirm nitrogen limitation or for simultaneous monitoring of a second parameter. Other nutrient sensor strains could be designed in a similar manner. However, there is a certain restriction in this proposition. As mentioned in Section 4.3.2, TurboRFP is detectable in the green fluorescence channel and resulted both in higher basic and nitrogen limitation-induced fluorescence of dual-colour GAP1 sensor cells. Because of the general strength of the GAP1-TurboGFP detection construct, induction of green fluorescence after shift to nitrogen limitation medium was still detectable. But weaker green fluorescence reporter gene expression in other yeast sensor strains could be completely covered by TurboRFP bleed-through effects. Different strategies could be considered as a countermeasure. Sticking to the reporter pair TurboGFP/TurboRFP, the red reporter should be fused to the weaker promoter. Alternatively, green fluorescent reporter could be combined with red reporters that promise less bleed-trough (e.g. DsRed variants) or deep/far-red reporters. The most useful, so-called 'mFruit' fluorescent protein from Clontech, mCherry, features peak emission at 610 nm but theoretically yields only 50% the brightness level of EGFP (Day and Davidson, 2009). In preliminary yeast expression studies, virtually no fluorescence was detectable (data not shown). In other studies with yeast, cyan and yellow fluorescent reporters were used in combination (Colman-Lerner et al., 2005; Raser and O'Shea, 2004; Warren et al., 2002). But ECFP and EYFP function as a donor–acceptor pair for fluorescence resonance energy transfer which may result in unintentional quenching of ECFP fluorescence (Pollok and Heim, 1999). In all experiments presented here, ECFP reporter cells displayed poor brightness as well as high autofluorescence background. Thus, no optimal solution can be proposed but this option must be investigated further.

4.4 Advances to yeast cell entrapment

4.4.1 Necessity of immobilisation

Immobilisation of yeast cells as the sensing element is a preferable but also critical step during microbial biosensor fabrication (Baronian, 2004; D'Souza, 2001). From a technical point of view, close conjunction of sensing cells and the transducer element promotes efficient signal transmission. At the same time, the immobilisation matrix is a physical barrier that fixes sensor cells at a defined position for precise measurements and protects the transducer surface from biofilm development or fouling. It is often stated that entrapped cells themselves are less susceptible to contamination.

During and after the immobilisation process, cells are exposed to a hyperosmotic microenvironment that can have both positive and negative effects on sensor cell performance. Osmotic stress during the immobilisation procedure can enhance viability and tolerance of yeast cells to toxic compounds or further stress inducers (Melzoch et al., 1994; Norton and D'Amore, 1994; Sun et al., 2007). This can be beneficial for sensor durability and long-term storage. There is evidence that the physiology of immobilised yeast cells is different from that of free ones (Verbelen et al., 2006). For alginate-entrapped yeast cells, improved heterologous gene expression rates, reduced plasmid loss and delayed overgrowth of plasmid-free cells have been reported, which may be advantageous using plasmid-based sensor cells (Bleve et al., 2008; Chau et al., 2000). However, immobilisation may have an impact on the plasma membrane properties of yeast cells, which can, in turn, cause modifications of some transport systems (Shen et al., 2003). Considering the fact that the created sensor cells perceive signalling molecules or nutrient concentrations by surface receptors, there could be an impact also on performance.

In the framework of the MBC projects FOBIO and MaBioS, immobilisation of tailored cells on non-biological surfaces was of particular interest. In order to extend the capability of the MBC technology and to address new markets such as microbial biosensor development for white biotechnology or other purposes, exhaustive examination of sensor cell performance after immobilisation was needed. The Institute of Genetics/TU Dresden was primarily responsible for the generation and evaluation of genetically engineered yeast cells for sensing purposes, but detailed examination of immobilisation strategies was not realisable in this work. However, general functionality of fluorescent yeast sensor and reporter cells after entrapment and their accessibility to several fluorescence readout (i.e. transducer) methods were successfully probed as a proof of concept. Collaboration partners such as the Institute of Materials Science/TU Dresden or the GMBU e. V., Department Dresden kindly shared their expertise in cell immobilisation strategies. With regard to the fact that physical entrapment methods are the most gentle and, therefore, promising immobilisation techniques for living cells, hydrogels primarily based on calcium-alginate have been used in MBC projects and this work.

4.4.2 Immobilisation in large calcium-alginate beads

The entrapment of yeast cells in large calcium-alginate beads for purposes of luminescence measurements or enzyme production were demonstrated in previous studies (Bleve et al., 2008; Fine et al., 2006). In a first attempt, the successful induction and acquisition of fluorescence signals from calcium-alginate beads with entrapped yeast sensor and reporter cells was demonstrated in this work and was recently published as a part of these studies (Gross et al., 2011).

Like from cells in batch cultures, constitutive or inducible fluorescence signals were detectable by fluorescence microscopy or microplate reader-based fluorometry. Importantly, a certain decrease in sensitivity was observed for sensor cells with inducible fluorescence when compared to cell suspension measurements. In detail, immobilised GAP1 sensor cells with higher fluorescence in nitrogen limitation displayed significantly lower signal differences than in batch cultures, and pheromone-responsive FIG1 reporter cells responded to a slightly lower α-factor concentration after entrapment. Several reasons were assumed. Firstly, the immobilisation matrix represents a diffusion/mass transfer barrier between the bulk medium and entrapped cells (external barrier) as well as within the hydrogel (internal barrier). Diffusion properties are determined by porosity and size of the matrix. Thus, the alginate concentration is a quite critical parameter. While beads with a high alginate concentration may result in a too high diffusion barrier for nutrients or signalling molecules, beads with too low alginate concentrations may be too fragile (Bleve et al., 2008; Konsoula and Liakopoulou-Kyriakides, 2006; Mehmetoglu et al., 1996). According to literature, the pore size of hydrogels with a 2% (w/v) alginate content are sufficient to let pass molecules that were of interest here, i.e. α-factor with an expected size of about 1,700 Daltons and even smaller ions such as ammonium, inorganic phosphate or sulphate (Dembczynski and Jankowski, 2001; Klein et al., 1983). Secondly, the term 'hydrogel' implies that the immobilisation matrix includes a high liquid content. The batch cultivation volume for the microplate reader-based fluorescence assays after immobilisation was significantly lower than for suspension cultures. It is likely that lower fluorescence signal differences between cultivation conditions were caused by preservation of equilibration medium and subsequent dilution effects after transfer. Thirdly, there may be disturbing electrostatic interactions of charged ions with also charged alginate that delay diffusion (Holte et al., 2007). Pheromone α-factor[10] and ammonium ions have a net positive charge which could result in attraction by the negatively charged alginate hydrogel. In contrast, anions such as inorganic phosphate or sulphate may be repulsed.

Yeast sensor cell entrapment in large-scale beads allowed for easy handling and faster measurement than routine suspension fluorescence assays. In fact, cells from one batch could be stored at 4°C and used for numerous measurements. During one

[10] The α-factor peptide contains three potential positively charged groups (N-terminal amino group, His2 and Lys7) and one potential negatively charged group (terminal carboxyl group).

experiment the identical cells could be monitored repetitively. As a consequence, both the required biomass and observed variation between measurements were reduced. A disadvantage with this immobilisation-based assay was that total fluorescence could not be referenced to constant cell densities like determined during assays with free cells by OD_{600} measurements. This likely results in non-proportional correlation of observed total fluorescence values and actual fluorescence per cell due to increasing autofluorescence and scattering, shielding or quenching effects. Moreover, hand-made production of spherical beads is not appropriate for technical large-scale fabrication of microbial biosensors. Laboratory-scale devices for machine-made production of alginate beads with a diameter ranging from 50 μm up to 2 mm have been developed and partially commercialised (Serp et al., 2000; Sugiura et al., 2005). However, the interest in this technology is primarily settled in the area of medical and bioprocess engineering.

4.4.3 Automated and miniaturised immobilisation in calcium-alginate hydrogels

Immobilisation strategies must be tailored with regard to geometry and mode of fabrication to suit a certain purpose. Recent and future trends in microbial biosensor development tend towards lab-on-chip technology or micro- or even nano-scale fabrication (Su et al., 2011). Instead of bulk immobilisation methods, a reliable technology for precise deposition of viable microbial cells in thin layers on dominantly planar surfaces is required. The 'Nano-Plotter' system developed by the local industry partner GeSiM GmbH is a promising automatic instrument for accurate and arbitrary deposition of nanolitre volumes on material surfaces. In cooperation with the Institute of Materials Science/TU Dresden, miniaturised arrays of viable yeast sensor and reporter cells with strong constitutive or inducible fluorescence were successfully tested. An area of about 5×5 cm^2 with approximately 1,500 cells was sufficient for unambiguous detection of fluorescence signals. However, optimisation of the immobilisation conditions is still recommended. The nano-printing of sensor arrays was extremely time-consuming and troublesome in comparison to the hand-made production of calcium-alginate beads. Small pipetting volumes caused severe problems with evaporation as well as reduced viability and functionality due to excessive pressure during piezoelectric micro-dispensation. Calcium-alginate/cell-arrays were also less robust than beads and patches were washed off the glass surface to some extent during handling. The reduced biomass in such thin layers also resulted in lower signal yield. In fact, fluorescence of GAP1 sensor cells with strong fluorescence under nitrogen limitation was clearly detectable while fluorescence of phosphorus-limited PHO11 sensor cells or sulphur-limited PDC6 sensor cells was not. As a countermeasure, multiple layers may be plotted but prior to this the nano-printing procedure must be optimised in terms of faster completion of array preparation.

4.4.4 Tailored geometry and composition of the immobilisation matrix

One type or even mixtures of yeast sensor and reporter cells could be entrapped in calcium-alginate beads. With regard to the cellular communication and signal amplification system, there is a particular interest in the separation of pheromone-producing (sensor) cells and pheromone-responsive (reporter) cells in adjacent compartments with a shared boundary (Section 4.5.1). Neither the bead-based immobilisation method (for geometrical reason) nor the disappointing status quo of nano-printing technology could meet these demands. As an alternative, plasmid-based sensor and reporter cells were immobilised in an agarose-based two-compartment setup that was recently validated (Jahn, 2011).[11] In line with the results of the nano-printed arrays, a dimension of 5×5 mm^2 was apparently sufficient for detection by fluorescence scanning and, remarkably, can be bridged by α-factor. In addition, the use of thicker layers and brighter fluorescent reporters (Section 4.3) can demonstrably and strikingly enhance signal output. Some concerns in widespread use of agarose for industrial biosensors are higher costs than of alginate and the necessity of heating the natural polymer over 37°C during the immobilisation procedure.

It should be noted that immobilisation strategies need to be tailored for structural stability in diverse fields of application. Calcium-alginate hydrogels were remarkably stable in the presence of low amounts of calcium (10 mmol l^{-1}). With regard to application of prospective yeast biosensors in white biotechnology, calcium addition to the batch or chemostat operation should be unproblematic for the majority of fermentation processes. Alternatively, calcium could be added after process sampling in a bypass solution. It must be emphasised that the use of developed yeast sensor and reporter cells is not restricted to applications in white biotechnology (Section 4.6.2). Other samples such as wastewater or salt-rich liquids though can contain chelators, phosphates and monovalent cations that may destabilise or even dissolve calcium-alginate hydrogels. Additional modifications, e.g. cross-linking or stabilisation with polyelectrolytes could prevent this (Kwon and Peng, 2002; Li, 1996). In any case, a compromise between matrix stability, remaining porosity and biological compatibility of the technique has to be made.

4.4.5 Viability and growth of immobilised yeast cells

The survival and vitality of yeast cells after immobilisation was not quantified.[12] For the recent experiments, budding or formation of mating projections of the major fraction of

[11] There is a significant body of evidence for sufficient diffusion of α-factor and comparable behaviour of the developed set of yeast sensor/reporter strains for a cellular communication and signal amplification system in agarose and alginate hydrogels. Moreover, transparency of agarose is sufficient for fluorescence detection.

[12] This issue was examined by the Institute of Materials Science/TU Dresden. According to presented results in internal FOBIO and MaBioS project meetings, immobilisation did not significantly decrease viability of yeast cells (B. Soltmann, Institute of Materials Science/TU Dresden, pers. comm.).

immobilised cells was taken as a surrogate for viability. However, during long-term use in embedded state in prospective microbial biosensor applications, growth of yeast cells can be quite obstructive. Massive propagation may lead to higher background fluorescence which can result in a highly questionable signal output during measurements with expected fluorescence decay. In addition, the immobilisation matrix may be disintegrated. This reduces biosensor durability and increases the effort for disposal of contaminated analyte solutions.

Perception of α-factor resulted in noticeable cell cycle arrest but there are applications possible where pheromone response is either not triggered or not intended. The application of so-called *cdc* mutants which can grow at a permissive but not at a restrictive temperature could prevent undesired growth (Hartwell et al., 1973). Numerous *cdc* mutant strains with W303-background – already validated for biosensor purposes in this work – are available and a selection was kindly provided by the Research Group of W. Zachariae (MPI-CBG, Dresden). Initial studies considering the applicability of cell cycle mutants *cdc15–2*, *cdc16–123* and *cdc28–13* (restrictive temperature 37°C) for biosensor purposes were recently performed (Spitzweg, 2010). The high restrictive temperature could cause higher cost during construction, storage or operation due to energy supply. Although *cdc* mutants with lower restrictive temperature (25°C) exist as well, their applicability must be exhaustively probed as handling is more sophisticated.

4.5 Advances to improve signal yield

4.5.1 Signal amplification by α-factor-based signalling

Paradigm of the cellular communication and signal amplification system

Biosensor assays using cells as the sensing element often suffer from poor signal yield that can not be improved solely by implementation of a stronger promoter or a brighter reporter. This work documents the applicability of the authentic *S. cerevisiae* pheromone system in conjunction with artificial constructs for secretion and detection of the pheromone α-factor in order to generate a versatile cellular communication and signal amplifier system. An international patent was issued to claim utilisation of the system for cell-to-cell signalling and signal amplification purposes (Ostermann et al., 2008b). Parts of the present work have also been published recently (Gross et al., 2011).

The generated system can be considered as an extended unicellular biosensor concept where the two fundamental steps – detection of analytes and production of fluorescence output signals – are spatially separated by means of implementation in two different cell types. In order to reconnect these two functions, the small diffusible α-factor was used as a signalling molecule. In fact, α-factor was preferred for this purpose as it needs no modifications and its biogenesis requires only the classical secretory pathway – cell's

ubiquitous protein secretion machinery. To probe the versatility of this system, it was implemented in yeast cells of mating type **a** that inherently do not produce α-factor but can respond to it. The made observations indicated that this strategy is sufficient but strictly requires deletion of the *BAR1* gene encoding α-factor protease in respective cells for effective signalling. However, there may be some less obvious drawbacks in the use of **a** cells. For this reason, two *matα*Δ deletion strains lacking expression of both α-factor-encoding genes, *MFα1* and *MFα2*, were generated for further analyses. One of these strains was additionally deleted for *BAR1* whose expression is negatively regulated by *MFα2* – lacking in the deletion mutant – and triggered by α-factor (Manney, 1983). In preliminary examinations, a setup with implemented *matα*Δ deletion strains for plasmid-based α-factor production yielded comparable fluorescence signal levels to that of the original system exclusively based on *bar1*Δ cells of mating type **a**. Thus, all α-factor-secreting strains are likely used to capacity. A noticeable difference, however, was that the *matα*Δ-based strains displayed no such bizarre mating projections like exploited **a** cells (data not shown).

Reporter gene expression was driven from the pheromone-inducible *FIG1* promoter and yielded sufficient fluorescence levels after four hours. According to other studies, *FIG1* exhibits the strongest change in transcript abundance (about 100-fold) after stimulation with α-factor (Roberts et al., 2000; Spellman et al., 1998). It is questionable whether other promoters could mediate stronger or faster expression. *PRM2* for instance has a similar expression profile like *FIG1* but respective reporter cells yielded fourfold lower brightness. In other studies, promoters of *FUS1* and *PRM1* were exploited for expression of several fluorescence reporter genes (Colman-Lerner et al., 2005; Ishii et al., 2006; Yu et al., 2008a). It is noteworthy that reporter gene expression in these studies was successfully monitored after insertion into (the native) genomic loci. Suitability of the promoters for this work's purpose should, therefore, be probed as well. In addition, the genome integration strategy is surely lucrative for sensor fidelity (Section 4.1.1).

Activation of all pheromone-responsive genes is Ste12p-dependent and thus most likely subjected to identical expression kinetics. Recent examinations by Su et al. (2010), however, showed that the number and position of Ste12p binding motifs in pheromone-responsive promoters strongly affected expression efficiency of *lacZ* reporter gene. These findings are valuable with regard to optimisation strategies by modifying authentic promoters or even the creation of artificial ones (Section 4.5.2).

To date, nearly all studies dealing with activation of pheromone-responsive genes use synthetic α-factor. In the presented work, it could be demonstrated that fluorescence of reporter cells can be triggered with cell-secreted α-factor too. The moderate *ADH* promoter mediated sufficient α-factor production for activation of reporter cells that were at least in tenfold excess. Signal amplification is also achieved by the fact that the gene *MFα1* encodes four copies of α-factor and expression is driven from a multicopy

2μ-based plasmid. Thus, a single α-factor-secreting cell can activate multiple reporter cells. The utilisation of amplifier cells harbouring the *MFα1* gene under the control of the pheromone-inducible *FIG1* promoter offers another amplification circuit.

Weaknesses and unique features of the system

Three important drawbacks of the systems must be examined carefully. Firstly, in comparison to other studies relatively high threshold concentrations of synthetic α-factor in control experiments (at least 0.1 μmol l^{-1} in suspension and 0.5 μmol l^{-1} after immobilisation[13]) were necessary to trigger detectable fluorescence in BY4741 *bar1*Δ reporter cells. According to Moore et al. (2008), this strain is capable to sense steady gradients in concentrations ranging from 1 nmol l^{-1} to 1 μmol l^{-1} α-factor. In presented experiments, a static or dynamically produced pheromone source was applied. Due to binding of α-factor to the cell surface of reporter cells it is probably exhausted over time. Roberts et al. (2000) observed a relatively invariant transcript response profile in batch cultures after already 30 minutes with α-factor concentrations above 15 nmol l^{-1} indicating this is a saturating pheromone concentration. In own experiments, batch cultures with higher cell densities were used and detection of pheromone response on the protein level was presumably delayed as there is additional time required for translation and maturation of the fluorescent reporter. Although in experiments with cell-secreted α-factor continuous production is ensured, certain time is required for accumulation of sufficient pheromone concentrations to activate reporter cells. Quantification of cell-secreted α-factor is difficult. Precipitation and conventional Western blot analysis is troublesome for such small peptides (J. L. Gaugler, Institute of Genetics/TU Dresden, pers. comm.; Jahn, 2011). Other attempts rely on indirect measurements such as halo assays (Kurjan and Herskowitz, 1982). HPLC could be conducted for direct detection but establishment and validation of this sensitive method is laborious and costly. Thus, a rough estimation must be made from comparison with fluorescence yield generated with synthetic α-factor.

Secondly, there are dilution effects of total fluorescence signal yield if reporter cells are cocultivated or coimmobilised with α-factor-secreting cells that do not fluoresce. As a countermeasure these cells could be simultaneously transformed with a direct detection construct but this may result in reduced expression capacity due to limitation of transcription factors (see Section 4.5.2). Alternatively, the recently validated two-compartment setup with a shared boundary between the source of α-factor (e.g. cells) and fluorescent reporter cells could be beneficial. With this approach, a 1:20 ratio of pheromone-secreting and responsive cells was sufficient for detection and a 1:1 ratio may be applied to trigger strong signals without 'dilution' of fluorescent cells. In addition, separated entrapment is advantageous because that way pheromone-secreting and pheromone-responsive cells

[13] Reasons for impaired sensitivity of entrapped cells have been already discussed in Section 4.4.2.

do not compete for space or nutrients.

The third drawback is the prolonged time between analyte sensing and fluorescence acquisition in comparison to a unicellular sensor since additional time is required for α-factor production and secretion. In proof of concept experiments, reporter cells were cocultivated with permanently α-factor-secreting cells (plasmid p426ADH–MFα1). During a traditional 'lights on' biosensor approach in contrast, the production of α-factor would be conditionally triggered under one particular condition, for instance, nutrient limitation. However, the real benefit of this setup is signal amplification. In fact, a tenfold lower amount of phosphorus-responsive, α-factor-secreting PHO11 sensor cells was employed for generation of an adequate fluorescence signal in reporter cells in comparison to a strain harbouring the direct PHO11–EGFP construct. Apart from this example, the cellular communication and signal amplification system could be exploited for numerous other applications. A detailed vision is discussed in Section 4.6.2.

Benefits from cell cycle arrest and morphological changes

The inherent mating response of *S. cerevisiae* mating type **a** cells in response to α-factor leads to cell cycle arrest and formation of mating projections. Both phenomena may be advantageous in biosensor applications as well. With regard to immobilised sensor cells, limited propagation minimises outgrowth or shift of background fluorescence and thus improves biosensor durability and performance. In order to prevent destructive effects due to formation of mating projections, *afr1*Δ deletion mutants could be applied. Creation and phenotypic characterisation of an deletion strain was previously reported (Groba, 2007). On the other hand, the formation of mating projections could be exploited for sensor purposes itself. Patents were issued that claim the use of these morphological changes as a detection principle in yeast-based sensor assays (Ostermann et al., 2010, 2009). Morphological changes can be detected by flow cytometry or even with a simple spectrophotometer. The mating response of yeast results in production and display of cell adhesion facilitators and the degree of agglutination could be assayed by spectrophotometry too (Lipke and Kurjan, 1992). A sophisticated approach would be the detection of mating projections via particle plasmon resonance or particle-mediated fluorescence. As recently shown by Thierfelder (2011), mating projections of *S. cerevisiae* can be labelled with fluorescence- or nanoparticle-conjugated antibodies which target also immunolabelled, shmoo tip-concentrating protein Fus1p.

4.5.2 Fidelity, reliability and capacity of promoters

As mentioned at the very beginning of this chapter, the cell-to-cell variance in expression could be an obstacle to signal output fidelity, and genome-integrated reporter constructs could render sensor cells more reliable (Section 4.1.1). Expression of multiple reporter

genes in dual-colour sensor cells resulted in a noticeable signal loss of constitutively expressed *TurboRFP* fluorescence in comparison to reporter cells expressing the reporter gene alone. This may result from insufficient levels or titration of transcription factors in cells carrying multicopy plasmids (Irani et al., 1987; Mumberg et al., 1995; Weber et al., 1992). Overexpression could consequently distort the correlation between analyte concentration and output signal strength. This is not expected from a genome-integrated detection construct with authentic or low copy number.

It was also found that expression noise is promoter-dependent. TATA-box containing promoters (about 20% in yeast including the promoters of *GNP1*, *PHO11* and *PDC6*[14]) tend to be more susceptible to stochastic fluctuations (Basehoar et al., 2004; Dong et al., 2011; Raser and O'Shea, 2004). Raser and O'Shea (2004) showed that the noise can be already altered by small mutations in the promoter sequences. Moreover, there is no strict dependency of the noise level on the absolute rate of expression or the identity of sequence-specific transcriptional activators. This makes the idea of optimised or artificial/tailored promoters quite attractive. The presence of TATA-like sequences in perspective signature promoters should be checked and probably removed on demand. In order to increase the expression level, either motifs for binding of known activators from particular metabolic pathways could be added or putative binding sites for repressors could be removed (Hartner et al., 2008; Liu et al., 2008). How the expression capacity of pheromone-responsive promoters can be altered by changing number, spacing and orientation of pheromone-responsive elements was recently published by Su et al. (2010).

4.6 Outlook

4.6.1 Political and biosafety concerns

According to the Genetically Modified Organisms (Contained Use) Regulations, application of genetically engineered strains is primarily confined to the laboratory environment and must be reported to governmental agencies. For use in large-scale industrial production, facilities must receive authorisation before commercial use. European Union-wide laws govern the facilities and microorganisms used for genetic engineering as well as the safety and quality of end products.[15] Yeast-based biosensors are likely valid systems for authorisation as the use of baker's yeast possesses GRAS status. A major issue during any operation – whether implemented in bioreactors or in portable devices – is contained use of these cells, i.e. limited contact to humans and environment. For portable devices outside laboratory use, a protective membrane could prevent accidental release of cells, and contact to disinfecting solutions may ensure their killing after use. In addition, there is an inherent safety in the experimental design of sensor cells. In fact, auxotrophic cells

[14] Recently, the predicted intrinsic noise of *PDC6* was experimentally validated (Li et al., 2010).
[15] `http://www.gmo-compass.org/eng/home/` [URL was last accessed on 28 September 2011.]

will not grow without sufficient supply of supplements. Genuine application of a microbial biosensor employing genetically engineered microorganisms outside a laboratory was recently demonstrated by the Helmholtz Centre of Environmental Research (UFZ), Leipzig. Their patented ARSOlux bacterial arsenic-biosensor has been field tested in Dhaka, Bangladesh.[16] Whether such technology including genetically modified organisms can be placed on the European or German market is questionable due to conflicts of law.

4.6.2 Constraints and capabilities of application

Considering detectable threshold concentrations, the generation of nutrient sensor strains in order to cope with conventional analysis methods is most probably comparable to fighting a loosing battle. A colourimetric microplate reader-based assay for quantification of ammonium, nitrate and inorganic phosphate in aquatic environments with detection limits below 2 μmol l^{-1} was recently published (Ringuet et al., 2011). However, conventional methods for quantification of nutrients typically require laborious procedures with multiple steps and reagents that must be performed repetitively if there is a demand for time-resolved analysis. Despite the development of modern flow autoanalyser instruments, monitoring is still performed off-line (Cook and Frum, 2004). The remarkably unique feature of cell-based sensors is their ability to detect the biologically available fraction of nutrients and the potential use for continuous and near-line analysis over longer periods of time. These advantages primarily meet demands of a microbial biosensor for monitoring of fermentation processes. As discussed in Section 4.4.1, immobilisation can result in a changed microenvironment – also for entrapped producing microorganisms. A coimmobilised microbial biosensor in close proximity can thus provide more relevant information about the nutritional state than off-line measurements. The microbial biosensor could be placed in the same matrix or in an adjacent containment which can be autonomously maintained, replaced and fed with additional supplements.

The title of this dissertation probably implies a too biased view on prospective applications of the generated yeast sensor and reporter strains to the reader. In fact, yeast nutrient sensor cells could also be particularly useful for environmental monitoring or wastewater treatment, a branch of grey biotechnology. The developed nitrogen and phosphorus sensor strains may be beneficial for the monitoring of biological nutrient removal in sequencing batch reactors. An enzyme-based biosensor for on-line monitoring of phosphorus removal was proposed by Mak et al. (2003). However, its major drawback is that phosphorus is measured indirectly by referencing to hydrogen peroxide concentrations produced by the enzyme. Moreover, many lakes or rivers suffer from poor water quality due to pollution with inorganic phosphate by fertilisers or phosphated detergents. A transportable (and disposal) yeast biosensor could be used for simple and routine

[16] `http://www.arsolux.ufz.de/` [URL was last accessed on 28 September 2011.]

detection of biologically available phosphorus 'on the spot'. Thereby, effort and time of sampling, transport and laboratory analysis is omitted which compensates the relative long response of a microbial sensor. A respective bacterial sensor was already published by Dollard and Billard (2003) but there is a lucrative niche for a yeast-based assay with more relevance for higher eukaryotes.

A possible implementation of the generated α-factor-based cellular communication and signal amplification system into a monitoring assay for the biological availability of nutrients (phosphorus) was demonstrated. Application in any other yeast-based biosensor approach is reasonable, too (Tab. 1.1). This spectrum may range from fermentation process control (nutrients, metabolic intermediates, final products) over environmental monitoring (pollutants, toxins) to medical and pharmaceutical questions (glucose, hormone-active substances). Besides, due to modularisation and spatial separation of the sensor and reporter unit, the system could be implemented in any sensor–actor system. As an example, the system could enhance performance of a yeast biosensor–biocatalyst that detects and degrades toxins (Schofield et al., 2007). In another approach, the α-factor-secreting cells could activate actor cells with different tasks in parallel or succession. The signalling principle is not restricted to the pheromone α-factor of *S. cerevisiae*. For a start, the second pheromone **a**-factor could be utilised. More excitingly, an interspecies communication network based on yeasts with similar mating pheromones like *Schizosaccharomyces pombe*, *Candida albicans* or *Kluyveromyces lactis* may be created (Alby et al., 2009; Davey et al., 1998; Ongay-Larios et al., 2007). Successful pheromone-based communication in *S. cerevisiae* cells expressing cognate pairs of pheromones and receptors from distantly related ascomycetes and basidomycetes was recently reported by Gonçalves-Sá and Murray (2011). The study opens a remarkable degree of freedom in the selection of α/**a**-factor-like signalling molecules. Even the engineering of artificial cellular communication systems in *S. cerevisiae* – for instance, based on signalling elements of *Arabidopsis thaliana* – is a promising perspective (Chen and Weiss, 2005). Virtually endless opportunities are feasible considering the fact that foreign or chimeric receptors for numerous target molecules can be expressed in *S. cerevisiae* and linked to the natural mating pheromone response pathway (Dowell and Brown, 2009; Janiak et al., 2005).

Summary

This work was performed in the framework of two application-oriented research projects that focus on the generation and evaluation of fluorescent *Saccharomyces* (*S.*) *cerevisiae*-based sensor and reporter cells for white biotechnology as well as the extension of the conventional single-cell/single-construct principle of ordinary yeast biosensor approaches. Numerous products are currently generated by biotechnological processes which require continuous and precise process control and monitoring. These demands are only partially met by physical or physiochemical sensors since they measure parameters off-line or use surrogate parameters that consequently provide only indirect information about the actual process performance. Biosensors, in particular whole cell-based biosensors, have the unique potential to near-line and long-term monitor parameters such as nutrient availability during fermentation processes. Moreover, they allow for the assessment of an analyte's biological relevance.

Prototype yeast sensor and reporter strains derived from common laboratory strains were transformed with multicopy expression plasmids that mediate constitutive or inducible expression of a fluorescence reporter gene. Performance of these cells was examined by various qualitative and quantitative detection methods – representative of putative transducer technologies. Analyses were performed on the population level by microplate reader-based fluorometry and Western blot as well as on the single-cell level by fluorescence microscopy and flow cytometry.

'Signature' promoters that are activated or repressed during particular nutrient-limited growth conditions were selected in order to generate yeast nutrient sensor strains for monitoring the biological availability of nitrogen, phosphorus or sulphur. For each category, at least one promoter mediating at least threefold changed green fluorescence levels between sensor cells in non-limited and nutrient-limited conditions was identified. Sensor strains were evaluated in detail regarding sensitivity, analyte selectivity and the ability to restore basic fluorescence after shift from nutrient-limited to non-limited conditions (regeneration). The applicability for bioprocess monitoring purposes was tested by growth of yeast nutrient sensor cells in microalgae media and supernatants. Despite successful proof of principle, numerous challenges still need to be solved to realise prospective implementation in this field of white biotechnology.

The major drawback of plasmid-borne detection constructs is a high fluorescence variance between individual cells. By generation of a nitrogen sensor strain with a genome-integrated detection construct, uniform expression on the single-cell level and simultaneous maintenance of basic properties (ability of fluorescence induction/regeneration and lack of cross-reactivity) was achieved. However, due to the singular detection construct per cell, significantly weaker overall fluorescence was observed.

The traditional single-cell/single-construct approach was expanded upon in two ways. Firstly, a practical dual-colour sensor strain was created by simultaneous, constitutive expression of a red fluorescence reporter gene in green fluorescent nitrogen sensor cells. This opens the possibility to use the additional fluorescent reporter as a surrogate for the cell number or to monitor a further parameter.

Secondly, an innovative cellular communication and signal amplification system inspired by the natural *S. cerevisiae* pheromone system and mating response was established successfully. It features the yeast pheromone α-factor as a trigger and α-factor-responsive reporter cells which express a fluorescence reporter gene from the pheromone-inducible *FIG1* promoter as an output signal. The system was functional both with synthetic and cell-secreted α-factor, provided that recombinant cells were deleted for the α-factor protease Bar1p. Integration of amplifier cells which secrete α-factor in response to stimulation with the pheromone itself could increase the system's sensitivity further. Signal amplification was demonstrated for phosphorus sensor cells as a proof of concept. Therefore, the α-factor-based cellular communication and signal amplification system might be useful in applications that suffer from poor signal yield. Due to its modular design, the system could be applied in basically any cell-based biosensor or sensor–actor system.

Immobilisation of the generated sensor and reporter cells in transparent natural polymers can be beneficial considering biosensor fabrication. Functionality of sensor and reporter cells in calcium-alginate beads or nano-printed arrays was successfully demonstrated. For the latter setup, fluorescence scanning and software-assisted fluorescence quantification was applied as a new detection method. In an experiment using an agarose-based two-compartment setup proposed by Jahn (2011), properties of the α-factor-based cellular communication and signal amplification system after immobilisation were tested. These studies provide an initial experimental basis for an appropriate geometry of miniaturised immobilisation matrices with fluorescent yeast sensor and reporter cells in prospective biosensor designs.

Bibliography

Afanassiev, V., Sefton, M., Anantachaiyong, T., Barker, G., Walmsley, R., Wölfl, S., Jan 2000. Application of yeast cells transformed with GFP expression constructs containing the *RAD54* or *RNR2* promoter as a test for the genotoxic potential of chemical substances. Mutat Res 464 (2), 297–308. 11

Aguilar, P. S., Engel, A., Walter, P., Feb 2007. The plasma membrane proteins Prm1 and Fig1 ascertain fidelity of membrane fusion during yeast mating. Mol Biol Cell 18 (2), 547–556. 26

Akyilmaz, E., Erdoğan, A., Oztürk, R., Yaşa, I., Jan 2007. Sensitive determination of L-lysine with a new amperometric microbial biosensor based on *Saccharomyces cerevisiae* yeast cells. Biosens Bioelectron 22 (6), 1055–1060. 10

Akyilmaz, E., Yaşa, I., Dinçkaya, E., Jul 2006. Whole cell immobilized amperometric biosensor based on *Saccharomyces cerevisiae* for selective determination of vitamin B1 (thiamine). Anal Biochem 354 (1), 78–84. 10

Alby, K., Schaefer, D., Bennett, R. J., Aug 2009. Homothallic and heterothallic mating in the opportunistic pathogen *Candida albicans*. Nature 460 (7257), 890–893. 157

Almaguer, C., Cheng, W., Nolder, C., Patton-Vogt, J., Jul 2004. Glycerophosphoinositol, a novel phosphate source whose transport is regulated by multiple factors in *Saccharomyces cerevisiae*. J Biol Chem 279 (30), 31937–31942. 19

Andersen, J. B., Sternberg, C., Poulsen, L. K., Bjorn, S. P., Givskov, M., Molin, S., Jun 1998. New unstable variants of green fluorescent protein for studies of transient gene expression in bacteria. Appl Environ Microbiol 64 (6), 2240–2246. 14

Arkowitz, R. A., Aug 2009. Chemical gradients and chemotropism in yeast. Cold Spring Harb Perspect Biol 1 (2), a001958. 22

Ballensiefen, W., Schmitt, H. D., Jul 1997. Periplasmic Bar1 protease of *Saccharomyces cerevisiae* is active before reaching its extracellular destination. Eur J Biochem 247 (1), 142–147. 23

Bardwell, L., Feb 2005. A walk-through of the yeast mating pheromone response pathway. Peptides 26 (2), 339–350. 21, 23

Barkai, N., Rose, M. D., Wingreen, N. S., Dec 1998. Protease helps yeast find mating partners. Nature 396 (6710), 422–423. 22, 23

Baronian, K. H. R., Apr 2004. The use of yeast and moulds as sensing elements in biosensors. Biosens Bioelectron 19 (9), 953–962. 9, 14, 15, 144, 147

Baronian, K. H. R., Gurazada, S., May 2007. Electrochemical detection of wild type *Saccharomyces cerevisiae* responses to estrogens. Biosens Bioelectron 22 (11), 2493–2499. 10

Barthelmebs, L., Calas-Blanchard, C., Istamboulie, G., Marty, J.-L., Noguer, T., 2010. Biosensors as analytical tools in food fermentation industry. Adv Exp Med Biol 698, 293–307. 7

Basehoar, A. D., Zanton, S. J., Pugh, B. F., Mar 2004. Identification and distinct regulation of yeast TATA box-containing genes. Cell 116 (5), 699–709. 135, 155

Beck, T., Hall, M. N., Dec 1999. The TOR signalling pathway controls nuclear localization of nutrient-regulated transcription factors. Nature 402 (6762), 689–692. 18

Belizario, J. E., Alves, J., Garay-Malpartida, M., Occhiucci, J. M., Jun 2008. Coupling caspase cleavage and proteasomal degradation of proteins carrying PEST motif. Curr Protein Pept Sci 9 (3), 210–220. 14

Belkin, S., Jun 2003. Microbial whole-cell sensing systems of environmental pollutants. Curr Opin Microbiol 6 (3), 206–212. 7

Benton, M. G., Glasser, N. R., Palecek, S. P., Sep 2007. The utilization of a *Saccharomyces cerevisiae HUG1P*-GFP promoter-reporter construct for the selective detection of DNA damage. Mutat Res 633 (1), 21–34. 11

Bettaieb, F., Ponsonnet, L., Lejeune, P., Ouada, H. B., Martelet, C., Bakhrouf, A., Jaffrézic-Renault, N., Othmane, A., Nov 2007. Immobilization of *E. coli* bacteria in three-dimensional matrices for ISFET biosensor design. Bioelectrochemistry 71 (2), 118–125. 15

Bevis, B. J., Glick, B. S., Jan 2002. Rapidly maturing variants of the *Discosoma* red fluorescent protein (DsRed). Nat Biotechnol 20 (1), 83–87. 13, 30, 143

Beyer, A., Hollunder, J., Nasheuer, H.-P., Wilhelm, T., Nov 2004. Post-transcriptional expression regulation in the yeast *Saccharomyces cerevisiae* on a genomic scale. Mol Cell Proteomics 3 (11), 1083–1092. 135

Bähler, J., Wu, J. Q., Longtine, M. S., Shah, N. G., McKenzie, A., Steever, A. B., Wach, A., Philippsen, P., Pringle, J. R., Jul 1998. Heterologous modules for efficient and versatile PCR-based gene targeting in *Schizosaccharomyces pombe*. Yeast 14 (10), 943–951. 48

Birnboim, H. C., Doly, J., Nov 1979. A rapid alkaline extraction procedure for screening recombinant plasmid DNA. Nucleic Acids Res 7 (6), 1513–1523. 42

Blaiseau, P. L., Isnard, A. D., Surdin-Kerjan, Y., Thomas, D., Jul 1997. Met31p and Met32p, two related zinc finger proteins, are involved in transcriptional regulation of yeast sulfur amino acid metabolism. Mol Cell Biol 17 (7), 3640–3648. 20

Bleve, G., Lezzi, C., Mita, G., Rampino, P., Perrotta, C., Villanova, L., Grieco, F., Jul 2008. Molecular cloning and heterologous expression of a laccase gene from *Pleurotus eryngii* in free and immobilized *Saccharomyces cerevisiae* cells. Appl Microbiol Biotechnol 79 (5), 731–741. 16, 147, 148

Blinder, D., Coschigano, P. W., Magasanik, B., Aug 1996. Interaction of the GATA factor Gln3p with the nitrogen regulator Ure2p in *Saccharomyces cerevisiae*. J Bacteriol 178 (15), 4734–4736. 18

Boer, V. M., de Winde, J. H., Pronk, J. T., Piper, M. D. W., Jan 2003. The genome-wide transcriptional responses of *Saccharomyces cerevisiae* grown on glucose in aerobic chemostat cultures limited for carbon, nitrogen, phosphorus, or sulfur. J Biol Chem 278 (5), 3265–3274. 6, 17, 20, 21, 40, 41, 68, 69, 70, 76, 134, 135, 136, 137, 138, 202

Bovee, T. F. H., Helsdingen, R. J. R., Hamers, A. R. M., van Duursen, M. B. M., Nielen, M. W. F., Hoogenboom, R. L. A. P., Nov 2007. A new highly specific and robust yeast androgen bioassay for the detection of agonists and antagonists. Anal Bioanal Chem 389 (5), 1549–1558. 12

Bovee, T. F. H., Helsdingen, R. J. R., Koks, P. D., Kuiper, H. A., Hoogenboom, R. L. A. P., Keijer, J., Jan 2004a. Development of a rapid yeast estrogen bioassay, based on the expression of green fluorescent protein. Gene 325, 187–200. 12

Bovee, T. F. H., Helsdingen, R. J. R., Rietjens, I. M. C. M., Keijer, J., Hoogenboom, R. L. A. P., Jul 2004b. Rapid yeast estrogen bioassays stably expressing human estrogen receptors α and β, and green fluorescent protein: a comparison of different compounds with both receptor types. J Steroid Biochem Mol Biol 91 (3), 99–109. 12

Bovee, T. F. H., Lommerse, J. P. M., Peijnenburg, A. A. C. M., Fernandes, E. A., Nielen, M. W. F., Jan 2008. A new highly androgen specific yeast biosensor, enabling optimisation of (Q)SAR model approaches. J Steroid Biochem Mol Biol 108 (1–2), 121–131. 12

Braschler, T., Johann, R., Heule, M., Metref, L., Renaud, P., May 2005. Gentle cell trapping and release on a microfluidic chip by *in situ* alginate hydrogel formation. Lab Chip 5 (5), 553–559. 16

Brent, R., Dec 2009. Cell signaling: what is the signal and what information does it carry? FEBS Lett 583 (24), 4019–4024. 22, 23

Breton, A., Surdin-Kerjan, Y., Oct 1977. Sulfate uptake in *Saccharomyces cerevisiae*: biochemical and genetic study. J Bacteriol 132 (1), 224–232. 20

Bun-Ya, M., Harashima, S., Oshima, Y., Jul 1992. Putative GTP-binding protein, Gtr1, associated with the function of the Pho84 inorganic phosphate transporter in *Saccharomyces cerevisiae*. Mol Cell Biol 12 (7), 2958–2966. 19

Cahill, P. A., Knight, A. W., Billinton, N., Barker, M. G., Walsh, L., Keenan, P. O., Williams, C. V., Tweats, D. J., Walmsley, R. M., Mar 2004. The GreenScreen genotoxicity assay: a screening validation programme. Mutagenesis 19 (2), 105–119. 11

Campanella, L., Favero, G., Mastrofini, D., Tomassetti, M., Jun 1996. Toxicity order of cholanic acids using an immobilised cell biosensor. J Pharm Biomed Anal 14 (8–10), 1007–1013. 9

Caplan, S., Green, R., Rocco, J., Kurjan, J., Jan 1991. Glycosylation and structure of the yeast *MFα1* α-factor precursor is important for efficient transport through the secretory pathway. J Bacteriol 173 (2), 627–635. 22

Carpenter, A. E., Jones, T. R., Lamprecht, M. R., Clarke, C., Kang, I. H., Friman, O., Guertin, D. A., Chang, J. H., Lindquist, R. A., Moffat, J., Golland, P., Sabatini, D. M., 2006. CellProfiler: image analysis software for identifying and quantifying cell phenotypes. Genome Biol 7 (10), R100. 57

Chalfie, M., Tu, Y., Euskirchen, G., Ward, W. W., Prasher, D. C., Feb 1994. Green fluorescent protein as a marker for gene expression. Science 263 (5148), 802–805. 10

Chau, T. L., Guillán, A., Roca, E., Núñez, M., Lema, J., Aug 2000. Enhancement of plasmid stability and enzymatic expression by immobilising recombinant *Saccharomyces cerevisiae*. Biotechnol Lett 22 (15), 1247–1250. 147

Chen, E. J., Kaiser, C. A., Nov 2002. Amino acids regulate the intracellular trafficking of the general amino acid permease of *Saccharomyces cerevisiae*. Proc Natl Acad Sci U S A 99 (23), 14837–14842. 19

Chen, M., Tang, H., Ma, H., Holland, T. C., Ng, K. Y. S., Salley, S. O., Jan 2011. Effect of nutrients on growth and lipid accumulation in the green algae *Dunaliella tertiolecta*. Bioresour Technol 102 (2), 1649–1655. 140

Chen, M.-T., Weiss, R., Dec 2005. Artificial cell-cell communication in yeast *Saccharomyces cerevisiae* using signaling elements from *Arabidopsis thaliana*. Nat Biotechnol 23 (12), 1551–1555. 157

Chen, P., Sapperstein, S. K., Choi, J. D., Michaelis, S., Jan 1997. Biogenesis of the *Saccharomyces cerevisiae* mating pheromone **a**-factor. J Cell Biol 136 (2), 251–269. 22

Chenevert, J., Nov 1994. Cell polarization directed by extracellular cues in yeast. Mol Biol Cell 5 (11), 1169–1175. 23

Cherest, H., Davidian, J. C., Thomas, D., Benes, V., Ansorge, W., Surdin-Kerjan, Y., Mar 1997. Molecular characterization of two high affinity sulfate transporters in *Saccharomyces cerevisiae*. Genetics 145 (3), 627–635. 20

Cherest, H., Surdin-Kerjan, Y., Antoniewski, J., Robichon-Szulmajster, H., Jun 1973. S-adenosyl methionine-mediated repression of methionine biosynthetic enzymes in *Saccharomyces cerevisiae*. J Bacteriol 114 (3), 928–933. 20

Cherest, H., Surdin-Kerjan, Y., Robichon-Szulmajster, H., Jun 1971. Methionine-mediated repression in *Saccharomyces cerevisiae*: a pleiotropic regulatory system involving methionyl transfer ribonucleic acid and the product of gene *eth2*. J Bacteriol 106 (3), 758–772. 20

Christianson, T. W., Sikorski, R. S., Dante, M., Shero, J. H., Hieter, P., Jan 1992. Multifunctional yeast high-copy-number shuttle vectors. Gene 110 (1), 119–122. 132

Chudakov, D. M., Matz, M. V., Lukyanov, S., Lukyanov, K. A., Jul 2010. Fluorescent proteins and their applications in imaging living cells and tissues. Physiol Rev 90 (3), 1103–1163. 10, 13, 142, 143

Clark-Walker, G. D., Miklos, G. L., Jan 1974. Localization and quantification of circular DNA in yeast. Eur J Biochem 41 (2), 359–365. 132

Coffman, J. A., Rai, R., Loprete, D. M., Cunningham, T., Svetlov, V., Cooper, T. G., Jun 1997. Cross regulation of four GATA factors that control nitrogen catabolic gene expression in *Saccharomyces cerevisiae*. J Bacteriol 179 (11), 3416–3429. 19

Coiffier, A., Coradin, T., Roux, C., Bouvetb, O. M. M., Livage, J., 2001. Sol-gel encapsulation of bacteria: a comparison between alkoxide and aqueous routes. J Mater Chem 11, 2039–2044. 16

Colman-Lerner, A., Gordon, A., Serra, E., Chin, T., Resnekov, O., Endy, D., Pesce, C. G., Brent, R., Sep 2005. Regulated cell-to-cell variation in a cell-fate decision system. Nature 437 (7059), 699–706. 26, 146, 152

Cook, D. L., Frum, N. L., 2004. Evaluation of total phosphorus and total nitrogen methods in pulp mill effluents. Water Sci Technol 50 (3), 79–86. 156

Cooper, T. G., Sumrada, R. A., Aug 1983. What is the function of nitrogen catabolite repression in *Saccharomyces cerevisiae*? J Bacteriol 155 (2), 623–627. 18

Coradin, T., Livage, J., Sep 2007. Aqueous silicates in biological sol-gel applications: new perspectives for old precursors. Acc Chem Res 40 (9), 819–826. 16

Coradin, T., Nassif, N., Livage, J., Jun 2003. Silica-alginate composites for microencapsulation. Appl Microbiol Biotechnol 61 (5–6), 429–434. 16

Cormack, B. P., Bertram, G., Egerton, M., Gow, N. A., Falkow, S., Brown, A. J., Feb 1997. Yeast-enhanced green fluorescent protein (yEGFP) a reporter of gene expression in *Candida albicans*. Microbiology 143 (Pt 2), 303–311. 13, 143

Cormack, B. P., Valdivia, R. H., Falkow, S., 1996. FACS-optimized mutants of the green fluorescent protein (GFP). Gene 173 (1 Spec No), 33–38. 13, 30, 144

Cormier, L., Barbey, R., Kuras, L., Aug 2010. Transcriptional plasticity through differential assembly of a multiprotein activation complex. Nucleic Acids Res 38 (15), 4998–5014. 20

Craene, J. O. D., Soetens, O., Andre, B., Nov 2001. The Npr1 kinase controls biosynthetic and endocytic sorting of the yeast Gap1 permease. J Biol Chem 276 (47), 43939–43948. 19

Crameri, A., Whitehorn, E. A., Tate, E., Stemmer, W. P., Mar 1996. Improved green fluorescent protein by molecular evolution using DNA shuffling. Nat Biotechnol 14 (3), 315–319. 13, 30, 60, 143

Crick, F. H., 1958. On protein synthesis. Symp Soc Exp Biol 12, 138–163. 134

Cunningham, T. S., Andhare, R., Cooper, T. G., May 2000. Nitrogen catabolite repression of *DAL80* expression depends on the relative levels of Gat1p and Ure2p production in *Saccharomyces cerevisiae*. J Biol Chem 275 (19), 14408–14414. 18

Daum, G., Tuller, G., Nemec, T., Hrastnik, C., Balliano, G., Cattel, L., Milla, P., Rocco, F., Conzelmann, A., Vionnet, C., Kelly, D. E., Kelly, S., Schweizer, E., Schüller, H. J., Hojad, U., Greiner, E., Finger, K., May 1999. Systematic analysis of yeast strains with possible defects in lipid metabolism. Yeast 15 (7), 601–614. 134

Davey, J., Davis, K., Hughes, M., Ladds, G., Powner, D., Feb 1998. The processing of yeast pheromones. Semin Cell Dev Biol 9 (1), 19–30. 157

Day, R. N., Davidson, M. W., Oct 2009. The fluorescent protein palette: tools for cellular imaging. Chem Soc Rev 38 (10), 2887–2921. 10, 13, 14, 143, 146

Dembczynski, R., Jankowski, T., 2001. Determination of pore diameter and molecular weight cut-off of hydrogel-membrane liquid-core capsules for immunoisolation. J Biomater Sci Polym Ed 12 (9), 1051–1058. 148

Dhanasekaran, D. N., Radhika, V., Proikas-Cezanne, T., Jayaraman, M., Ha, J., Jul 2009. Heterologous expression of olfactory receptors for targeted chemosensing. Ann N Y Acad Sci 1170, 157–160. 12

Diderich, J. A., Schepper, M., van Hoek, P., Luttik, M. A., van Dijken, J. P., Pronk, J. T., Klaassen, P., Boelens, H. F., de Mattos, M. J., van Dam, K., Kruckeberg, A. L., May 1999. Glucose uptake kinetics and transcription of *HXT* genes in chemostat cultures of *Saccharomyces cerevisiae*. J Biol Chem 274 (22), 15350–15359. 138

Dohlman, H. G., Thorner, J. W., 2001. Regulation of G protein-initiated signal transduction in yeast: paradigms and principles. Annu Rev Biochem 70, 703–754. 23

Dolan, J. W., Fields, S., Feb 1991. Cell-type-specific transcription in yeast. Biochim Biophys Acta 1088 (2), 155–169. 21

Dollard, M. A., Billard, P., Oct 2003. Whole-cell bacterial sensors for the monitoring of phosphate bioavailability. J Microbiol Methods 55 (1), 221–229. 157

Dong, D., Shao, X., Deng, N., Zhang, Z., Jan 2011. Gene expression variations are predictive for stochastic noise. Nucleic Acids Res 39 (2), 403–413. 132, 155

Dorer, R., Pryciak, P. M., Hartwell, L. H., Nov 1995. *Saccharomyces cerevisiae* cells execute a default pathway to select a mate in the absence of pheromone gradients. J Cell Biol 131 (4), 845–861. 23

Dowell, S. J., Brown, A. J., 2009. Yeast assays for G protein-coupled receptors. In: Leifert, W. R., Walker, J. M. (Eds.), G Protein-Coupled Receptors in Drug Discovery. Vol. 552 of Methods in Molecular Biology. Humana Press, pp. 213–229. 157

Driessche, B. V., Tafforeau, L., Hentges, P., Carr, A. M., Vandenhaute, J., Oct 2005. Additional vectors for PCR-based gene tagging in *Saccharomyces cerevisiae* and *Schizosaccharomyces pombe* using nourseothricin resistance. Yeast 22 (13), 1061–1068. 35

D'Souza, S. F., Aug 2001. Microbial biosensors. Biosens Bioelectron 16 (6), 337–353. 7, 14, 15, 16, 147

Duchen, M. R., Biscoe, T. J., May 1992. Mitochondrial function in type I cells isolated from rabbit arterial chemoreceptors. J Physiol 450, 13–31. 143

Dyke, N. V., Baby, J., Dyke, M. W. V., May 2006. Stm1p, a ribosome-associated protein, is important for protein synthesis in *Saccharomyces cerevisiae* under nutritional stress conditions. J Mol Biol 358 (4), 1023–1031. 137

Eide, D. J., Clark, S., Nair, T. M., Gehl, M., Gribskov, M., Guerinot, M. L., Harper, J. F., 2005. Characterization of the yeast ionome: a genome-wide analysis of nutrient mineral and trace element homeostasis in *Saccharomyces cerevisiae*. Genome Biol 6 (9), R77. 136

Eldridge, M. L., Sanseverino, J., Layton, A. C., Easter, J. P., Schultz, T. W., Sayler, G. S., Oct 2007. *Saccharomyces cerevisiae* BLYAS, a new bioluminescent bioreporter for detection of androgenic compounds. Appl Environ Microbiol 73 (19), 6012–6018. 12

Emter, O., Mechler, B., Achstetter, T., Müller, H., Wolf, D. H., Nov 1983. Yeast pheromone α-factor is synthesized as a high molecular weight precursor. Biochem Biophys Res Commun 116 (3), 822–829. 22

Erdman, S., Lin, L., Malczynski, M., Snyder, M., Feb 1998. Pheromone-regulated genes required for yeast mating differentiation. J Cell Biol 140 (3), 461–483. 25

Evdokimov, A. G., Pokross, M. E., Egorov, N. S., Zaraisky, A. G., Yampolsky, I. V., Merzlyak, E. M., Shkoporov, A. N., Sander, I., Lukyanov, K. A., Chudakov, D. M., Oct 2006. Structural basis for the fast maturation of Arthropoda green fluorescent protein. EMBO Rep 7 (10), 1006–1012. 13, 30, 144

Fabregas, J., Domínguez, A., Regueiro, M., Maseda, A., Otero, A., May 2000. Optimization of culture medium for the continuous cultivation of the microalga *Haematococcus pluvialis*. Appl Microbiol Biotechnol 53 (5), 530–535. 203

Farré, M., Barceló, D., 2003. Toxicity testing of wastewater and sewage sludge by biosensors, bioassays and chemical analysis. Trends Anal Chem 22 (5), 299–310. 8

Fauchon, M., Lagniel, G., Aude, J. C., Lombardia, L., Soularue, P., Petat, C., Marguerie, G., Sentenac, A., Werner, M., Labarre, J., Apr 2002. Sulfur sparing in the yeast proteome in response to sulfur demand. Mol Cell 9 (4), 713–723. 20, 136, 137

Fine, T., Leskinen, P., Isobe, T., Shiraishi, H., Morita, M., Marks, R. S., Virta, M., Jun 2006. Luminescent yeast cells entrapped in hydrogels for estrogenic endocrine disrupting chemical biodetection. Biosens Bioelectron 21 (12), 2263–2269. 12, 16, 148

Finkelstein, D. B., Strausberg, S., Feb 1979. Metabolism of α-factor by **a** mating type cells of *Saccharomyces cerevisiae*. J Biol Chem 254 (3), 796–803. 22

Fleischer, T. C., Weaver, C. M., McAfee, K. J., Jennings, J. L., Link, A. J., May 2006. Systematic identification and functional screens of uncharacterized proteins associated with eukaryotic ribosomal complexes. Genes Dev 20 (10), 1294–1307. 136

Fukuda, T., Tsuchiya, K., Makishima, H., Tsuchiyama, K., Mulchandani, A., Kuroda, K., Ueda, M., ichiro Suye, S., May 2010. Organophosphorus compound detection on a cell chip with yeast coexpressing hydrolase and *eGFP*. Biotechnol J 5 (5), 515–519. 11

Futcher, A. B., Cox, B. S., May 1983. Maintenance of the 2μm circle plasmid in populations of *Saccharomyces cerevisiae*. J Bacteriol 154 (2), 612–622. 132

Futcher, A. B., Cox, B. S., Jan 1984. Copy number and the stability of 2-μm circle-based artificial plasmids of *Saccharomyces cerevisiae*. J Bacteriol 157 (1), 283–290. 132

Gacesa, P., 1988. Alginates. Carbohydr Polym 8, 161–182. 15

García-Alonso, J., Fakhrullin, R. F., Paunov, V. N., Mar 2010. Rapid and direct magnetization of GFP-reporter yeast for micro-screening systems. Biosens Bioelectron 25 (7), 1816–1819. 11

García-Alonso, J., Greenway, G. M., Hardege, J. D., Haswell, S. J., Jan 2009. A prototype microfluidic chip using fluorescent yeast for detection of toxic compounds. Biosens Bioelectron 24 (5), 1508–1511. 11

García-Martínez, J., González-Candelas, F., Pérez-Ortín, J. E., 2007. Common gene expression strategies revealed by genome-wide analysis in yeast. Genome Biol 8 (10), R222. 135

Garjonyte, R., Melvydas, V., Malinauskas, A., May 2006. Mediated amperometric biosensors for lactic acid based on carbon paste electrodes modified with baker's yeast *Saccharomyces cerevisiae*. Bioelectrochemistry 68 (2), 191–196. 10

Gietz, R. D., Woods, R. A., 2002. Transformation of yeast by lithium acetate/single-stranded carrier DNA/polyethylene glycol method. Methods Enzymol 350, 87–96. 47

Giordano, M., Norici, A., Ratti, S., Raven, J. A., 2008. Role of sulfur for algae: acquisition, metabolism, ecology and evolution. In: Hell, R., Dahl, C., Knaff, D., Leustek, T. (Eds.), Sulfur Metabolism in Phototrophic Organisms. Vol. 27 of Advances in Photosynthesis and Respiration. Springer Netherlands, pp. 397–415. 141

Girish, V., Vijayalakshmi, A., Jan–Mar 2004. Affordable image analysis using NIH Image/ImageJ. Indian J Cancer 41 (1), 47. 57

Gompel, J. V., Woestenborghs, F., Beerens, D., Mackie, C., Cahill, P. A., Knight, A. W., Billinton, N., Tweats, D. J., Walmsley, R. M., Nov 2005. An assessment of the utility of the yeast GreenScreen assay in pharmaceutical screening. Mutagenesis 20 (6), 449–454. 11

Gonçalves-Sá, J., Murray, A., Aug 2011. Asymmetry in sexual pheromones is not required for ascomycete mating. Curr Biol 21 (16), 1337–1346. 157

Groba, C., Dec 2007. Herstellung rekombinanter Hefen zur Nutzung des Hefepheromonsystems in der Biosensorik. Diploma thesis, Technische Universität Dresden, Institut für Genetik. 6, 34, 35, 36, 113, 114, 125, 126, 154

Gross, A., Rödel, G., Ostermann, K., May 2011. Application of the yeast pheromone system for controlled cell-cell communication and signal amplification. Lett Appl Microbiol 52 (5), 521–526. 148, 151

Gu, M. B., Mitchell, R. J., Kim, B. C., 2004. Whole-cell-based biosensors for environmental biomonitoring and application. Adv Biochem Eng Biotechnol 87, 269–305. 8, 9

Hagen, D. C., McCaffrey, G., Sprague, G. F., Mar 1986. Evidence the yeast *STE3* gene encodes a receptor for the peptide pheromone **a** factor: gene sequence and implications for the structure of the presumed receptor. Proc Natl Acad Sci U S A 83 (5), 1418–1422. 21

Hartner, F. S., Ruth, C., Langenegger, D., Johnson, S. N., Hyka, P., Lin-Cereghino, G. P., Lin-Cereghino, J., Kovar, K., Cregg, J. M., Glieder, A., Jul 2008. Promoter library designed for fine-tuned gene expression in *Pichia pastoris*. Nucleic Acids Res 36 (12), e76. 155

Hartwell, L. H., Mortimer, R. K., Culotti, J., Culotti, M., Jun 1973. Genetic control of the cell division cycle in yeast: V. Genetic analysis of *cdc* mutants. Genetics 74 (2), 267–286. 151

Heim, R., Cubitt, A. B., Tsien, R. Y., Feb 1995. Improved green fluorescence. Nature 373 (6516), 663–664. 13

Heim, R., Prasher, D. C., Tsien, R. Y., Dec 1994. Wavelength mutations and posttranslational autoxidation of green fluorescent protein. Proc Natl Acad Sci U S A 91 (26), 12501–12504. 13

Heim, R., Tsien, R. Y., Feb 1996. Engineering green fluorescent protein for improved brightness, longer wavelengths and fluorescence resonance energy transfer. Curr Biol 6 (2), 178–182. 13

Heiman, M. G., Walter, P., Oct 2000. Prm1p, a pheromone-regulated multispanning membrane protein, facilitates plasma membrane fusion during yeast mating. J Cell Biol 151 (3), 719–730. 25

Henry, S. A., Atkinson, K. D., Kolat, A. I., Culbertson, M. R., Apr 1977. Growth and metabolism of inositol-starved *Saccharomyces cerevisiae*. J Bacteriol 130 (1), 472–484. 137

Henry, S. A., White, M. J., Jun 1996. Inositol-excreting yeast. U.S. Patent 5,529,912. 138

Hentges, P., Driessche, B. V., Tafforeau, L., Vandenhaute, J., Carr, A. M., Oct 2005. Three novel antibiotic marker cassettes for gene disruption and marker switching in *Schizosaccharomyces pombe*. Yeast 22 (13), 1013–1019. 35, 128

Herskowitz, I., Dec 1988. Life cycle of the budding yeast *Saccharomyces cerevisiae*. Microbiol Rev 52 (4), 536–553. 21

Hever, N., Belkin, S., Jun 2006. A dual-color bacterial reporter strain for the detection of toxic and genotoxic effects. Eng Life Sci 6 (3), 319–323. 146

Hicke, L., Riezman, H., Jan 1996. Ubiquitination of a yeast plasma membrane receptor signals its ligand-stimulated endocytosis. Cell 84 (2), 277–287. 23

Hoffman, C. S., Winston, F., 1987. A ten-minute DNA preparation from yeast efficiently releases autonomous plasmids for transformation of *Escherichia coli*. Gene 57 (2–3), 267–272. 43

Hofman-Bang, J., Aug 1999. Nitrogen catabolite repression in *Saccharomyces cerevisiae*. Mol Biotechnol 12 (1), 35–73. 18

Hohmann, S., Dec 1991. Characterization of *PDC6*, a third structural gene for pyruvate decarboxylase in *Saccharomyces cerevisiae*. J Bacteriol 173 (24), 7963–7969. 137

Hollis, R. P., Killham, K., Glover, L. A., Apr 2000. Design and application of a biosensor for monitoring toxicity of compounds to eukaryotes. Appl Environ Microbiol 66 (4), 1676–1679. 11

Holte, Ø., Tønnesen, H. H., Karlsen, J., Dec 2007. Effect of charge and size of diffusing probe on the diffusion through calcium alginate gel matrices. Pharmazie 62 (12), 914–918. 148

Hosaka, K., Nikawa, J., Kodaki, T., Ishizu, H., Yamashita, S., Dec 1994. Cloning and sequence of the *SCS3* gene which is required for inositol prototrophy in *Saccharomyces cerevisiae*. J Biochem 116 (6), 1317–1321. 81, 137

Ichikawa, K., Eki, T., Jan 2006. A novel yeast-based reporter assay system for the sensitive detection of genotoxic agents mediated by a DNA damage-inducible LexA-GAL4 protein. J Biochem 139 (1), 105–112. 11

Ino, K., Kitagawa, Y., Watanabe, T., Shiku, H., Koide, M., Itayama, T., Yasukawa, T., Matsue, T., Oct 2009. Detection of hormone active chemicals using genetically engineered yeast cells and microfluidic devices with interdigitated array electrodes. Electrophoresis 30 (19), 3406–3412. 12

Inukai, M., Yonese, M., 1999. Effects of charge density on drug permeability through alginate gel membranes. Chem Pharm Bull 47 (8), 1059–1063. 15

Irani, M., Taylor, W. E., Young, E. T., Mar 1987. Transcription of the *ADH2* gene in *Saccharomyces cerevisiae* is limited by positive factors that bind competitively to its intact promoter region on multicopy plasmids. Mol Cell Biol 7 (3), 1233–1241. 155

Ishii, J., Matsumura, S., Kimura, S., Tatematsu, K., Kuroda, S., Fukuda, H., Kondo, A., 2006. Quantitative and dynamic analyses of G protein-coupled receptor signaling in yeast using Fus1, enhanced green fluorescence protein (EGFP), and His3 fusion protein. Biotechnol Prog 22 (4), 954–960. 26, 152

Jackson, C. L., Hartwell, L. H., Nov 1990. Courtship in *S. cerevisiae*: both cell types choose mating partners by responding to the strongest pheromone signal. Cell 63 (5), 1039–1051. 22

Jahn, M., Apr 2011. Dynamic mating pheromone gradients for induction of mating projection and fluorescence in baker's yeast. Diploma thesis, Technische Universität Dresden, Institut für Genetik. 16, 55, 56, 119, 120, 125, 133, 150, 153, 160

Janiak, A. M., Sargsyan, H., Russo, J., Naider, F., Hauser, M., Becker, J. M., Apr 2005. Functional expression of the *Candida albicans* α-factor receptor in *Saccharomyces cerevisiae*. Fungal Genet Biol 42 (4), 328–338. 157

Jauniaux, J. C., Grenson, M., May 1990. *GAP1*, the general amino acid permease gene of *Saccharomyces cerevisiae*. Nucleotide sequence, protein similarity with the other bakers yeast amino acid permeases, and nitrogen catabolite repression. Eur J Biochem 190 (1), 39–44. 19

Jayaraman, M., Radhika, V., Bamne, M. N., Ramos, R., Briggs, R., Dhanasekaran, D. N., Sep–Oct 2005. Engineered *Saccharomyces cerevisiae* strain BioS–OS1/2, for the detection of oxidative stress. Biotechnol Prog 21 (5), 1373–1379. 11

Jenness, D. D., Burkholder, A. C., Hartwell, L. H., Dec 1983. Binding of α-factor pheromone to yeast **a** cells: chemical and genetic evidence for an α-factor receptor. Cell 35 (2 Pt 1), 521–529. 21

Jenness, D. D., Burkholder, A. C., Hartwell, L. H., Jan 1986. Binding of α-factor pheromone to *Saccharomyces cerevisiae* **a** cells: dissociation constant and number of binding sites. Mol Cell Biol 6 (1), 318–320. 23

Jia, X., Zhu, Y., Xiao, W., Aug 2002. A stable and sensitive genotoxic testing system based on DNA damage induced gene expression in *Saccharomyces cerevisiae*. Mutat Res 519 (1–2), 83–92. 11

Jin, H.-F., Lim, B.-R., Lee, K., 2006. Influence of nitrate feeding on carbon dioxide fixation by microalgae. J Environ Sci Health A Tox Hazard Subst Environ Eng 41 (12), 2813–2824. 140

Julius, D., Schekman, R., Thorner, J., Feb 1984. Glycosylation and processing of prepro-α-factor through the yeast secretory pathway. Cell 36 (2), 309–318. 22

Kaiser, P., Flick, K., Wittenberg, C., Reed, S. I., Aug 2000. Regulation of transcription by ubiquitination without proteolysis: Cdc34/SCF(Met30)-mediated inactivation of the transcription factor Met4. Cell 102 (3), 303–314. 20

Karube, I., Matsunaga, T., Mitsuda, S., Suzuki, S., Oct 1977. Microbial electrode BOD sensors. Biotechnol Bioeng 19 (10), 1535–1547. 7

Karube, I., Suzuki, M., 1990. Microbial biosensors. In: Cass, A. E. G. (Ed.), Biosensors – A Practical Approach. IRL Press, Oxford, pp. 155–169. 9

Keenan, P. O., Knight, A. W., Billinton, N., Cahill, P. A., Dalrymple, I. M., Hawkyard, C. J., Stratton-Campbell, D., Walmsley, R. M., Dec 2007. Clear and present danger? The use of a yeast biosensor to monitor changes in the toxicity of industrial effluents subjected to oxidative colour removal treatments. J Environ Monit 9 (12), 1394–1401. 11

Kissinger, P. T., Jun 2005. Biosensors – a perspective. Biosens Bioelectron 20 (12), 2512–2516. 1

Klein, J., Stock, J., Vorlop, K.-D., 1983. Pore size and properties of spherical Ca-alginate biocatalysts. Eur J Appl Microbiol Biotechno 18, 86–91. 148

Klis, F. M., Mol, P., Hellingwerf, K., Brul, S., Aug 2002. Dynamics of cell wall structure in *Saccharomyces cerevisiae*. FEMS Microbiol Rev 26 (3), 239–256. 142

Klosinska, M. M., Crutchfield, C. A., Bradley, P. H., Rabinowitz, J. D., Broach, J. R., Feb 2011. Yeast cells can access distinct quiescent states. Genes Dev 25 (4), 336–349. 40, 138

König, A., Riedel, K., Metzger, J. W., Oct 1998. A microbial sensor for detecting inhibitors of nitrification in wastewater. Biosens Bioelectron 13 (7–8), 869–874. 8

Kogure, H., Kawasaki, S., Nakajima, K., Sakai, N., Futase, K., Inatsu, Y., Bari, M. L., Isshiki, K., Kawamoto, S., Jan 2005. Development of a novel microbial sensor with baker's yeast cells for monitoring temperature control during cold food chain. J Food Prot 68 (1), 182–186. 9

Kolkman, A., Daran-Lapujade, P., Fullaondo, A., Olsthoorn, M. M. A., Pronk, J. T., Slijper, M., Heck, A. J. R., 2006. Proteome analysis of yeast response to various nutrient limitations. Mol Syst Biol 2, 2006.0026. 135

Konsoula, Z., Liakopoulou-Kyriakides, M., Aug 2006. Thermostable α-amylase production by *Bacillus subtilis* entrapped in calcium alginate gel capsules. Enzyme M 39 (4), 690–696. 148

Kuchler, K., Sterne, R. E., Thorner, J., Dec 1989. *Saccharomyces cerevisiae STE6* gene product: a novel pathway for protein export in eukaryotic cells. EMBO J 8 (13), 3973–3984. 22

Kudla, B., Nicolas, A., Sep 1992. A multisite integrative cassette for the yeast *Saccharomyces cerevisiae*. Gene 119 (1), 49–56. 133

Kulaev, I., Vagabov, V., Kulakovskaya, T., 1999. New aspects of inorganic polyphosphate metabolism and function. J Biosci Bioeng 88 (2), 111–129. 19, 136

Kuras, L., Barbey, R., Thomas, D., May 1997. Assembly of a bZIP–bHLH transcription activation complex: formation of the yeast Cbf1–Met4–Met28 complex is regulated through Met28 stimulation of Cbf1 DNA binding. EMBO J 16 (9), 2441–2451. 20

Kurischko, C., Kim, H. K., Kuravi, V. K., Pratzka, J., Luca, F. C., Feb 2011. The yeast Cbk1 kinase regulates mRNA localization via the mRNA-binding protein Ssd1. J Cell Biol 192 (4), 583–598. 146

Kurjan, J., Herskowitz, I., Oct 1982. Structure of a yeast pheromone gene (*MF*α): a putative α-factor precursor contains four tandem copies of mature α-factor. Cell 30 (3), 933–943. 22, 153

Kuroda, K., Ueda, M., Jan 2011. Cell surface engineering of yeast for applications in white biotechnology. Biotechnol Lett 33 (1), 1–9. 142

Kwon, Y. J., Peng, C.-A., Jul 2002. Calcium-alginate gel bead cross-linked with gelatin as microcarrier for anchorage-dependent cell culture. Biotechniques 33 (1), 212–4, 216, 218. 150

Laemmli, U. K., Aug 1970. Cleavage of structural proteins during the assembly of the head of bacteriophage T4. Nature 227 (5259), 680–685. 51

Lange, H. C., Heijnen, J. J., Nov 2001. Statistical reconciliation of the elemental and molecular biomass composition of *Saccharomyces cerevisiae*. Biotechnol Bioeng 75 (3), 334–344. 136

Lehmann, M., Riedel, K., Adler, K., Kunze, G., Jun 2000. Amperometric measurement of copper ions with a deputy substrate using a novel *Saccharomyces cerevisiae* sensor. Biosens Bioelectron 15 (3–4), 211–219. 11

Lei, Y., Chen, W., Mulchandani, A., May 2006. Microbial biosensors. Anal Chim Acta 568 (1–2), 200–210. 7, 8, 14, 15, 144

Leskinen, P., Michelini, E., Picard, D., Karp, M., Virta, M., Oct 2005. Bioluminescent yeast assays for detecting estrogenic and androgenic activity in different matrices. Chemosphere 61 (2), 259–266. 12

Leskinen, P., Virta, M., Karp, M., Oct 2003. One-step measurement of firefly luciferase activity in yeast. Yeast 20 (13), 1109–1113. 11, 12

Li, J., Min, R., Vizeacoumar, F. J., Jin, K., Xin, X., Zhang, Z., Jun 2010. Exploiting the determinants of stochastic gene expression in *Saccharomyces cerevisiae* for genome-wide prediction of expression noise. Proc Natl Acad Sci U S A 107 (23), 10472–10477. 155

Li, P., Anumanthan, A., Gao, X.-G., Ilangovan, K., Suzara, V. V., Düzgüneş, N., Renugopalakrishnan, V., Aug 2007. Expression of recombinant proteins in *Pichia pastoris*. Appl Biochem Biotechnol 142 (2), 105–124. 141

Li, X., Jun 1996. The use of chitosan to increase the stability of calcium alginate beads with entrapped yeast cells. Biotechnol Appl Biochem 23 (Pt 3), 269–272. 150

Li, X., Zhao, X., Fang, Y., Jiang, X., Duong, T., Fan, C., Huang, C. C., Kain, S. R., Dec 1998. Generation of destabilized green fluorescent protein as a transcription reporter. J Biol Chem 273 (52), 34970–34975. 14, 144

Li, Y. R., Chu, J., 1991. Study of BOD microbial sensors for waste water treatment control. Appl Biochem Biotechnol 28-29, 855–863. 8

Lichtenberg-Fraté, H., Schmitt, M., Gellert, G., Ludwig, J., Oct–Dec 2003. A yeast-based method for the detection of cyto and genotoxicity. Toxicol In Vitro 17 (5–6), 709–716. 11

Lipke, P. N., Kurjan, J., Mar 1992. Sexual agglutination in budding yeasts: structure, function, and regulation of adhesion glycoproteins. Microbiol Rev 56 (1), 180–194. 154

Liu, T., Wang, T., Li, X., Liu, X., Feb 2008. Improved heterologous gene expression in *Trichoderma reesei* by cellobiohydrolase I gene (*cbh1*) promoter optimization. Acta Biochim Biophys Sin (Shanghai) 40 (2), 158–165. 155

Ludwig, D. L., Ugolini, S., Bruschi, C. V., Sep 1993. High-level heterologous gene expression in *Saccharomyces cerevisiae* from a stable 2μ plasmid system. Gene 132 (1), 33–40. 133

MacKay, V. L., Armstrong, J., Yip, C., Welch, S., Walker, K., Osborn, S., Sheppard, P., Forstrom, J., 1991. Characterization of the Bar proteinase, an extracellular enzyme from the yeast *Saccharomyces cerevisiae*. Adv Exp Med Biol 306, 161–172. 23

MacKay, V. L., Welch, S. K., Insley, M. Y., Manney, T. R., Holly, J., Saari, G. C., Parker, M. L., Jan 1988. The *Saccharomyces cerevisiae BAR1* gene encodes an exported protein with homology to pepsin. Proc Natl Acad Sci U S A 85 (1), 55–59. 23, 113

Magasanik, B., 1992. Regulation of nitrogen utilization. In: Jones, E. W., Pringle, J. R., Broach, J. R. (Eds.), The Molecular and Cellular Biology of the Yeast *Saccharomyces*, Vol. 2: Gene Expression. Cold Spring Harbour Laboratory Press, Cold Spring Harbour, New York, pp. 283–317. 18

Magasanik, B., Kaiser, C. A., May 2002. Nitrogen regulation in *Saccharomyces cerevisiae*. Gene 290 (1–2), 1–18. 18, 134

Mak, W. C., Chan, C., Barford, J., Renneberg, R., Nov 2003. Biosensor for rapid phosphate monitoring in a sequencing batch reactor (SBR) system. Biosens Bioelectron 19 (3), 233–237. 156

Malínská, K., Malínský, J., Opekarová, M., Tanner, W., Nov 2003. Visualization of protein compartmentation within the plasma membrane of living yeast cells. Mol Biol Cell 14 (11), 4427–4436. 146

Manney, T. R., Jul 1983. Expression of the *BAR1* gene in *Saccharomyces cerevisiae*: induction by the α mating pheromone of an activity associated with a secreted protein. J Bacteriol 155 (1), 291–301. 23, 128, 152

Marini, A. M., Soussi-Boudekou, S., Vissers, S., Andre, B., Aug 1997. A family of ammonium transporters in *Saccharomyces cerevisiae*. Mol Cell Biol 17 (8), 4282–4293. 18

Marini, A. M., Vissers, S., Urrestarazu, A., André, B., Aug 1994. Cloning and expression of the *MEP1* gene encoding an ammonium transporter in *Saccharomyces cerevisiae*. EMBO J 13 (15), 3456–3463. 18

Marrakchi, M., Vidic, J., Jaffrezic-Renault, N., Martelet, C., Pajot-Augy, E., Nov 2007. A new concept of olfactory biosensor based on interdigitated microelectrodes and immobilized yeasts expressing the human receptor OR17-40. Eur Biophys J 36 (8), 1015–1018. 11

Marsh, L., Neiman, A. M., Herskowitz, I., 1991. Signal transduction during pheromone response in yeast. Annu Rev Cell Biol 7, 699–728. 23

Martineau, R. L., Towe, B. C., Stout, V., 2006. An optical micro-instrumentation system for measurement of fluorescent proteins in whole-cell biosensors. In: Proc. Bio Micro and Nanosystems Conf. BMN '06. pp. 90–93. 141

Martinez, P., Zvyagilskaya, R., Allard, P., Persson, B. L., Apr 1998. Physiological regulation of the derepressible phosphate transporter in *Saccharomyces cerevisiae*. J Bacteriol 180 (8), 2253–2256. 19

Martínez, M., Hilding-Ohlsson, A., Viale, A. A., Cortón, E., Apr 2007. Membrane entrapped *Saccharomyces cerevisiae* in a biosensor-like device as a generic rapid method to study cellular metabolism. J Biochem Biophys Methods 70 (3), 455–464. 9

Mascini, M., Memoli, A., 1986. Comparison of microbial sensors based on amperometric and potentiometric electrodes. An 182, 113–122. 9

Mateus, C., Avery, S. V., Oct 2000. Destabilized green fluorescent protein for monitoring dynamic changes in yeast gene expression with flow cytometry. Yeast 16 (14), 1313–1323. 14, 30, 143, 144, 145

Matz, M. V., Fradkov, A. F., Labas, Y. A., Savitsky, A. P., Zaraisky, A. G., Markelov, M. L., Lukyanov, S. A., Oct 1999. Fluorescent proteins from nonbioluminescent Anthozoa species. Nat Biotechnol 17 (10), 969–973. 13

Mehmetoglu, U., Ates, S., Berber, R., Mar 1996. Oxygen diffusivity in calcium alginate gel beads containing *Gluconobacter suboxydans*. Artif Cells Blood Substit Immobil Biotechnol 24 (2), 91–106. 148

Melzoch, K., Rychtera, M., Hábová, V., Jan 1994. Effect of immobilization upon the properties and behaviour of *Saccharomyces cerevisiae* cells. J Biot 32 (1), 59–65. 147

Merzlyak, E. M., Goedhart, J., Shcherbo, D., Bulina, M. E., Shcheglov, A. S., Fradkov, A. F., Gaintzeva, A., Lukyanov, K. A., Lukyanov, S., Gadella, T. W. J., Chudakov, D. M., Jul 2007. Bright monomeric red fluorescent protein with an extended fluorescence lifetime. Nat Methods 4 (7), 555–557. 14, 30

Michaelis, S., Herskowitz, I., Mar 1988. The **a**-factor pheromone of *Saccharomyces cerevisiae* is essential for mating. Mol Cell Biol 8 (3), 1309–1318. 22

Michelini, E., Leskinen, P., Virta, M., Karp, M., Roda, A., May 2005. A new recombinant cell-based bioluminescent assay for sensitive androgen-like compound detection. Biosens Bioelectron 20 (11), 2261–2267. 12

Minic, J., Persuy, M.-A., Godel, E., Aioun, J., Connerton, I., Salesse, R., Pajot-Augy, E., Jan 2005. Functional expression of olfactory receptors in yeast and development of a bioassay for odorant screening. FEBS J 272 (2), 524–537. 11

Mirisola, M. G., Colomba, L., Gallo, A., Amodeo, R., Leo, G. D., Sep 2007. Yeast vectors for the integration/expression of any sequence at the *TYR1* locus. Yeast 24 (9), 761–766. 34, 100, 132, 193

Moore, T. I., Chou, C.-S., Nie, Q., Jeon, N. L., Yi, T.-M., Dec 2008. Robust spatial sensing of mating pheromone gradients by yeast cells. PLoS One 3 (12), e3865. 23, 153

Mouillon, J.-M., Persson, B. L., Mar 2006. New aspects on phosphate sensing and signalling in *Saccharomyces cerevisiae*. FEMS Yeast Res 6 (2), 171–176. 19

Moukadiri, I., Jaafar, L., Zueco, J., Aug 1999. Identification of two mannoproteins released from cell walls of a *Saccharomyces cerevisiae mnn1 mnn9* double mutant by reducing agents. J Bacteriol 181 (16), 4741–4745. 23

Muddana, S. S., Peterson, B. R., Sep 2003. Fluorescent cellular sensors of steroid receptor ligands. Chembiochem 4 (9), 848–855. 12

Mulholland, J., Konopka, J., Singer-Kruger, B., Zerial, M., Botstein, D., Mar 1999. Visualization of receptor-mediated endocytosis in yeast. Mol Biol Cell 10 (3), 799–817. 25

Muller, E. M., Mackin, N. A., Erdman, S. E., Cunningham, K. W., Oct 2003. Fig1p facilitates Ca^{2+} influx and cell fusion during mating of *Saccharomyces cerevisiae*. J Biol Chem 278 (40), 38461–38469. 25

Mumberg, D., Müller, R., Funk, M., Apr 1995. Yeast vectors for the controlled expression of heterologous proteins in different genetic backgrounds. Gene 156 (1), 119–122. VII, 34, 35, 37, 59, 68, 132, 155, 191

Nakamura, H., Shimomura-Shimizu, M., Karube, I., 2008. Development of microbial sensors and their application. Adv Biochem Eng Biotechnol 109, 351–394. 7, 9

Nelissen, B., Wachter, R. D., Goffeau, A., Sep 1997. Classification of all putative permeases and other membrane plurispanners of the major facilitator superfamily encoded by the complete genome of *Saccharomyces cerevisiae*. FEMS Microbiol Rev 21 (2), 113–134. 136

Nern, A., Arkowitz, R. A., May 2000. G proteins mediate changes in cell shape by stabilizing the axis of polarity. Mol Cell 5 (5), 853–864. 23

Nevoigt, E., Sep 2008. Progress in metabolic engineering of *Saccharomyces cerevisiae*. Microbiol Mol Biol Rev 72 (3), 379–412. 141

Norton, S., D'Amore, T., May 1994. Physiological effects of yeast cell immobilization: applications for brewing. Enzyme Microb Technol 16, 365–375. 147

Olmo, V. N., Grote, E., Oct 2010. Prm1 targeting to contact sites enhances fusion during mating in *Saccharomyces cerevisiae*. Eukaryot Cell 9 (10), 1538–1548. 25

Ongay-Larios, L., Navarro-Olmos, R., Kawasaki, L., Velázquez-Zavala, N., Sánchez-Paredes, E., Torres-Quiroz, F., Coello, G., Coria, R., Aug 2007. *Kluyveromyces lactis* sexual pheromones. Gene structures and cellular responses to α-factor. FEMS Yeast Res 7 (5), 740–747. 157

Ormö, M., Cubitt, A. B., Kallio, K., Gross, L. A., Tsien, R. Y., Remington, S. J., Sep 1996. Crystal structure of the *Aequorea victoria* green fluorescent protein. Science 273 (5280), 1392–1395. 10

Oshima, Y., Dec 1997. The phosphatase system in *Saccharomyces cerevisiae*. Genes Genet Syst 72 (6), 323–334. 19

Ostermann, K., Groß, A., Zierau, O., Diel, P., Vollmer, G., Lehmann, S., Rataj, F., Rödel, G., Jul 2010. Method for verification and/or identifying hormonally effective substances. WO Patent 2010072767. 154

Ostermann, K., Pompe, W., Böttcher, H., Rödel, G., Groß, A., Nov 2008a. Whole-cell sensor. WO Patent 2008132178. 2

Ostermann, K., Pompe, W., Rödel, G., Groß, A., Dec 2008b. Device and a method for the detection and amplification of a signal. WO Patent 2009000918. 4, 151

Ostermann, K., Pompe, W., Wersing, D., Lakatos, M., Mertig, M., Rödel, G., Thierfelder, S., Dec 2009. Device and method for detecting a substance by means of particle resonance (PPR) or particle-mediated fluorescence based on cell surface polarizations. WO Patent 2009000920. 154

Pancrazio, J. J., Whelan, J. P., Borkholder, D. A., Ma, W., Stenger, D. A., Nov–Dec 1999. Development and application of cell-based biosensors. Ann Biomed Eng 27 (6), 697–711. 7

Park, H., Bakalinsky, A. T., Jul 2000. *SSU1* mediates sulphite efflux in *Saccharomyces cerevisiae*. Yeast 16 (10), 881–888. 21

Park, J.-N., Sohn, M. J., Oh, D.-B., Kwon, O., Rhee, S. K., Hur, C.-G., Lee, S. Y., Gellissen, G., Kang, H. A., Oct 2007. Identification of the cadmium-inducible *Hansenula polymorpha SEO1* gene promoter by transcriptome analysis and its application to whole-cell heavy-metal detection systems. Appl Environ Microbiol 73 (19), 5990–6000. 135

Parry, J. M., 1999. Use of tests in yeasts and fungi in the detection and evaluation of carcinogens. IARC Sci Publ (146), 471–485. 9

Parvez, S., Venkataraman, C., Mukherji, S., Feb 2006. A review on advantages of implementing luminescence inhibition test (*Vibrio fischeri*) for acute toxicity prediction of chemicals. Environ Int 32 (2), 265–268. 8

Patterson, G., Day, R. N., Piston, D., Mar 2001. Fluorescent protein spectra. J Cell Sci 114 (Pt 5), 837–838. 30

Patterson, G. H., Knobel, S. M., Sharif, W. D., Kain, S. R., Piston, D. W., Nov 1997. Use of the green fluorescent protein and its mutants in quantitative fluorescence microscopy. Biophys J 73 (5), 2782–2790. 30

Patton-Vogt, J. L., Henry, S. A., Aug 1998. *GIT1*, a gene encoding a novel transporter for glycerophosphoinositol in *Saccharomyces cerevisiae*. Genetics 149 (4), 1707–1715. 19

Payne, W. J., Dec 1973. Reduction of nitrogenous oxides by microorganisms. Bacteriol Rev 37 (4), 409–452. 141

Peijnenburg, A., Riethof-Poortman, J., Baykus, H., Portier, L., Bovee, T., Hoogenboom, R. L. A. P., Sep 2010. AhR-agonistic, anti-androgenic, and anti-estrogenic potencies of 2-isopropylthioxanthone (ITX) as determined by *in vitro* bioassays and gene expression profiling. Toxicol In Vitro 24 (6), 1619–1628. 12

Pernodet, N., Maaloum, M., Tinland, B., Jan 1997. Pore size of agarose gels by atomic force microscopy. Electrophoresis 18 (1), 55–58. 16

Persson, B. L., Lagerstedt, J. O., Pratt, J. R., Pattison-Granberg, J., Lundh, K., Shokrollahzadeh, S., Lundh, F., Jul 2003. Regulation of phosphate acquisition in *Saccharomyces cerevisiae*. Curr Genet 43 (4), 225–244. 19

Petrezselyova, S., Zahradka, J., Sychrova, H., Feb–Mar 2010. *Saccharomyces cerevisiae* BY4741 and W303–1A laboratory strains differ in salt tolerance. Fungal Biol 114 (2–3), 144–150. 82

Pham, M. T., Jan 2008. Herstellung rekombinanter Hefen als Ganzzellsensoren. Diploma thesis, Technische Universität Dresden, Institut für Genetik. 36, 69, 71, 75

Pickup, J. C., Hussain, F., Evans, N. D., Rolinski, O. J., Birch, D. J. S., Jun 2005. Fluorescence-based glucose sensors. Biosens Bioelectron 20 (12), 2555–2565. 8

Planta, R. J., Mager, W. H., Mar 1998. The list of cytoplasmic ribosomal proteins of *Saccharomyces cerevisiae*. Yeast 14 (5), 471–477. 137

Plessis, A., Dujon, B., Nov 1993. Multiple tandem integrations of transforming DNA sequences in yeast chromosomes suggest a mechanism for integrative transformation by homologous recombination. Gene 134 (1), 41–50. 133

Pollok, B. A., Heim, R., Feb 1999. Using GFP in FRET-based applications. Trends Cell Biol 9 (2), 57–60. 146

Prasher, D. C., Eckenrode, V. K., Ward, W. W., Prendergast, F. G., Cormier, M. J., Feb 1992. Primary structure of the *Aequorea victoria* green-fluorescent protein. Gene 111 (2), 229–233. 10

Pulz, O., Gross, W., Nov 2004. Valuable products from biotechnology of microalgae. Appl Microbiol Biotechnol 65 (6), 635–648. 140

Radhika, V., Milkevitch, M., Audigé, V., Proikas-Cezanne, T., Dhanasekaran, N., Apr 2005. Engineered *Saccharomyces cerevisiae* strain BioS–1, for the detection of water-borne toxic metal contaminants. Biotechnol Bioeng 90 (1), 29–35. 11

Radhika, V., Proikas-Cezanne, T., Jayaraman, M., Onesime, D., Ha, J. H., Dhanasekaran, D. N., Jun 2007. Chemical sensing of DNT by engineered olfactory yeast strain. Nat Chem Biol 3 (6), 325–330. 12

Raser, J. M., O'Shea, E. K., Jun 2004. Control of stochasticity in eukaryotic gene expression. Science 304 (5678), 1811–1814. 132, 135, 136, 146, 155

Regenberg, B., Holmberg, S., Olsen, L. D., Kielland-Brandt, M. C., Mar 1998. Dip5p mediates high-affinity and high-capacity transport of L-glutamate and L-aspartate in *Saccharomyces cerevisiae*. Curr Genet 33 (3), 171–177. 76, 137

Ringuet, S., Sassano, L., Johnson, Z. I., Feb 2011. A suite of microplate reader-based colorimetric methods to quantify ammonium, nitrate, orthophosphate and silicate concentrations for aquatic nutrient monitoring. J Environ Monit 13 (2), 370–376. 156

Rippka, R., Herdman, M., 1993. Catalogue and Taxonomic Handbook Vol. 1. Insitut Pasteur, Paris. 203

Roberts, C. J., Nelson, B., Marton, M. J., Stoughton, R., Meyer, M. R., Bennett, H. A., He, Y. D., Dai, H., Walker, W. L., Hughes, T. R., Tyers, M., Boone, C., Friend, S. H., Feb 2000. Signaling and circuitry of multiple MAPK pathways revealed by a matrix of global gene expression profiles. Science 287 (5454), 873–880. 23, 25, 127, 152, 153

Roda, A., Roda, B., Cevenini, L., Michelini, E., Mezzanotte, L., Reschiglian, P., Hakkila, K., Virta, M., May 2011. Analytical strategies for improving the robustness and reproducibility of bioluminescent microbial bioreporters. Anal Bioanal Chem. 11

Rodrigues, F., van Hemert, M., Steensma, H. Y., Côrte-Real, M., Leão, C., Jun 2001. Red fluorescent protein (DsRed) as a reporter in *Saccharomyces cerevisiae*. J Bacteriol 183 (12), 3791–3794. 146

Rogers, S., Wells, R., Rechsteiner, M., Oct 1986. Amino acid sequences common to rapidly degraded proteins: the PEST hypothesis. Science 234 (4774), 364–368. 14

Rogowska-Wrzesinska, A., Larsen, P. M., Blomberg, A., Görg, A., Roepstorff, P., Norbeck, J., Fey, S. J., 2001. Comparison of the proteomes of three yeast wild type strains: CEN.PK2, FY1679 and W303. Comp Funct Genomics 2 (4), 207–225. 133, 134

Rouillon, A., Barbey, R., Patton, E. E., Tyers, M., Thomas, D., Jan 2000. Feedback-regulated degradation of the transcriptional activator Met4 is triggered by the SCF(Met30) complex. EMBO J 19 (2), 282–294. 20

Salama, S. R., Hendricks, K. B., Thorner, J., Dec 1994. G1 cyclin degradation: the PEST motif of yeast Cln2 is necessary, but not sufficient, for rapid protein turnover. Mol Cell Biol 14 (12), 7953–7966. 14

Saldanha, A. J., Brauer, M. J., Botstein, D., Sep 2004. Nutritional homeostasis in batch and steady-state culture of yeast. Mol Biol Cell 15 (9), 4089–4104. 40, 138

Sanseverino, J., Eldridge, M. L., Layton, A. C., Easter, J. P., Yarbrough, J., Schultz, T. W., Sayler, G. S., Jan 2009. Screening of potentially hormonally active chemicals using bioluminescent yeast bioreporters. Toxicol Sci 107 (1), 122–134. 12

Sanseverino, J., Gupta, R. K., Layton, A. C., Patterson, S. S., Ripp, S. A., Saidak, L., Simpson, M. L., Schultz, T. W., Sayler, G. S., Aug 2005. Use of *Saccharomyces cerevisiae* BLYES expressing bacterial bioluminescence for rapid, sensitive detection of estrogenic compounds. Appl Environ Microbiol 71 (8), 4455–4460. 12

Schofield, D. A., Westwater, C., Barth, J. L., DiNovo, A. A., Oct 2007. Development of a yeast biosensor-biocatalyst for the detection and biodegradation of the organophosphate paraoxon. Appl Microbiol Biotechnol 76 (6), 1383–1394. 11, 72, 134, 157

Schwartz, M. A., Madhani, H. D., 2004. Principles of MAP kinase signaling specificity in *Saccharomyces cerevisiae*. Annu Rev Genet 38, 725–748. 22

Segall, J. E., Sep 1993. Polarization of yeast cells in spatial gradients of α mating factor. Proc Natl Acad Sci U S A 90 (18), 8332–8336. 23

Serp, D., Cantana, E., Heinzen, C., Stockar, U. V., Marison, I. W., Oct 2000. Characterization of an encapsulation device for the production of monodisperse alginate beads for cell immobilization. Biotechnol Bioeng 70 (1), 41–53. 149

Shagin, D. A., Barsova, E. V., Yanushevich, Y. G., Fradkov, A. F., Lukyanov, K. A., Labas, Y. A., Semenova, T. N., Ugalde, J. A., Meyers, A., Nunez, J. M., Widder, E. A., Lukyanov, S. A., Matz, M. V., May 2004. GFP-like proteins as ubiquitous metazoan superfamily: evolution of functional features and structural complexity. Mol Biol Evol 21 (5), 841–850. 13, 30

Shen, H. Y., Moonjai, N., Verstrepen, K., Delvaux, F., Apr 2003. Impact of attachment immobilization on yeast physiology and fermentation performance. Amer Soc Brewing Chemists Inc (2), 79–87. 147

Shetty, R. S., Deo, S. K., Liu, Y., Daunert, S., Dec 2004. Fluorescence-based sensing system for copper using genetically engineered living yeast cells. Biotechnol Bioeng 88 (5), 664–670. 11

Shibasaki, S., Ninomiya, Y., Ueda, M., Iwahashi, M., Katsuragi, T., Tani, Y., Harashima, S., Tanaka, A., Dec 2001. Intelligent yeast strains with the ability to self-monitor the concentrations of intra- and extracellular phosphate or ammonium ion by emission of fluorescence from the cell surface. Appl Microbiol Biotechnol 57 (5–6), 702–707. 142

Shibasaki, S., Tanaka, A., Ueda, M., Nov 2003. Development of combinatorial bioengineering using yeast cell surface display–order-made design of cell and protein for bio-monitoring. Biosens Bioelectron 19 (2), 123–130. 12, 142

Shimomura, O., Johnson, F. H., Saiga, Y., Jun 1962. Extraction, purification and properties of aequorin, a bioluminescent protein from the luminous hydromedusan, *Aequorea*. J Cell Comp Physiol 59, 223–239. 10

Sicko-Goad, L., Jensen, T. E., Feb 1976. Phosphate metabolism in blue-green algae. II. Changes in phosphate distribution during starvation and the 'polyphosphate overplus' phenomenon in *Plectonema boryanum*. Am J Bot 63 (2), 183–188. 140, 141

Singh, A., Chen, E. Y., Lugovoy, J. M., Chang, C. N., Hitzeman, R. A., Seeburg, P. H., Jun 1983. *Saccharomyces cerevisiae* contains two discrete genes coding for the α-factor pheromone. Nucleic Acids Res 11 (12), 4049–4063. 22

Smidsrød, O., Skjåk-Braek, G., Mar 1990. Alginate as immobilization matrix for cells. Trends Biotechnol 8 (3), 71–78. 15, 16

Spellman, P. T., Sherlock, G., Zhang, M. Q., Iyer, V. R., Anders, K., Eisen, M. B., Brown, P. O., Botstein, D., Futcher, B., Dec 1998. Comprehensive identification of cell cycle-regulated genes of the yeast *Saccharomyces cerevisiae* by microarray hybridization. Mol Biol Cell 9 (12), 3273–3297. 152

Spitzweg, C., Oct 2010. Thermosensitive *Saccharomyces cerevisiae* W303-Stämme für die Anwendung in der Hefe-Ganzzellsensorik. Bachelor thesis, Technische Universität Dresden, Institut für Genetik. 151

Sprague, G. F., Blair, L. C., Thorner, J., 1983. Cell interactions and regulation of cell type in the yeast *Saccharomyces cerevisiae*. Annu Rev Microbiol 37, 623–660. 21

Springael, J. Y., André, B., Jun 1998. Nitrogen-regulated ubiquitination of the Gap1 permease of *Saccharomyces cerevisiae*. Mol Biol Cell 9 (6), 1253–1263. 19

Stanbrough, M., Magasanik, B., Jan 1995. Transcriptional and posttranslational regulation of the general amino acid permease of *Saccharomyces cerevisiae*. J Bacteriol 177 (1), 94–102. 136

Su, L., Jia, W., Hou, C., Lei, Y., Jan 2011. Microbial biosensors: a review. Biosens Bioelectron 26 (5), 1788–1799. 7, 8, 9, 14, 16, 144, 149

Su, T.-C., Tamarkina, E., Sadowski, I., Aug 2010. Organizational constraints on Ste12 *cis*-elements for a pheromone response in *Saccharomyces cerevisiae*. FEBS J 277 (15), 3235–3248. 152, 155

Sugiura, S., Oda, T., Izumida, Y., Aoyagi, Y., Satake, M., Ochiai, A., Ohkohchi, N., Nakajima, M., Jun 2005. Size control of calcium alginate beads containing living cells using micro-nozzle array. Biomaterials 26 (16), 3327–3331. 16, 149

Sun, Z.-J., Lv, G.-J., Li, S.-Y., Xie, Y.-B., Yu, W.-T., Wang, W., Ma, X.-J., Jan 2007. Probing the role of microenvironment for microencapsulated *Sacchromyces cerevisiae* under osmotic stress. J Biotechnol 128 (1), 150–161. 147

Svitel, J., Curilla, O., Tkác, J., Apr 1998. Microbial cell-based biosensor for sensing glucose, sucrose or lactose. Biotechnol Appl Biochem 27 (Pt 2), 153–158. 8

Tai, S. L., Boer, V. M., Daran-Lapujade, P., Walsh, M. C., de Winde, J. H., Daran, J.-M., Pronk, J. T., Jan 2005. Two-dimensional transcriptome analysis in chemostat cultures. Combinatorial effects of oxygen availability and macronutrient limitation in *Saccharomyces cerevisiae*. J Biol Chem 280 (1), 437–447. 6, 17, 20, 21, 68, 69, 70, 76, 134, 135, 136, 137, 138, 202

Tamiya, H., Iwamura, T., Shibata, K., Hase, E., Nihei, T., 1953. Correlation between photosynthesis and light-independent metabolism in the growth of *Chlorella*. Biochim Biophys Acta 12 (1–2), 23–40. 203

Tao, W., Evans, B.-G., Yao, J., Cooper, S., Cornetta, K., Ballas, C. B., Hangoc, G., Broxmeyer, H. E., Mar 2007. Enhanced green fluorescent protein is a nearly ideal long-term expression tracer for hematopoietic stem cells, whereas DsRed-express fluorescent protein is not. Stem Cells 25 (3), 670–678. 142

ter Schure, E. G., van Riel, N. A., Verrips, C. T., Jan 2000. The role of ammonia metabolism in nitrogen catabolite repression in *Saccharomyces cerevisiae*. FEMS Microbiol Rev 24 (1), 67–83. 18

Thierfelder, S., Jul 2011. Entwicklung rekombinanter *Saccharomyces cerevisiae* Zellen als Ganzzellsensor zum Nachweis von Glucoselimitation. Doctoral thesis, Technische Universität Dresden, Institut für Genetik. 154

Thierfelder, S., Ostermann, K., Göbel, A., Rödel, G., Apr 2011. Vectors for glucose-dependent protein expression in *Saccharomyces cerevisiae*. Appl Biochem Biotechnol 163 (8), 954–964. 135, 139, 145

Thomas, B. J., Rothstein, R., Feb 1989. Elevated recombination rates in transcriptionally active DNA. Cell 56 (4), 619–630. 38

Thomas, D., Surdin-Kerjan, Y., Dec 1997. Metabolism of sulfur amino acids in *Saccharomyces cerevisiae*. Microbiol Mol Biol Rev 61 (4), 503–532. 20, 134

Tirosh, I., Berman, J., Barkai, N., Jul 2007. The pattern and evolution of yeast promoter bendability. Trends Genet 23 (7), 318–321. 69, 135

Tønnesen, H. H., Karlsen, J., Jul 2002. Alginate in drug delivery systems. Drug Development and Industrial Pharmacy 28 (6), 621–630. 15

Tsien, R. Y., Oct 1999. Rosy dawn for fluorescent proteins. Nat Biotechnol 17 (10), 956–957. 143

Tusher, V. G., Tibshirani, R., Chu, G., Apr 2001. Significance analysis of microarrays applied to the ionizing radiation response. Proc Natl Acad Sci U S A 98 (9), 5116–5121. 17

Usaite, R., Patil, K. R., Grotkjaer, T., Nielsen, J., Regenberg, B., Sep 2006. Global transcriptional and physiological responses of *Saccharomyces cerevisiae* to ammonium, L-alanine, or L-glutamine limitation. Appl Environ Microbiol 72 (9), 6194–6203. 18

Vagabov, V. M., Trilisenko, L. V., Kulaev, I. S., Mar 2000. Dependence of inorganic polyphosphate chain length on the orthophosphate content in the culture medium of the yeast *Saccharomyces cerevisiae*. Biochemistry (Mosc) 65 (3), 349–354. 19

Verbelen, P. J., Schutter, D. P. D., Delvaux, F., Verstrepen, K. J., Delvaux, F. R., Oct 2006. Immobilized yeast cell systems for continuous fermentation applications. Biotechnol Lett 28 (19), 1515–1525. 147

Verduyn, C., Postma, E., Scheffers, W. A., Dijken, J. P. V., Jul 1992. Effect of benzoic acid on metabolic fluxes in yeasts: a continuous-culture study on the regulation of respiration and alcoholic fermentation. Yeast 8 (7), 501–517. 40

Välimaa, A.-L., Kivistö, A. T., Leskinen, P. I., Karp, M. T., Jan 2010. A novel biosensor for the detection of zearalenone family mycotoxins in milk. J Microbiol Methods 80 (1), 44–48. 12

Wachter, R. M., Elsliger, M. A., Kallio, K., Hanson, G. T., Remington, S. J., Oct 1998. Structural basis of spectral shifts in the yellow-emission variants of green fluorescent protein. Structure 6 (10), 1267–1277. 13

Walmsley, R. M., Keenan, P., 2000. The eukaryote alternative: advantages of using yeasts in place of bacteria in microbial biosensor development. Biotechnol Bioprocess Eng 5, 387–394. 9

Warren, D. T., Andrews, P. D., Gourlay, C. W., Ayscough, K. R., Apr 2002. Sla1p couples the yeast endocytic machinery to proteins regulating actin dynamics. J Cell Sci 115 (Pt 8), 1703–1715. 146

Waters, M. G., Evans, E. A., Blobel, G., May 1988. Prepro-α-factor has a cleavable signal sequence. J Biol Chem 263 (13), 6209–6214. 22

Weber, G., Jun 1950. Fluorescence of riboflavin and flavin-adenine dinucleotide. Biochem J 47 (1), 114–121. 143

Weber, J. M., Ponti, C. G., Käppeli, O., Reiser, J., Jul 1992. Factors affecting homologous overexpression of the *Saccharomyces cerevisiae* Lanosterol 14α-demethylase gene. Yeast 8 (7), 519–533. 97, 155

Wee, S., Gombotz, W. R., May 1998. Protein release from alginate matrices. Adv Drug Deliv Rev 31 (3), 267–285. 15, 16

Wozei, E., Hermanowicz, S. W., Holman, H.-Y. N., Feb 2006. Developing a biosensor for estrogens in water samples: study of the real-time response of live cells of the estrogen-sensitive yeast strain RMY/ER-ERE using fluorescence microscopy. Biosens Bioelectron 21 (8), 1654–1658. 12

Wulf, P. D., Brambilla, L., Vanoni, M., Porro, D., Alberghina, L., Sep 2000. Real-time flow cytometric quantification of *GFP* expression and Gfp-fluorescence generation in *Saccharomyces cerevisiae*. J Microbiol Methods 42 (1), 57–64. 144, 145

Wykoff, D. D., O'Shea, E. K., Dec 2001. Phosphate transport and sensing in *Saccharomyces cerevisiae*. Genetics 159 (4), 1491–1499. 19

Xiong, J.-Y., Narayanan, J., Liu, X.-Y., Chong, T. K., Chen, S. B., Chung, T.-S., Mar 2005. Topology evolution and gelation mechanism of agarose gel. J Phys Chem B 109 (12), 5638–5643. 15

Xu, T., Baicu, C., Aho, M., Zile, M., Boland, T., Sep 2009. Fabrication and characterization of bio-engineered cardiac pseudo tissues. Biofabrication 1 (3), 035001. 16

Yagi, K., Jan 2007. Applications of whole-cell bacterial sensors in biotechnology and environmental science. Appl Microbiol Biotechnol 73 (6), 1251–1258. 9

Yang, H.-C., Lim, B.-S., k. Lee, Y., 2005. *In vitro* assessment of biocompatibility of biomaterials by using fluorescent yeast biosensor. Curr Appl Phys 5, 444–448. 11

Yanisch-Perron, C., Vieira, J., Messing, J., 1985. Improved M13 phage cloning vectors and host strains: nucleotide sequences of the M13mp18 and pUC19 vectors. Gene 33 (1), 103–119. 34, 35

Yu, D., Volponi, J., Chhabra, S., Brinker, C. J., Mulchandani, A., Singh, A. K., Jan 2005. Aqueous sol-gel encapsulation of genetically engineered *Moraxella* spp. cells for the detection of organophosphates. Biosens Bioelectron 20 (7), 1433–1437. 16

Yu, R. C., Pesce, C. G., Colman-Lerner, A., Lok, L., Pincus, D., Serra, E., Holl, M., Benjamin, K., Gordon, A., Brent, R., Dec 2008a. Negative feedback that improves information transmission in yeast signalling. Nature 456 (7223), 755–761. 26, 152

Yu, R. C., Resnekov, O., Abola, A. P., Andrews, S. S., Benjamin, K. R., Bruck, J., Burbulis, I. E., Colman-Lerner, A., Endy, D., Gordon, A., Holl, M., Lok, L., Pesce, C. G., Serra, E., Smith, R. D., Thomson, T. M., Tsong, A. E., Brent, R., Sep 2008b. The alpha project: a model system for systems biology research. IET Syst Biol 2 (5), 222–233. 24

Zaman, S., Lippman, S. I., Zhao, X., Broach, J. R., 2008. How *Saccharomyces* responds to nutrients. Annu Rev Genet 42, 27–81. 18

Zhang, N.-N., Dudgeon, D. D., Paliwal, S., Levchenko, A., Grote, E., Cunningham, K. W., Aug 2006. Multiple signaling pathways regulate yeast cell death during the response to mating pheromones. Mol Biol Cell 17 (8), 3409–3422. 26

Zhang, Z., Moo-Young, M., Chisti, Y., 1996. Plasmid stability in recombinant *Saccharomyces cerevisiae*. Biotechnol Adv 14 (4), 401–435. 131

Zhou, J., Lin, J., Zhou, C., Deng, X., Xia, B., Mar 2011. Cytotoxicity of red fluorescent protein DsRed is associated with the suppression of Bcl-xL translation. FEBS Lett 585 (5), 821–827. 142

Zhu, J., Zhang, M. Q., Jul–Aug 1999. SCPD: a promoter database of the yeast *Saccharomyces cerevisiae*. Bioinformatics 15 (7–8), 607–611. 69

Zhu, X., Garrett, J., Schreve, J., Michaeli, T., Jul 1996. *GNP1*, the high-affinity glutamine permease of *S. cerevisiae*. Curr Genet 30 (2), 107–114. 18, 136

Appendix A

Promoter sequences

A.1 *DAL80* promoter region

The cloned promoter region of *DAL80* carries an A→G transition at position –811 before the start of translation. The position is highlighted.

```
  1 TTTCTTAAAA GCGTGGCCAA ACTCTTTCTT CCAGCCATTG AACTGCTGTT
 51 GGGTGTAAGC TACAGAAGAA GAACGCCTTT GAGGGGCTCT TTCTTCCTCT
101 CTTTTAGAAT TCCGCTTAGA ATGAACATTA TTGTTACTGC TATGGAGATT
151 GTTGTAGAGC CGGTGCATAT TTTCCTCATC AGAACCTCGA CGAGGATCAT
201 GTTCATTAGA GTGCATAATA TGGTCTAATG AGTGGTTCGG TGACACATCA
251 CTCAGGTTTC TATCTACAAA GGATTTGGGC AATGCATGCT TCCTCTCCGC
301 CTCCTTGCCG TTGGGAGTTC TTCGTTTTTC TCTTTGTAAA CTGCTAGTCA
351 GATTGCCATT CTCAGGTAAT TGCCGCAATA CTTCTTGGTT TTCTAACTCA
401 TCTGGTCTCG AATTTACTCT ATCTACTTCT TCAGTCACCG ATCTATCTGC
451 CTGAGGTGGA GCGAAGTGAG TTCCAGACGC TGTTGACACG TTAGACATCA
501 CCCTTGTTTA TCTATCCTAC CTTTTCTTCT TGCGTACGTG CCTCTCAATG
551 CGTCGTGTGA ATTATCAGTG ACCGGTCGTG CCTATAATGT CCTGCTAATT
601 TCCCACTAAA TCTTTCCCCA TGGCGTATTC ATCGTTATGT TTGTGTCTTT
651 TGTTCAACCC AAAGGGCTGT AGCAATCTTC ACCCGTTTGT CGTTGATAAC
701 GAGTTTCCAC CTTATCACTT ATCACTAGTG CTAATCAAAC AGCAAAGAAT
751 GCTTGATAGA AACCGATCCT GGGCTTATCT CGCTGCATTG TGGCGGCATC
801 CCTGGACTGT AATCAGCAAG TGTTGCTTAG TATATATATA CATCCAGCGT
851 CAGCTTGAAT TTGGATACAG TTACTGTTTT TTCGATTTTC TCTTGGTTAT
901 TCTTTCTGAG ACAGTAGTAA TTTTGTATTA CTGAGCGGGA TATTGTTTAT
951 CTGCCGTCAT ACTATATTAC ATTATATTAT ATCATATTAT ATATAAGAGA
```

A.2 *DIP5* promoter region

The cloned promoter region of *DIP5* carries a T→C transition at position –556 before the start of translation. The position is highlighted.

```
  1 ATGCTTTTCA CCAGGTTGGT ATCCATTTTT CATGAGCTCT CTTATCAATT
 51 ATGTAAGTGC TTGTATACTA TTTACCTAAG ATAAGAAAAA AAAAAGCAAT
101 TCAAAATTAA GCTTATCTTG ACAGCGGGGC TGGTTTGTTT CTAGAAGACA
151 AAAAGTGGGG AATCATTTTT ACGTAACTCC CCCTGATAAG AAGGACTCAC
201 ATCCTTATAG GTACGATAAA GAATGGTTGT ATCTTTCCTA TTTTTCGAAA
251 TCGTTATCTT ATATAGTTGA ACTACTACGG TTAAAAAGCT TAAGCCTCAG
301 CCCTCTTAGT CAAACTTCTT TTTTGAAGGC ACCAGGGTGC ATAAAAGTGC
351 GTCTATTGTT TCCCAGTGGA ACTCTGTTGA GATAGCGATG TTTGTTTTTT
401 TTTCACTTAA CGGCAACCAA TACCGATAGC GACGTCGCTG GCAGTGTAGA
451 GTGGCCGTAC GGCGTCGCTA GATGGCACGG CACTGATTGC GGCGGGAGTC
501 GCTAGGCGGT GATGCATTTC CGCACAGGGA CCAGAGGAAG CTTCCCAGGC
551 GGTGACAGTA AGTGAACTCA TTATCATGTC TTCTCCAAAA CATTCGTGAC
601 ATCTAGTCAT GCTCCTCGCA ATTCACTCCG ATTGGTATAG CTTTTTCGGT
651 AGTTTTAGCT ACTATGCTTA GGGGAAAGAG GAGAAACCGT ACCGTCAGTC
701 TCAGTCAAAA AATTTTGATA TTCAATCTGA TAGCAAAGTT GGAACTTGGG
751 GTTATCTGGC CCTTTTTTGT TATCATATTC GTATACCCAA CAACATATCG
801 GTTCCACCGG TCCTTTTTAT ATATAAAAGA CGATGTGTAG ATGCACTCGA
851 GTATTCTTGG AGAACGTAAC TTGTATTGAG CTAGAGTGCT GGATAAAGTA
901 CCACATACTA ACGTTCTTTT ATAGAGCCAA ACATAATTCT TTTGCACTTT
951 CAATATAAGG TACAAGTGAA ACACAGGAAA AAAAGAACTA ACTCTAAGTA
```

A.3 *TMA10* promoter region

The cloned promoter region of *TMA10* carries a T→C transition at position –517 before the start of translation. The position is highlighted.

```
  1 GCAGGCATCG CCTTAACCAC TCGGCCACTG GGACGGTTGA ACAACGATCT
 51 AAAAATGAAT CGTTATATTG TCCAAATTTT GTGTCACATC AAATGCCCAT
101 TTGCGCATTC CTATATCCTC GAGGGAGAAC TTCTAGTATA TTTTGTACCC
151 CTAATATTAA CACCGAATCG ACAATGAAAT AAACGGAATA GCGCAATTTC
201 TGCAAATTTT TACAGTTCAT CAACAAGATA CATATCTTTC ATGACAGCTC
251 CTAAAACGAC TCTCATGAAT GGTAGTACAC CTCACGAAAA AGCGTACCAA
301 AACCGCACAC AATAAACGGA CTCGAACTGT TATGATCTCG TATTTTCTTG
351 TGCCCCGGGT CTTACTTCGT CGTGAGGGTG GATGAGCCAT CACAATGGGC
401 ATTTAGCGTT TTGGTGCAAG AGCGGGAAGA GGGGCGGCAG TTGGTTGCAA
451 TACCAAAAGC AAGTGACTCA CTACGGTCCG ATATTATCTT GCCCTTTCCA
501 TTCTCATACG TATGTTTTTT TAGATTATGC ACCTTCTTTG CCACAGTAAA
551 TGTGGCGGGG AAGATGTTGA GCTAGCGCCG TGCACAGTGG AAGAGACGGA
601 GGCGATTGTG GGGTTTCATC GGATTGTGCG GGAAGAAGGC CTACACCGTG
651 TTGAGCCACC CCCCCCTCAG GAGTAAATTT ACACAAACAG TGGTGGTGCC
701 TATGGTGGTA TACGAGATAG TGATAGAAGC TGCTGGATTG GGGTAGAAAT
751 TTTGTAGGCG TTTATGGATA TGGTATGGAT ATGGTATGGC TTGAGGTAGG
801 TAATCCAGAC ACCACTGGAA ATATATATAA GGAGAGAGTT CTGGCAGGTA
851 GATTTGTACT CCTCTCTACC ACTTTCTTCT ACTCCTTTTA TTATGTAATG
901 TTTATTATAA GCACAGCAAA AACGTTAAAT AAATCTAATA AGATTTCATT
951 ATAACATAAC ATTAAAGCAC ACAAATTTCT AACACAAACA CAATTCAAAC
```

A.4 *RPS22B* promoter region

The cloned promoter region of *RPS22B* carries a C→A transversion at position –267 before the start of translation. The position is highlighted.

```
  1 ACTGCAACTA TTCTTACAAT CTTTCATTTA CATGGCTCAA GAAGTGTTGC
 51 TGCTCAAAAT TTCATTCTAT TTCATGATTA TTTACATTAA ACAAGTATGA
101 TCCGTTATTC TTCTCGCAAC CGGAGTGCTC GAGAAGTGCC AGTAAGACGA
151 CACCCTATTT TTCAAGTCCA GCATTGGAAG ACTTCCAATG AACACTCTTA
201 TCATTATTCT TTATGCATTA CGTTTCGCAG TAATCCTAGA ACCCTAACTT
251 TTTCTAAAAT TACCGTCAAA AATGACGGAC GCAACTTTTC TCAGAAATTT
301 TTTTTTTCAT TTCTCTTAAA AAGTTTTCTA CGCTGGATAA ATTGTTCTCT
351 TCCCTTTGAA ATATGGAGAC GTTCAAAGTC AATTTCCACA CATTTAAGGT
401 GAACAAATAA ATTATAAGAT ACCACATTAA CAACAAGTAT GTGGACGAGG
451 TGTGGTAAGA TCTCCGCTGA GGTTGATTGA AAAGTATTGG GTAAATTTGT
501 ACTTTTTGTC TGCTGCTGGT CGTTTGTCTT TCGTTTTAAA ATTGCGCTAG
551 ACAAGTAAAC AGGGATTGCT TAAGAATCAA AGTAGCTTAA CTCTAAAGTA
601 TTATTTTCCT CAGTTGTGGG CCCATGTGTT GGAGGGAAGG AATATATTGA
651 AATGTAAATG TTCTTAAGTT CGGTTGAACT TGGATATTGT TACAAGAGTT
701 CTAGTCTTTG ATACCATTTT TACGCAATTA CAACCGCATT ATTTACCTTT
751 TCATCTTCAG TTTTACGGTT CAGTTTATTC TGTTACGAAA GAACTATGGT
801 GATTCAAAGG CGAAGTGCGT AGGATTGTAA CTCCTATATC TTTAGGATAC
851 TTACAATTTT GTACTGTTTT CAAGACCACT GTAACCGATA ATAAACCGGA
901 GGACACATTT TAACCCACTA TTTTTTTCAG AAGATCAGAT GCGAGAGCTC
951 GAAGCATAAG TATAATACTA ACGTTTCAAA ACATAGTAAT TAGGTAAAAA
```

A.5 *SOL1* promoter region

The cloned promoter region of *SOL1* carries a T→C transition at position –236 before the start of translation. The position is highlighted.

```
  1 CCCCGCCAAG ATGAAACGCC TCCAGTTTTG TGCTTCTTAA GTACTTCTCC
 51 AGAAAGGTTT TTGAAGTGGG ATGCAGACAC ATGCGAGCTA CGTCCCATCA
101 AGGGAACTGT GAAAAAAGGA CCGCAAATGA ACTTGGCAAA AGCCACACGA
151 ATCCTGAAGA CACCAAAAGA ATTTGGTGAG AACTTAATGA TTTTGGACTT
201 AATCAGAAAT GACCTTTACG AGTTGGTTCC TGACGTTCGG GTGGAGGAGT
251 TCATGTCCGT GCAAGAATAT GCCACCGTTT ACCAACTCGT TAGCGTCGTA
301 AAGGCACATG GATTGACCTC TGCCAGTAAG AAGACGAGAT ATTCAGGCAT
351 TGATGTCCTT AAACACTCGC TTCCTCCGGG ATCTATGACG GGAGCCCCCA
401 AGAAGATTAC TGTGCAATTA TTGCAGGACA AGATAGAAAG CAAGCTAAAC
451 AAACATGTCA ATGGTGGAGC ACGTGGTGTT TACAGCGGTG TCACGGGATA
501 TTGGTCTGTG AATTCCAACG GAGATTGGTC TGTTAACATT AGATGTATGT
551 ATTCCTACAA CGGCGGAACC AGCTGGCAAC TCGGTGCAGG GGGGGCCATA
601 ACAGTCTTAA GCACACTAGA TGGCGAACTA GAGGAAATGT ACAACAAGTT
651 GGAGAGCAAC TTACAAATTT TCATGTAGAT ATTTGTATAT TATTAGATAT
701 GTATGCAAAC ATTTTCTTTA GAATAATATA CTATTCTTGT ACGATGCAGA
751 ATTTTTTTTT TTTTTCGCTT TAGGAAAATG ACGTTTTGTG CCGTGGAAAA
801 CCCTGGAAAA GGATATTGGA AAAAAGTTAA AGCATGGTCA TTTAGGGAAG
851 ACTTTCCTTC CAATTTACTT ATCAATAGGT TATAATGTAT GCTTGACGGA
901 GCAGAATTCT TTCAAACCAT AAGATAATAG ATATTATAAC ATTTTAGTAC
951 ATAAAAGAGG CCCGAGAAAA TAGATTTTAA CTGGAATAAT TTTTTGCAAG
```

Appendix B

Vector and plasmid maps

B.1 Generation of plasmid p426GPD–FP

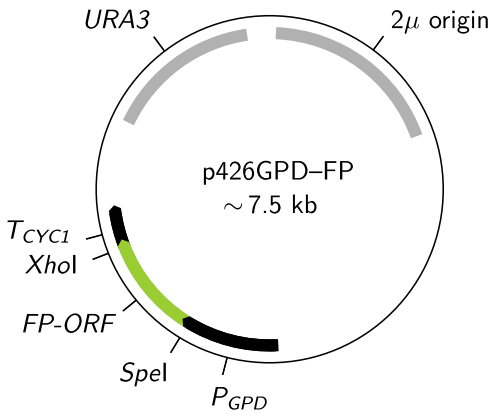

Figure B.1: Plasmid map of p426GPD–FP for strong and constitutive expression of fluorescence reporter genes (indicated with *FP-ORF*) in *S. cerevisiae*. Plasmids were derived from yeast expression vector p426GPD (Mumberg et al., 1995). For details see Section 3.1.1 and Figure 2.1 in Section 2.2.7.

B.2 Generation of nutrient detection plasmids

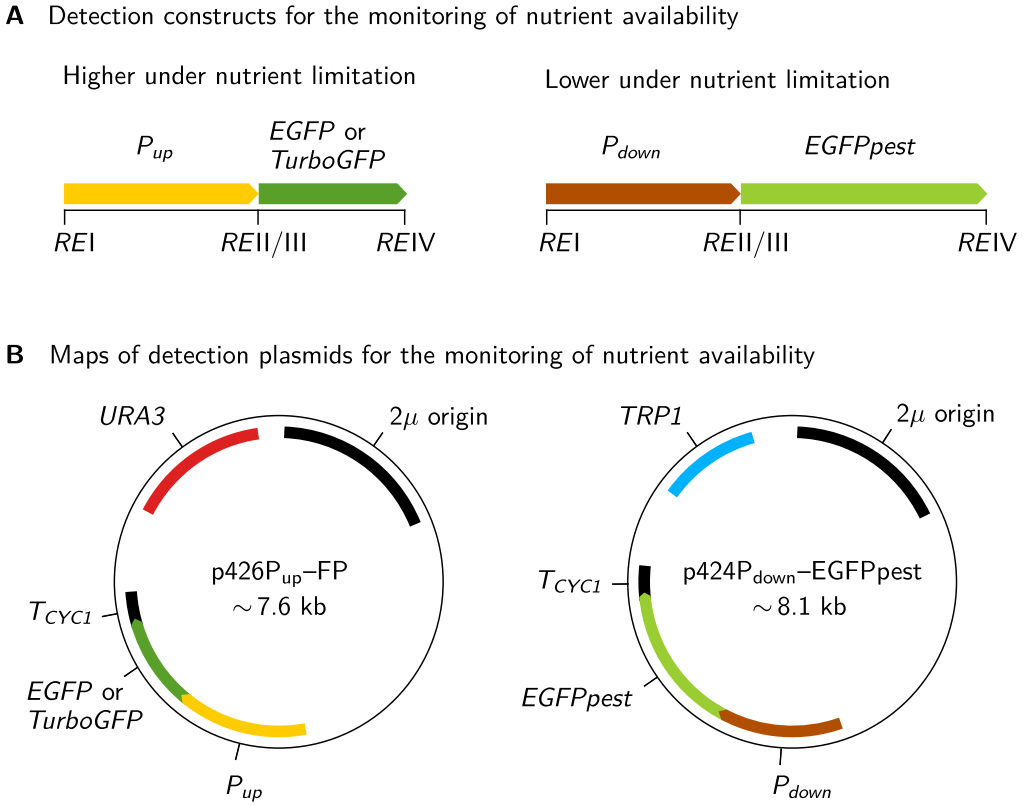

Figure B.2: Detection constructs and plasmids for the monitoring of nutrient availability with recombinant *S. cerevisiae* sensor strains. **A** Signature promoters drive specifically higher (P_{up}) or lower (P_{down}) expression of reporter genes encoding green fluorescent proteins (EGFP, TurboGFP or EGFPpest) under nutrient limitation. **B** Fragments with restriction site-extensions (*RE*I–IV) were PCR-generated for promoter replacement or reporter gene insertion into vectors p426ADH and p424GPD. See Tables 2.7 and 2.8 in Section 2.2.6 for primer sequences. Plasmids feature a 2μ origin for replication, selection markers for complementation of uracil (*URA3*) or tryptophan (*TRP1*) auxotrophic yeasts and the detection construct comprising the nutrient-responsive promoter ($P_{up/down}$), one of the three reporter genes and the *CYC1* terminator (T_{CYC1}).

B.3 Generation of plasmid pTT–GAP1

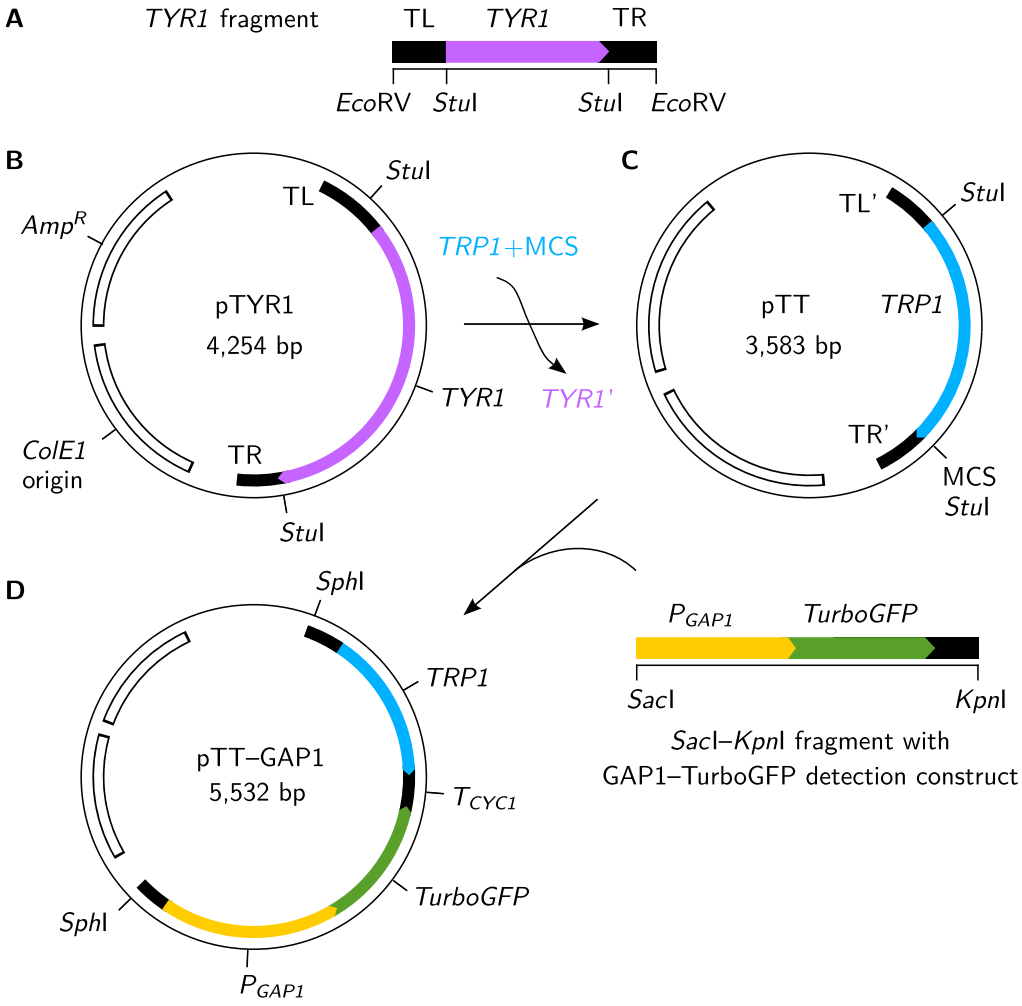

Figure B.3: Generation of a genome-integration cassette with a GAP1–TurboGFP nitrogen detection construct [strategy adapted from Mirisola et al. (2007)]. **A** Fragment *TYR1* including the *TYR1*-encoding sequence (1,359 bp) and flanking regions with *Stu*I recognition sites (TL, TR) was PCR-amplified from genomic DNA of BY4741 using primers F100 and R100 (Tab. 2.10, Section 2.2.6). **B** The fragment was cut with *Eco*RV and ligated to *Pvu*II-digested pUC18, yielding pTYR1. **C** The *TRP1* cassette (823 bp) was PCR-amplified from plasmid p424GPD with primers TRP1-ka-for and TRP1-Li-rev yielding a *TRP1* fragment linked to a small multiple cloning site (*TRP1*+MCS). Vector pTYR1 was digested with *Stu*I and the backbone with residual TL'/TR'-sites was ligated with *TRP1*+MCS. This vector was named pTT. **D** The *Sac*I–*Kpn*I fragment from detection plasmid p426GAP1–TurboGFP comprising the nitrogen-responsive *GAP1* promoter (P_{GAP1}), *TurboGFP* reporter gene and *CYC1* terminator (T_{CYC1}) was integrated into the small MCS cloning site of pTT. For genome integration, pTT–GAP1 was digested with *Sph*I to release the cassette comprising the GAP1 detection construct and *TRP1*.

Appendix C

Supplemental data for analysis of reporter and nutrient sensor cells

C.1 Flow cytometry analysis data

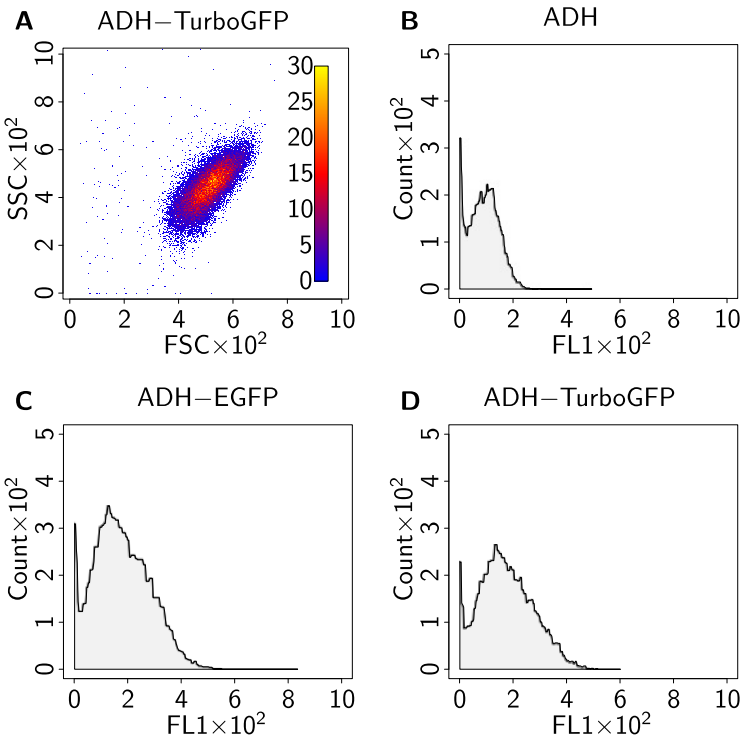

Figure C.1: Single-cell analysis of *S. cerevisiae* reporter cells with intermediate levels of green fluorescent protein by flow cytometry. Cells of strain BY4741 were transformed with plasmids p426ADH–EGFP or p426ADH–TurboGFP for moderate fluorescence, or parental vector p426ADH as a control (no fluorescence). For each strain, 40,000 cells were analysed using a Partec CyFlow SL flow cytometer with identical settings. **A** The representative scatter plot of recombinant cells is shown for reporter cells with p426ADH–TurboGFP. FSC (forward scatter channel) and SSC (side scatter channel) intensities provide information about cell size and granular content, respectively. The coloured legend specifies the count of cells at given positions in the plot. **B**–**D** Green fluorescence histograms (FL1) depict fluorescence distribution for recombinant strains.

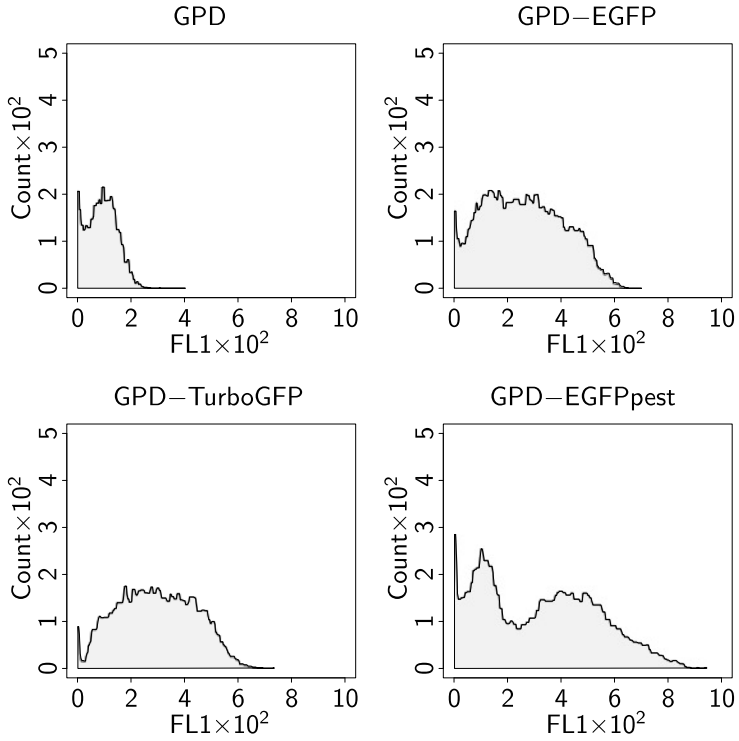

Figure C.2: Single-cell analysis of *S. cerevisiae* reporter cells with high levels of green fluorescent protein by flow cytometry. Cells of strain BY4741 were transformed with plasmids p426GPD–EGFP, p426GPD–TurboGFP or p426GPD–EGFPpest for strong fluorescence, or parental vector p426GPD as a control (no fluorescence). For each strain, 40,000 cells were analysed using a Partec CyFlow SL flow cytometer with identical settings. Green fluorescence histograms (FL1) depict fluorescence distribution for recombinant strains. Respective scatter plots (data not shown) were in line with the plot depicted in Figure C.1A.

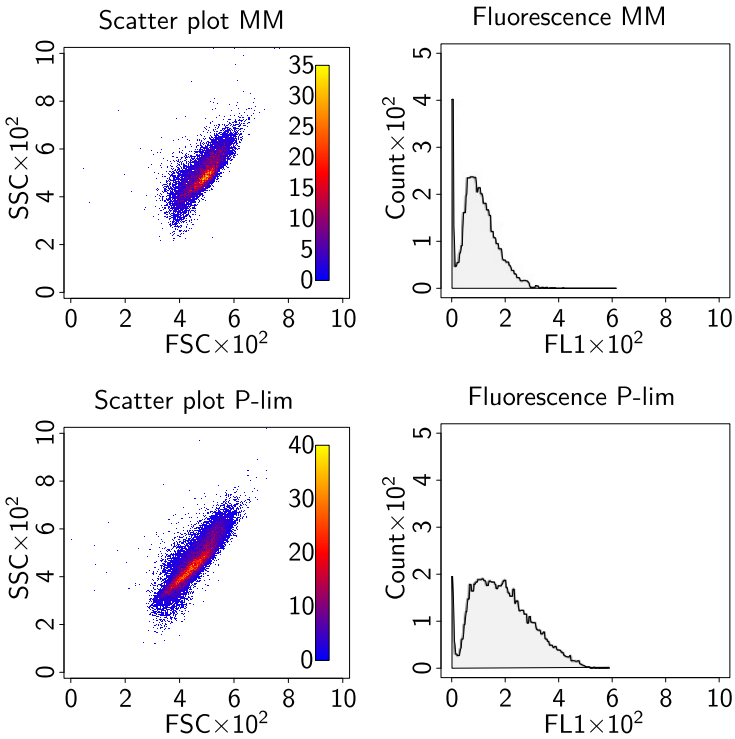

Figure C.3: Analysis of PHO11 phosphorus sensor cells by flow cytometry. Cells of BY4741 harbouring sensor plasmid p426PHO11–EGFP were cultivated in mineral medium and then shifted to fresh mineral medium (upper panels) or phosphorus limitation medium (lower panels) for eight hours. For each condition, 40,000 cells were analysed using a Partec CyFlow SL flow cytometer with identical settings. Scatter plots of FSC (forward scatter channel) and SSC (side scatter channel) intensities which provide information about cell size and granular content, respectively, and green fluorescence histograms (FL1) are shown. Coloured legends in scatter plots specify the count of cells at given positions in plots.

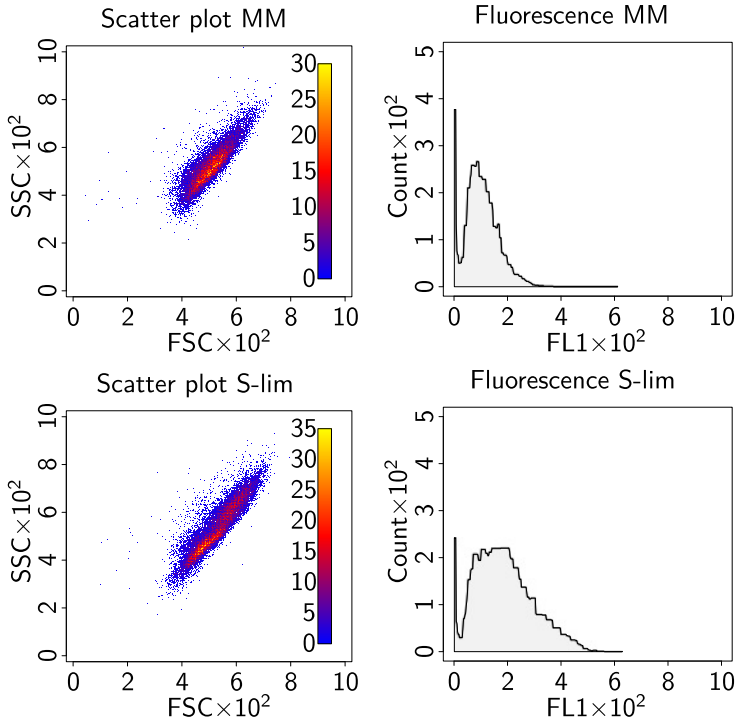

Figure C.4: Analysis of PDC6 sulphur sensor cells by flow cytometry. Cells of W303–1A harbouring sensor plasmid p426PDC6–EGFP were cultivated in mineral medium and then shifted to fresh mineral medium (upper panels) or sulphur limitation medium (lower panels) for eight hours. For each condition, 40,000 cells were analysed using a Partec CyFlow SL flow cytometer with identical settings. Scatter plots of FSC (forward scatter channel) and SSC (side scatter channel) intensities which provide information about cell size and granular content, respectively, and green fluorescence histograms (FL1) are shown. Coloured legends in scatter plots specify the count of cells at given positions in plots.

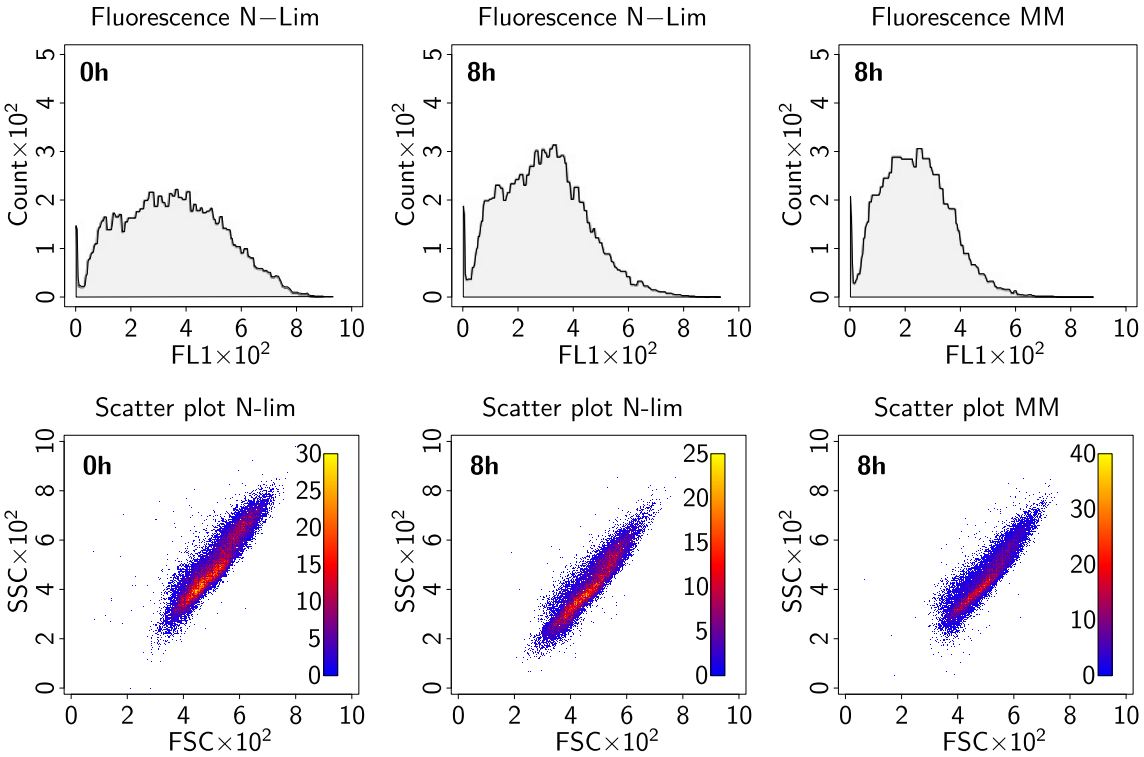

Figure C.5: Flow cytometry analysis of GAP1 sensor cell regeneration from nitrogen limitation. Cells of BY4741 harbouring detection plasmid p426GAP1–TurboGFP were shifted from nitrogen limitation medium (N-lim) to mineral medium (MM) for regeneration or transferred to fresh limitation medium for control. Per analysis, 40,000 cells were monitored using a Partec CyFlow SL flow cytometer with identical settings. Green fluorescence histograms and scatter plots are shown. FSC (forward scatter channel) and SSC (side scatter channel) intensities were similar for all samples. Coloured legends in scatter plots specify the count of cells at given positions in plots.

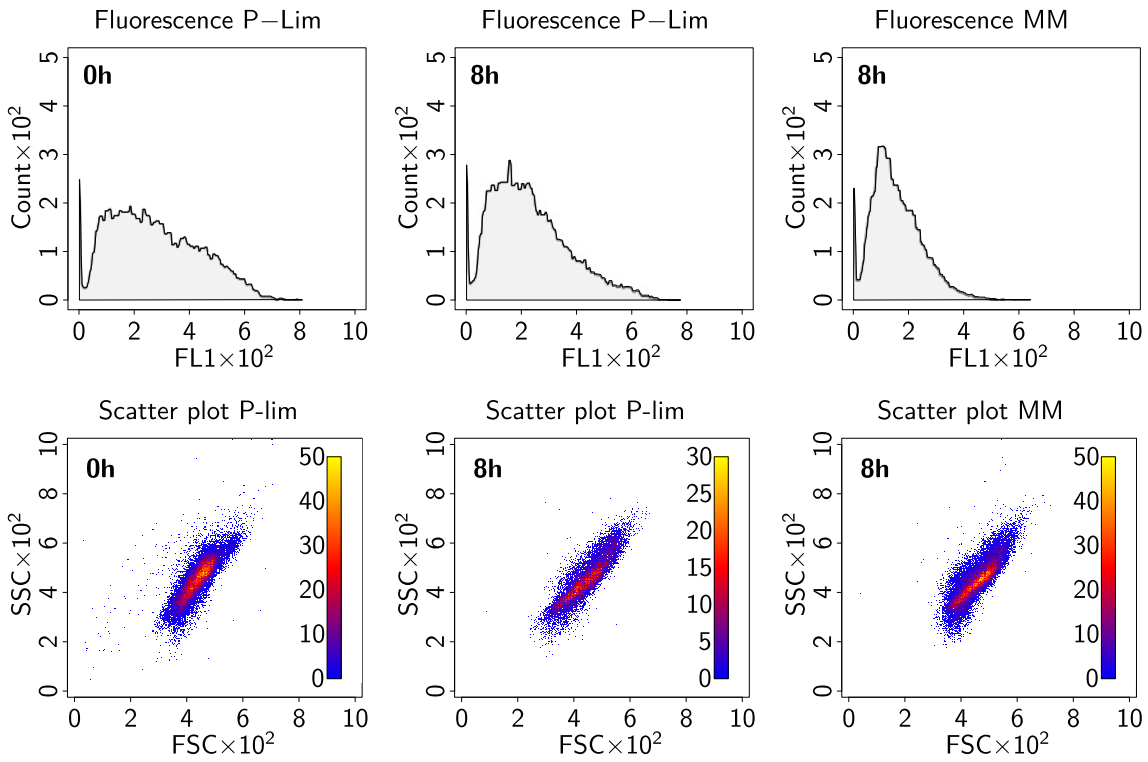

Figure C.6: Flow cytometry analysis of PHO11 sensor cell regeneration from phosphorus limitation. Cells of BY4741 harbouring detection plasmid p426PHO11–EGFP were shifted from phosphorus limitation medium (P-lim) to mineral medium (MM) for regeneration or transferred to fresh limitation medium for control. Per analysis, 40,000 cells were monitored using a Partec CyFlow SL flow cytometer with identical settings. Green fluorescence histograms and scatter plots are shown. FSC (forward scatter channel) and SSC (side scatter channel) intensities were similar for all samples. Coloured legends in scatter plots specify the count of cells at given positions in plots.

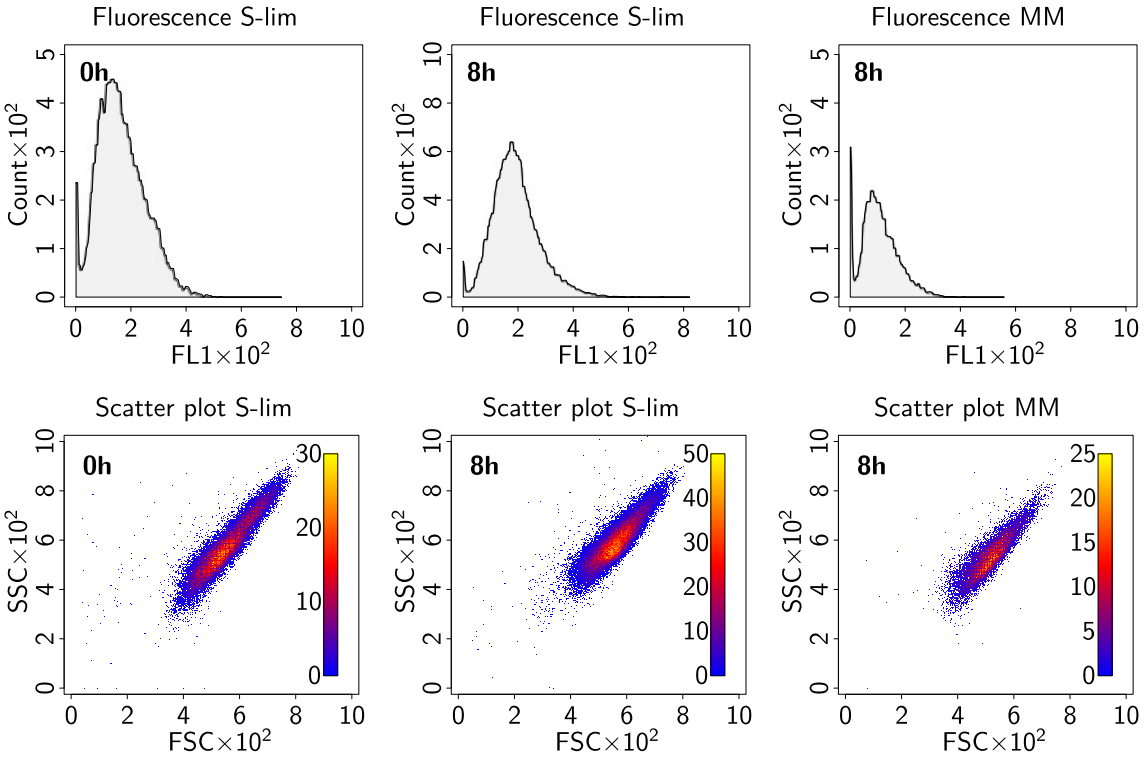

Figure C.7: Flow cytometry analysis of PDC6 sensor cell regeneration from sulphur limitation. Cells of W303–1A harbouring detection plasmid p426PDC6–EGFP were shifted from sulphur limitation medium (S-lim) to mineral medium (MM) for regeneration or transferred to fresh limitation medium for control. Per analysis, 40,000 cells were monitored using a Partec CyFlow SL flow cytometer with identical settings. Green fluorescence histograms and scatter plots are shown. FSC (forward scatter channel) and SSC (side scatter channel) intensities were similar for all samples. Coloured legends in scatter plots specify the count of cells at given positions in plots.

C.2 Signature genes indicating nutrient limitation

Table C.1: Transcript abundance (± sd) of selected signature genes that are indicative for *S. cerevisiae* growth limited by either nitrogen, phosphorus or sulphur. Values were extracted from supplemental data of publications by Boer et al. (2003) and Tai et al. (2005). The average fold-change (FC_{AV}) gives the average abundance in limitation of interest and average abundance in all three other conditions.

Gene	Glucose	Nitrogen	Phosphorus	Sulphur	FC_{AV}
Higher in nitrogen limitation					
GAP1	522.0 ± 82.9	2898.3 ± 203.9	426.8 ± 92.0	276.9 ± 24.8	7.6 ± 2.6
DAL5	90.8 ± 18.0	2436.8 ± 167.9	102.3 ± 14.6	105.5 ± 7.3	24.6 ± 2.0
DAL80	112.7 ± 3.0	829.6 ± 180.2	44.4 ± 6.8	12.0 ± 2.7	51.0 ± 28.1
DAL4	20.5 ± 2.3	238.4 ± 21.2	23.6 ± 8.7	12.0 ± 1.6	13.9 ± 5.3
Lower in nitrogen limitation					
HPF1	1133.3 ± 588.4	214.0 ± 144.1	2196.0 ± 343.1	1827.5 ± 111.2	-7.7 ± 11.2
NSR1	518.4 ± 127.2	137.3 ± 76.4	408.4 ± 111.0	367.8 ± 238.0	-1.5 ± 0.7
GNP1	78.5 ± 9.9	16.7 ± 2.6	64.2 ± 16.2	273.1 ± 33.7	-8.3 ± 7.0
Higher in phosphorus limitation					
PHO84	332.4 ± 512.3	19.7 ± 5.0	3244.6 ± 353.9	16.4 ± 6.2	124.1 ± 100.4
VTC1	348.8 ± 141.5	671.9 ± 34.3	2381.2 ± 74.7	551.6 ± 35.4	16.0 ± 13.2
PHO11	55.2 ± 37.1	68.2 ± 12.1	2357.2 ± 114.0	44.7 ± 4.2	43.3 ± 9.1
PHO3	279.8 ± 334.0	210.9 ± 33.8	2012.5 ± 165.6	64.6 ± 2.0	16.0 ± 13.2
Lower in phosphorus limitation					
TMA10	1969.8 ± 169.5	312.7 ± 71.3	85.5 ± 9.5	363.7 ± 34.7	-10.3 ± 11.0
SUL1	1035.2 ± 67.4	487.2 ± 30.5	42.0 ± 8.1	1885.4 ± 396.9	-27.0 ± 16.8
DIP5	28.1 ± 9.7	696.8 ± 44.4	13.2 ± 2.6	445.6 ± 71.1	-29.6 ± 25.6
RPS22B	520.1 ± 92.1	517.4 ± 93.4	234.8 ± 15.3	519 ± 92	-2.2 ± 0.0
Higher in sulphur limitation					
JLP1	12.0 ± 4.3	12.0 ± 2.1	12.0 ± 4.1	2232.7 ± 354.1	186.1 ± 0.0
PDC6	66.0 ± 43.9	161.1 ± 30.3	37.4 ± 7.3	1874.3 ± 235.7	30.0 ± 19.3
BDS1	25.9 ± 12.4	40.8 ± 8.3	41.6 ± 11.9	1738.9 ± 192.8	50.5 ± 14.4
AGP3	31.6 ± 4.8	12.0 ± 0.2	12.0 ± 2.3	773.8 ± 111.3	51.2 ± 23.1
Lower in sulphur limitation					
SOL1	835.7 ± 234.4	233.8 ± 20.4	92.4 ± 6.7	42.3 ± 3.1	-9.2 ± 9.3
SCS3	369.3 ± 289.8	438.9 ± 206.2	602.7 ± 251.5	12.0 ± 3.7	-39.2 ± 10.0
SSU1	449.7 ± 149.5	287.5 ± 10.9	193.8 ± 21.3	60.1 ± 4.7	-5.2 ± 2.2
GPH1	303.6 ± 44.3	431.6 ± 100.6	393.6 ± 33.3	35.0 ± 2.4	-10.8 ± 1.9

C.3 Microalgae media formulations

BG11 medium	Macronutrients	1.5 g l^{-1} $NaNO_3$
adapted from		40 mg l^{-1} $K_2HPO_4 \cdot 3\ H_2O$
Rippka and Herdman (1993)		75 mg l^{-1} $MgSO_4 \cdot 7\ H_2O$
		36 mg l^{-1} $CaCl_2 \cdot 2\ H_2O$
		6 mg l^{-1} Citric acid
		6 mg l^{-1} Ferric ammonium citrate
		1 mg l^{-1} EDTA–Na_2
		20 mg l^{-1} Na_2CO_3
	Trace minerals	61 μg l^{-1} H_3BO_3
		169 μg l^{-1} $MnSO_4 \cdot H_2O$
		287 μg l^{-1} $ZnSO_4 \cdot 7\ H_2O$
		2.5 μg l^{-1} $CuSO_4 \cdot 5\ H_2O$
		12.5 μg l^{-1} $(NH_4)6Mo_7O_{24} \cdot 4\ H_2O$
OHM medium	Macronutrients	410 mg l^{-1} KNO_3
described by		30 mg l^{-1} Na_2HPO_4
Fabregas et al. (2000)		246 mg l^{-1} $MgSO_4 \cdot 7\ H_2O$
		110 mg l^{-1} $CaCl_2 \cdot 2\ H_2O$
	Vitamins	15 μg l^{-1} Vitamin B_{12}
		25 μg l^{-1} Biotin
		17.5 μg l^{-1} Thiamine
	Trace minerals	2.62 mg l^{-1} Fe(III)citrate $\cdot\ H_2O$
		11 μg l^{-1} $CoCl_2 \cdot 6\ H_2O$
		12 μg l^{-1} $CuSO_4 \cdot 5\ H_2O$
		75 μg l^{-1} Cr_2O_3
		980 μg l^{-1} $MnCl_2 \cdot 4\ H_2O$
		120 μg l^{-1} $Na_2MoO_4 \cdot 2\ H_2O$
		5 μg l^{-1} SeO_2
Tamiya medium	Macronutrients	2.5 g l^{-1} KNO_3
described by		1.25 g l^{-1} $MgSO_4 \cdot 7\ H_2O$
Tamiya et al. (1953)		625 mg l^{-1} KH_2PO_4
		4.5 mg l^{-1} $FeSO_4 \cdot 7\ H_2O$
		18.6 m g l^{-1} EDTA–Na_2
	Trace minerals	1.43 m g l^{-1} H_3BO_4
		900 μg l^{-1} $MnCl_2 \cdot 4\ H_2O$
		111 μg l^{-1} $ZnSO_4 \cdot 7\ H_2O$
		9 μg l^{-1} MoO_3
		11.5 μg l^{-1} NH_4VO_3

C.4 Evaluation of nutrient sensor strains in microalgae media

Table C.2: Evaluation of nitrogen sensor cells in microalgae media and supernatants. Cells of BY4741 were transformed with detection plasmid p426GAP–TurboGFP and probed by microplate reader-based fluorometry as described in Section 3.2.12. For each cultivation condition (see Table 3.3 for microalgae media/supernatants, yeast-optimised mineral medium and nitrogen limitation medium are denoted as MM and N-lim, respectively), the fluorescence (RFU) after eight hours, the ratio of fluorescence in this medium to fluorescence in yeast-optimised mineral medium, and its evaluation are given.

Medium	**RFU ± sd (8 h)**	**RFU ratio (medium/MM)**	**Evaluation**
MM	670.0 ± 38.2	1.0	No limitation
N-lim	3485.0 ± 9.8	5.2	Limitation
BG11	5021.3 ± 239.9	7.5	$\gg$ N-lim
BG11 + *B. b.*	3300.7 ± 84.1	4.9	$\sim$ N-lim, $<$ BG11
OHM	3696.0 ± 44.2	5.5	$\sim$ N-lim
OHM + *H. p.*	3087.0 ± 46.1	4.6	$<$ N-lim, $<$ OHM
Tamiya	5516.0 ± 237.7	8.2	$\gg$ N-lim
Tamiya + *C. v.*	3525.3 ± 99.5	5.3	$\sim$ N-lim, $<$ Tamiya

Table C.3: Evaluation of phosphorus sensor cells in microalgae media and supernatants. Cells of BY4741 were transformed with detection plasmid p426PHO11–EGFP and probed by microplate reader-based fluorometry as described in Section 3.2.12. For each cultivation condition (see Table 3.3 for microalgae media/supernatants, yeast-optimised mineral medium and phosphorus limitation medium are denoted as MM and P-lim, respectively), the fluorescence (RFU) after eight hours, the ratio of fluorescence in this medium to fluorescence in yeast-optimised mineral medium, and its evaluation are given.

Medium	**RFU ± sd (8 h)**	**RFU ratio (medium/MM)**	**Evaluation**
MM	117.7 ± 2.3	1.0	No limitation
P-lim	591.7 ± 12.1	5.0	Limitation
BG11	221.0 ± 1.0	1.9	$>$ MM, $<$ P-lim
BG11 + *B. b.*	128.7 ± 3.2	1.1	$\sim$ MM, $<$ BG11
OHM	148.3 ± 2.5	1.3	$\sim$MM
OHM + *H. p.*	120.3 ± 15.3	1.0	$\sim$ MM, $<$ OHM
Tamiya	156.7 ± 7.1	1.3	$\sim$MM
Tamiya + *C. v.*	113.0 ± 6.1	1.0	$\sim$ MM, $<$ Tamiya

Table C.4: Evaluation of sulphur sensor cells in microalgae media and supernatants. Cells of W303–1A were transformed with detection plasmid p426PDC6–EGFP and probed by microplate reader-based fluorometry as described in Section 3.2.12. For each cultivation condition (see Table 3.3 for microalgae media/supernatants, yeast-optimised mineral medium and sulphur limitation medium are denoted as MM and S-lim, respectively), the fluorescence (RFU) after eight hours, the ratio of fluorescence in this medium to fluorescence in yeast-optimised mineral medium, and its evaluation are given.

Medium	**RFU ± sd (8 h)**	**RFU ratio (medium/MM)**	**Evaluation**
MM	123.9 ± 14.5	1.0	No limitation
S-lim	313.6 ± 32.3	2.5	Limitation
BG11	288.5 ± 12.3	2.3	$\sim$ S-lim
BG11 + *B. b.*	199.5 ± 8.8	1.6	$>$ MM, $<$ S-lim, $<$ BG11
OHM	261.8 ± 15.1	2.1	$>$ MM, $<$ S-lim
OHM + *H. p.*	188.3 ± 7.6	1.5	$>$ MM, $<$ S-lim, $<$ OHM
Tamiya	302.8 ± 6.7	2.4	$\sim$ S-lim
Tamiya + *C. v.*	224.4 ± 10.1	1.8	$>$ MM, $<$ S-lim, $<$ Tamiya